Simultaneous Chemical and Phase Equilibrium Calculations with Non-Stoichiometric Method

Tsanas, Christos

Publication date:
2018

Document Version
Publisher's PDF, also known as Version of record

Technical University of Denmark

Simultaneous Chemical and Phase Equilibrium Calculations with Non-Stoichiometric Methods

Christos Tsanas

Ph.D. Thesis
January 2018

DTU Chemistry
Department of Chemistry

Technical University of Denmark

Simultaneous Chemical and Phase Equilibrium Calculations with Non-Stoichiometric Methods

Christos Tsanas

Associate Professor Wei Yan
Professor Erling H. Stenby

Center for Energy Resources Engineering
Department of Chemistry
Technical University of Denmark

Kongens Lyngby, Denmark
January 2018

DTU Chemistry
Department of Chemistry

Science must begin with myths, and with the criticism of myths

— Karl R. Popper

Preface

This thesis is submitted in partial fulfillment of the requirements for the Ph.D. degree at the Technical University of Denmark, DTU. The research was carried out from December 2014 to January 2018 in the Department of Chemistry, DTU, under the supervision of Associate Professor Wei Yan (main supervisor) and Professor Erling H. Stenby (co-supervisor). The Ph.D. program was supported by the scholarship provided by DTU Chemistry and the research on dimethyl ether phase equilibrium modeling was supported by the Danish Hydrocarbon Research and Technology Centre (DHRTC).

January 2018
Christos Tsanas

Acknowledgments

First and foremost, I would like to express my utmost gratitude to my supervisors, Dr. Wei Yan and Prof. Erling H. Stenby, for their trust and guidance throughout this project. This work would not have been possible without their optimism and reassurance, but most importantly this academic adventure would not have been as enjoyable. I am also thankful to Prof. Michael L. Michelsen for his comments and suggestions. He was not directly involved in the supervision of this project, and this is why I appreciate immensely his help in the beginning of this study.

I am grateful to my colleges in CERE for the countless casual discussions that would suddenly escalate to detailed model comparisons and ruthless criticism of algorithms. I greatly appreciate the help of Anders Schlaikjer with the danish translation of the abstract.

I shared the same office with amazing people in DTU Chemistry. It was a complete pleasure to work with Farhad, Diego and Duncan. The things I learned and the inspiration I got from them are invaluable.

Last but certainly not least, I would like to thank my family and friends, the unsung heroes during my Ph.D. years in Denmark. This new chapter in my life did not come without difficulties, but their encouragement made everything much easier.

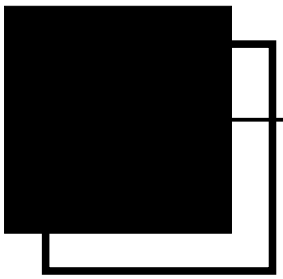

Abstract

Simultaneous chemical and phase equilibrium (CPE) calculations constitute a major class of challenging equilibrium problems, with applications in diverse scientific disciplines and engineering fields, such as the chemical industry, oil and gas production, and geochemistry. Robustness and efficiency of computational procedures are essential for demanding simulations of industrial processes, such as reactive distillation, heterogeneous organic synthesis, and fuel synthesis from renewable feedstocks. Most association equations of state, such as the popular SAFT family models, are essentially special cases of physical models incorporating chemical (association) equilibrium. Solution and further improvement of these association models can benefit from the advance in CPE calculations.

Over 70 years of research on CPE computation have resulted in a long list of algorithms with many variants but there seems to be no clear consensus on the most adequate methods. The deterministic algorithms can be roughly divided into stoichiometric and non-stoichiometric methods. The stoichiometric methods are more intuitive but less efficient for systems with many reactions. They are usually implemented with inefficient nested loops, whereas quadratic formulation can involve quite a cumbersome implementation for multiple phases. The non-stoichiometric methods are less common but suitable to systems with many reactions. However, most applications of non-stoichiometric methods are for ideal single-phase mixtures to slightly non-ideal two-phase systems and the reported algorithms are mostly non-quadratic for non-ideal systems.

The primary aim of this work is to develop a general and systematic non-stoichiometric approach which can determine the equilibrium state of multicomponent multiphase systems with multiple reactions at specified temperature and pressure. Two methods based on Gibbs energy minimization under material balance constraints are derived and presented in their extended form for non-ideal multiphase reaction systems. Both can be classified under the same category of using the Lagrange multipliers (and the phase molar amounts) as variables. For distinction, they are called the Lagrange multipliers method and the modified

RAND method, respectively. In the Lagrange multipliers method, successive substitution is employed to solve a modified set of equations originating from the Lagrangian conditions at the minimum. Convergence is quadratic for ideal systems (ideal gas/ideal solution) and linear for non-ideal systems. In the modified RAND method, one of the Lagrangian conditions is linearized around the current estimate of mole numbers. Composition derivatives of fugacity or activity coefficients are utilized to achieve quadratic convergence. The methods can be combined to form a robust and efficient approach: the Lagrange multipliers method is used for the first iterations of successive substitution and the modified RAND method for the second-order convergence. The resulting algorithm is called the combined algorithm in this thesis. For comparison, a successive substitution based algorithm using only the first-order Lagrange multipliers method is also investigated in this study. Both algorithms incorporate a reliable initialization procedure, where initial estimates are provided by the minimization of a convex function, and stability analysis to introduce additional phases when needed. The combined algorithm, as the recommended approach for CPE problems, has several advantages including a smaller system of equations (fewer variables), less sensitivity to initial estimates, the same treatment for all components and all phases, and the ability to monitor the decrease in Gibbs energy in the modified RAND steps to guide convergence.

The algorithms were applied to vapor-liquid (VLE), liquid-liquid (LLE) and vapor-liquid-liquid (VLLE) equilibrium of ideal as well as non-ideal systems that are commonly tested in the literature, including acid/alcohol esterifications, alkene/alcohol etherefications, hydration, hydrogenation and isomer separation. Additionally, predictions were made for the more complex transesterification of two individual triglycerides with methanol, which entails five chemical reactions and can result in one-, two- or even three-phase equilibrium. Finally, CPE calculations were attempted for electrolyte systems. The electroneutrality equation is satisfied by the material balance constraints, therefore there is no need to change the working equations of the algorithms. The equilibrium solution was obtained for aqueous mixtures of electrolytes in contact with a vapor and a solid phase. Consideration of the solid phase did not affect the convergence of the initialization procedure or the CPE calculations. This makes the algorithms potentially applicable to more complicated geological systems with an electrolyte aqueous phase and multiple solids. From the simple one-reaction ideal systems to the highly non-ideal electrolyte mixtures with speciation reactions and solids, both algorithms could converge without problems to the equilibrium solution. The CPU time and the reasonable number of iterations, allowed us to conclude that the methods presented are efficient and robust for the equilibrium determination of reaction systems.

The thesis also involves a small study on the dimethyl ether (DME) phase equilibrium modeling. DME is a slightly polar compound able to dissolve in both water/brine and hydrocarbon phases. It has been considered as a novel solvent in enhanced oil recovery, and more specifically in DME enhanced waterflood (DEW) process. DME is dissolved in water/brine and injected into the reservoir. It partitions preferably into the oil phase

to improve the mobility of the oil by swelling it and reducing its viscosity. DME itself is first-contact miscible with the oil. Accurate phase equilibrium modeling is necessary in DEW simulations. Parameters for CPA and PR/SRK EoS with Huron-Vidal mixing rules are regressed from experimental data of DME binary systems with water, hydrocarbons and inert gases. With satisfactory phase equilibrium modeling, predictions are made focusing on the K-value of DME between oil and aqueous phases in DME/water/oil mixtures (oil modeled as a mixture of methane, n-butane and n-decane). Different oil compositions appear to slightly affect the partitioning of DME, which could possibly simplify simulations of the DEW process. Finally, sensitivity of the K-value is investigated with respect to temperature, pressure and salinity of the aqueous phase. K-values increase with temperature and salinity but slightly decrease with pressure. Dependence on temperature is larger, while high salinity in the aqueous phase favors markedly the DME partitioning into the oil phase.

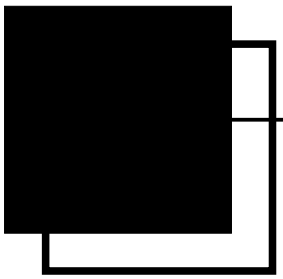

Resumé på dansk

Samtidig beregning af kemisk ligevægt og fase ligevægt (CPE) udgør en betragtelig klasse af udfordrende ligevægts problemer, med applikationer i et bredt spektre af videnskabelige discipliner og ingeniør felter som fx den kemiske industri, olie og gas produktion, og geokemi. Robusthed og effektivitet af de beregningsmæssige processor er essentielle for krævende simulationer af industrielle processor, som fx reaktiv destillation, heterogen organisk syntese og brændstof syntese fra bæredygtige råmaterialer. De fleste associations tilstandsligninger som de populærere SAFT modeller er egentlig særlige tilfælde hvor fysiske modeller inkorporer kemisk (association) ligevægt. Løsning af og yderlige forbedring af disse associations modeller kan drage fordel fra fremskridt i CPE beregninger.

Over 70 års forskning i CPE beregninger har resulteret i en lang liste af algoritmer med mange varianter, men der synes ikke at være en klar konsensus mod de mest passende metoder. De deterministiske algoritmer kan groft fordels i støkiometriske og ikke støkiometriske metoder. De støkiometriske metoder er mere intuitive men også mindre effektive i systemer med mange reaktioner. De er som regel implementeret med ineffektive nestede løkker, hvorimod kvadratisk formulering kan involvere en meget besværlig implementering for flere faser. De ikke støkiometriske metoder er mindre almindelige, men passende for systemer med mange reaktioner. De fleste applikationer af ikke støkiometriske metoder er dog for ideelle enkelt fase blandinger op til en smule ikke ideelle 2-fase systemer og de rapporterede algoritmer er hovedsageligt ikke kvadratiske for ikke ideelle systemer.

Det primære mål med dette arbejde er at udvikle en generel systematisk ikke støkiometrisk tilgang som kan bestemme ligevægts tilstanden af multikomponent multifase systemer med flere reaktioner ved specificeret temperatur og tryk. To metoder baseret på Gibbs energi minimering under forudsætning af materialer balance begrænsninger er udledt og præsenteret i deres udvidet form for ikke ideelle multifase reaktions systemer. Begge kan blive klassificeret under den samme kategori ved at bruge Lagrange multiplikatorer (og fase

molar mængder) som variable. For at skelne er de kaldet; Lagrange multiplikator metoden og modificeret RAND metoden. I Lagrange multiplikator metoden bruges successiv substitution til at løse et modificeret set ligninger der stammer fra Lagrange betingelser ved minimum. Dette konvergerer kvadratisk for ideelle systemer (ideal gas/ideelle opløsninger) og lineært for ikke ideelle systemer. I den modificeret RAND metode er en af Lagrange betingelserne lineariseret omkring det nuværende estimat af mol mængde. De sammensætnings aflede af fugacitet or aktivitets koefficient er udnyttet til at opnå den kvadratiske konvergering. De to metoder kan kombineres til at forme en robust og effektive tilgang; Lagrange multiplikator metoden er brugt til de første iterationer af successiv substitution og den modificerede RAND metoder er brugt for anden grads konvergeringen. Resultatet er en algoritme kaldet den kombinerede algoritme i denne afhandling. En successiv substitions baseret algoritme der kun burger første ordens Lagrange multiplikatorer metoden er også undersøgt i dette studie for at kunne blive brugt som sammenligning. Begge algoritmer inkorporer en troværdig initierings procedure, hvor indledende værdier er fundet ved minimering af en konveks funktion, og stabilitets analyse til at introducere yderligere faser når nødvendigt. Den kombinerede algoritme, som den anbefalede tilgang til CPE problemer, har flere fordele inklusive et mindre system af ligninger (færre variable), den er mindre sensitiv to initiale værdier, har samme behandling af alle komponenter og alle faser og har muligheden for at overvåge faldet i Gibbs energi per skidt i den modificerede RAND for at guide mod konvergering.

Algoritmerne er anvendt på gas-væske, væske-væske og gas-væske-væske ligevægte i ideelle såvel som ikke ideelle systemer der er regelmæssigt testet i litteraturen, inklusive syre/alkohol esterficeringer, alkene/alkohol etherficeringer, hydrering, hydrogenering, og isomer separation. Forudsigelser er derudover lavet for mere komplekse transesterficeringer af 2 individuelle triglycerider med metanol, en proces der har 5 kemiske reaktioner og kan resultere i 1, 2 eller 3 fasers ligevægt. Slutteligt har CPE beregninger været forsøgt anvendt på elektrolyt systemer. Elektroneutralitets ligningen er opfyldt ved masse balance begrænsninger, og derfor er der ingen ændring i arbejdes ligningerne i algoritmerne. Ligevægts opløsningen er fundet ved vandig blanding af elektrolytter i kontakt med en gas og en fast fase. At tage den faste fase i betragtning har ikke nogen effekt på konvergeringen af den initiale procedure eller CPE beregningerne. Dette gør potentiellet algoritmerne anvendelige på mere komplekse geologiske systemer med en vandig elektrolyt fase og indtil flere faste faser. Begge algoritmer kan konvergere, såvel det simpelt 1 reaktions ideelle system til det meget ikke ideelle elektrolyt system med speciations reaktioner og faste faser, uden problemer med ligevægts opløsningen. CPU beregningstiden og et passende antal iterationer, tillader os at konkludere at de præsenterede metoder er effektive og robuste for ligevægts fastsættelse i reaktions systemer.

Afhandlingen indeholder også et mindre studie om modellering af dimethyl ethers (DME) fase ligevægt. DME er et mildt polært stof der er kan opløses i såvel vand/brine og carbonhydrid faser. Det har været betragtet som et nyt solvent i udvidet olieudvinding (EOR) og mere specifikt i DME forbedret waterflood (DEW) processer. DME er opløst i

vand/brine og bliver pumpet ned i reservoiret. Her skilles det helst ind i olie fasen for at forbedre mobiliteten af olien ved at få det til at hæve op og derved reducere viskositeten. DME er første kontakts opløseligt i olien. Præcis fase ligevægt modellering er nødvendig i DEW simulationer. Parametre fra CPA og PR/SRK tilstandsligninger med Huron-Vidal blandings regler er estimeret til eksperimentelle data for binære DME systemer med vand, carbonhydrider og inerte gaser. Med tilfredsstillende faseligevægts modellering er forudsigelser af K-værdien for DME mellem olie og vand faserne i DME/vand/olie blandinger (olie modelleret som en blanding af metan, n-butan og n-dekan) beregnet. Forskellige olie sammensætninger synes at have en mindre effekt på fordeling af DME, hvilket potentielt kunne forsimple simuleringen af DEW processen. Til slut er sensitiviteten af K-værdien undersøgt i forhold til temperatur, tryk og saltindhold i vand fasen. K-værdierne stiger med temperatur og saltindhold men falder svagt med tryk. Afhængighed af temperatur er større, mens højt saltindhold i vandfasen kraftigt favoriserer DME i olie fasen.

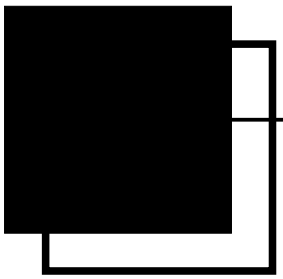

Contents

List of figures

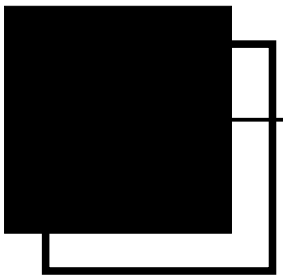

List of tables

CHAPTER

1 Introduction

1.1 Literature review

Calculation of simultaneous chemical and phase equilibrium (CPE) is essential in the chemical and petroleum industry. Fast and reliable algorithms are necessary in process simulations that combine phase separation and transformation of compounds into valuable products. CPE calculations are useful in:

- reactive distillation (Saito et al., 1971; Barbosa and Doherty, 1988; Ung and Doherty, 1995a,b,c,d,e). Reactions allow us to bypass restrictions of purely physical processes, such as infeasibility of separation due to azeotropes or close-boiling components (e.g. isomers).
- reactive extraction (Kanth et al., 2014; Pal et al., 2015; Shah et al., 2016). Reacting components tend to have higher partition coefficients.
- heterogeneous organic synthesis (Toikka et al., 2012). Reactants can impede the progress of the reaction if they separate into different phases. On the other hand, partitioning of products can shift equilibrium to favorable yields.
- biodiesel production (Kiss et al., 2006; Anikeev et al., 2012; Osorio-Viana et al., 2013). A mixture of fatty acid esters is mainly produced by transesterification of triglycerides.
- weak electrolytes/geochemical systems (Gautam and Seider, 1979c; Venkatraman et al., 2015; Leal et al., 2016a). Speciation of electrolytes takes place in an aqueous phase, which is potentially at equilibrium with vapor and solid phases.
- reactor design (Solsvik et al., 2016). Gibbs energy minimization is combined with current feasibility and design models to improve them.
- metallurgical applications (Rao, 1983; Sander et al., 1986)
- reactive crystallization (Jiménez and Costa-López, 2002; Jaime-Leal et al., 2012)

- air pollution control equipment (Sanderson and Chien, 1973; Pérez Cisneros et al., 1997)

Various algorithms and solution strategies were published and applied to a range of ideal/non-ideal single- or multiphase systems. Some common reaction mixtures reported in literature include:

- esterification of acetic acid/ethanol (Castillo and Grossmann, 1981; Barbosa and Doherty, 1988; Xiao et al., 1989; Castier et al., 1989; McDonald and Floudas, 1995, 1997; Pérez Cisneros et al., 1997)
- esterification of acetic acid/1-butanol (Suzuki et al., 1970; Grob and Hasse, 2005; Bonilla-Petriciolet et al., 2006; Mandagaran and Campanella, 2009)
- MTBE (methyl-*tert*-butyl ether) synthesis (Ung and Doherty, 1995e; Seider and Widagdo, 1996; Fateen et al., 2012; Moodley et al., 2015)
- TAME (*tert*-amyl methyl ether) synthesis (Chen et al., 2002; Bonilla-Petriciolet et al., 2008a, 2011; Elnabawy et al., 2014)
- methanol synthesis (Chang et al., 1986; Castier et al., 1989; Gupta et al., 1991; Stateva and Wakeham, 1997; Phoenix and Heidemann, 1998; Avami and Saboohi, 2011)
- propene hydration (Castier et al., 1989; Stateva and Wakeham, 1997; Bonilla-Petriciolet et al., 2012)
- transesterification of fatty acids (Schuchardt et al., 1998; Darnoko and Cheryan, 2000; Omota et al., 2001, 2003; Kiss et al., 2006; Chong et al., 2014)
- benzene hydrogenation (George et al., 1976; Castillo and Grossmann, 1981; Burgos-Solórzano et al., 2004)
- xylene separation (Ung and Doherty, 1995a,c,e; Pérez Cisneros et al., 1997)
- reactions in aqueous solution of formaldehyde (Ung and Doherty, 1995a,e; Pérez Cisneros et al., 1997; Avami and Saboohi, 2011)
- blast furnace problem (Madeley and Toguri, 1973; Cavallotti et al., 1980; Castillo and Grossmann, 1981)
- steam cracking of ethane (Castillo and Grossmann, 1981; Gautam and Wareck, 1986; Lantagne et al., 1988)
- geological reactions with solid calcite/dolomite/quartz (Leal et al., 2016a,b)

CPE applications are not limited to these lists. Although there are cases where a process is subject to kinetic limitations and the equilibrium solution has little to no weight in decision making (e.g. optimization of process parameters), CPE can still provide a thermodynamic limit as reference to judge the overall efficiency of the process.

This work uses terminology that appears in Smith and Missen (1982), who published

a systematic categorization and review of CPE procedures. Two main categories exist, solution of equilibrium algebraic equations and Gibbs energy minimization. Minimization problems are further divided into stoichiometric and non-stoichiometric. The former use reaction extents as independent variables and the later material balance constraints, which are incorporated in the Lagrangian of the Gibbs energy. Later publications usually follow this convention when they refer to CPE calculation methods.

Solution of equilibrium equations

One of the oldest algorithms for CPE calculations was published by Brinkley (1946, 1947), using a nested-loop scheme to solve the equilibrium equations. Activity coefficients are kept constant in the inner loop (secondary iterations) and updated in the outer loop (primary iterations). A "representative phase" and a basis of reference components are selected for the calculations. Different basis components and representative phases affect the speed of convergence. According to Brinkley (1946) determination of an optimum basis is possible but can be too inconvenient for practical application. Nevertheless, a number of publications have addressed the issue of the basis optimization (Prigogine and Defay, 1947; Schott, 1964; Cruise, 1964). Usually it consists of the most abundant components.

Stoichiometric algorithms

Ma and Shipman (1972) presented a two-step method for ideal multiphase mixtures approximating major components in the beginning (high truncation error) and subsequently solving for the exact equilibrium solution, where minor components re-enter calculations. Sanderson and Chien (1973) developed a procedure transforming the Gibbs energy minimization into an unconstrained minimization using a penalty function. The solution is based on the Rachford-Rice equation using values of chemical equilibrium constants in nested-loop calculations. Marquardt's method was chosen to solve the non-linear equations. Phase equilibrium is solved in the inner loop, updating the reaction extents in the outer loop. Sanderson and Chien (1973) made a distinction between the two solution approaches for the chemical and phase equilibrium problem. According to them, solution of algebraic equations should be advantageous in data correlation and simulations whereas Gibbs energy minimization in larger systems or for predictions. Xiao et al. (1989) studied VLE of reaction systems with a K-value based method. They proposed an improvement of the S-C algorithm (Sanderson and Chien, 1973), called the KZ algorithm. Still with a nested-loop procedure, chemical equilibrium is solved in the inner loop and phase equilibrium in the outer loop with a modified Marquardt method (S-C algorithm loops switched). For improved efficiency, variables are also scaled by the total amount of components at equilibrium. Stateva and Wakeham (1997) presented a modified KZ algorithm (Xiao et al., 1989) partitioning the system into linear and non-linear equations. In the inner loop chemical equilibrium is solved, whereas in the outer loop phase equilibrium equations with constant K-values are converged. In general, their three-step method involves initialization, stability analysis with phase split/flash and final convergence to the equilibrium solution.

Castier et al. (1989) derived the only stoichiometric second-order method to our knowledge. Initial steps involve accelerated direct substitution with the General Dominant Eigenvalue Method (GDEM) (Crowe and Nishio, 1975). Rachford-Rice equations are solved in the inner loop and reaction extents and K-values are updated in the outer loop. The efficient Murry's minimization is employed for final convergence. Yield factors are introduced to account for the separation of the components between the phases. Components need to be divided into primary or secondary and revision of their mole numbers is necessary when they attain negative values.

Non-stoichiometric algorithms

The non-stoichiometric formulation was extensively explained by Zeleznik and Gordon (1968). Perturbation calculations were used to initialize computations for challenging systems, accounting for non-ideality. Elimination of the Lagrange multipliers reduces the minimization to a "chemical equilibrium constant" method. Sensitivity with respect to initial conditions was also mentioned. The potentially large difference of thermodynamic derivatives between reaction and non-reaction systems was addressed but it is kinetics that decides which derivatives should be used. The overall strategy for CPE problems was considered by the authors as "an interplay between thermodynamic fundamentals and numerical analysis". George et al. (1976) used exponential functions instead of penalty functions to eliminate the constraints for two- or three-phase equilibrium with Powell's method (Powell, 1971) with independent treatment of trace components. Castillo and Grossmann (1981) presented a non-stoichiometric method with a phase elimination procedure using steepest descent coupled with optimum step sizes. A non-linear programming algorithm allowed direct treatment of the non-negativity constraints of mole numbers. They took provision in the neighborhood of zero compositions, since the gradient is unbound and convergence is impeded. They presented results for both reaction and non-reaction mixtures. There was no need for a feasible starting point, linear independence of the constraints and fugacity analytical derivatives, the latter being especially useful for complex thermodynamic models. Phases with zero mole numbers were not eliminated in the event that they were needed later. Harvie et al. (1987) identified automatically orthogonal reaction paths needed in the poorly conditioned chemical equilibrium problems, as they are more stable in calculations. Gibbs energy was minimized with Newton's method and phases were removed when the Hessian was singular. Instability could occur when assuming more phases than the Gibbs phase rule allows or when concentrations approach zero. They noted the need for second-order derivatives to increase efficiency in the phase removal procedure. Different specifications from isothermal and isobaric chemical and phase equilibrium are mentioned in Gautam and Wareck (1986). In their formulation, equations for an electrolyte phase were also included. They started calculations with one phase or more and used the phase splitting algorithm of Gautam and Seider (1979b). Although the authors believed that the method "is robust enough", they admit that there was not extensive testing concerning the phase-splitting algorithm. Uchida (1987) used logarithms of mole fractions as variables to speed up the convergence. Initialization

was provided by the Simplex method and components were separated into primary and secondary based on their abundance. Instead of trying all the possible phase combinations, they introduced imaginary components to decide which phases of the ones initially assumed actually exist at equilibrium. Saim and Subramaniam (1988) applied the non-stoichiometric formulation to systems with solvents at supercritical conditions solving the equations of the Lagrangian at the minimum. Lantagne et al. (1988) showed a second-order Newton's and quasi-Newton method based on the penalty function formulation, allowing the existence of electrolyte phases. The efficiency of the algorithm strongly depends on the choice of the penalty parameter. The authors compared their procedure with a sequential quadratic programming (SQP) method for reaction and non-reaction systems. Their algorithm showed similar performance to the SQP procedure, with the additional advantage that it is able to deal with low concentrations. Michelsen (1989) stressed that away from critical conditions, CPE calculations can approach the efficiency of second-order methods coupled with an acceleration method. To overcome problems associated with trace components, Michelsen (1989) defined the dual problem. Linear programming was used to initialize calculations. In the same work, an augmented Lagrangian using penalty functions was also applied and resulted in more stable iterations.

Lucia and Xu (1990) applied a general SQP algorithm in VLE with trust region as a stabilization method. The Hessian matrix was approximated and the quadratic problem was solved by two methods, a linear programming based method and the active set method. In their work, their formulations involved Gibbs energy minimization and entropy maximization. Hildebrandt and Glasser (1994) developed a geometric algorithm that constructs the boundary of the convex hull of the Gibbs energy. This provides an alternative way to find equilibrium number of phases and compositions. Pérez Cisneros et al. (1997) presented two procedures for chemical and phase equilibrium calculations: the chemical model using elements in the mass balance equation and the ideal solution approach with two-loops (inner loop calculation for constant fugacity coefficients, outer loop updating the non-ideality). They also stressed that the reader should take caution with the sensitivity of the equilibrium solution on the model parameters. Phoenix and Heidemann (1998) developed two first-order methods, a stoichiometric with reaction extents and phase amounts as iteration variables and a non-stoichiometric with Lagrange multipliers and phase amounts. The usual scheme was considered, where fugacity coefficients are constant in the inner loop and updated in the outer loop. Stability analysis and damping coefficients to control the non-stoichiometric convergence were also used. Lee et al. (1999) employed direct search optimization to minimize the Gibbs energy, that can converge even when the phases assumed in the beginning were more than the equilibrium phases. Wasylkiewicz and Ung (2000) using transformed variables form Ung and Doherty (1995d) developed a procedure that can systematically track all the stationary points of the tangent plane distance function. Transformed mole fractions for reaction systems introduced by Ung and Doherty (1995a,b,c,d,e), were widely used in different algorithms in the literature. Their work was based on the study of Barbosa and Doherty (1988) in the VLE of systems with one

reaction. The authors addressed the issue of reactive azeotropes and the conditions under they are likely to appear. They showed that mole fractions in the vapor and liquid phase are not necessarily equal at a reactive azeotrope and ideal systems can also exhibit such behavior. Jalali-Farahani and Seader (2000) and Jalali et al. (2008) determined equilibrium with the homotopy-continuation method. Homotopy function provides a smooth transition to the solution by gradually introducing non-linearities and the continuation method is capable of finding all the roots of a function. Koukkari and Pajarre (2007) illustrated how kinetic constraints can be incorporated in a non-stoichiometric method, implying however that the dependence of the reaction extents on time is known. Rossi et al. (2011) studied a number of systems with models that behave as pseudo-convex functions, covering both PT and PH flash with non-linear programming, pointing out that the assumption of convexity might limit applicability. Avami and Saboohi (2011) worked on the simultaneous solution of equilibrium and stability analysis, relaxing the constraint of the known phases number before the calculations. Their method is referred to as an extended τ method. Variables τ are called phase characteristic variables and are linked to the existence of a phase at equilibrium. The authors suggest that this method could be used in reactive distillation simulations. Leal et al. (2016a,b) combined the Gibbs energy minimization with geochemical reactions, electrolytes and solid precipitation. They start with the maximum number of phases allowed, removing those that do not exist at equilibrium. Their observation is that the electroneutrality equation is not an additional constraint, but is forced by the formula matrix of the system.

The RAND method

White et al. (1958) presented a non-stoichiometric method, the original RAND method, named after the company where the authors were working. It is a Gibbs energy minimization approach that does not distinguish between the components during calculations (primary/secondary). Linear programming was used for initialization with a safeguard for zero concentrations. The method was proposed for ideal gas reaction phases. A similar method was developed by Huff et al. (1951), known as the NASA method. Their key difference is that during RAND iterations, the material balance is satisfied in contrast to NASA iterations. Boynton (1960) extended calculations to multiple ideal phases, with the assumption that all condensed phases were known beforehand. The author mentioned the possibility of application to non-ideal systems with an outer loop updating the activity coefficients. Gautam and Seider (1979a,b,c) and White and Seider (1981) in a series of four research papers, covered different topics pertinent to equilibrium calculations. They mentioned solid existence criteria and referred to the procedures presented in Sanderson and Chien (1973) (S-C algorithm), White et al. (1958) (RAND algorithm), Huff et al. (1951) (NASA algorithm) and George et al. (1976) (Powell's method). They found that quadratic programming and the RAND algorithm are faster than Powell's method. They combined the RAND algorithm with a phase-splitting procedure that allows even poor guesses for trial phases. Furthermore, they accounted for dissociation reactions by including additional terms for electrolytes in the Gibbs energy expression. Finally, they

discussed characteristic of stoichiometric and non-stoichiometric methods, presenting an extension of the RAND algorithm for multiphase systems. There is no direct mention of how they used the RAND method to account for non-ideality. In their final paper (White and Seider, 1981) they refer to the extended RAND as the "augmented" RAND, that can be applied to systems with reactions, electrolytes and solid components. Michelsen (1989) commented on the difficulty of the RAND method to determine small concentrations (trace components). Greiner (1988a,b,c) presented an extensive analysis of the Gibbs energy minimization. The analysis was based on the elemental abundance approach. The author showed with rigorous mathematical proofs how the non-ideal non-convex problem can be formulated as an equivalent "convexified" problem, avoiding metastable points as final solutions. Moreover, he demonstrated how the formulation can be transformed into a generalized linear program to approximate the solution without the need of second-order derivatives. However, this approach achieved linear converge rate. Generalization of the RAND algorithm to non-ideal multiphase systems with quadratic convergence rate is attributed to Greiner (1991), but a similar formulation appears in Michelsen and Mollerup (2007) with different derivation. Voňka and Leitner (1995) showed calculations with the RAND method in non-ideal systems by performing RAND steps under the ideal system approximation (constant fugacity or activity coefficients) and then updated the non-ideality part using the new compositions. New initial estimates were created in the case of a singular matrix. In general implementations based on the ideal system approximation are not expected to be fast and there is no guarantee that the Gibbs energy decreases between outer-loop iterations. Recently Paterson et al. (2017) presented two RAND-based formulations: modified RAND with TP based thermodynamics and vol-RAND with TV based thermodynamics. Nevertheless, their study is primarily focused on multiphase equilibrium calculations without reactions.

Global optimization methods

Floudas and Visweswaran (1990) provided an extensive study with mathematical proofs on global optimization of non-linear programming. Their treatment involved the solution of a number of subproblems with partitioning and transformation of variables (GOP algorithm). McDonald and Floudas (1995, 1997) developed GLOPEQ, guaranteed to convergence to the global minimum combining two procedures: minimization of Gibbs energy and minimization of the tangent plane distance. Gupta et al. (1991) presented an alternative treatment for stability analysis with a multiphase reaction equilibrium algorithm. Algebraic equations of equilibrium and stability are solved in a nested-loop. In the inner loop fugacity coefficients are kept constant while phase fractions, stability variables and reaction extents are converged. In the outer loop mole fractions are updated and an acceleration factor is calculated based on the dominant eigenvalue method. Incipient phases, phase removal and reintroduction of phases were not a problem. Burgos-Solórzano et al. (2004) developed a validation tool to provide a guarantee of convergence to the Gibbs energy global minimum. Due to the additional computation time it requires, the authors suggest its use at the end of a simulation.

A large part of the literature is devoted to deterministic methods. In recent decades, a number of stochastic methods has been utilized for equilibrium calculations. Stochastic methods require only evaluation of the objective function. Bonilla-Petriciolet and Segovia-Hernández (2010), and Bonilla-Petriciolet et al. (2008b, 2011, 2012) worked largely on stochastic methods in Gibbs energy minimization for reacting systems. They proposed algorithms for two-phase equilibrium (VLE and LLE) using different algorithms such as swarm optimization and its modifications, genetic algorithms, differential evolution with tabu list, simulated annealing and harmony search. A local optimization method is used during final convergence to improve efficiency. Fateen et al. (2012) compared three global optimization algorithms (CMA-ES, SCE, Firefly). Elnabawy et al. (2014) presented different variations of the Charged System Search method, inspired by the Coulombic forces between charged particles. Both works mention the possibility of a local optimization method for final convergence to improve global success rate, an indication of the successful convergence to the minimum with different initial estimates. Moodley et al. (2015) presented modifications of the Krill Herd optimization on CPE and stability analysis. The method simulates the herding behavior of the krill crustacean and requires a smaller number of function evaluations than other stochastic methods. Yet, the stochastic approach is in general computationally expensive and more efficient methods exist for CPE. Stability analysis coupled with a local minimization method is the conventional way to check if we have converged to the Gibbs energy global minimum. Even strictly formulated deterministic global minimization can be too time consuming (Floudas and Visweswaran, 1990; McDonald and Floudas, 1995, 1997). Bonilla-Petriciolet and Segovia-Hernández (2010), and Bonilla-Petriciolet et al. (2008b, 2011, 2012) provide a more comprehensive listing of various stochastic methods.

1.2 Scope of this work

In our work, we introduce the non-stoichiometric Lagrange multipliers and modified RAND methods to integrate them in algorithms for equilibrium calculations of non-ideal multicomponent multiphase systems with multiple reactions. These methods are extensions of the Lagrange multipliers method for ideal systems mentioned in Michelsen (1989) and the ideal RAND for a single vapor phase mentioned in White et al. (1958). The successive substitution algorithm utilizes only the first-order Lagrange multipliers method and results in linear convergence rate for non-ideal systems. In the combined algorithm, after a few steps of successive substitution, the second-order modified RAND method is chosen for final convergence. The use of fugacity or activity coefficient composition derivatives and the Gibbs energy monitoring during modified RAND steps enhances the efficiency and robustness of the combined algorithm, which is the recommended general, quick and reliable approach for CPE calculations. Initialization and stability analysis are included in both algorithms, which start with the assumption of a single phase and additional phases are considered whenever needed. The algorithms were extensively applied to multiphase equilibrium of reaction systems that appear in the literature (VLE, LLE, VLLE

of one/two-reaction mixtures). Furthermore, calculations for more complex systems are shown, such as in the transesterification of fatty acid triglycerides with methanol (five reactions and up to three phases) as well as highly non-ideal electrolyte speciation in an aqueous phase at equilibrium with a vapor and/or a pure solid phase.

A secondary project is also included in this thesis. Dimethyl ether (DME) phase equilibrium was modeled with CPA EoS and PR/SRK EoS with Huron-Vidal mixing rules, intended for the DME enhanced waterflood (DEW) process. Experimental data of DME binary systems with water, hydrocarbons, carbon dioxide and nitrogen were used in parameter regression. Predictions for the partitioning between aqueous and oil phases as well as K-value sensitivity with respect to temperature, pressure, oil composition and salinity of the aqueous phase are presented.

A brief outline of the remaining chapters in this thesis is given below, where the most important elements are described.

Chapter 2 Thermodynamic principles and terms relevant to this work are explained. Starting with the definition of the Gibbs energy, conditions that characterize phase and chemical equilibrium are described. This chapter serves as a reference for the equations that will be used throughout the thesis and can be viewed as an introduction to the analysis of CPE calculation.

Chapter 3 Stoichiometric and non-stoichiometric Gibbs energy minimization methods for CPE are analyzed. The emphasis is on non-stoichiometric methods and more specifically on the Lagrange multipliers and the modified RAND method. At the end of the chapter both methods are integrated in complete algorithms with initialization and stability analysis, intended for multiphase CPE calculations.

Chapter 4 The algorithms developed in Chapter 3 are applied to the most common systems in the literature and calculations are compared with published results. Moreover, predictions are made for the complex ester mixture resulting from the transesterification of two fatty acid triglycerides with methanol. Finally, the speed of calculations as CPU time and the convergence rate with iteration plots are shown.

Chapter 5 Chemical and phase equilibrium in electrolyte systems is investigated. The basic equations for electrolyte analysis are presented. Systems containing water, ammonia, carbon dioxide, calcium chloride and calcium carbonate can lead to the equilibrium of vapor, liquid and pure solid phases. Calculations are made without changes in the working equations developed for non-electrolyte mixtures.

Chapter 6 Dimethyl ether binary systems are modeled with CPA EoS and PR/SRK

EoS with Huron-Vidal mixing rules. Parameters for different regression strategies are shown. Predictions based on the regressed parameters are made, especially for the change of the DME K-value between the aqueous and the oil phase with temperature, pressure, oil composition and salinity.

CHAPTER

2

General thermodynamic definitions

The purpose of the following sections is to clarify necessary thermodynamic terms and notions relevant to the algorithm development and application in succeeding chapters. The Gibbs energy of a closed system is defined and basic equations of phase and chemical equilibrium are presented. Finally, the ideal gas and the pure component reference state are explained, two different reference states that will be used in calculations of reaction systems.

2.1 System and state functions

Fundamental concepts in thermodynamics are the system, material entities it contains and the interactions between these entities. Some of the following terms might not adhere to the classical definitions of chemistry or physical chemistry but are based on their use in thermodynamics and engineering practices:

- system: arbitrarily defined part of the universe regardless of form or size (McNaught and Wilkinson, 1997). The remaining part of the universe is called the surroundings. Systems can be further divided into:
  - isolated: cannot exchange either matter or energy with the surroundings, e.g. a mixture inside a thermally insulated closed container.
  - closed: can only exchange energy with the surroundings, e.g. a reaction mixture in a closed flask that is cooling over an ice bath.
  - open: can exchange matter and energy with the surroundings, e.g. a semi-batch reactor with a constant feed flow of reactants with heating.
- components: entities of a material system with identical chemical structure. For example, different components are H_2O, CH_3OH, *o*-xylene and *p*-xylene. This term is not used with the formal physical chemistry definition mentioned in McNaught and

Wilkinson (1997).

- elements: entities of a mixture whose amount or concentration can be varied independently. They represent the minimum number of independent entities necessary to define compositions in all the phases of a system. Their number may vary with external conditions, since additional chemical equilibria will reduce their number (Rao, 1985). This definition corresponds to the formal physical chemistry definition of the term "component" (McNaught and Wilkinson, 1997).
- phase: an entity of a material system which is uniform in chemical composition and physical state (McNaught and Wilkinson, 1997). Phases are regions in space characterized by the same values of properties, such as density, refractive index and component composition. They are separated by distinct boundaries called interfaces.
- reaction: a process that results in the interconversion of chemical species (McNaught and Wilkinson, 1997). Chemical reactions may be elementary or step-wise, involving a single or at least two consecutive steps, respectively.

The state of a system is formally described by state functions, also known as thermodynamic potentials (Michelsen and Mollerup, 2007). State functions have the following features:

- they have exact differentials
- they are zero or first order homogeneous functions
- a unique value of the function corresponds to a specific state
- the change of the function value between two states A and B does not depend on the path of the transition from A to B but only on the individual states

Along with their derivatives, state functions can provide complete characterization of the system state. A state function postulated by the first law of thermodynamics is the internal energy, U:

$$U = f(S, V, \mathbf{n}, ...) \tag{2.1}$$

where:

S	entropy
V	volume
$\mathbf{n}$	component abundance matrix

The entries of matrix $\mathbf{n}$ are n_{ik}, the mole numbers of component i in phase k. It is implied that the internal energy depends on additional variables, such as the surface area or the total charge. We assume that the systems are not affected by external fields, the total charge is zero and that multiple phases contribute additively to the total value of the function:

$$U = \sum_{i=1}^{N_P} U_k(S_k, V_k, \mathbf{n}_k) \tag{2.2}$$

where:

U_k	internal energy of phase k
S_k	entropy of phase k
V_k	volume of phase k
$\mathbf{n}_k$	component abundance vector in phase k
N_P	number of phases

Eq. 2.2 is not applicable for systems of phases thinly dispersed in another phase (e.g. colloid systems), because surface energy contributions must be also included. In this work the internal energy is a function of entropy, volume and mole numbers:

$$U = f(S, V, \mathbf{n}) \tag{2.3}$$

The differential of the internal energy (Eq. 2.3) is:

$$dU = TdS - pdV + \sum_{k=1}^{N_P} \sum_{i=1}^{N_C} \mu_{ik} dn_{ik} \tag{2.4}$$

with the following definitions:

$$\left(\frac{\partial U}{\partial S}\right)_{V,\mathbf{n}} = T \qquad \left(\frac{\partial U}{\partial V}\right)_{S,\mathbf{n}} = -p \qquad \left(\frac{\partial U}{\partial n_{ik}}\right)_{S,V,n_{(j\neq i)k}} = \mu_{ik} \tag{2.5}$$

where:

T	temperature
p	pressure
μ_{ik}	chemical potential of component i in phase k
N_C	number of components

From Euler's theorem for homogeneous functions:

$$U = TS - pV + \sum_{k=1}^{N_P} \sum_{i=1}^{N_C} \mu_{ik} n_{ik} \tag{2.6}$$

Different state functions can be defined by applying Legendre transformations to the internal energy:

$$\mathcal{F}_i^U[x_{j\neq i}, (\partial U/\partial x_i)_{x_{j\neq i}}] = U - x_i \left(\frac{\partial U}{\partial x_i}\right)_{x_{j\neq i}} \tag{2.7}$$

where:
$\mathcal{F}_i^f$ Legendre transformation of function $f(\mathbf{x})$ with respect to variable x_i

In terms of function $f(\mathbf{x})$, variables $\mathbf{x}$ are called natural variables, whereas x_i and $(\partial f/\partial x_i)_{x_{j\neq i}}$ are called conjugate variables. Legendre transformation creates a new function $\mathcal{F}_i^f$ with natural variables all $x_{j\neq i}$, and $(\partial f/\partial x_i)_{x_{j\neq i}}$ in place of x_i. Intensive variables of state functions do not depend on the size or amount of matter in the system. When such a dependency exists, the variables are called extensive.

Three of the most useful state functions derived from internal energy are:

- Enthalpy (Legendre transformation of U with respect to V)

$$H(S, p, \mathbf{n}) = U - V \left(\frac{\partial U}{\partial V}\right)_{S,\mathbf{n}} = U + pV = TS + \sum_{k=1}^{N_P} \sum_{i=1}^{N_C} \mu_{ik} n_{ik} \tag{2.8}$$

  Enthalpy is the internal energy of a system plus the work exerted on the surroundings by the system, to attain final volume V and pressure p. Mathematical treatment of open systems with mass flow or closed systems under constant entropy and pressure is usually based on enthalpy analysis.

- Helmholtz energy (Legendre transformation of U with respect to S)

$$A(T, V, \mathbf{n}) = U - S \left(\frac{\partial U}{\partial S}\right)_{V,\mathbf{n}} = U - TS = -pV + \sum_{k=1}^{N_P} \sum_{i=1}^{N_C} \mu_{ik} n_{ik} \tag{2.9}$$

  Helmholtz energy represents the maximum reversible work that can be performed by a closed system at constant temperature and volume.

- Gibbs (free) energy (Legendre transformation of U with respect to S and V):

$$\begin{aligned} G(T, p, \mathbf{n}) = U - S \left(\frac{\partial U}{\partial S}\right)_{V,\mathbf{n}} - V \left(\frac{\partial U}{\partial V}\right)_{S,\mathbf{n}} = \\ = U - TS + pV = H - TS = \sum_{k=1}^{N_P} \sum_{i=1}^{N_C} \mu_{ik} n_{ik} \end{aligned} \tag{2.10}$$

  Gibbs energy represents the maximum reversible work that can be performed by a closed system at constant temperature and pressure. These are frequently the conditions of physical and chemical processes, therefore the Gibbs energy is usually selected for thermodynamic analysis. The total differential of the Gibbs energy is:

$$dG = \left(\frac{\partial G}{\partial T}\right)_{p,\mathbf{n}} dT + \left(\frac{\partial G}{\partial p}\right)_{T,\mathbf{n}} dp + \sum_{k=1}^{N_P}\sum_{i=1}^{N_C}\left(\frac{\partial G}{\partial n_{ik}}\right)_{T,p,n_{(j\neq i)k}} dn_{ik} \tag{2.11}$$

Taking the total differential of Eq. 2.10 results in:

$$dG = -SdT + Vdp + \sum_{k=1}^{N_P}\sum_{i=1}^{N_C}\mu_{ik}dn_{ik} \tag{2.12}$$

Therefore:

$$\left(\frac{\partial G}{\partial T}\right)_{p,\mathbf{n}} = -S \qquad \left(\frac{\partial G}{\partial p}\right)_{T,\mathbf{n}} = V \qquad \left(\frac{\partial G}{\partial n_{ik}}\right)_{T,p,n_{(j\neq i)k}} = \mu_{ik} \tag{2.13}$$

Additional derivatives of the Gibbs energy are:

$$\left[\frac{\partial(G/T)}{\partial T}\right]_{p,\mathbf{n}} = -\frac{H}{T^2} \tag{2.14}$$

and

$$\left[\frac{\partial(G/T)}{\partial p}\right]_{T,\mathbf{n}} = \frac{V}{T} \tag{2.15}$$

2.2 Equilibrium

Equilibrium in thermodynamics refers to a state of balance between the driving forces of change in the system, so that no macroscopic change is observed. It is an internal state of a system insensitive to small temporary perturbations. Thermodynamic analysis of processes is not concerned about how fast we reach equilibrium, but the feasible limits of the process. Two types of equilibrium on which we focus are:

- phase equilibrium: balance between the transfer of components between different phases (e.g. in a vapor-liquid system, the rate of evaporation is equal to the rate of condensation)
- chemical equilibrium: balance between the transformation of reactants to products and vice versa (rates of forward and backward reaction are equal)

2.2.1 Phase equilibrium

We assume a system consisting of N_P phases in contact that allow exchange of components. From the second law of thermodynamics, when the system attains conditions of thermodynamic equilibrium, entropy has its maximum value. It follows that for two arbitrary phases k and q:

- $T_k = T_q$ (thermal equilibrium)
- $p_k = p_q$ (mechanical equilibrium)
- $\mu_{ik} = \mu_{iq}$, for $i = 1, ..., N_C$ (diffusive equilibrium)

where:

T_k	temperature of phase k
p_k	pressure of phase k

Entropy maximization is not the only criterion for thermodynamic equilibrium. Different conditions in terms of equivalent thermodynamic potentials are shown in Table 2.1 (Michelsen and Mollerup, 2007).

Table 2.1: Thermodynamic equilibrium conditions for closed systems.

Natural variables	State function	Extremum
U, V, $\mathbf{n}$ or H, p, $\mathbf{n}$	S	max
S, V, $\mathbf{n}$	U	min
S, p, $\mathbf{n}$	H	min
T, V, $\mathbf{n}$	A	min
T, p, $\mathbf{n}$	G	min

Chemical potentials are particularly important in equilibrium determination. The differential of the chemical potential of an ideal gas in phase k at constant temperature is given by:

$$d\mu_{ik} = v_{ik}dp = RT\frac{dp}{p} \tag{2.16}$$

where:

v_{ik}	molar volume of component i in phase k
R	gas constant

For non-ideal phases, we introduce fugacities:

$$d\mu_{ik} = \bar{V}_{ik}dp = RT\frac{d\hat{f}_{ik}}{\hat{f}_{ik}} \tag{2.17}$$

After integration:

$$\mu_{ik} = \mu_{ik}^{\circ} + RT \ln \frac{\hat{f}_{ik}}{f_{ik}^{\circ}} \tag{2.18}$$

where:

$\bar{V}_{ik}$	partial molar volume of component i in phase k
μ_{ik}°	reference state chemical potential of component i in phase k
$\hat{f}_{ik}$	fugacity of component i in phase k
f_{ik}°	reference state fugacity of component i in phase k

Diffusive equilibrium is not uniquely expressed in terms of chemical potentials. The equality of chemical potentials at equilibrium results in the fugacity equality in two arbitrary phases k and q:

$$\begin{gathered} \hat{f}_{ik} = \hat{f}_{iq} \\ i = 1, ..., N_C \end{gathered} \tag{2.19}$$

However, the changes of chemical potentials are not independent in a particular phase. The Gibbs-Duhem equation shows the dependence between different chemical potentials in the same phase. If we use Eq. 2.10 and 2.12 for an arbitrary phase k, we have:

$$G_k = \sum_{i=1}^{N_C} \mu_{ik} n_{ik} \tag{2.20}$$

$$dG_k = -S_k dT + V_k dp + \sum_{i=1}^{N_C} \mu_{ik} dn_{ik} \tag{2.21}$$

where:

G_k	Gibbs energy of phase k

By differentiating Eq. 2.20, and subtracting Eq. 2.21, we get:

$$\begin{gathered} \sum_{i=1}^{N_C} n_{ik} d\mu_{ik} = -S_k dT + V_k dp \\ k = 1, ..., N_P \end{gathered} \tag{2.22}$$

At constant temperature and pressure:

$$\begin{aligned} &\sum_{i=1}^{N_C} n_{ik} d\mu_{ik} = 0 \\ &k = 1, ..., N_P \end{aligned} \tag{2.23}$$

It must be underlined, that the above expressions for the Gibbs-Duhem equation are not general. In fact, their application is valid only in systems where the internal energy is given by Eq. 2.3. Nevertheless, this is a reasonable assumption for the purpose of this work.

2.2.2 Chemical equilibrium

Studying chemical equilibrium involves identifying the reactions between the components of a mixture. There are different ways to write the formula of a chemical reaction but a systematic way to represent it is:

$$\nu_1 \mathcal{A}_1 + ... + \nu_{N_C} \mathcal{A}_{N_C} = 0 \tag{2.24}$$

or, for multiple reactions:

$$\begin{aligned} &\sum_{i=1}^{N_C} \nu_{ir} \mathcal{A}_i = 0 \\ &r = 1, ..., N_R \end{aligned} \tag{2.25}$$

where:

$\mathcal{A}_i$	component i in a chemical reaction
ν_{ir}	stoichiometric coefficient of component i in reaction r
N_R	number of independent chemical reactions

Stoichiometric coefficients indicate the number of molecules that take part in a reaction. Values of the stoichiometric coefficients follow this convention:

$$\nu_{ir} \begin{cases} < 0 & i \text{ is a reactant in reaction } r \\ = 0 & i \text{ does not participate in reaction } r \\ > 0 & i \text{ is a product in reaction } r \end{cases} \tag{2.26}$$

Stoichiometric coefficients can be combined in the stoichiometric matrix $\mathbf{N}$, which is a compact way to document all the reactions between the components. It is also common to refer to the total stoichiometric coefficient of reaction r as:

$$\nu_{t,r} = \sum_{i=1}^{N_C} \nu_{ir} \tag{2.27}$$

When $\nu_{t,r} = 0$, there is no change in the total mole numbers due to reaction r. In other words, reactants and products have each the same number of molecules. An essential quantity in reaction analysis is the reaction extent. These are defined to demonstrate the degree of progression of each transformation from reactants to products. For multiple reactions in a single phase:

$$dn_i = \sum_{r=1}^{N_R} \nu_{ir} d\xi_r \tag{2.28}$$

where:
ξ_r extent of reaction r

Despite that an arbitrary component i appears in the definition of Eq. 2.28, the reaction extent does not depend on the component used in its calculation. Positive values imply that the reaction proceeds from reactants to products and negative values from products to reactants. The following example clarifies the essence of the reaction extent. Components $\mathcal{A}$, $\mathcal{B}$ and $\mathcal{C}$ react according to the scheme:

$$\nu_{\mathcal{A}}\mathcal{A} + \nu_{\mathcal{B}}\mathcal{B} \rightleftharpoons \nu_{\mathcal{C}}\mathcal{C} \tag{2.29}$$

If the extent of the above reaction is ξ, then $\nu_{\mathcal{A}}\xi$ moles of $\mathcal{A}$ reacted with $\nu_{\mathcal{B}}\xi$ moles of $\mathcal{B}$ to produce $\nu_{\mathcal{C}}\xi$ moles of $\mathcal{C}$. For multiple phases, Eq. 2.28 becomes:

$$d\left(\sum_{k=1}^{N_P} n_{ik}\right) = \sum_{r=1}^{N_R} \nu_{ir} d\xi_r \tag{2.30}$$

and:

$$\sum_{k=1}^{N_P} n_{ik} = n_{F,i} + \sum_{r=1}^{N_R} \nu_{ir}\xi_r \tag{2.31}$$

or, in matrix-vector form:

$$\sum_{k=1}^{N_P} \mathbf{n}_k = \mathbf{n}_F + \mathbf{N}\boldsymbol{\xi} \tag{2.32}$$

where:

$\mathbf{n}_k$ component abundance vector in phase k
$\mathbf{n}_F$ component abundance vector in the feed
$\mathbf{N}$ stoichiometric matrix
$\boldsymbol{\xi}$ vector of reaction extents
$n_{F,i}$ mole numbers of component i in the feed

The degree to which reactions progress is governed by the chemical equilibrium constants. For reaction r in phase k, the chemical equilibrium constant is defined as:

$$K_{rk}^{\mathrm{eq}} = \exp\left(-\frac{\Delta_r G_{rk}^{\circ}}{RT}\right) = \exp\left(-\frac{\sum_{i=1}^{N_C} \nu_{ir}\mu_{ik}^{\circ}}{RT}\right) = \prod_{i=1}^{N_C}\left(\frac{\hat{f}_{ik}}{f_{ik}^{\circ}}\right)^{\nu_{ir}} \tag{2.33}$$

where:
K_{rk}^{eq} thermodynamic equilibrium constant of reaction r in phase k
$\Delta_r G_{rk}^{\circ}$ reference state Gibbs energy of reaction r in phase k

Since the Gibbs energy is a state function, formation or combustion Gibbs energies of components can be used to calculate the Gibbs energy of reaction:

$$\Delta_r G_{rk}^{\circ} = \sum_{i=1}^{N_C} \nu_{ir}\Delta_f G_{ik}^{\circ} = -\sum_{i=1}^{N_C} \nu_{ir}\Delta_c G_{ik}^{\circ} \tag{2.34}$$

where:
$\Delta_f G_{ik}^{\circ}$ reference state Gibbs energy of formation of component i in phase k
$\Delta_c G_{ik}^{\circ}$ reference state Gibbs energy of combustion of component i in phase k

The chemical equilibrium constant is a function of the same independent variables as the standard state chemical potentials. Therefore, reference state quantities in Eq. 2.33 and 2.34 must correspond to the same temperature and pressure. Derivatives of the chemical equilibrium constant with respect to T and p, combining Eq. 2.33, 2.14 and 2.15, are given by the following relations:

$$\left(\frac{\partial \ln K_{rk}^{\mathrm{eq}}}{\partial T}\right)_p = \frac{\Delta_r H_{rk}^{\circ}}{RT^2} \tag{2.35}$$

with

$$\frac{\partial \Delta_r H_{rk}^{\circ}}{\partial T} = \sum_{i=1}^{N_C} \nu_{ir} C_{p,i}^{\circ} \tag{2.36}$$

and

$$\left(\frac{\partial \ln K_{rk}^{\mathrm{eq}}}{\partial p}\right)_T = -\frac{\Delta_r V_{rk}^{\circ}}{RT} \tag{2.37}$$

where:

$\Delta_r H_{rk}^{\circ}$	reference state enthalpy of reaction r in phase k
$\Delta_r V_{rk}^{\circ}$	reference state volume change of reaction r in phase k
$C_{p,i}^{\circ}$	reference state heat capacity at constant pressure of component i

When the enthalpies of reactions or heat capacities are not known, we can use formation or combustion enthalpies at the same temperature and pressure:

$$\Delta_r H_{rk}^{\circ} = \sum_{i=1}^{N_C} \nu_{ir} \Delta_f H_{ik}^{\circ} = -\sum_{i=1}^{N_C} \nu_{ir} \Delta_c H_{ik}^{\circ} \tag{2.38}$$

Phase equilibrium analysis utilizes the K-values of components. These are essentially distribution coefficients of a component between phase k and a reference phase q:

$$K_{ik} = \frac{x_{ik}}{x_{iq}} \tag{2.39}$$

2.2.3 Types of reference states

To calculate the absolute value of the chemical potential in Eq. 2.18, the reference state must be decided. Convenience of calculations is often the criterion to choose between chemical potential expressions with different reference states. It is important to be consistent with the use of reference states in Eq. 2.18. Two of the most widely used are the ideal gas and the pure component reference state.

- Ideal gas reference state:

$$f_{ik}^{\circ} = p^* \tag{2.40}$$

and

$$\mu_{ik}^{\circ} = \mu_i^*(T, p^*) \tag{2.41}$$

where:

p^*	ideal gas reference pressure
μ_i^*	ideal gas chemical potential of component i

Reference temperature is equal to the system temperature. Reference pressure is usually selected as $p^* = 1$ atm or $p^* = 1$ bar. Originally, it was supposed to refer to unit

fugacity, but at low pressures fugacity and pressure do not differ much. The ideal gas chemical potential depends only on temperature. We select this reference state when a phase is described by an equation of state that provides us with fugacity coefficients, defined as:

$$\hat{\phi}_{ik} \equiv \frac{\hat{f}_{ik}}{x_{ik}p} \tag{2.42}$$

where:
$\hat{\phi}_{ik}$ fugacity coefficient of component i in phase k

Fugacities are calculated from:

$$\hat{f}_{ik} = x_{ik}\hat{\phi}_{ik}p \tag{2.43}$$

and chemical potentials from:

$$\mu_{ik} = \mu_i^* + RT \ln \frac{x_{ik}\hat{\phi}_{ik}p}{p^*} \tag{2.44}$$

- Pure component reference state:

$$f_{ik}^{\circ} = f_{ik}(T, p) \tag{2.45}$$

and

$$\mu_{ik}^{\circ} = \mu_{ik}^{\text{pure}}(T, p) \tag{2.46}$$

where:
f_{ik} fugacity of pure component i in phase k
μ_{ik}^{pure} chemical potential of pure component i in phase k

Reference temperature and pressure are equal to the system temperature and pressure. Reference state chemical potential and pure component fugacity depend on T and p. We select the pure component reference state when a phase is described by an activity coefficient model that provides us with the symmetric activity coefficients, defined as:

$$\gamma_{ik} \equiv \frac{\hat{f}_{ik}}{x_{ik}f_{ik}} \tag{2.47}$$

where:

γ_{ik} symmetric activity coefficient of component i in phase k

Fugacities are calculated from:

$$\hat{f}_{ik} = x_{ik}\gamma_{ik}f_{ik} \tag{2.48}$$

and chemical potentials from:

$$\mu_{ik} = \mu_{ik}^{\text{pure}} + RT\ln(x_{ik}\gamma_{ik}) \tag{2.49}$$

Activity coefficient models usually describe non-ideal liquid phases. The fugacity of the liquid pure component i is expressed as:

$$f_{il} = p_i^s\phi_i^s Pe_i \tag{2.50}$$

where the Poynting effect (Poynting correction) of component i is calculated as:

$$Pe_i = \exp\left(\int_{p_i^s}^{p}\frac{v_{il}}{RT}dp\right) \approx \exp\left[\frac{v_{il}(p-p_i^s)}{RT}\right] \tag{2.51}$$

where:

p_i^s vapor pressure of component i

ϕ_i^s saturation fugacity coefficient of component i

v_{il} molar volume of component i in the liquid phase

The pure component reference state introduces the activity, which shows the deviation of the fugacity from the pure component fugacity. Activity is defined from the expression:

$$\alpha_{ik} \equiv \frac{\hat{f}_{ik}}{f_{ik}} \tag{2.52}$$

where:

α_{ik} activity of component i in phase k

Therefore, an alternative equation for the chemical potential calculation is:

$$\mu_{ik} = \mu_{ik}^{\text{pure}} + RT\ln\alpha_{ik} \tag{2.53}$$

When we account for non-ideality through fugacity coefficients for vapor and liquid phases,

we follow the ϕ-ϕ approach, whereas when an activity coefficient model is used for the liquid phases, we follow the γ-ϕ approach. In case there is a need to change between these two reference states we can use the following equation:

$$\mu_i^* - \mu_{ik}^{\text{pure}} = RT \ln \frac{p^*}{f_{ik}} \tag{2.54}$$

When using an activity coefficient model, an equivalent fugacity coefficient can be calculated by:

$$\hat{\phi}_{ik} = \frac{\gamma_{ik} f_{ik}}{p} \tag{2.55}$$

As a result, derivatives of fugacity and activity coefficients are equal when they refer to the same phase:

$$\left(\frac{\partial \ln \gamma_{ik}}{\partial n_{qk}}\right)_{T,p} = \left(\frac{\partial \ln \hat{\phi}_{ik}}{\partial n_{qk}}\right)_{T,p} \qquad i,q = 1,...,N_C \qquad k = 1,...,N_P \tag{2.56}$$

We define the symmetric matrix of mole number derivatives of fugacity coefficients:

$$\Phi_{iqk} = \left(\frac{\partial \ln \hat{\phi}_{ik}}{\partial n_{qk}}\right)_{T,p} \qquad k = 1,...,N_P \tag{2.57}$$

where

$$\Phi_{iqk} = \Phi_{qik} \qquad i,q = 1,...,N_C \qquad k = 1,...,N_P \tag{2.58}$$

The Gibbs-Duhem equation (Eq. 2.23) can also be expressed in terms of the fugacity coefficients:

$$\sum_{i=1}^{N_C} n_{ik} \left(\frac{\partial \mu_{ik}}{\partial n_{qk}}\right)_{T,p} = \sum_{i=1}^{N_C} n_{ik} \left(\frac{\partial \ln \hat{\phi}_{ik}}{\partial n_{qk}}\right)_{T,p} = \sum_{i=1}^{N_C} n_{ik} \Phi_{iqk} = 0 \qquad q = 1,...,N_C \qquad k = 1,...,N_P \tag{2.59}$$

or

$$\begin{gathered}\mathbf{\Phi}_k \mathbf{n}_k = \mathbf{0} \\ k = 1, ..., N_P\end{gathered} \tag{2.60}$$

The selection of the reference state has an effect on the dependence of the chemical equilibrium constant on T and p (Eq. 2.33). The ideal gas reference state renders the chemical equilibrium constant only temperature dependent. However, even if the pure component reference state is chosen and the resulting chemical equilibrium constant becomes pressure dependent, pressure effect is usually assumed minor at lower pressures (Eq. 2.37, $\Delta_r V^\circ_{rk} \approx 0$).

Finally, ideal behavior of vapor and liquid phases refers to composition independent fugacity or activity coefficients. More specifically, fugacity coefficients for ideal gases and activity coefficients for ideal liquids are equal to 1. Ideal vapor fugacity and chemical potential is given by:

$$\hat{f}_{ik} = x_{ik} p = p_i \tag{2.61}$$

and

$$\mu_{ik} = \mu_i^* + RT \ln \frac{x_{ik} p}{p^*} \tag{2.62}$$

where:

p_i partial pressure of component i

For ideal liquid we have:

$$\hat{f}_{ik} = x_{ik} f_{ik} \tag{2.63}$$

and

$$\mu_{ik} = \mu_{ik}^{\text{pure}} + RT \ln x_{ik} \tag{2.64}$$

At low pressures in liquid phases:

$$f_{ik} \approx p_i^s \tag{2.65}$$

Therefore, the K-value (Eq. 2.39) of an ideal vapor-liquid system at low pressures is (Raoult's law):

$$K_i = \frac{x_{iv}}{x_{il}} = \frac{p_i^s}{p} \tag{2.66}$$

A generalized K-value correlation of T_c, p_c and ω is the Wilson K-factor expression:

$$K_{W,i} = \frac{p_{c,i}}{p} \exp\left[5.373(1+\omega_i)\left(\frac{T_{c,i}}{T}\right)\right] \tag{2.67}$$

where:

$T_{c,i}$	critical temperature of component i
$p_{c,i}$	critical pressure of component i
ω_i	acentric factor of component i

The Wilson K-factors do not yield accurate results for polar components. They are usually preferred to initialize a non-ideal multicomponent flash procedure.

CHAPTER

3

Calculation of chemical and phase equilibrium

The first attempts to calculate simultaneous chemical and phase equilibrium were concerned with the solution of the algebraic equations valid at equilibrium. These are the relations that hold at the minimum of the Gibbs energy at constant temperature and pressure. For instance, in the early work of Brinkley (1946, 1947) the material balance is solved, ensuring that the sum of mole fractions in each phase is 1 and chemical potentials are equal. However, convergence of such an approach is not guaranteed because monitoring the Gibbs energy between iterations is not feasible.

An alternative route to the CPE solution is the direct minimization of the total Gibbs energy of a closed system at specified temperature and pressure. In contrast to solving algebraic equations, minimizing the Gibbs energy could allow monitoring of its value. It is possible then to conclude if the current iteration produced an acceptable direction, namely a descent direction pointing to the minimum. In the following sections stoichiometric and non-stoichiometric minimization methods are explained, with the focus on the non-stoichiometric approach. Finally, two non-stoichiometric calculation procedures are proposed, which are integrated in full algorithms with initialization of computations and stability analysis to confirm that the global minimum of the Gibbs energy is found.

3.1 Gibbs energy minimization

According to Smith and Missen (1982), minimization methods in chemical and phase equilibrium are divided into stoichiometric and non-stoichiometric based on the way the minimization is formulated. A common constraint of both formulations is that mole numbers cannot be negative. In general, algorithms do not account for this constraint explicitly in the derivation of the working equations and employ different checks that attempt to satisfy it internally.

3.1.1 Stoichiometric formulation

In stoichiometric methods, mole numbers are expressed as functions of the reaction extents, defined in Eq. 2.30. The Gibbs energy is then minimized with respect to the reaction extents:

$$\begin{aligned} &\min_{\boldsymbol{\xi}} G(T,p,\boldsymbol{\xi}) \\ \text{s.t.} \quad & n_{ik} \geq 0, \quad i = 1,...,N_C \qquad k = 1,...,N_P \end{aligned} \tag{3.1}$$

At the minimum, the equilibrium conditions are:

$$\frac{\partial G}{\partial \xi_r} = \sum_{k=1}^{N_P}\sum_{i=1}^{N_C} \frac{\partial G}{\partial n_{ik}} \frac{\partial n_{ik}}{\partial \xi_r} = \sum_{i=1}^{N_C} \mu_{ik} \frac{\partial \sum_{k=1}^{N_P} n_{ik}}{\partial \xi_r} \tag{3.2}$$

or

$$\begin{aligned} &\sum_{i=1}^{N_C} \nu_{ir}\mu_{ik} = 0 \\ &k = 1,...,N_P \end{aligned} \tag{3.3}$$

Disregarding the non-negativity constraints, the above problem is essentially an unconstrained minimization. The conventional approach involves nested loop calculations, solving phase equilibrium in the inner loop and updating the reaction extents in the outer loop. The work of Sanderson and Chien (1973) applies such a successive substitution-based method on reaction systems. This independent treatment of the two phenomena allows chemical equilibrium to be coupled with an existing reliable multiphase flash code. Nevertheless, in spite of their simple implementation, nested loop schemes are not expected to be very efficient.

The only second-order stoichiometric method we could find in the literature for non-ideal mixtures was presented by Castier et al. (1989). The authors applied successive substitution with acceleration as initialization, and the second-order calculations were used for final convergence. Castier et al. (1989) account simultaneously for reactions through the extents and for phase separation through the yield factors:

$$\begin{aligned} &\theta_{ik} = \frac{n_{ik}}{\sum_{q=1}^{N_C} n_{qk}} \\ &i = 1,...,N_C \qquad k = 1,...,N_P \end{aligned} \tag{3.4}$$

Stoichiometric formulation is advantageous when the number of independent chemical reactions is small (Michelsen and Mollerup, 2007). On the other hand, the main limitations

are initialization problems and susceptibility to round-off errors. To overcome round-off errors, an "optimum" basis of components can be selected, the primary components, which are the most abundant in the system (Michelsen and Mollerup, 2007). The rest of the components are called secondary and their mole numbers can be expressed as a function of the primary components. It is possible that primary components are the same at every iteration. If at the current estimate a previously secondary component becomes more abundant than a primary, the former should be included in the basis at the expense of the later. Various publications have studied how to select the proper basis (Brinkley, 1946, 1947; Prigogine and Defay, 1947; Schott, 1964).

3.1.2 Non-stoichiometric formulation

Components are not independent in reaction systems. Reactions dictate the relations between different components. At the same time, it is implied that the later are being produced or depleted. As a result, the material balance cannot be expressed in terms of component mole numbers. A new basis must be selected consisting of the independent entities, called elements. Elements usually represent building blocks of components and they can be single chemical elements or even groups of atoms. Isomers, although sharing the same chemical composition, must be "composed" by separate elements. Provided that there are no additional stoichiometric constraints and we choose a set of linearly independent reactions (Appendix B):

$$N_E = N_C - N_R \tag{3.5}$$

where:

N_E number of elements

Non-stoichiometric methods do not take into account the reactions in a direct way. The Gibbs energy is minimized under material balance constraints, which are expressed in terms of elements:

$$\begin{aligned} & \min_{\mathbf{n}} G(T,p,\mathbf{n}) = \min_{n_{ik}} \sum_{k=1}^{N_P} \sum_{i=1}^{N_C} n_{ik}\mu_{ik}(T,p,\mathbf{n}_k) \\ \text{s.t.} \quad & \sum_{k=1}^{N_P} \sum_{i=1}^{N_C} A_{ji} n_{ik} = b_j, \quad j = 1,...,N_E \\ & n_{ik} \geq 0, \quad i = 1,...,N_C \qquad k = 1,...,N_P \end{aligned} \tag{3.6}$$

where:

A_{ji} number of elements j in the chemical formula of component i

b_j total mole numbers of element j

More conveniently, the material balance in matrix-vector form is:

$$\mathbf{A}\sum_{k=1}^{N_P}\mathbf{n}_k = \mathbf{b} \tag{3.7}$$

where:

$\mathbf{A}$	formula matrix
$\mathbf{b}$	element abundance vector

The material balance constraint must be valid at all times and is independent of the reaction progress. It must be satisfied by the feed, unstable intermediate phase configurations or the equilibrium solution. The element abundance vector is constant and can be calculated by the feed:

$$\begin{gathered} b_j = \sum_{i=1}^{N_C} A_{ji} n_{F,i} = n_{t,F} \sum_{i=1}^{N_C} A_{ji} z_i \\ j = 1, ..., N_E \end{gathered} \tag{3.8}$$

or

$$\mathbf{b} = \mathbf{A}\mathbf{n}_F = n_{t,F}\mathbf{A}\mathbf{z} \tag{3.9}$$

where:

$\mathbf{n}_F$	component abundance vector in the feed
$\mathbf{z}$	vector of mole fractions in the feed
$n_{t,F}$	total mole numbers in the feed
z_i	mole fraction of component i in the feed

It might be preferable to present the distribution of elements in different phases instead of components. The following quantities are defined:

$$\mathbf{B}_k = \mathbf{A}\mathbf{n}_k \tag{3.10}$$

or collectively in a matrix:

$$\mathbf{B} = \mathbf{A}\mathbf{n} \tag{3.11}$$

Similar to component mole fractions, we have the element mole fractions:

$$x_{jk}^{\mathrm{el}} = \frac{B_{jk}}{\sum_{q=1}^{N_E} B_{qk}} \qquad k = 1, ..., N_P \tag{3.12}$$

where:

$\mathbf{B}_k$	element abundance vector in phase k
$\mathbf{B}$	element abundance matrix
B_{jk}	total mole numbers of element j in phase k
x_{jk}^{el}	mole fraction of element j in phase k

When working with non-stoichiometric methods, we define the Lagrangian of the function to eliminate the constraints. For convenience, we decided to minimize the reduced Gibbs energy $G/(RT)$, since it shares its minimizer with the Gibbs energy at constant temperature. The Lagrangian is given by:

$$\mathcal{L}(\mathbf{n}, \boldsymbol{\lambda}) = \sum_{k=1}^{N_P} \sum_{i=1}^{N_C} \frac{n_{ik}\mu_{ik}}{RT} - \sum_{j=1}^{N_E} \lambda_j \left(\sum_{k=1}^{N_P} \sum_{i=1}^{N_C} A_{ji} n_{ik} - b_j \right) \tag{3.13}$$

where:

$\boldsymbol{\lambda}$	vector of Lagrange multipliers
λ_j	Lagrange multiplier of element j

The equilibrium solution is a stationary point of the Lagrangian. Derivatives with respect to mole numbers and Lagrange multipliers must satisfy:

$$\frac{\partial \mathcal{L}}{\partial n_{ik}} = \frac{\mu_{ik}}{RT} - \sum_{j=1}^{N_E} A_{ji}\lambda_j = 0 \qquad i = 1, ..., N_C \qquad k = 1, ..., N_P \tag{3.14}$$

and

$$\frac{\partial \mathcal{L}}{\partial \lambda_j} = -\sum_{k=1}^{N_P} \sum_{i=1}^{N_C} A_{ji} n_{ik} + b_j = 0 \qquad j = 1, ..., N_E \tag{3.15}$$

The optimization theory concludes that Lagrange multipliers indicate how sensitive the solution is to the constraints. From Eq. 3.14 we get:

$$\begin{aligned}\frac{G_{\min}}{RT} &= \sum_{k=1}^{N_P}\sum_{i=1}^{N_C}\frac{n_{ik}\mu_{ik}}{RT} = \sum_{k=1}^{N_P}\sum_{i=1}^{N_C} n_{ik}\sum_{j=1}^{N_E} A_{ji}\lambda_j = \\ &= \sum_{j=1}^{N_E}\lambda_j\sum_{k=1}^{N_P}\sum_{i=1}^{N_C} A_{ji}n_{ik} = \sum_{j=1}^{N_E} b_j\lambda_j = \mathbf{b}^{\mathrm{T}}\boldsymbol{\lambda}\end{aligned} \tag{3.16}$$

and

$$\left(\frac{\partial}{\partial b_j}\frac{G_{\min}}{RT}\right)_{T,p,b_{q\neq j}} = \lambda_j \tag{3.17}$$

From the perspective of Eq. 3.16, Eq. 3.14 shows that the Lagrange multipliers represent the reduced chemical potentials of the elements at equilibrium (Michelsen and Mollerup, 2007). Eq. 3.15 is simply the constraint of the minimization. It should be stressed and clarified that the reduced Gibbs energy is minimized, not the Lagrangian. The minimum of the reduced Gibbs energy corresponds to a saddle point of the Lagrangian.

Stoichiometric and non-stoichiometric methods perform the same minimization in different ways. The link they share is established between the characteristic matrices of each method: the stoichiometric matrix $\mathbf{N}$ for stoichiometric methods and the formula matrix $\mathbf{A}$ for non-stoichiometric methods. Multiplying Eq. 2.32 with $\mathbf{A}$ from the left, we have:

$$\mathbf{A}\sum_{k=1}^{N_P}\mathbf{n}_k = \mathbf{A}\mathbf{n}_F + \mathbf{A}\mathbf{N}\boldsymbol{\xi} \tag{3.18}$$

Using Eq. 3.7 and 3.9, we get:

$$\mathbf{A}\mathbf{N}\boldsymbol{\xi} = \mathbf{0} \tag{3.19}$$

Assuming that at least one of the reactions progresses to some extent, there is at least one non-zero ξ_q. Therefore, for Eq. 3.19 to be valid for any $\boldsymbol{\xi}$:

$$\mathbf{A}\mathbf{N} = \mathbf{0} \tag{3.20}$$

Eq. 3.20 shows that we need to know only one of the matrices $\mathbf{A}$ or $\mathbf{N}$ to calculate the other. If the elements are selected, there can be found a consistent set of independent chemical reactions and vice versa (Appendix D). A similar comment can be found in Smith and Missen (1982). The solution of Eq. 3.20 for one of the two matrices is not unique.

3.1.3 Stability analysis

For a fixed number of phases, it might be possible to find the minimum Gibbs energy of the system. Nevertheless, a different number of phases could result in lower Gibbs energy. In other words, we might have determined a local minimum if the number of phases is allowed to change (formation or disappearance of phases). Only the global minimum of the Gibbs energy is the actual equilibrium solution. Stability analysis investigates whether additional phases should be considered to further decrease the Gibbs energy. If this is the case, our current phase set is unstable. The method used in this work was presented by Michelsen (1982) and later in Michelsen and Mollerup (2007). We check the stability of a feed phase with composition $\mathbf{z}$ and total mole numbers n_t. Its Gibbs energy is:

$$G_f = n_t \sum_{i=1}^{N_C} z_i \mu_i(\mathbf{z}) \tag{3.21}$$

The feed phase is separated into two phases. The Gibbs energy of the new phase with composition $\mathbf{w}$ and infinitesimal total mole numbers ϵ is:

$$G(\epsilon) = \epsilon \sum_{i=1}^{N_C} w_i \mu_i(\mathbf{w}) \tag{3.22}$$

The total change of the Gibbs energy for this process is:

$$\Delta G = G(n_t - \epsilon) + G(\epsilon) - G_f \tag{3.23}$$

The first term can be approximated with the Taylor expansion around the feed:

$$G(n_t - \epsilon) = G(n_t) - \epsilon \sum_{i=1}^{N_C} w_i \left(\frac{\partial G}{\partial n_i} \right)_{n_t} = G_f - \epsilon \sum_{i=1}^{N_C} w_i \mu_i(\mathbf{z}) \tag{3.24}$$

Finally, Eq. 3.23 becomes:

$$\Delta G = \epsilon \sum_{i=1}^{N_C} w_i \left[\mu_i(\mathbf{w}) - \mu_i(\mathbf{z}) \right] \tag{3.25}$$

For a spontaneous phase split, ΔG must be negative. Two equivalent functions can be defined, the tangent plane distance function:

$$TPD(\mathbf{w}) = \sum_{i=1}^{N_C} w_i \left[\mu_i(\mathbf{w}) - \mu_i(\mathbf{z}) \right] \tag{3.26}$$

and the reduced tangent plane distance function:

$$tpd(\mathbf{w}) = \frac{TPD(\mathbf{w})}{RT} = \sum_{i=1}^{N_C} w_i \left[\ln w_i + \ln \hat{\phi}_i(\mathbf{w}) - \ln z_i - \ln \hat{\phi}_i(\mathbf{z})\right] \tag{3.27}$$

The function used in Michelsen (1982) is a modified tangent plane distance function with mole numbers W_i as variables:

$$tm(\mathbf{W}) = 1 + \sum_{i=1}^{N_C} W_i \left[\ln W_i + \ln \hat{\phi}_i(\mathbf{W}) - \ln z_i - \ln \hat{\phi}_i(\mathbf{z}) - 1\right] \tag{3.28}$$

Negative values of tm indicate an unstable feed phase. Although instability can be identified by finding the minima of the above function (Michelsen, 1982; Michelsen and Mollerup, 2007), there is no need to fully converge to a minimum. If a negative tm is found during the search, the phase split will occur. Mole fractions of the trial phase can be then found as:

$$w_i = \frac{W_i}{\sum_{q=1}^{N_C} W_q} \tag{3.29}$$

In case of a multiphase system, stability is essentially the same as for a two-phase system. Any phase can be used to test the overall stability, since:

$$\begin{gathered} \mu_{ik} = \mu_{iq} \\ i = 1, ..., N_C \qquad \forall\ k \neq q \end{gathered} \tag{3.30}$$

However, initialization of this minimization for multiphase calculations requires special care (Michelsen, 1982; Michelsen and Mollerup, 2007). Suitable initial estimates must be chosen to ensure that no minimum is overlooked.

3.2 Non-stoichiometric methods for CPE calculations

3.2.1 Lagrange multipliers method[†]

Eq. 3.14 and 3.15 define a system of $N_C N_P + N_E$ equations for $N_C N_P$ unknown mole numbers n_{ik} and N_E unknown Lagrange multipliers λ_j. In practice reaction mixtures involve many components and consequently the dimensions of the system can be large.

[†]Appears in Tsanas et al. (2017b)

Instead of solving directly the Lagrangian conditions for all n_{ik} and λ_j, we introduce mole fractions and phase amounts:

$$n_{ik} = x_{ik} n_{t,k} \tag{3.31}$$

where:

x_{ik}	mole fraction of component i in phase k
$n_{t,k}$	amount of phase k

Substitution of Eq. 3.31 in Eq. 3.15, gives:

$$\begin{gathered} F_j^A = \sum_{k=1}^{N_P} n_{t,k} \sum_{i=1}^{N_C} A_{ji} x_{ik} - b_j = 0 \\ j = 1, ..., N_E \end{gathered} \tag{3.32}$$

Mole fractions in each phase must also satisfy:

$$\begin{gathered} F_k^B = \sum_{i=1}^{N_C} x_{ik} - 1 = 0 \\ k = 1, ..., N_P \end{gathered} \tag{3.33}$$

Mole fractions appearing in 3.32 and 3.33 can be further expressed as functions of the Lagrange multipliers. From Eq. 3.14:

$$\ln x_{ik} = \sum_{j=1}^{N_E} A_{ji} \lambda_j - \frac{\mu_{ik}^\circ}{RT} - \ln \frac{\hat{\phi}_{ik} p}{f_{ik}^\circ} \tag{3.34}$$

For the ideal gas reference state, Eq. 3.34 becomes:

$$\ln x_{ik} = \sum_{j=1}^{N_E} A_{ji} \lambda_j - \frac{\mu_i^*}{RT} - \ln \frac{\hat{\phi}_{ik} p}{p^*} \tag{3.35}$$

and for the pure component reference state:

$$\ln x_{ik} = \sum_{j=1}^{N_E} A_{ji} \lambda_j - \frac{\mu_{ik}^{\text{pure}}}{RT} - \ln \gamma_{ik} \tag{3.36}$$

The working equations of the Lagrange multipliers method are given by Eq. 3.32 and 3.33. Independent variables are $\boldsymbol{\lambda}$ and $\mathbf{n}_t$, which are roots of function $\mathbf{F}$ at equilibrium:

$$\mathbf{F}(\boldsymbol{\lambda}, \mathbf{n}_t) = \begin{bmatrix} \mathbf{F}^A \\ \mathbf{F}^B \end{bmatrix} \tag{3.37}$$

where:

$\mathbf{n}_t$ phase amount vector

The system of equations is solved with Newton's method. Derivatives of x_{ik} with respect to the independent variables are required to find the Jacobian of $\mathbf{F}$. Whenever we use the Jacobian in calculations, we assume that the fugacity or activity coefficients are constant (ideal system approximation). As a result, differentiation of Eq. 3.34 gives:

$$\begin{aligned} \frac{\partial x_{ik}}{\partial \lambda_q} &= A_{qi} x_{ik} \\ q &= 1, ..., N_E \end{aligned} \tag{3.38}$$

and

$$\begin{aligned} \frac{\partial x_{ik}}{\partial n_{t,q}} &= 0 \\ q &= 1, ..., N_P \end{aligned} \tag{3.39}$$

The Jacobian matrix of function $\mathbf{F}$ has the form:

$$\mathbf{J}(\boldsymbol{\lambda}, \mathbf{n}_t) = \begin{bmatrix} \mathbf{J}^A & \mathbf{J}^B \\ \mathbf{J}^C & \mathbf{J}^D \end{bmatrix} \tag{3.40}$$

where:

$$\begin{aligned} J^A_{jq} = \frac{\partial F^A_j}{\partial \lambda_q} &= \sum_{k=1}^{N_P} n_{t,k} \sum_{i=1}^{N_C} A_{ji} A_{qi} x_{ik} \\ j = 1, ..., N_E \qquad & q = 1, ..., N_E \end{aligned} \tag{3.41}$$

$$\begin{aligned} J^B_{jq} = \frac{\partial F^A_j}{\partial n_{t,q}} &= \sum_{i=1}^{N_C} A_{ji} x_{iq} \\ j = 1, ..., N_E \qquad & q = 1, ..., N_P \end{aligned} \tag{3.42}$$

$$\begin{aligned} J^C_{kq} = \frac{\partial F^B_k}{\partial \lambda_q} &= \sum_{i=1}^{N_C} A_{qi} x_{ik} = J^B_{qk} \\ k = 1, ..., N_P \qquad & q = 1, ..., N_E \end{aligned} \tag{3.43}$$

$$J_{kq}^{D} = \frac{\partial F_k^B}{\partial n_{t,q}} = 0 \qquad k = 1, ..., N_P \qquad q = 1, ..., N_P \tag{3.44}$$

Finally, the system of equations in the Lagrange multipliers method is:

$$\mathbf{J} \begin{bmatrix} \Delta\boldsymbol{\lambda} \\ \Delta\mathbf{n}_t \end{bmatrix} = -\mathbf{F} \tag{3.45}$$

or

$$\begin{bmatrix} \mathbf{A}\,\mathrm{diag}\left(\sum_{k=1}^{N_P}\mathbf{n}_k\right)\mathbf{A}^{\mathrm{T}} & \mathbf{Ax} \\ (\mathbf{Ax})^{\mathrm{T}} & \mathbf{0} \end{bmatrix} \begin{bmatrix} \Delta\boldsymbol{\lambda} \\ \Delta\mathbf{n}_t \end{bmatrix} = - \begin{bmatrix} \mathbf{A}\sum_{k=1}^{N_P}\mathbf{n}_k - \mathbf{b} \\ \mathbf{x}^{\mathrm{T}}\mathbf{e}_{N_C} - \mathbf{e}_{N_P} \end{bmatrix} \tag{3.46}$$

where:

$\mathbf{e}_X$ vector of ones with dimensions $X \times 1$

The Lagrange multipliers method is based on the work of Michelsen (1989). If the system is ideal, the solution of Eq. 3.46 is the equilibrium solution. Conversely, when we are dealing with non-ideal systems, a nested loop procedure is required: the solution of Eq. 3.46 in the inner loop must be used to update the values of the fugacity or activity coefficients in the outer loop, continuing until the update is smaller than a tolerance.

3.2.2 The modified RAND method[†]

The RAND method was originally proposed by White et al. (1958) only for single-phase ideal gases, with $N_E + 1$ working equations. Boynton (1960) calculated multiphase ideal system equilibrium with $N_E + N_P$ equations and suggested extension to non-ideal calculations using the ideal system approximation: a nested loop scheme with constant fugacity or activity coefficients in the inner loop and non-ideality updates in the outer loop. Smith and Missen (1982) showed calculations for ideal multiphase systems, mentioning the RAND method in the algorithm group "BNR" (Brinkley-NASA-RAND). They discussed application in non-ideal mixtures and provided N_C linearized equilibrium equations for a single phase, but did not comment on how the equations should be solved. For the multiphase case, this strategy would result in $N_C N_P + N_E$ equations.

Different authors applied the RAND method to non-ideal mixtures with the ideal system approximation (Gautam and Seider, 1979a,b,c; White and Seider, 1981; Voňka and Leitner, 1995) but this approach does not exhibit quadratic convergence. A second-order non-ideal RAND formulation for multiple phases was published by Greiner (1991) with $N_E + N_P$

[†]Appears in Tsanas et al. (2017a)

equations, but no calculations for reaction systems were included in his work. Michelsen and Mollerup (2007) presented in brief a modified formulation, preserving the same number of equations as in Greiner (1991). Paterson et al. (2017) showed RAND based formulations for TP and TV thermodynamics, titled modified and vol-RAND respectively, intended for phase equilibrium calculations. In this work the modified RAND is presented based on the extension of the original RAND to the general case of non-ideal multiple phases. The modified RAND method is faster and more reliable than implementations based on the ideal system approximation. Eq. 3.14 can be linearized around the estimate of mole numbers:

$$\begin{gathered}\frac{\mu_{ik}}{RT}+\sum_{q=1}^{N_C}\frac{\partial}{\partial n_{qk}}\left(\frac{\mu_{ik}}{RT}\right)_{T,p}\Delta n_{qk}-\sum_{j=1}^{N_E}\lambda_j A_{ji}=0\\ i=1,...,N_C \qquad k=1,...,N_P\end{gathered} \tag{3.47}$$

Mole number derivatives of the chemical potentials are calculated as:

$$\frac{\partial}{\partial n_{qk}}\left(\frac{\mu_{ik}}{RT}\right)_{T,p}=\frac{\delta_{iq}}{n_{ik}}-\frac{1}{n_{t,k}}+\left(\frac{\partial \ln\hat{\phi}_{ik}}{\partial n_{qk}}\right)_{T,p} \tag{3.48}$$

where:

δ_{ij} Kronecker delta

If an activity coefficient model is used for a liquid phase, derivatives of the activity coefficients are equivalent, as shown in Eq. 2.56. Corrections to the mole numbers Δn_{ik} must be isolated. According to the Gibbs-Duhem equation, the matrix of the mole number derivatives of the chemical potentials in a specific phase is singular and therefore not invertible (Eq. 2.59 and 2.60). We define the following:

$$M_{iqk}=\frac{\delta_{iq}}{n_{ik}}+\left(\frac{\partial \ln\hat{\phi}_{ik}}{\partial n_{qk}}\right)_{T,p}=\frac{\delta_{iq}}{n_{ik}}+\Phi_{iqk} \tag{3.49}$$

and

$$s_k=\frac{\sum_{i=1}^{N_C}\Delta n_{ik}}{n_{t,k}}=\frac{\Delta n_{t,k}}{n_{t,k}}=\frac{\Delta n_{t,k}}{\mathbf{e}_{N_C}^{\mathrm{T}}\mathbf{n}_k} \tag{3.50}$$

The matrix-vector form of Eq. 3.47 for different phases is:

$$\begin{gathered}\frac{\boldsymbol{\mu}_k}{RT}+\mathbf{M}_k\Delta\mathbf{n}_k-s_k\mathbf{e}_{N_C}-\mathbf{A}^{\mathrm{T}}\boldsymbol{\lambda}=0\\ k=1,...,N_P\end{gathered} \tag{3.51}$$

where:

$\boldsymbol{\mu}_k$	vector of chemical potentials in phase k
s_k	correction for the amount of phase k

Corrections to the component abundance vectors are given by:

$$\begin{gathered}\Delta\mathbf{n}_k = \mathbf{M}_k^{-1}\mathbf{e}_{N_C}s_k + \mathbf{M}_k^{-1}\left(\mathbf{A}^{\mathrm{T}}\boldsymbol{\lambda} - \frac{\boldsymbol{\mu}_k}{RT}\right) \\ k = 1, ..., N_P\end{gathered} \tag{3.52}$$

From the definition of matrix $\mathbf{M}_k$ (Eq. 3.49), we have:

$$\begin{gathered}\mathbf{M}_k\mathbf{n}_k = \mathbf{e}_{N_C} + \boldsymbol{\Phi}_k\mathbf{n}_k \\ k = 1, ..., N_P\end{gathered} \tag{3.53}$$

From Eq. 2.59, Eq. 3.53 becomes:

$$\begin{gathered}\mathbf{M}_k\mathbf{n}_k = \mathbf{e}_{N_C} \\ k = 1, ..., N_P\end{gathered} \tag{3.54}$$

and by inverting matrix $\mathbf{M}_k$:

$$\begin{gathered}\mathbf{n}_k = \mathbf{M}_k^{-1}\mathbf{e}_{N_C} \\ k = 1, ..., N_P\end{gathered} \tag{3.55}$$

Substituting Eq. 3.55 in Eq. 3.52:

$$\begin{gathered}\Delta\mathbf{n}_k = \mathbf{n}_k s_k + \mathbf{M}_k^{-1}\left(\mathbf{A}^{\mathrm{T}}\boldsymbol{\lambda} - \frac{\boldsymbol{\mu}_k}{RT}\right) \\ k = 1, ..., N_P\end{gathered} \tag{3.56}$$

Linearizing Eq. 3.7 around the estimate of mole numbers, we obtain:

$$\mathbf{A}\sum_{k=1}^{N_P}(\mathbf{n}_k + \Delta\mathbf{n}_k) = \mathbf{b} \tag{3.57}$$

or

$$\mathbf{A}\sum_{k=1}^{N_P}\Delta\mathbf{n}_k = \mathbf{b} - \sum_{k=1}^{N_P}\mathbf{B}_k \tag{3.58}$$

We define:

$$\Delta \mathbf{b} \equiv \mathbf{b} - \sum_{k=1}^{N_P} \mathbf{B}_k \tag{3.59}$$

If the mole numbers satisfy the material balance, $\Delta \mathbf{b}$ is equal to zero. There are two conditions the correction vectors $\Delta \mathbf{n}_k$ must meet:

$$\mathbf{A} \sum_{k=1}^{N_P} \Delta \mathbf{n}_k = \Delta \mathbf{b} \tag{3.60}$$

and

$$\begin{gathered} \mathbf{e}_{N_C}^{\mathrm{T}} \Delta \mathbf{n}_k = \Delta n_{t,k} \\ k = 1, ..., N_P \end{gathered} \tag{3.61}$$

Substitution of Eq. 3.56 in Eq. 3.60 results in:

$$\mathbf{A} \sum_{k=1}^{N_P} \mathbf{n}_k s_k + \mathbf{A} \sum_{k=1}^{N_P} \mathbf{M}_k^{-1} \mathbf{A}^{\mathrm{T}} \boldsymbol{\lambda} - \mathbf{A} \sum_{k=1}^{N_P} \mathbf{M}_k^{-1} \frac{\boldsymbol{\mu}_k}{RT} = \Delta \mathbf{b} \tag{3.62}$$

or

$$\left(\mathbf{A} \sum_{k=1}^{N_P} \mathbf{M}_k^{-1} \mathbf{A}^{\mathrm{T}} \right) \boldsymbol{\lambda} + \mathbf{B}\mathbf{s} = \mathbf{A} \sum_{k=1}^{N_P} \mathbf{M}_k^{-1} \frac{\boldsymbol{\mu}_k}{RT} + \Delta \mathbf{b} \tag{3.63}$$

where:

$\mathbf{s}$ phase amount correction vector

Substitution of Eq. 3.56 in Eq. 3.61 results in:

$$\begin{gathered} \mathbf{e}_{N_C}^{\mathrm{T}} \mathbf{n}_k s_k + \mathbf{e}_{N_C}^{\mathrm{T}} \mathbf{M}_k^{-1} \left(\mathbf{A}^{\mathrm{T}} \boldsymbol{\lambda} - \frac{\boldsymbol{\mu}_k}{RT} \right) = \Delta n_{t,k} \\ k = 1, ..., N_P \end{gathered} \tag{3.64}$$

Matrix $\mathbf{M}_k$ is symmetric (Eq. 2.58), therefore, when we take the transpose of Eq. 3.55:

$$\begin{gathered} \mathbf{n}_k^{\mathrm{T}} = \mathbf{e}_{N_C}^{\mathrm{T}} \mathbf{M}_k^{-1} \\ k = 1, ..., N_P \end{gathered} \tag{3.65}$$

Combining Eq. 3.50 with 3.65 and substituting them in Eq. 3.64 gives:

$$\begin{gathered} \mathbf{n}_k^{\mathrm{T}} \left(\mathbf{A}^{\mathrm{T}} \boldsymbol{\lambda} - \frac{\boldsymbol{\mu}_k}{RT} \right) = 0 \\ k = 1, ..., N_P \end{gathered} \tag{3.66}$$

or

$$\begin{gathered} \mathbf{B}_k^{\mathrm{T}} \boldsymbol{\lambda} = \frac{\mathbf{n}_k^{\mathrm{T}} \boldsymbol{\mu}_k}{RT} \\ k = 1, ..., N_P \end{gathered} \tag{3.67}$$

Finally, the modified RAND method for non-ideal multiphase mixtures requires solving the system of Eq. 3.63 and Eq. 3.67:

$$\begin{bmatrix} \mathbf{A} \sum_{k=1}^{N_P} \mathbf{M}_k^{-1} \mathbf{A}^{\mathrm{T}} & \mathbf{B} \\ \mathbf{B}^{\mathrm{T}} & \mathbf{0} \end{bmatrix} \begin{bmatrix} \boldsymbol{\lambda} \\ \mathbf{s} \end{bmatrix} = \begin{bmatrix} \mathbf{A} \sum_{k=1}^{N_P} \mathbf{M}_k^{-1} (\boldsymbol{\mu}_k / RT) + \Delta \mathbf{b} \\ \mathbf{d} \end{bmatrix} \tag{3.68}$$

where:

$$d_k = \frac{\mathbf{n}_k^{\mathrm{T}} \boldsymbol{\mu}_k}{RT} \tag{3.69}$$

Monitoring of the Gibbs energy is the major advantage of the RAND method (original and modified). Mole numbers satisfy the material balance at every iteration, if the initial estimate satisfies it. In this case, the value of the Gibbs energy can be calculated and compared with previous values, to ensure the descent to a minimum. At every iteration, $\boldsymbol{\lambda}$ and $\mathbf{s}$ are determined from Eq. 3.68 to calculate corrections to the mole numbers from Eq. 3.56. The mole numbers at iteration q are then updated as:

$$\begin{gathered} \mathbf{n}_k^{(q+1)} = \mathbf{n}_k^{(q)} + \alpha \Delta \mathbf{n}_k^{(q)} \\ k = 1, ..., N_P \end{gathered} \tag{3.70}$$

using parameter α to control the step when the Gibbs energy increases or corrections lead to negative mole numbers. In Eq. 3.68, $\Delta \mathbf{b}$ can be omitted if the initial estimate of $\mathbf{n}$ satisfies the material balance. However, in our implementation we preserve it in the general form defined by Eq. 3.59, in order to mitigate the effect of round-off errors and cover the cases where the initial estimates do not meet the constraint.

3.2.3 Initialization

To obtain initial estimates for CPE calculations, we usually need to solve a linear programming problem (Michelsen and Mollerup, 2007). This involves the determination of non-zero mole numbers for N_E components, allowing the estimation of $\boldsymbol{\lambda}$ and $\mathbf{n}_t$. The main disadvantages associated with this method are degenerate cases, poor estimation of small concentrations and a solution with fewer than N_E present components. In the last case, there is not enough information to estimate $\boldsymbol{\lambda}$ (Michelsen and Mollerup, 2007).

A different approach can be followed to avoid the linear programming problem. First, we guess the values of the phase amounts. Based on the minimum and maximum reaction extents, total mole numbers of a phase will be between a minimum and a maximum number. In the special case where all reactions do not change the number of molecules, the estimate will be equal to the total mole numbers in the feed. In this way, we can find reasonable starting values for the phase amounts. When the $\mathbf{n}_t$ is decided, it is kept constant and the following function is defined:

$$Q(\boldsymbol{\lambda}) = \sum_{k=1}^{N_P} n_{t,k} \left(\sum_{i=1}^{N_C} x_{ik} - 1 \right) - \sum_{j=1}^{N_E} \lambda_j b_j \tag{3.71}$$

The unconstrained minimization of function Q can provide initial estimates for the Lagrange multipliers. To find the minimizer, we need to solve:

$$\nabla^2 Q \Delta\boldsymbol{\lambda} = -\nabla Q \tag{3.72}$$

Assuming composition independent fugacity or activity coefficients, and comparing Eq. 3.72 with Eq. 3.32 and 3.41:

$$\mathbf{J}^A \Delta\boldsymbol{\lambda} = -\mathbf{F}^A \tag{3.73}$$

or

$$\left[\mathbf{A} \operatorname{diag} \left(\sum_{k=1}^{N_P} \mathbf{n}_k \right) \mathbf{A}^{\mathrm{T}} \right] \Delta\boldsymbol{\lambda} = - \left(\mathbf{A} \sum_{k=1}^{N_P} \mathbf{n}_k - \mathbf{b} \right) \tag{3.74}$$

The entries of the diagonal matrix are the total mole numbers of each component, which are all positive. Since the diagonal matrix is positive definite and $\mathbf{A}$ has full rank, matrix $\mathbf{J}^A$ is also positive definite. This means that Q is a strongly convex function and it has a unique minimizer. During the minimization, parameter α controls the step at iteration q in case of an increase in the value of function Q:

$$\boldsymbol{\lambda}^{(q+1)} = \boldsymbol{\lambda}^{(q)} + \alpha \Delta \boldsymbol{\lambda}^{(q)} \tag{3.75}$$

The minimizer $\boldsymbol{\lambda}$ corresponds to the equilibrium of a hypothetical mixture of ideal phases, with the initially assumed phase amounts. Consequently, when the guess of the phase amounts is exactly equal to their actual equilibrium values and the phases are ideal, Q function minimization converges to the final solution of Eq. 3.46.

3.3 Non-stoichiometric algorithms for multiphase chemical equilibrium

In sections 3.2.1 and 3.2.2 we presented two numerical methods for CPE calculations of ideal and non-ideal systems. Each method represents the core of a different algorithm we tested for the multiphase chemical equilibrium of multicomponent systems, when multiple reactions take place. The first algorithm is entirely based on the Lagrange multipliers method (successive substitution algorithm). The second algorithm uses successive substitution for the first steps and then switches to the modified RAND for rapid convergence (combined algorithm). The most essential steps of both algorithms are explained below and are also presented in Figure 3.1.

- Successive substitution algorithm

  1. Set temperature, pressure, specify the feed composition, assume that only a single phase exists and guess the phase amount. It is more straightforward to guess the mole numbers of the single phase, based on how much reactions can progress. Although systematic generalization for a multiphase system is not addressed here, initial estimates of phase amounts were found less critical for convergence (Appendix E).

  2. Minimize function Q mentioned in section 3.2.3 with respect to $\boldsymbol{\lambda}$ for the $\mathbf{n}_t$ guessed in step 1. Update mole fractions from Eq. 3.34 as $\mathbf{x} = f(\boldsymbol{\lambda})$ at each iteration until convergence. Assume ideal vapor (ideal gas) or ideal solution (ideal liquid): set for the vapor phase all $\hat{\phi}_{ik} = 1$ and for the liquid phase $\hat{\phi}_{ik} = K_{ik}$. Find the K-values from Eq. 2.67 when an EoS is used or from Eq. 2.66 when an activity coefficient model is used. When converged, calculate mole numbers as $\mathbf{n} = f(\boldsymbol{\lambda}, \mathbf{n}_t)$.

  3. Use as initial estimates the $\mathbf{n}_t$ guessed in step 1 and the $\boldsymbol{\lambda}$ at the minimum of function Q in step 2. Calculate fugacity or activity coefficients as $\hat{\phi}_{ik} = f(\mathbf{n}_k)$ or $\gamma_{ik} = f(\mathbf{n}_k)$ and keep them constant. Solve the full system of Eq. 3.46, updating mole fractions from Eq. 3.34 as $\mathbf{x} = f(\boldsymbol{\lambda})$ at each iteration until convergence. When converged, calculate mole numbers as $\mathbf{n} = f(\boldsymbol{\lambda}, \mathbf{n}_t)$. This step constitutes the inner loop.

4. Check if all phases are ideal:
   - If all phases are ideal, proceed.
   - If at least one phase is non-ideal, update fugacity or activity coefficients with the solution of the inner loop and go to step 3. Repeat until convergence. This step constitutes the outer loop.
5. Check if current phase set is stable:
   - If the phase set is stable, the equilibrium solution has been found.
   - If the phase set is unstable, add one phase and go to step 3. Re-initialization is not required. Stability analysis provides reasonable estimates for the mole fractions of the new phase. The amount of the new phase is set to zero and the $\boldsymbol{\lambda}$ used is the one from the previously converged phase set.

- Combined algorithm
  1. Set conditions, assume a single phase and guess the phase amount.
  2. Miminize function Q for $\boldsymbol{\lambda}$ initial estimates.
  3. Repeat steps 3 and 4 of the successive substitution algorithm for up to three outer-loop iterations.
     - If converged at three or fewer iterations, proceed.
     - If not converged at three iterations, change to the modified RAND method solving the system of Eq. 3.68 until convergence. Fugacity or activity coefficients are updated as $\hat{\phi}_{ik} = f(\mathbf{n}_k)$ or $\gamma_{ik} = f(\mathbf{n}_k)$ at every iteration.
  4. Check if current phase set is stable:
     - If the phase set is stable, the equilibrium solution has been found.
     - If the phase set is unstable, add one phase and go to step 3.

Convergence is assumed when the error is less than 10^{-10}. The error in the Q-function minimization is defined at iteration q as:

$$\text{error}^{(q)} = \sqrt{\sum_{j=1}^{N_E} \left[\lambda_j^{(q)} - \lambda_j^{(q-1)}\right]^2} \tag{3.76}$$

For successive substitution (inner/outer loop):

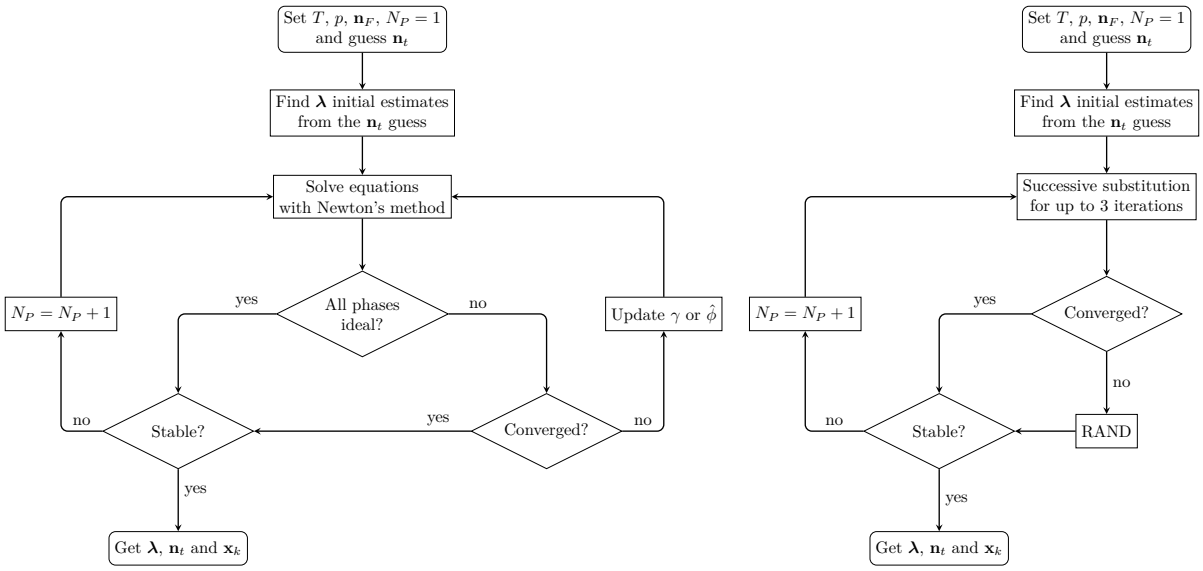

Figure 3.1: Main steps of the algorithms in this work: (a) successive substitution and (b) successive substitution combined with the modified RAND.

$$\text{error}^{(q)} = \sqrt{\sum_{j=1}^{N_E} \left[\lambda_j^{(q)} - \lambda_j^{(q-1)}\right]^2 + \sum_{k=1}^{N_P} \left[n_{t,k}^{(q)} - n_{t,k}^{(q-1)}\right]^2} \tag{3.77}$$

and for the modified RAND method:

$$\text{error}^{(q)} = \sqrt{\sum_{k=1}^{N_P} \sum_{i=1}^{N_C} \left[n_{ik}^{(q)} - n_{ik}^{(q-1)}\right]^2} \tag{3.78}$$

The unknown variables in the algorithms (Eq. 3.46 and 3.68) are $N_E + N_P$. The original working equations of the Lagrangian (Eq. 3.14 and 3.15) require a total of $N_C N_P + N_E$ variables, whereas the Lagrange multipliers method and the modified RAND method use $(N_C - 1)N_P$ fewer variables. In multiphase multicomponent mixtures this difference becomes more prominent.

The successive substitution algorithm is expected to be slower as it utilizes a first-order method that does not take advantage of fugacity or activity composition derivatives. An accelerated technique could be employed, such as the the General Dominant Eigenvalue Method (GDEM) (Crowe and Nishio, 1975). Although acceleration can reduce computation time, calculation could become unstable. To validate if an accelerated step should be accepted, the value of the Gibbs energy must be decreasing. Checking the value of $G = f(\boldsymbol{\lambda}, \mathbf{n}_t)$ is not possible because the constraints are not satisfied at every iteration. Instead, the material balance is a working equation.

The Q function minimization initializes calculations for both algorithms with the ideal system approximation and a single phase. This minimization could be also achieved under different assumptions. A multiphase mixture can be chosen ($N_P > 1$) and fugacity/activity coefficients can be calculated for an ideal mixture. Alternatively, the system can be considered non-ideal and fugacity/activity coefficients can be calculated for the current composition estimate and kept constant. The Hessian of function Q is always positive definite, thus the minimization is a safe procedure.

The algorithms presented in Figure 3.1 are intended to provide a general solution, without prior knowledge of the phase number or the distribution of components in the different phases. Our trials showed that the algorithms can also converge if the initial assumption is $N_P > 1$, saving calculation time for more than one phase at equilibrium. However, the focus of this work was to determine the equilibrium solution by sequentially adding phases after the previous phase set has converged.

Finally, the CPE solvers and the thermodynamic routines are coded in FORTRAN with the Intel® Parallel Studio XE 2015 compiler. In this implementation, we used functions provided by the Intel® MKL libraries (LAPACK). Function `DSYTRF` is required to factorize a symmetric matrix (LDL decomposition), `DSYTRS` to solve the linear system and `DSYTRI` to invert a symmetric matrix. Similar performance is expected by other Cholesky decomposition routines. Furthermore, EoS or activity coefficient models are included in a modular way, to effectively make the algorithms "fugacity-expression" independent. The input of a fugacity routine is temperature, pressure and component mole numbers of a phase to calculate fugacity coefficients. This can be done directly from an EoS after solving for volume, or from an activity coefficient model using Eq. 2.55.

3.4 Conclusions

Gibbs energy minimization methods in CPE are classified as stoichiometric and non-stoichiometric. Stoichiometric methods with reaction extents as independent variables are associated with certain disadvantages, such as the selection of primary/secondary components to avoid round-off errors and challenging initialization. For this reason, we selected non-stoichiometric methods for CPE calculation in our work. The Lagrange multipliers method and the modified RAND method were derived and presented in their general form for non-ideal multiphase systems. Lagrange multipliers and phase amounts are the independent variables for both methods, a total of $(N_C-1)N_P$ fewer variables compared with the conventional method based on the Lagrangian conditions at equilibrium.

The Lagrange multipliers method for non-ideal systems is a first-order nested-loop method. Although the inner loop is a second-order procedure, inner-loop calculations are performed under constant fugacity or activity coefficients with outer-loop non-ideality updates. For ideal gas/ideal solution phases, no outer-loop updates are required and the procedure shows quadratic convergence. Logarithms of mole fractions are expressed as a function

of Lagrange multipliers, therefore the actual mole fractions are always expected to be positive.

The modified RAND is a second-order method for both ideal and non-ideal systems. The material balance is not a working equation as in the Lagrange multipliers method. Instead, it is satisfied at every iteration, allowing monitoring of the Gibbs energy and enhancing the robustness of the method. Corrections for trace components might lead to negative mole numbers, but this can be overcome with the control of the Newton step. Compared with different nested (first-order) RAND implementations published in the literature, the modified RAND method can be used for multiphase reaction systems, while preserving its quadratic convergence rate even for non-ideal systems.

Initialization is required for the numerical methods presented in this section. Values for phase amounts must be assumed based on the mole number changes caused by the reactions. At constant phase amounts, a convex function Q is defined and minimized under the ideal system approximation. The minimizer represents the initial estimates for the Lagrange multipliers. With a positive definite Hessian, the minimization of function Q is always a safe procedure and control of the Newton step is only needed when its value is increasing due to overstepping. This minimization results in the equilibrium of a hypothetical ideal gas/ideal solution system with the initially assumed phase amounts. If the phase amount guesses coincide with the actual equilibrium phase amounts and the systems are ideal, the CPE solution can be obtained from this minimization. It was found that the convergence of the Lagrange multipliers method or the modified RAND method are not particularly influenced by initial estimates of the phase amounts during this step.

Finally, CPE methods, initialization and stability analysis are coupled in non-stoichiometric algorithms. The first algorithm uses only the Lagrange multipliers method (successive substitution algorithm). The second algorithm combines the Lagrange multipliers method for the first few iterations with the much faster modified RAND method that accelerates convergence (combined algorithm). The algorithms are intended for calculations where no information about the equilibrium phases is available. Therefore, initialization is performed in the beginning assuming one phase and when the single phase converges, stability analysis investigates if a second phase should be considered. Stability analysis provides a good estimate of the new phase composition and there is no need to re-initialize with the new phase set. In the same fashion, new phases are added and converged until the current phase set is stable, which means that the Gibbs energy global minimum has been found. More than one phase can be initially assumed to save computation time but this work is focused on presenting and applying a more general approach by starting calculations with one phase.

CHAPTER

4 Application of CPE algorithms to reaction systems

The most common reaction systems in the literature are tested with the successive substitution and the combined algorithm. Calculations in this work are compared with published results of two- and three-phase mixtures where one or two reactions can take place. Then, the algorithms are applied to a more complex five-reaction system, which is the basis of the biodiesel synthesis: transesterification of fatty acid triglycerides with methanol. For this purpose we used two different starting triglycerides that lead to two separate mixtures of esters. Finally, speed of calculations and convergence behavior is presented for all the systems in this chapter to evaluate the efficiency of the proposed algorithms.

4.1 CPE calculations for systems in the literature[†]

For convenience, components and elements are numbered in each mixture. Table 4.1 illustrates the identity of components and the chemical composition of elements in the systems included in this work. Apart from the calculations of component mole fractions, a useful measure to quantify phase distribution is the mole fraction of phase k:

$$\beta_k = \frac{n_{t,k}}{\sum_{q=1}^{N_P} n_{t,q}} \tag{4.1}$$

Calculations concern VLE, LLE and VLLE systems. All equations where developed using "x_{ik}" as the mole fraction of component i in phase k. Nevertheless, to avoid using double subscripts (e.g. x_{31} component 3 in the 1st phase), we refer to mole fractions of component i in vapor phase as "y_i", in the first liquid phase as "x_i" and in the second liquid phase as

[†]Appears in Tsanas et al. (2017a,b)

"x_i'".

Table 4.1: Component and element numbering for the systems examined.

System		1	2	3	4	5	6	7
Formaldehyde/ water	Component	formaldehyde	water	methylene glycol	oxydimethanol			
	Element	CH_2O	H_2O					
Xylene separation	Component	di-*tert*-butylbenzene	*m*-xylene	*tert*-butyl-*m*-xylene	*tert*-butylbenzene	benzene	*p*-xylene	
	Element	C_6H_6	C_4H_8	C_8H_{10}	C_8H_{10}			
Acetic acid/ethanol esterification	Component	acetic acid	ethanol	water	ethyl acetate			
	Element	C_2H_2O	C_2H_6O	H_2O				
Acetic acid/1-butanol esterification	Component	acetic acid	1-butanol	water	butyl acetate			
	Element	C_2H_2O	$C_4H_{10}O$	H_2O				
MTBE synthesis	Component	isobutene	methanol	*n*-butane	MTBE			
	Element	C_4H_8	CH_4O	C_4H_{10}				
TAME synthesis 1 reaction 2 reactions	Component	2-methyl-1-butene	2-methyl-2-butene	methanol	TAME	*n*-pentane		
	Element	$C_{2.5}H_5$	$C_{2.5}H_5$	CH_4O	C_5H_{12}			
	Element	C_5H_{10}	CH_4O	C_5H_{12}				
Propene hydration	Component	propene	water	2-propanol				
	Element	C_3H_6	H_2O					
Cyclohexane synthesis	Component	benzene	hydrogen	cyclohexane				
	Element	C_6H_6	H_2					
Methanol synthesis	Component	carbon monoxide	carbon dioxide	hydrogen	water	methanol	methane	octadecane
	Element	CO	O	H_2	CH_4	$C_{18}H_{38}$		

For the analysis of reaction systems, Ung and Doherty (1995b,d) introduced a set of N_E transformed composition variables based on a set of N_R reference components. Transformed mole fractions X_i defined as:

$$X_i = \frac{x_i - \boldsymbol{\nu}_i \boldsymbol{\mathcal{V}}^{-1} \mathbf{x}_{\text{ref}}}{1 - \boldsymbol{\nu}_t^{\text{T}} \boldsymbol{\mathcal{V}}^{-1} \mathbf{x}_{\text{ref}}} \tag{4.2}$$

where:

$\boldsymbol{\nu}_i$	vector of all stoichiometric coefficients for component i
$\boldsymbol{\nu}_t$	vector of total stoichiometric coefficients
$\boldsymbol{\mathcal{V}}$	stoichiometric matrix of reference components in Ung and Doherty (1995b,d)
$\mathbf{x}_{\text{ref}}$	reference component mole fractions in Ung and Doherty (1995b,d)

A property of the transformed mole fractions is:

$$\sum_{i=1}^{N_E} X_i = 1 \tag{4.3}$$

When mole fractions of different phases are selected, such as y_i or x_i', we can calculate transformed Y_i or X_i' respectively. In phase equilibrium of non-reaction systems, azeotropes are identified when:

$$\mathbf{y} = \mathbf{x} \tag{4.4}$$

Ung and Doherty (1995b,d) have proven that this is not necessarily true for reaction

systems. However, the use of transformed compositions can preserve this equality at the reactive azeotrope:

$$\mathbf{Y} = \mathbf{X} \tag{4.5}$$

Derivation and implications of transformed variables can be found in Ung and Doherty (1995b,d). In some publications, only equilibrium transformed mole fractions are available for comparison.

4.1.1 Formaldehyde/water mixture

Maurer (1986) presented a number of reactions occurring in aqueous solutions of formaldehyde:

$$\mathrm{CH_2O + H_2O \rightleftharpoons CH_4O_2} \tag{4.6}$$

$$\mathrm{HO\text{-}(CH_2O)_{n-1}\text{-}H + CH_4O_2 \rightleftharpoons HO\text{-}(CH_2O)_n\text{-}H + H_2O} \tag{4.7}$$

$$n \geq 2$$

We base our calculations on the approach of Ung and Doherty (1995e), who studied the reaction system for $n = 2$:

$$\mathrm{CH_2O + H_2O \rightleftharpoons CH_4O_2} \tag{4.8}$$

$$\mathrm{2CH_4O_2 \rightleftharpoons C_2H_6O_3 + H_2O} \tag{4.9}$$

where formaldehyde reacts with water to produce methylene glycol and two molecules of methylene glycol produce oxydimethanol and water. The number of elements is $N_E = N_C - N_R = 4 - 2 = 2$. The formula matrix and stoichiometric matrix of the system are given by:

$$\mathbf{A} = \begin{bmatrix} 1 & 0 & 1 & 2 \\ 0 & 1 & 1 & 1 \end{bmatrix} \qquad \mathbf{N} = \begin{bmatrix} -1 & -1 & 1 & 0 \\ 0 & 1 & -2 & 1 \end{bmatrix}^{\mathrm{T}} \tag{4.10}$$

Vapor phase is ideal gas and liquid phase is ideal solution (Ung and Doherty, 1995e). Chemical equilibrium constants and vapor pressures were taken from Maurer (1986). Oxydimethanol is considered non-volatile and its vapor concentration is zero, as for all oligomers in the original study from Maurer (1986). Equilibrium T-y-x diagrams at 1 atm

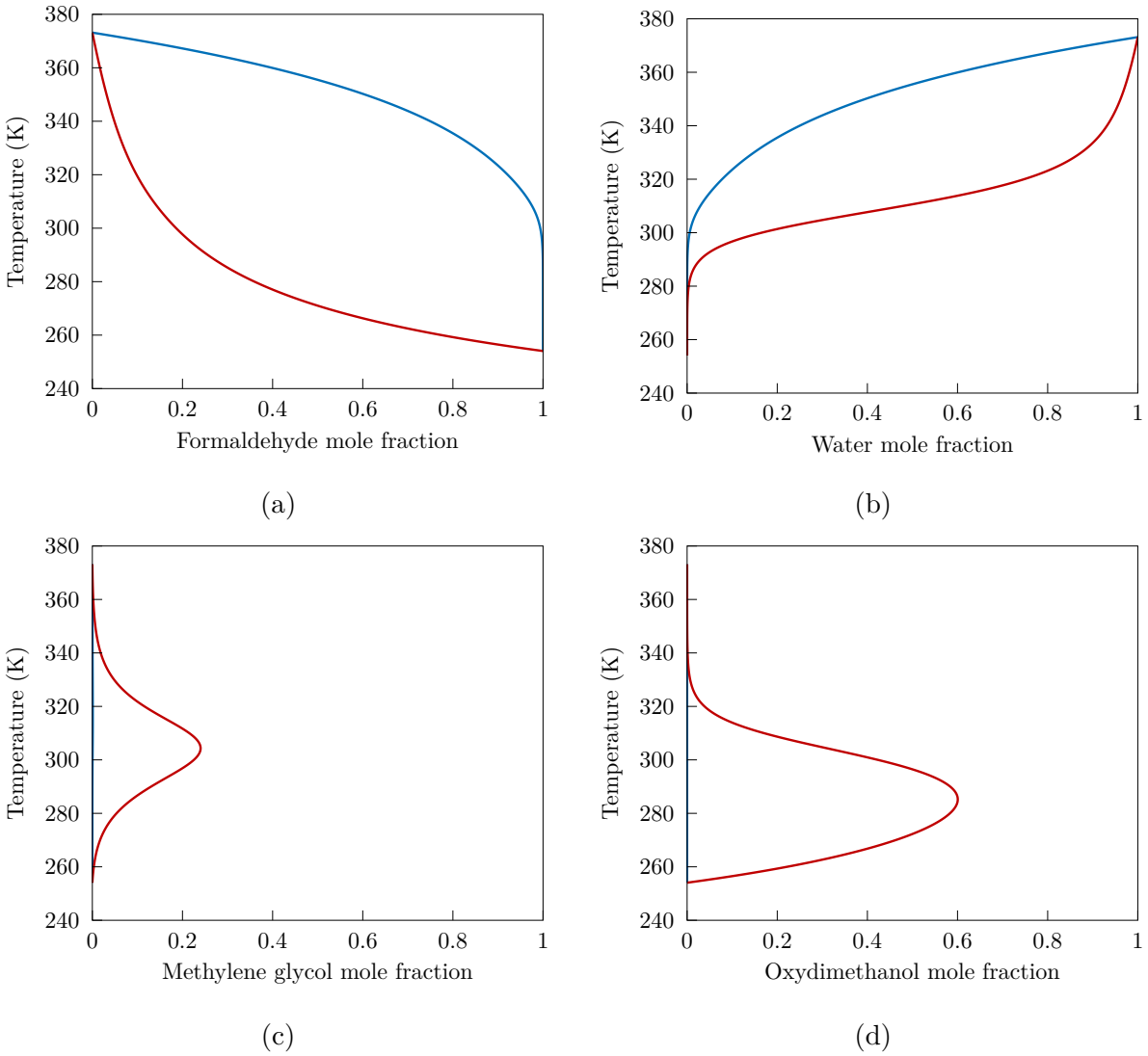

Figure 4.1: Equilibrium T-y-x diagrams in formaldehyde/water mixture at 1 atm: (a) formaldehyde, (b) water, (c) methylene glycol, (d) oxydimethanol [vapor (—), liquid (—)].

for all components are presented in Figure 4.1, matching the results published by Ung and Doherty (1995e).

Reaction system components do not always cover the full mole fraction range [0,1] (Ung and Doherty, 1995e). For instance, Eq. 4.9 shows that methylene glycol cannot be pure, since it reacts with other methylene glycol molecules to produce oxydimethanol. Methylene glycol is relatively non-volatile with maximum concentration in the vapor phase less than 0.1% mol at 315.98 K. Maximum mole fractions in the liquid phase are 0.24 at 304.07 K for methylene glycol and 0.60 at 285.02 K for oxydimethanol. Equilibrium diagrams at 1 atm are presented in Figure 4.2 using transformed compositions. For this system, transformed compositions are calculated by:

$$X_1 = \frac{x_1 + x_3 + 2x_4}{1 + x_3 + 2x_4} \qquad X_2 = \frac{x_2 + x_3 + x_4}{1 + x_3 + 2x_4} \tag{4.11}$$

using methylene glycol and oxydimethanol as reference components. At the current pressure, no reactive azeotrope is identified.

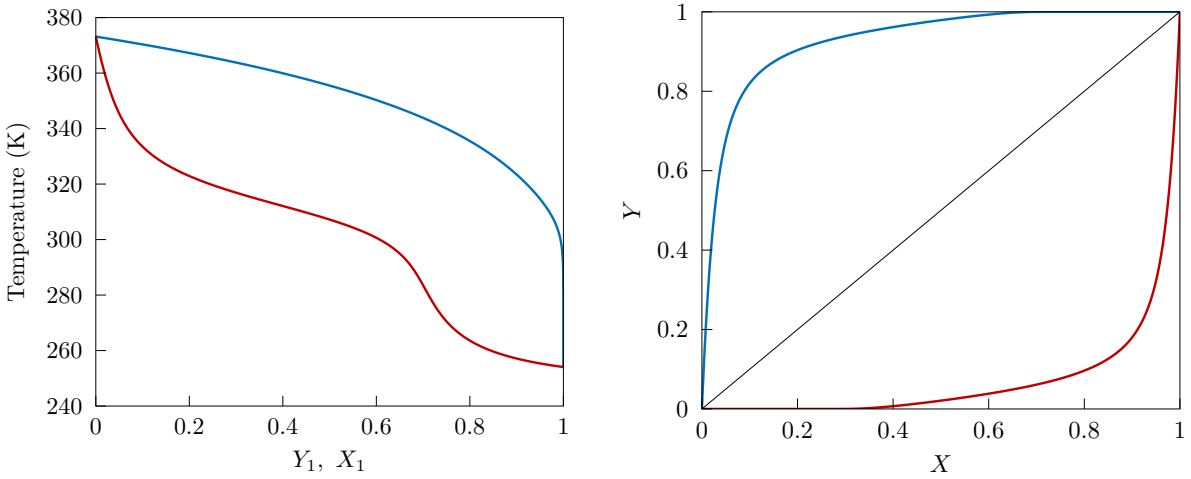

(a) (b)

Figure 4.2: Equilibrium in formaldehyde/water mixture at 1 atm: (a) T-Y-X diagram of formaldehyde [vapor (—), liquid (—)], (b) Y-X diagram of formaldehyde and water [formaldehyde (—), water (—)].

4.1.2 Xylene separation

Separating a mixture of isomers is not usually achieved by simple distillation, because boiling points are too close for distillation to be advantageous. Saito et al. (1971) attempted to separate *m*- and *p*-xylene in a reactive distillation column, seeing that the former participates in the following reactions:

$$C_{14}H_{22} + m\text{-}C_8H_{10} \rightleftharpoons C_{12}H_{18} + C_{10}H_{14} \tag{4.12}$$

$$C_{10}H_{14} + m\text{-}C_8H_{10} \rightleftharpoons C_{12}H_{18} + C_6H_6 \tag{4.13}$$

where di-*tert*-butylbenzene reacts with *m*-xylene to give *tert*-butyl-*m*-xylene and *tert*-butylbenzene, while *tert*-butylbenzene reacts with *m*-xylene to produce *tert*-butyl-*m*-xylene and benzene (*p*-xylene is an inert). The number of elements is $N_E = N_C - N_R = 6 - 2 = 4$. The formula matrix and stoichiometric matrix of the system are given by:

$$\mathbf{A} = \begin{bmatrix} 1 & 0 & 0 & 1 & 1 & 0 \\ 2 & 0 & 1 & 1 & 0 & 0 \\ 0 & 1 & 1 & 0 & 0 & 0 \\ 0 & 0 & 0 & 0 & 0 & 1 \end{bmatrix} \qquad \mathbf{N} = \begin{bmatrix} -1 & -1 & 1 & 1 & 0 & 0 \\ 0 & -1 & 1 & -1 & 1 & 0 \end{bmatrix}^{\mathrm{T}} \tag{4.14}$$

Vapor phase is ideal gas and liquid phase is ideal solution (Ung and Doherty, 1995e). Chemical equilibrium constants and vapor pressures were taken from Saito et al. (1971). The authors determined experimentally mole fractions in the main alkylation columun of *m*-xylene at 44 mmHg, and in a second recovery column of *m*-xylene and alkylating reagent at 86 mmHg. We compared bubble point calculations with the experimental data at the first plate/condenser stage of the columns in Saito et al. (1971). Results are presented in Tables 4.2 and 4.3. Benzene concentrations deviate the most at both pressures, while overall deviations are larger at the higher pressure. At the lower pressure there is higher overestimation of the bubble point.

Table 4.2: Equilibrium mole fractions in xylene separation at 44 mmHg (bubble point).

Component	Feed	Our work: 336.54 K		Saito et al. (1971): 331.15 K
		Vapor	Liquid	Vapor
di-*tert*-butylbenzene	0.29	0.01	0.29	0.02
m-xylene	0.08	0.10	0.08	0.14
tert-butyl-*m*-xylene	0.07	0.01	0.07	0.01
tert-butylbenzene	0.19	0.08	0.19	0.11
benzene	0.03	0.34	0.03	0.22
p-xylene	0.34	0.47	0.34	0.50

Figure 4.3 shows the temperature range of the two-phase system using the same feed compositions as in Tables 4.2 and 4.3. Most mole fractions curves exhibit monotonic behavior. Although xylene isomer compositions might have maxima in the two different pressures and phases, *p*-xylene shows the clearest maximum at 347.52 K and 44 mmHg with a vapor phase mole fraction of 0.557 (Figure 4.3c).

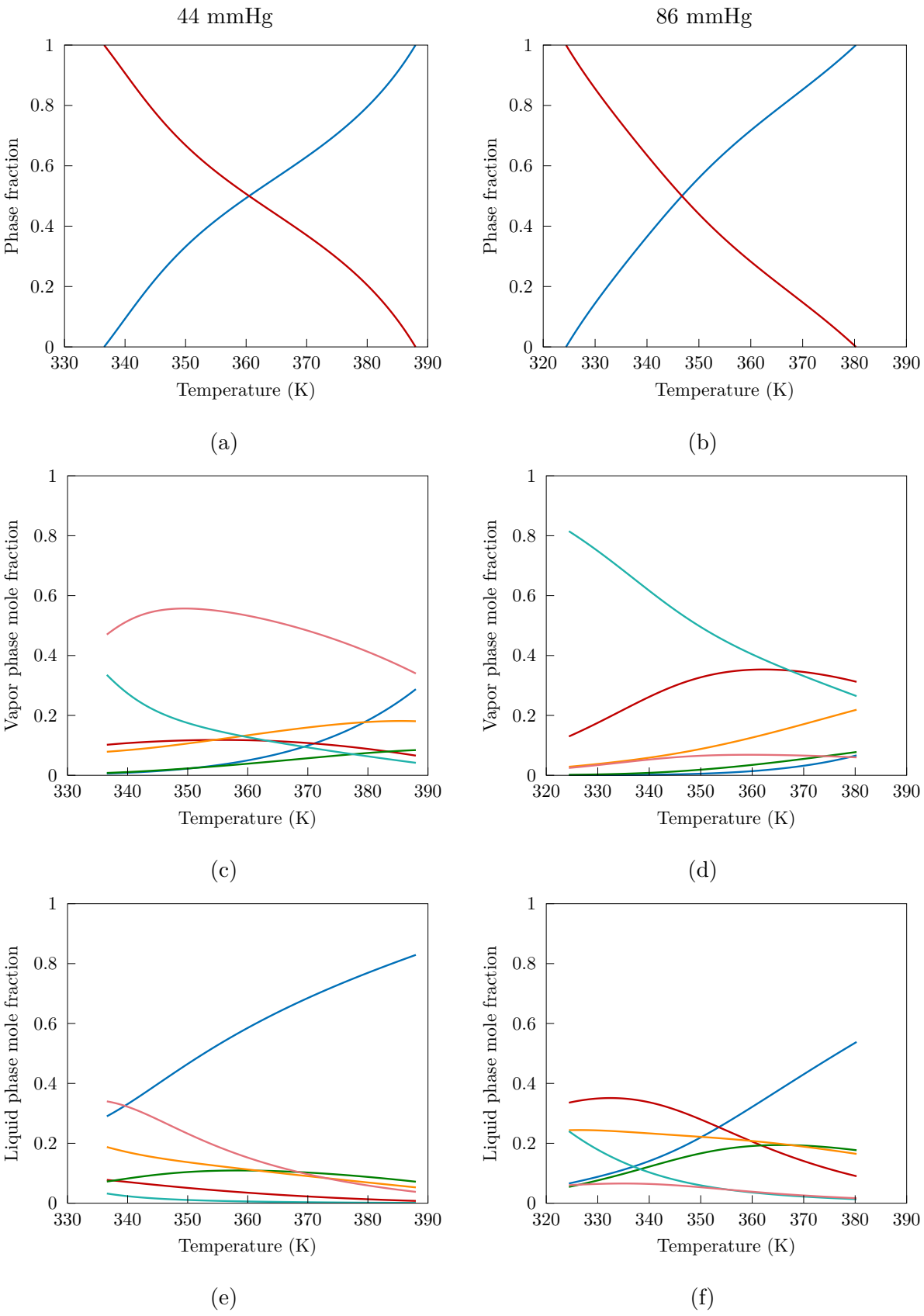

Figure 4.3: Equilibrium in xylene separation at 44 mmHg and 86 mmHg: (a, b) phase fractions [vapor (—), liquid (—)], (c, d, e, f) mole fractions [di-*tert*-butylbenzene (—), *m*-xylene (—), *tert*-butyl-*m*-xylene (—), *tert*-butylbenzene (—), benzene (—), *p*-xylene (—)].

Table 4.3: Equilibrium mole fractions in xylene separation at 86 mmHg (bubble point).

Component	Feed	Our work: 324.40 K		Saito et al. (1971): 323.15 K
		Vapor	Liquid	Vapor
di-*tert*-butylbenzene	0.09	0.00	0.07	0.00
m-xylene	0.35	0.13	0.34	0.29
tert-butyl-*m*-xylene	0.04	0.00	0.05	0.00
tert-butylbenzene	0.21	0.03	0.24	0.05
benzene	0.25	0.82	0.24	0.59
p-xylene	0.06	0.02	0.06	0.07

When the inert *p*-xylene is not included in the calculations, the number of elements reduces to three. It is possible to depict phase behavior of this reaction system in a ternary diagram, where the coordinates correspond to the element mole fractions (Eq. 3.12). Figure 4.4 shows the VLE region at 350 K for 44 and 86 mmHg. As expected, the vapor phase region is larger at the lower pressure.

A ternary diagram expressed in element mole fractions might not allow us to see the actual component distribution in the phases. Nevertheless, a ternary diagram can reveal if a phase split will take place, based on the element mole fractions in a feed we want to test. To determine the component mole fractions, we need to solve the CPE problem for the corresponding element abundance vector of the specific phase. The components that do not appear as vertices of the triangle refer to combinations of the elements and are defined, according to the formula matrix, by:

$$\text{DTBB: } 2b_1 = b_2 \qquad \text{TBB: } b_2 = b_3 \qquad \text{TBMX: } b_1 = b_2 \tag{4.15}$$

These points represent pure di-*tert*-butylbenzene, *tert*-butylbenzene and *tert*-butyl-*m*-xylene respectively. In this ternary diagram, there is a region that corresponds to infeasible mole fractions of the elements (non-physical mixture). Such a region exists because element 2 can be used only as part of a component – there is no component in the physical mixture with chemical composition C_4H_8. Elements 1 and 3 can exist as pure, because their chemical composition corresponds to benzene and *m*-xylene. In other words, pure element 1 or 3 is a system of pure benzene and *m*-xylene respectively. Concentration of elements 1 and 3 must be high enough to be combined with element 2 and deplete it completely when "building" the components in the system. The constraint on the elements that defines the infeasible region, according to the formula matrix, is:

$$b_2 \geq 2b_1 + b_3 \tag{4.16}$$

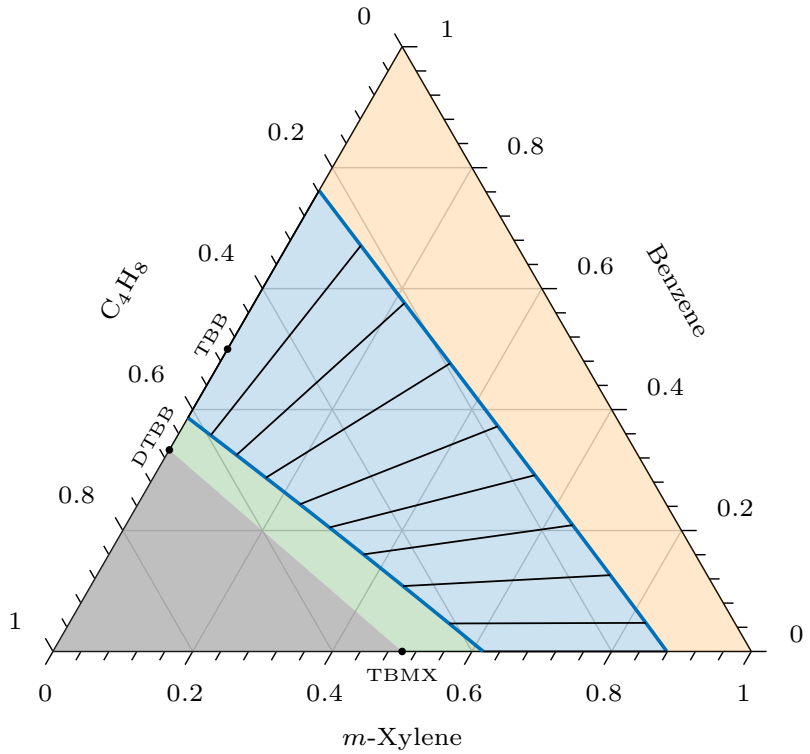

(a)

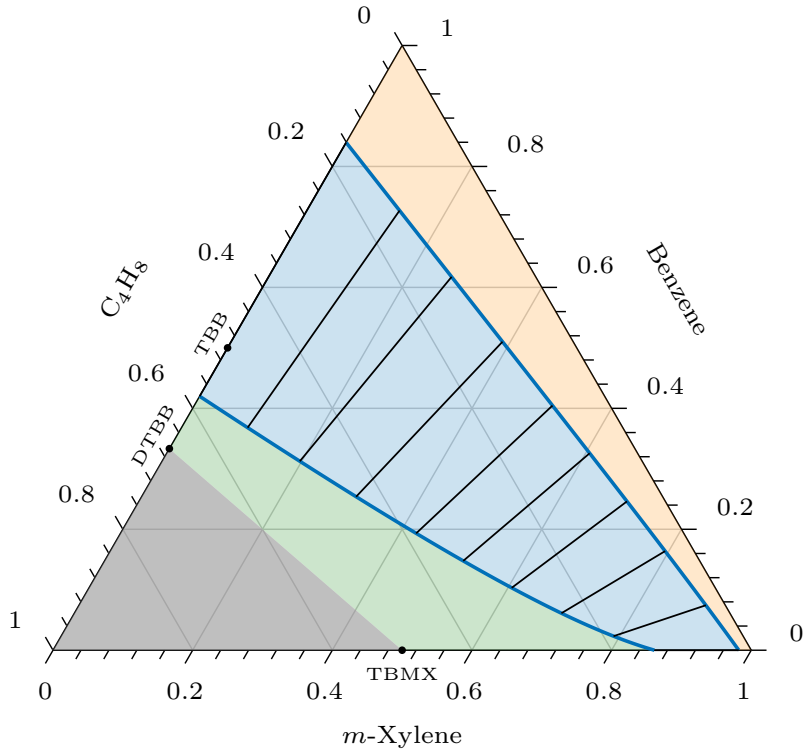

(b)

Figure 4.4: Ternary diagrams of elements in *m*-xylene alkylation without *p*-xylene at 350 K: (a) 44 mmHg, (b) 86 mmHg [binodal curve (—), tie lines (—), VLE region (▬), vapor region (▬), liquid region (▬), infeasible region (▬), DTTB (di-*tert*-butylbenzene), TBB (*tert*-butylbenzene), TBMX (*tert*-butyl-*m*-xylene)].

4.1.3 Esterification of acetic acid with ethanol

A benchmark system for chemical and phase equilibrium algorithms is the acetic acid and ethanol esterification, producing water and ethyl acetate:

$$C_2H_4O_2 + C_2H_6O \rightleftharpoons H_2O + C_4H_8O_2 \tag{4.17}$$

The number of elements is $N_E = N_C - N_R = 4 - 1 = 3$. The formula matrix and stoichiometric matrix of the system are given by:

$$\mathbf{A} = \begin{bmatrix} 1 & 0 & 0 & 1 \\ 0 & 1 & 0 & 1 \\ 1 & 0 & 1 & 0 \end{bmatrix} \qquad \mathbf{N} = \begin{bmatrix} -1 & -1 & 1 & 1 \end{bmatrix}^{\mathrm{T}} \tag{4.18}$$

Vapor phase is considered ideal gas and liquid phase is described by the UNIQUAC activity coefficient model (Abrams and Prausnitz, 1975). The chemical equilibrium constant, vapor pressures and parameters for the UNIQUAC model were taken from Xiao et al. (1989). Castier et al. (1989) studied this system considering the competitive conversion of ethanol to diethylether and the acetic acid dimerization in the vapor phase. The latter was not modeled by a reaction in Castier et al. (1989) but implicitly accounted for by the value of the fugacity coefficient (Nothnagel et al., 1973; Hayden and O'Connell, 1975). Xiao et al. (1989) and Stateva and Wakeham (1997) made similar calculations and the comparisons with this work are presented in Table 4.4. Larger deviations with Stateva and Wakeham (1997) are due to different chemical equilibrium constants. The behavior of the two-phase system at 1 atm is also shown in Figure 4.5 for an equimolar feed of the reactants.

Table 4.4: Equilibrium mole fractions, phase amounts and phase fractions in acetic acid/ethanol esterification at 355 K and 1 atm.

Component	Feed	Our work		Stateva and Wakeham (1997)		Xiao et al. (1989)	
		Vapor	Liquid	Vapor	Liquid	Vapor	Liquid
acetic acid	0.5	0.0629	0.2360	0.0554	0.2243	0.0624	0.2376
ethanol	0.5	0.0855	0.0670	0.1029	0.0675	0.0862	0.0686
water	0	0.3970	0.5630	0.3604	0.5537	0.3963	0.5565
ethyl acetate	0	0.4545	0.1339	0.4813	0.1545	0.4551	0.1373
n_t (mol)	20	17.636	2.364	–	–	–	–
β		0.882	0.118	0.767	0.233	0.877	0.123

The number of elements is equal to three. Figure 4.6 shows the VLE region of the system at 355 K and 1 atm in terms of element mole fractions. The components that do not appear as vertices of the triangle are acetic acid and ethyl acetate respectively:

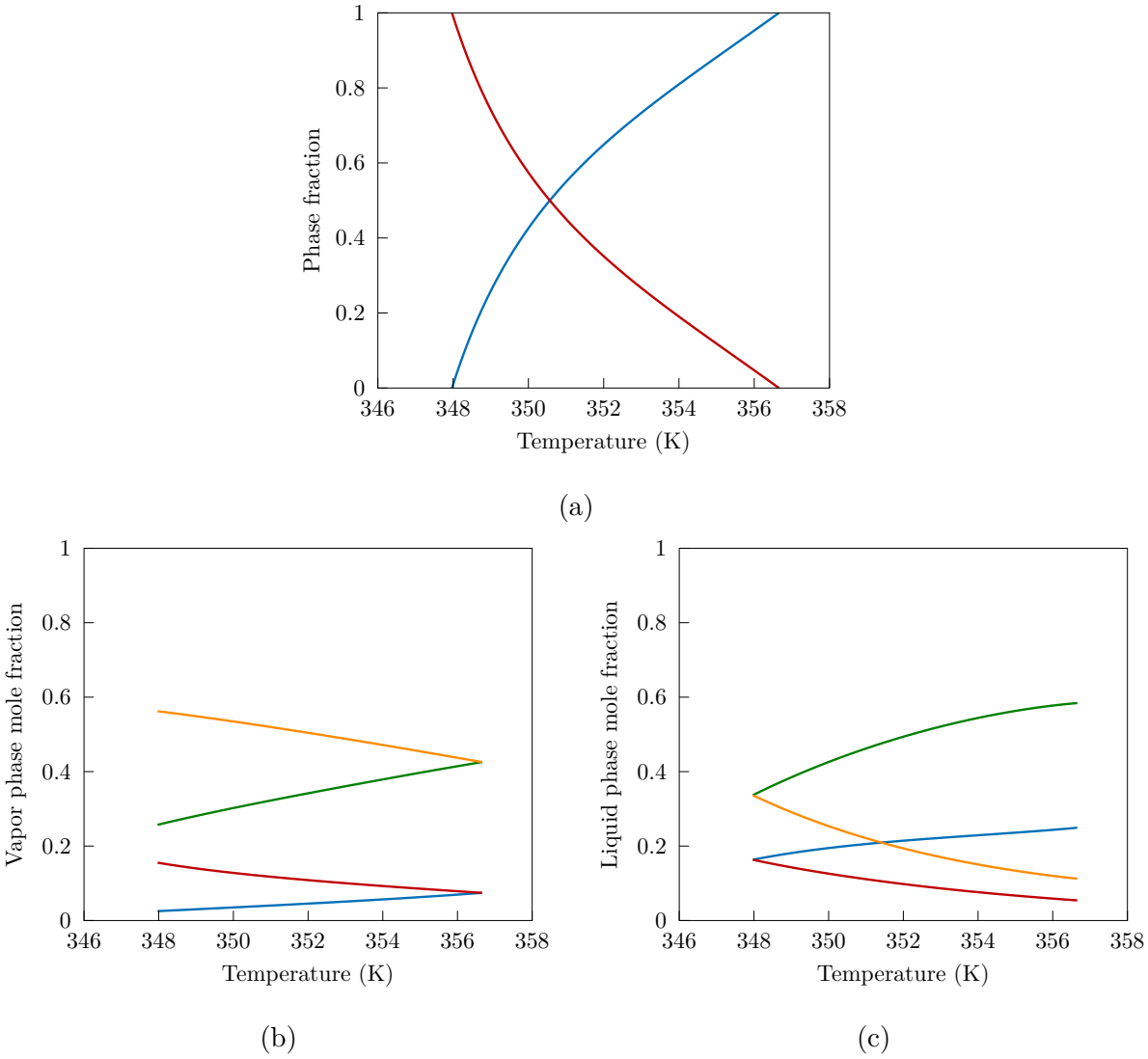

Figure 4.5: Equilibrium in acetic acid/ethanol esterification for an equimolar feed of reactants at 1 atm: (a) phase fractions [vapor (—), liquid (—)] and (b, c) mole fractions [acetic acid (—), ethanol (—), water (—), ethyl acetate (—)].

$$\text{HAc: } b_1 = b_3 \qquad \text{EtOAc: } b_1 = b_2 \tag{4.19}$$

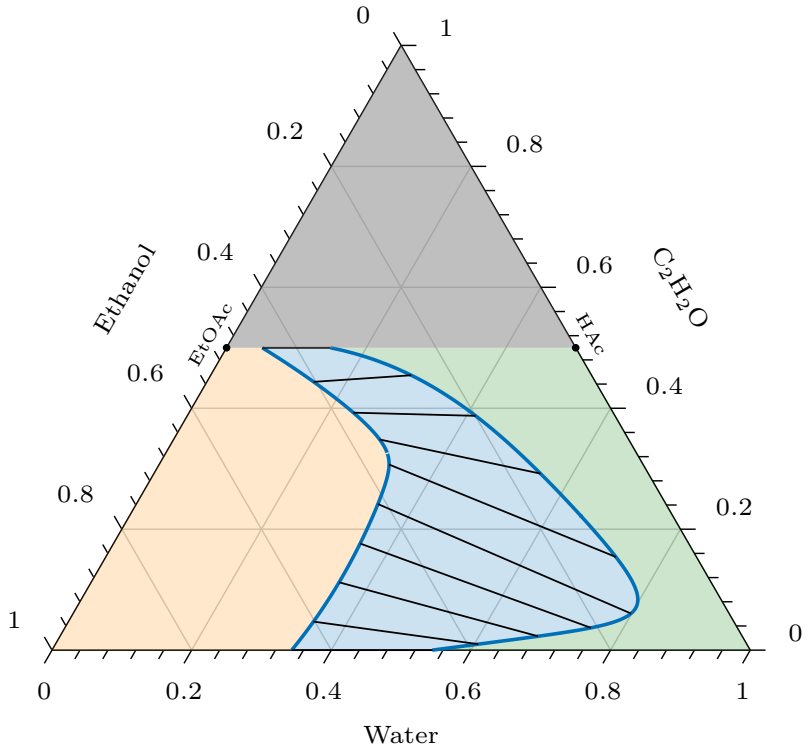

Figure 4.6: Ternary diagram of elements in acetic acid/ethanol esterification at 355 K and 1 atm [binodal curve (—), tie lines (——), VLE region (▭), vapor region (▭), liquid region (▭), infeasible region (▭), HAc (acetic acid), EtOAc (ethyl acetate)].

Element 1 represents part of a component molecule, therefore it cannot exist pure in the system and there is an infeasible region defined by:

$$b_1 \geq b_2 + b_3 \tag{4.20}$$

4.1.4 Esterification of acetic acid with 1-butanol

A different esterification was studied by Wasylkiewicz and Ung (2000), the LLE of acetic acid and 1-butanol reaction to water and butyl acetate:

$$C_2H_4O_2 + C_4H_{10}O \rightleftharpoons H_2O + C_6H_{12}O_2 \tag{4.21}$$

The number of elements is $N_E = N_C - N_R = 4 - 1 = 3$. The formula matrix and stoichiometric matrix of the system are given by:

$$\mathbf{A} = \begin{bmatrix} 1 & 0 & 0 & 1 \\ 0 & 1 & 0 & 1 \\ 1 & 0 & 1 & 0 \end{bmatrix} \qquad \mathbf{N} = \begin{bmatrix} -1 & -1 & 1 & 1 \end{bmatrix}^{\mathrm{T}} \tag{4.22}$$

Vapor phase is considered ideal gas and liquid phases is described by the UNIQUAC activity coefficient model (Abrams and Prausnitz, 1975). The chemical equilibrium constant was taken from Wasylkiewicz and Ung (2000), vapor pressures and parameters for the UNIQUAC model from Okasinski and Doherty (2000). Calculations for the LLE of the quaternary mixture are compared with Bonilla-Petriciolet et al. (2008a) in Table 4.5. Transformed mole fractions were calculated by Eq. 4.2, taking butyl acetate as the reference component:

$$X_1 = x_1 + x_4 \qquad X_2 = x_2 + x_4 \tag{4.23}$$

The first liquid phase is the organic liquid phase and calculation of the aqueous (water-rich) liquid phase transformed mole fractions X_1' and X_2' is similar. Bonilla-Petriciolet et al. (2008a) also defined slopes of the transformed tie lines as:

$$\begin{gathered} R_j = \frac{X_j - X_j'}{X_1 - X_1'} \\ j = 2, ..., N_E \end{gathered} \tag{4.24}$$

Table 4.5: Transformed tie line slopes R_2 in acetic acid/1-butanol esterification at 298.15 K and 1 atm.

Feed vector	Our work	Bonilla-Petriciolet et al. (2008a)
$[0.01\ 0.4\ 0.59\ 0]^{\mathrm{T}}$	46.1875	46.0948
$[0.1\ 0.2\ 0.7\ 0]^{\mathrm{T}}$	2.6801	2.6796
$[0.15\ 0.5\ 0.35\ 0]^{\mathrm{T}}$	3.7591	3.7574
$[0.2\ 0.3\ 0.5\ 0]^{\mathrm{T}}$	1.8917	1.8920
$[0.3\ 0.3\ 0.4\ 0]^{\mathrm{T}}$	1.3425	1.3410
$[0.3\ 0.4\ 0.3\ 0]^{\mathrm{T}}$	1.6227	1.6227
$[0.397\ 0.294\ 0.309\ 0]^{\mathrm{T}}$	1.0689	1.0649
$[0.394\ 0.274\ 0.332\ 0]^{\mathrm{T}}$	1.0368	1.0323
$[0.3\ 0.15\ 0.55\ 0]^{\mathrm{T}}$	0.9759	0.9692
$[0.27\ 0.1\ 0.63\ 0]^{\mathrm{T}}$	0.9257	0.9176

Moreover, calculations for the VLE of the system were made at 1 atm for an equimolar amount of reactants. The phase and mole fractions are presented in Figure 4.7.

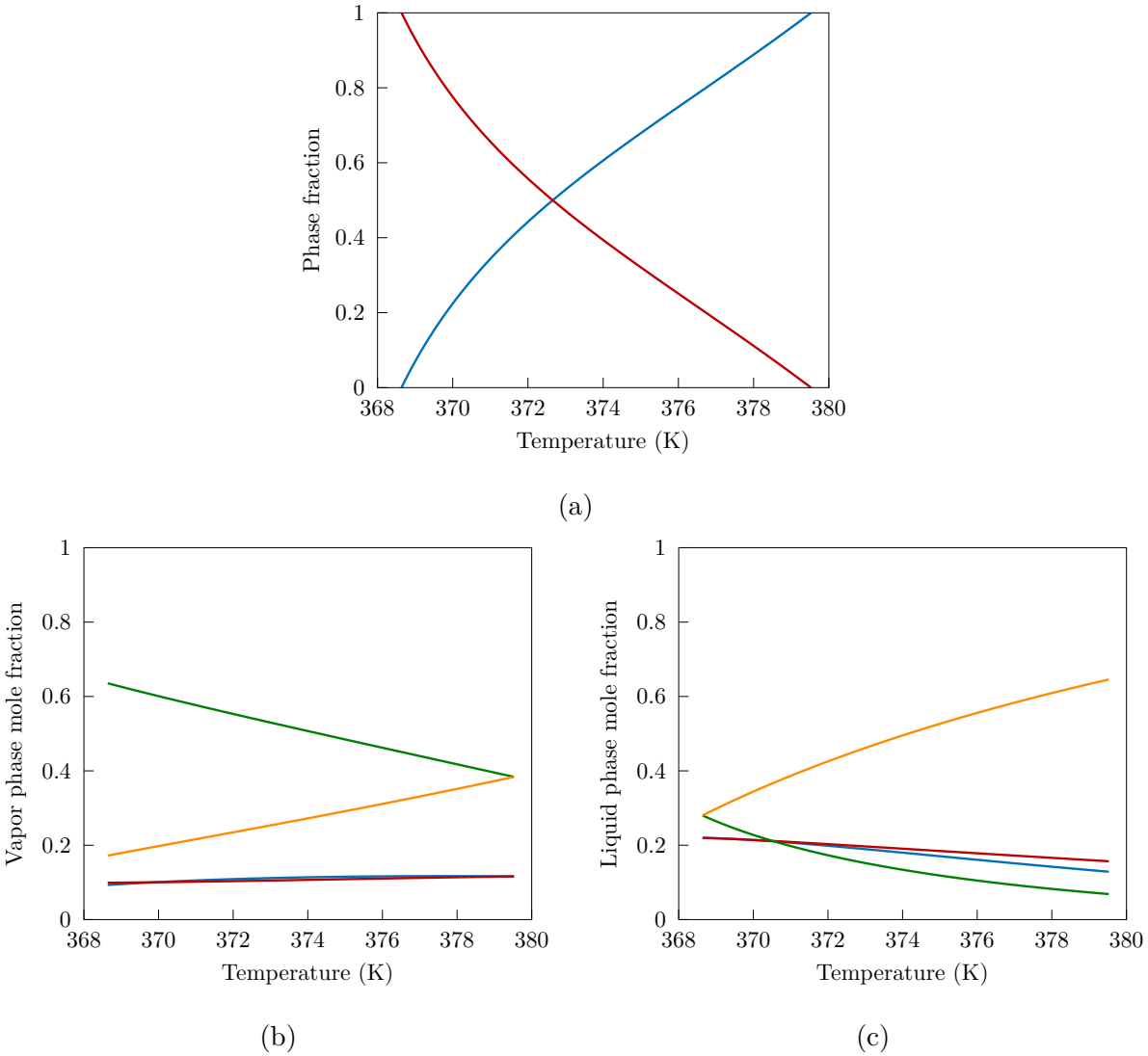

Figure 4.7: Equilibrium in acetic acid/1-butanol esterification for an equimolar feed of reactants at 1 atm: (a) phase fractions [vapor (—), liquid (—)], (b, c) mole fractions [acetic acid (—), 1-butanol (—), water (—), butyl acetate (—)].

The number of elements is equal to three. Figure 4.8 shows the LLE region of the system at 298.15 K and 1 atm in terms of element mole fractions. The components that do not appear as vertices of the triangle are acetic acid and butyl acetate respectively:

$$\text{HAc: } b_1 = b_3 \qquad \text{BuOAc: } b_1 = b_2 \tag{4.25}$$

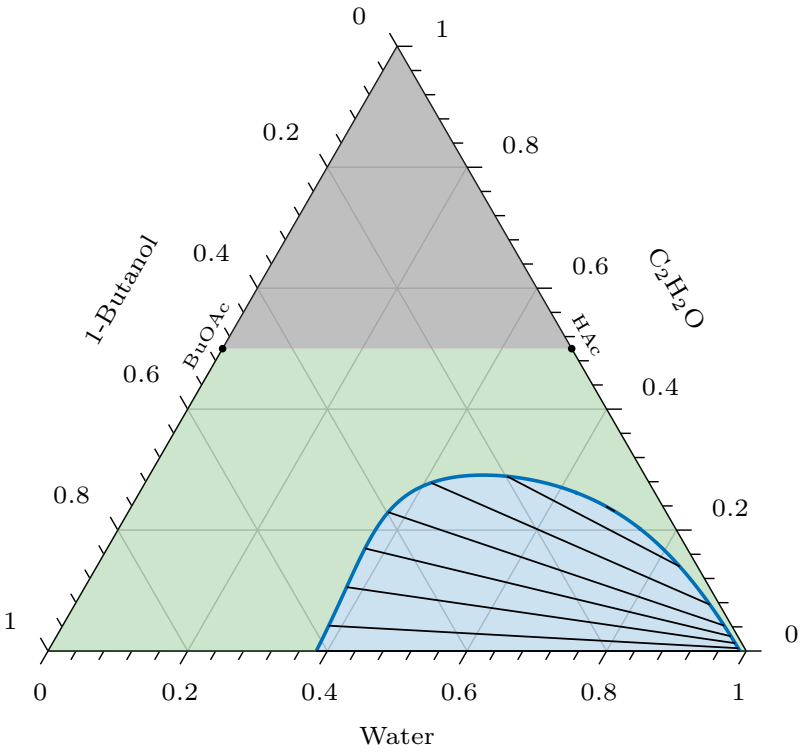

Figure 4.8: Ternary diagram of elements in acetic acid/1-butanol esterification at 298.15 K and 1 atm [binodal curve (—), tie lines (—), LLE region (▭), liquid region (▭), infeasible region (▭), HAc (acetic acid), BuOAc (butyl acetate)].

Element 1 represents part of a component molecule, therefore it cannot exist pure in the system and there is an infeasible region defined by:

$$b_1 \geq b_2 + b_3 \tag{4.26}$$

4.1.5 MTBE synthesis

Methyl-*tert*-butyl ether (MTBE) is synthesized from a mixture of isobutene and methanol:

$$C_4H_8 + CH_4O \rightleftharpoons C_5H_{12}O \tag{4.27}$$

Ung and Doherty (1995e) examined the VLE of the mixture in the presence of *n*-butane as inert. The number of elements is $N_E = N_C - N_R = 4 - 1 = 3$. The formula matrix and

stoichiometric matrix of the system are given by:

$$\mathbf{A} = \begin{bmatrix} 1 & 0 & 0 & 1 \\ 0 & 1 & 0 & 1 \\ 0 & 0 & 1 & 0 \end{bmatrix} \qquad \mathbf{N} = \begin{bmatrix} -1 & -1 & 0 & 1 \end{bmatrix}^{\mathrm{T}} \tag{4.28}$$

Vapor phase is considered ideal gas and liquid phase is described by the Wilson activity coefficient model (Wilson, 1964). The chemical equilibrium constant, vapor pressurs and parameters for the Wilson model were taken from Ung and Doherty (1995e). Calculations without n-butane are shown in Figure 4.9. The equilibrium diagram of MTBE at 1 atm is presented in Figure 4.9a. Due to the reaction in Eq. 4.27, pure MTBE cannot be achieved in any of the phases. Maximum mole fraction in the vapor phase is 0.70 at 320.56 K and in the liquid phase 0.93 at 317.70 K. Figures 4.9b and 4.9c show transformed mole fractions at equilibrium using MTBE as a reference component, calculated by:

$$X_1 = \frac{x_1 + x_4}{1 + x_4} \qquad X_2 = \frac{x_2 + x_4}{1 + x_4} \tag{4.29}$$

According to Ung and Doherty (1995e), an "intermediate-boiling inflection azeotrope" or a "pseudo-reactive azeotrope" is identified. This charecterization comes from the fact that the plot $Y_1 = f(X_1)$ approaches the diagonal $Y_1 = X_1$ (Eq. 4.5). We observed this point at 320.92 K.

Different mole numbers of n-butane were included in the feed to study the effect of the inert at 300 K and 1 atm. Isobutene and methanol were kept constant in the feed at 1 mol each. Figure 4.10 illustrates the phase fractions and the mole fractions of the components in each phase. An overall mole fraction is included in Figures 4.10b to 4.10e, calculated as:

$$\begin{gathered} \bar{x}_i = \sum_{k=1}^{N_P} \beta_k x_{ik} \\ i = 1, ..., N_C \end{gathered} \tag{4.30}$$

The overall mole fraction represents the average concentration of a component in the N_P-phase mixture. Vapor pressure for n-butane was taken from NIST Chemistry WebBook (2016) and parameters for the Wilson model from Ung and Doherty (1995e). Results are shown in Figure 4.10. The inert is a volatile component, therefore a vapor phase is expected to appear as its concentration in the feed increases (approximately after adding 0.36 mol of n-butane). After n-butane is abundant enough, we obtain 100% vapor. Increasing the concentration of the inert causes the reaction (Eq. 4.27) to shift to the left, decreasing the yield according to Le Chatelier's principle. This leads to the increase of isobutene

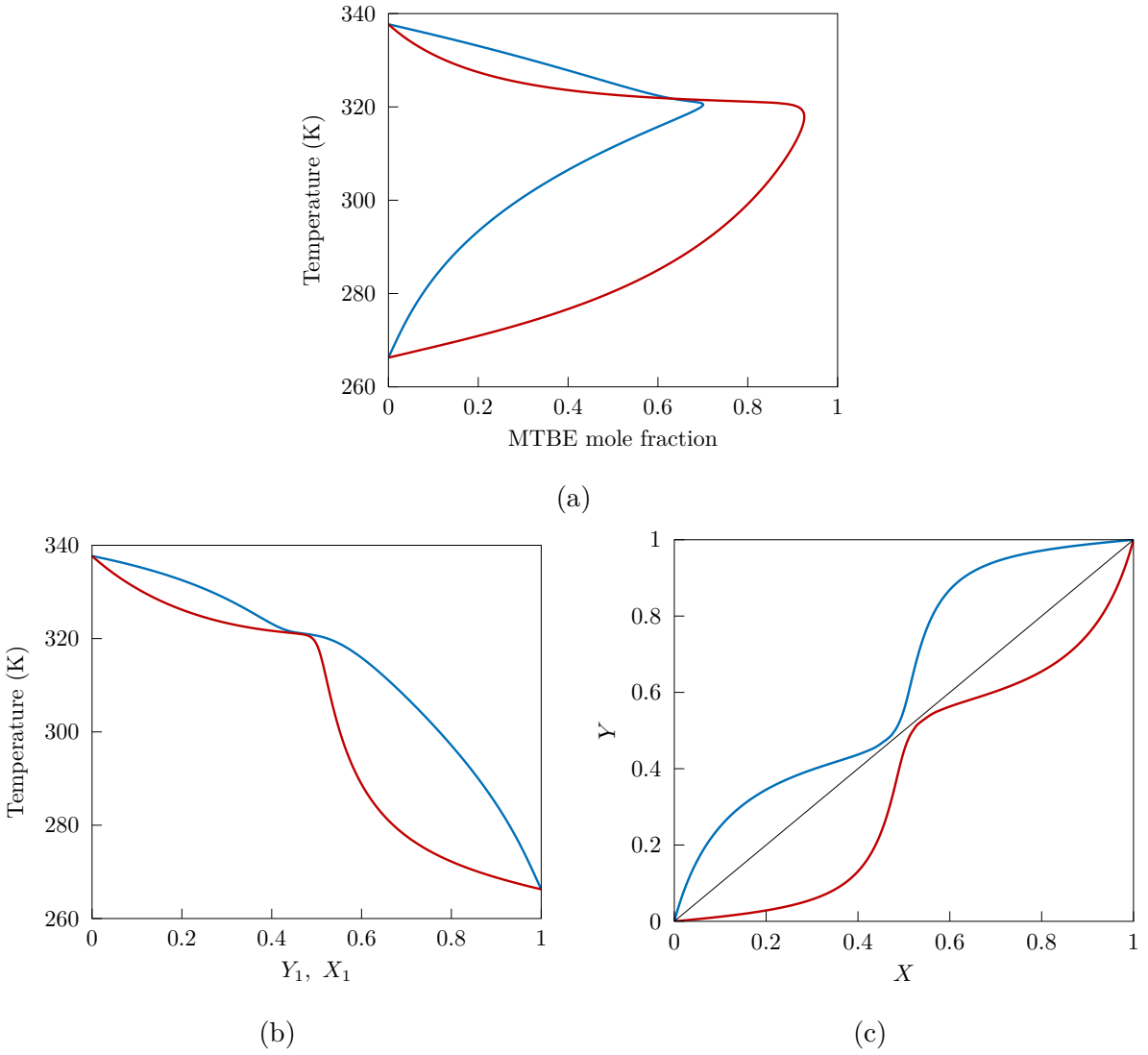

Figure 4.9: Equilibrium in MTBE synthesis at 1 atm: (a) T-y-x diagram for MTBE, (b) T-Y-X diagram for isobutene [vapor (—), liquid (—)], (c) Y-X diagram for isobutene and methanol [isobutene (—), methanol (—)].

and methanol mole numbers. However, the addition of the inert dilutes the remaining components of the mixture. As a result, the single-phase mole fractions of all components except for the inert decrease, with MTBE exhibiting the faster decrease. In Figures 4.10b, 4.10c and 4.10e it is evident that in the two-phase region the shift due to backward reaction is more prominent than the dilution of the reactants, with their overall mole fractions slightly increasing. In any case, the overall mole fraction of MTBE is expected to decreases continuously.

The number of elements is equal to three. Figure 4.11 shows the VLE region of the system at 1 atm for at 280 and 320 K and in terms of element mole fractions. At the higher temperature, the single liquid region shrinks appreciably compared to the one at the lower temperature. The component that does not appear as a vertice of the triangle is MTBE:

$$\text{MTBE: } b_1 = b_2 \tag{4.31}$$

All the elements can exist as pure, therefore there are no infeasible regions.

4.1.6 TAME synthesis

Bonilla-Petriciolet et al. (2008a) modeled the synthesis of *tert*-amyl methyl ether (TAME) from a mixture of 2-methyl-1-butene, 2-methyl-2-butene and methanol:

$$\text{2-CH}_3\text{-1-C}_4\text{H}_7 + \text{2-CH}_3\text{-2-C}_4\text{H}_7 + 2\text{CH}_4\text{O} \rightleftharpoons 2\text{C}_6\text{H}_{14}\text{O} \tag{4.32}$$

in the presence of inert *n*-pentane. The number of elements is $N_E = N_C - N_R = 5 - 1 = 4$. The formula matrix and stoichiometric matrix of the system are given by:

$$\mathbf{A} = \begin{bmatrix} 2 & 0 & 0 & 1 & 0 \\ 0 & 2 & 0 & 1 & 0 \\ 0 & 0 & 1 & 1 & 0 \\ 0 & 0 & 0 & 0 & 1 \end{bmatrix} \qquad \mathbf{N} = \begin{bmatrix} -1 & -1 & -2 & 2 & 0 \end{bmatrix}^{\mathrm{T}} \tag{4.33}$$

Vapor phase is considered ideal and liquid phase is described by the Wilson activity coefficient model (Wilson, 1964). The chemical equilibrium constant was taken from Bonilla-Petriciolet et al. (2008a), vapor pressures and parameters for the Wilson model were taken from Chen et al. (2002). Transformed compositions using TAME as the reference component are found by:

$$X_1 = \frac{x_1 + 0.5x_4}{1 + x_4} \qquad X_2 = \frac{x_2 + 0.5x_4}{1 + x_4} \qquad X_3 = \frac{x_3 + x_4}{1 + x_4} \tag{4.34}$$

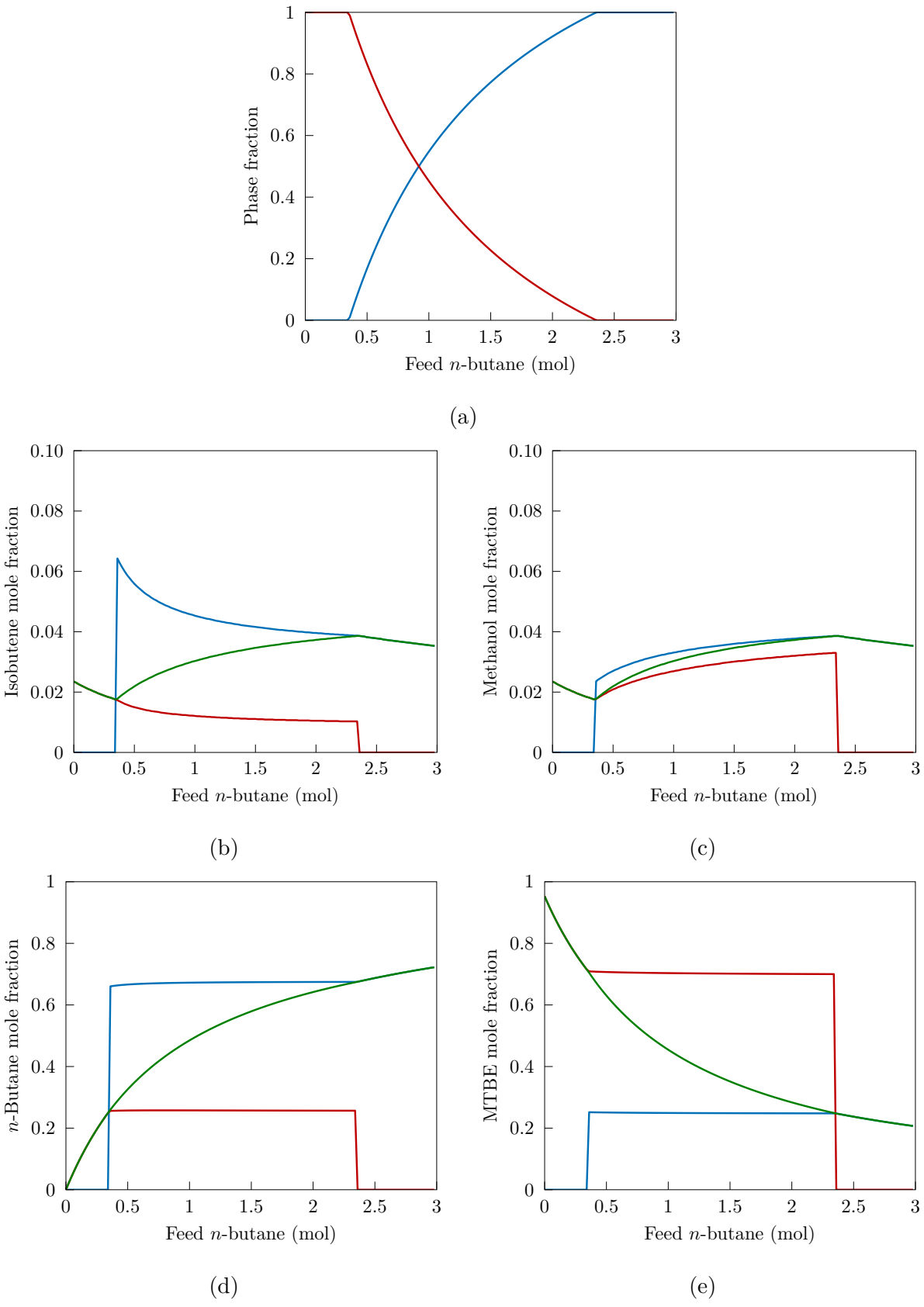

Figure 4.10: Effect of inert feed mole numbers in MTBE synthesis at 300 K and 1 atm: (a) phase fractions and mole fractions of (b) isobutene, (c) methanol, (d) n-butane, (e) MTBE [vapor (—), liquid (—), overall (—)].

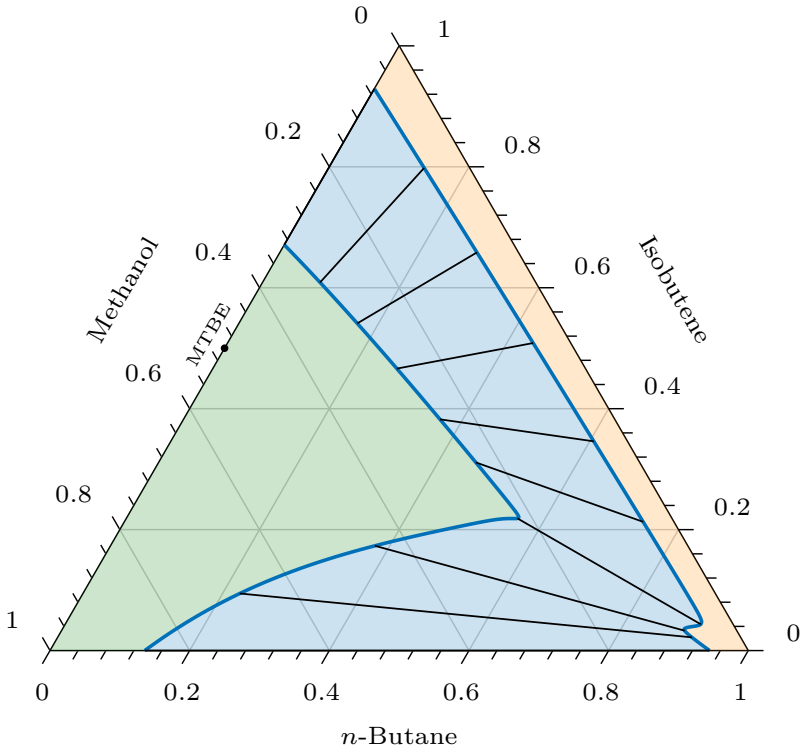

(a)

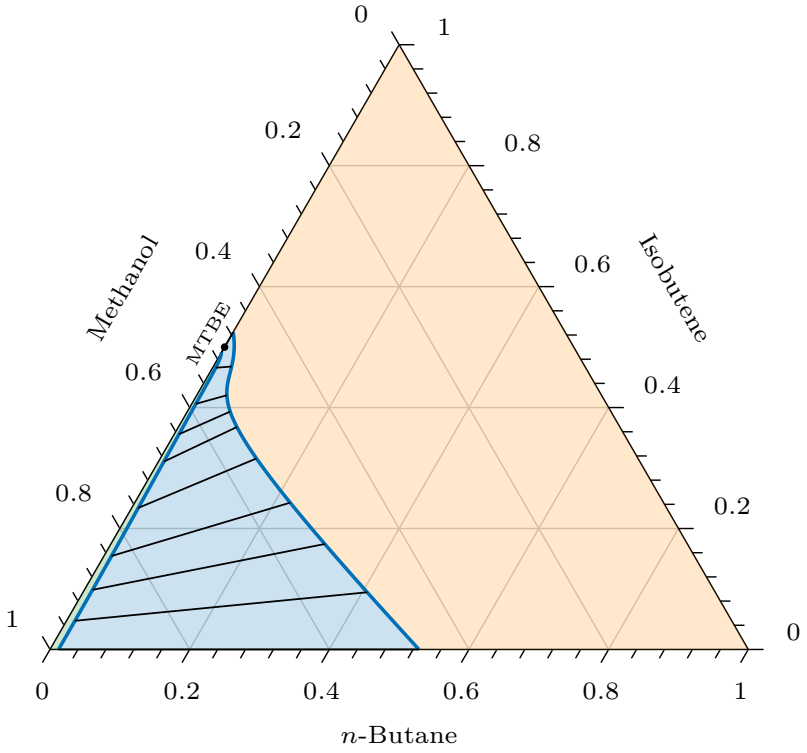

(b)

Figure 4.11: Ternary diagrams of elements in MTBE synthesis at 1 atm: (a) 280 K, (b) 320 K [binodal curve (—), tie lines (—), VLE region (▬), vapor region (▬), liquid region (▬)].

Transformed tie lines slopes are calculated by:

$$R_j = \frac{Y_j - X_j}{Y_1 - X_1} \qquad j = 2, ..., N_E \tag{4.35}$$

VLE results are compared with Bonilla-Petriciolet et al. (2008a) in Table 4.6. Chen et al. (2002) studied the kinetics in reactive distillation of TAME. In their analysis, two reactions take place in the column:

$$\text{2-CH}_3\text{-1-C}_4\text{H}_7 + \text{CH}_4\text{O} \rightleftharpoons \text{C}_6\text{H}_{14}\text{O} \tag{4.36}$$

$$\text{2-CH}_3\text{-2-C}_4\text{H}_7 + \text{CH}_4\text{O} \rightleftharpoons \text{C}_6\text{H}_{14}\text{O} \tag{4.37}$$

With the new reaction set, the number of elements is now $N_E = N_C - N_R = 5 - 2 = 3$. The formula matrix and stoichiometric matrix of the new system are given by:

$$\mathbf{A} = \begin{bmatrix} 1 & 1 & 0 & 1 & 0 \\ 0 & 0 & 1 & 1 & 0 \\ 0 & 0 & 0 & 0 & 1 \end{bmatrix} \qquad \mathbf{N} = \begin{bmatrix} -1 & 0 & -1 & 1 & 0 \\ 0 & -1 & -1 & 1 & 0 \end{bmatrix}^{\mathrm{T}} \tag{4.38}$$

The chemical equilibrium constants of reactions in Eq. 4.36 and 4.37 are K_1^{eq} and K_2^{eq} respectively. Bonilla-Petriciolet et al. (2008a) combined these reactions into a single reaction given by Eq. 4.32. The chemical equilibrium constant of the resulting reaction must be the product of the chemical equilibrium constants of the two reactions $K_{\mathrm{comb}}^{\mathrm{eq}} = K_1^{\mathrm{eq}} K_2^{\mathrm{eq}}$. Instead, Bonilla-Petriciolet et al. (2008a) disregarded the second chemical equilibrium constant and reported $K_{\mathrm{comb}}^{\mathrm{eq}} = K_1^{\mathrm{eq}}$. In this work we calculated the correct chemical equilibrium constant of the combined reaction and compared one- and two-reaction mixture VLE. A stoichiometric ratio of reactants and methanol/*n*-pentane ratio 2:1 was selected at 1.52 bar (Figure 4.12). According to Eq. 4.32, 2-methyl-1-butene and 2-methyl-2-butene are equivalent as reactants. In the single-phase regions, their concentrations are expected to be equal. Because they are isomers, their physical properties differ slightly and in the two-phase region their concentrations are not supposed to be very different (Figures 4.12b, 4.12d and 4.12f). Conversely, if we follow the two-reaction modeling of the system and subtract Eq. 4.37 from 4.36, we obtain:

$$\text{2-CH}_3\text{-1-C}_4\text{H}_7 \rightleftharpoons \text{2-CH}_3\text{-2-C}_4\text{H}_7 \tag{4.39}$$

Calculations are the same if Eq. 4.39 would replaced one of Eq. 4.36 or 4.37. Eq. 4.39 shows that one of the two isomer forms is more dominant and mole fractions are expected

to be different (Figures 4.12a, 4.12c and 4.12e). Finally, the chemical equilibrium constant of the combined reaction is larger, and we can expect higher concentrations of the heavier product (TAME) which will result in a heavier system, and therefore the vapor phase will appear at higher temperatures than the two-reaction system.

Table 4.6: Transformed tie line slopes R_2 and R_3 in TAME synthesis for the single-reaction system at 335 K and 1.52 bar.

Feed vector	Our work		Bonilla-Petriciolet et al. (2008a)	
	R_2	R_3	R_2	R_3
$[0.3\ 0.15\ 0.55\ 0\ 0]^{\mathrm{T}}$	-0.2083	–	-0.2072	–
$[0.32\ 0.2\ 0.48\ 0\ 0]^{\mathrm{T}}$	-0.2813	–	-0.2800	–
$[0.354\ 0.183\ 0.463\ 0\ 0]^{\mathrm{T}}$	-0.2869	–	-0.2856	–
$[0.2\ 0.07\ 0.73\ 0\ 0]^{\mathrm{T}}$	-0.0079	–	-0.0076	–
$[0.15\ 0.02\ 0.83\ 0\ 0]^{\mathrm{T}}$	0.0063	–	0.0064	–
$[0.27\ 0.3\ 0.43\ 0\ 0]^{\mathrm{T}}$	0.8050	–	0.8089	–
$[0.2\ 0.35\ 0.45\ 0\ 0]^{\mathrm{T}}$	-3.6530	–	-3.6767	–
$[0.1\ 0.35\ 0.55\ 0\ 0]^{\mathrm{T}}$	-8.4680	–	-8.5301	–
$[0.05\ 0.3\ 0.65\ 0\ 0]^{\mathrm{T}}$	-157.8824	–	-162.6184	–
$[0.025\ 0.3\ 0.675\ 0\ 0]^{\mathrm{T}}$	334.3359	–	327.5080	–
$[0.15\ 0.02\ 0.8\ 0\ 0.03]^{\mathrm{T}}$	0.0098	-1.2428	0.0099	-1.2428
$[0.1\ 0.1\ 0.6\ 0\ 0.2]^{\mathrm{T}}$	0.9404	-5.8388	0.9406	-5.8340
$[0.05\ 0.05\ 0.85\ 0\ 0.05]^{\mathrm{T}}$	0.8065	-6.2504	0.8069	-6.2438
$[0.1\ 0.15\ 0.7\ 0\ 0.05]^{\mathrm{T}}$	6.0678	-13.5463	6.0243	-13.4445
$[0.15\ 0.15\ 0.6\ 0\ 0.1]^{\mathrm{T}}$	0.8456	-4.0466	0.8465	-4.0396
$[0.07\ 0.17\ 0.64\ 0\ 0.12]^{\mathrm{T}}$	7.9465	-18.0942	7.9130	-18.0152

The number of elements in the two-reaction mixture is equal to three. Figure 4.13 shows the VLE region of the system at 335 K and 1.52 bar in terms of element mole fractions. The component that does not appear as a vertice of the triangle is TAME:

$$\text{TAME: } b_1 = b_2 \tag{4.40}$$

All the elements can exist as pure, therefore there are no infeasible regions.

4.1.7 Propene hydration

Castier et al. (1989), and Stateva and Wakeham (1997) examined the synthesis of 2-propanol by propene hydration:

$$C_3H_6 + H_2O \rightleftharpoons C_3H_8O \tag{4.41}$$

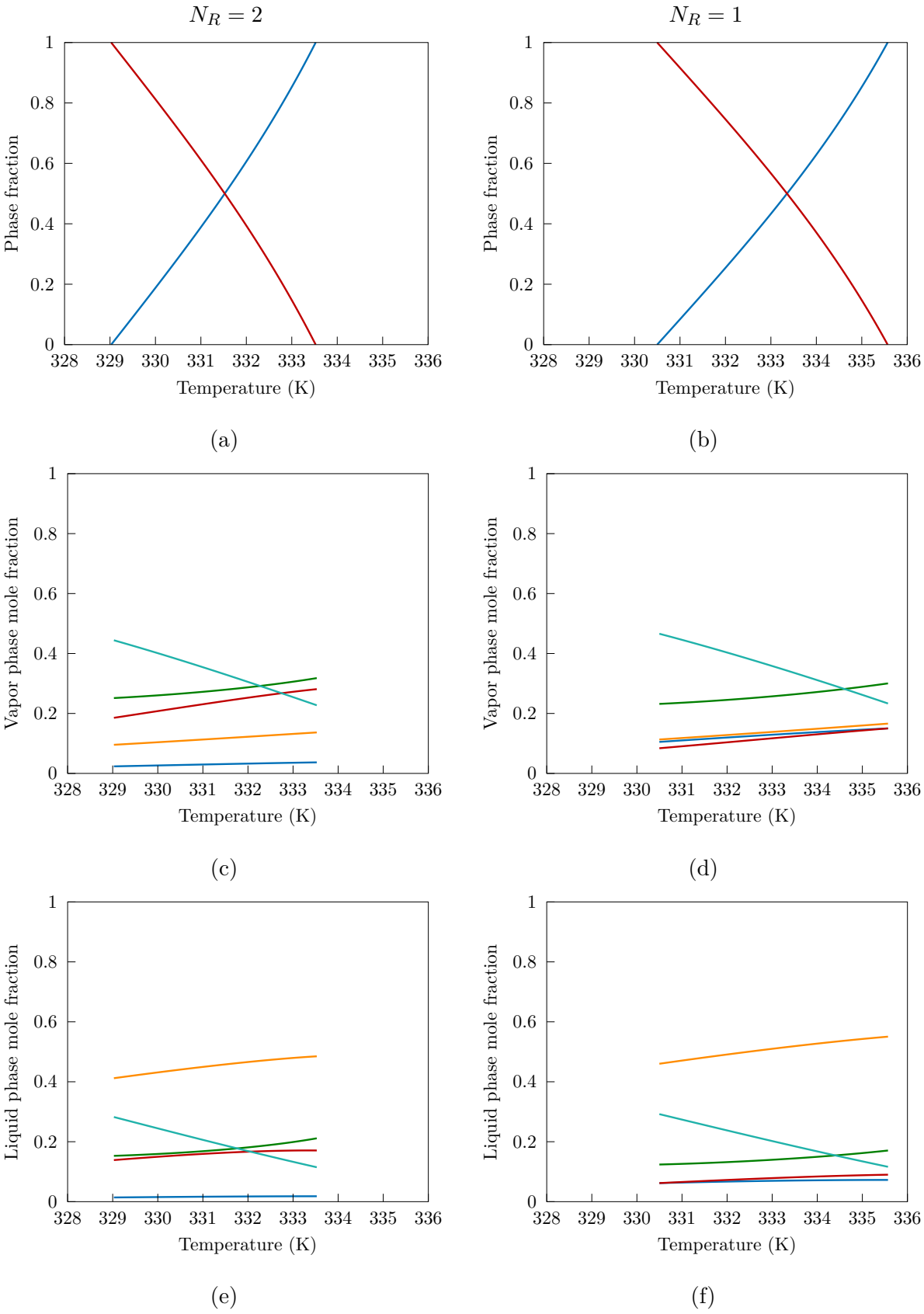

Figure 4.12: Equilibrium in the two- and one-reaction TAME synthesis for a stoichiometric ratio of reactants and methanol/*n*-pentane ratio equal to 2:1 at 1.52 bar: (a) phase fractions [vapor (—), liquid (—)], (b, c) mole fractions [2-methyl-1-butene (—), 2-methyl-2-butene (—), methanol (—), TAME (—), *n*-pentane (—)].

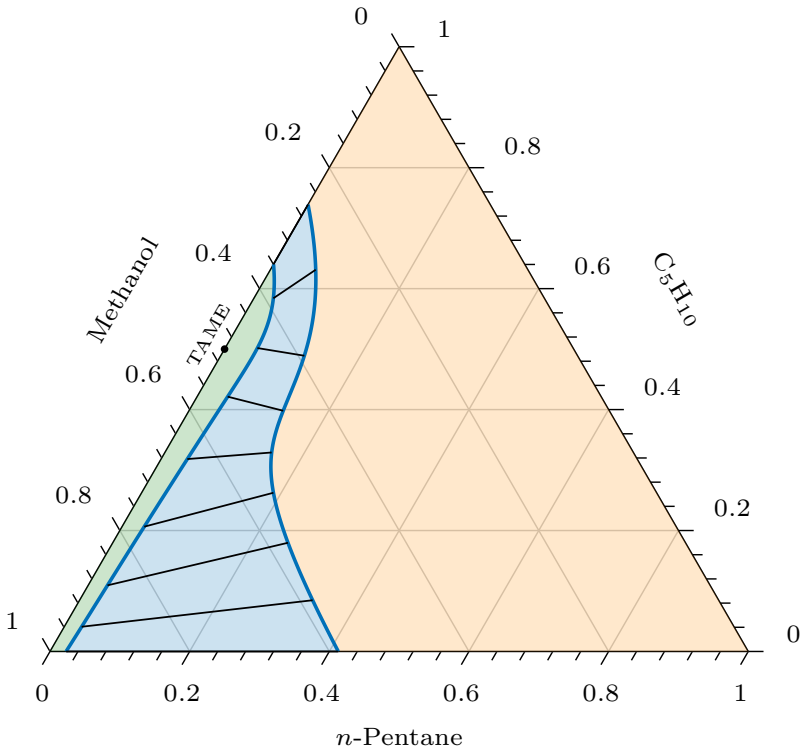

Figure 4.13: Ternary diagram of elements in the two-reaction TAME synthesis at 335 K and 1.52 bar [binodal curve (—), tie lines (—), VLE region (), vapor region (), liquid region ()].

in the presence of n-nonane as inert. The resulting equilibrium could lead to vapor-liquid and vapor-liquid-liquid mixtures, depending on the concentration of n-nonane in the feed. Bonilla-Petriciolet et al. (2008a) tested the same system without the inert and this is the approach we followed as well. The number of elements is $N_E = N_C - N_R = 3 - 1 = 2$. The formula matrix and stoichiometric matrix of the system are given by:

$$\mathbf{A} = \begin{bmatrix} 1 & 0 & 1 \\ 0 & 1 & 1 \end{bmatrix} \qquad \mathbf{N} = \begin{bmatrix} -1 & -1 & 1 \end{bmatrix}^{\mathrm{T}} \tag{4.42}$$

Vapor and liquid phases are described by the Soave-Redlich-Kwong equation of state (Soave, 1972) with all the binary interaction parameters k_{ij} set to zero (Bonilla-Petriciolet et al., 2008a). The chemical equilibrium constant was taken from Bonilla-Petriciolet et al. (2008a), and was considered temperature independent. Calculations are compared with Bonilla-Petriciolet et al. (2008a) in Table 4.7, using transformed compositions with 2-propanol as a reference component:

$$X_1 = \frac{x_1 + x_3}{1 + x_3} \tag{4.43}$$

If the chemical equilibrium constant is not temperature independent, we need to use

Table 4.7: Transformed compositions Y_1 and X_1 in propene hydration at 353.15 K.

Pressure (bar)	Our work		Bonilla-Petriciolet et al. (2008a)	
	Y_1	X_1	Y_1	X_1
1	0.3817	0.0002	0.3745	0.0002
10	0.9158	0.5673	0.9149	0.5663
30	0.9802	0.8648	0.9800	0.8649

equations Eq. 2.35 and 2.36 to determine its change with temperature. As a first approximation, we can assume that the non-zero enthalpy of reaction is temperature independent. Integrating Eq. 2.35 from a reference temperature T_0 to T:

$$\ln K^{\text{eq}}(T) = \ln K^{\text{eq}}(T_0) + \frac{\Delta_r H^\circ}{R}\left(\frac{1}{T_0} - \frac{1}{T}\right) \tag{4.44}$$

To calculate the enthalpy of reaction from Eq. 2.38, enthalpies of formation were taken from NIST Chemistry WebBook (2017). The reference temperature was selected as the temperature Bonilla-Petriciolet et al. (2008a) performed their calculations and the value of $\ln K^{\text{eq}}(T_0)$ is known ($T_0 = 353.15$ K). In Figure 4.14 the VLE of an equimolar feed of reactants at 1 bar is presented using a temperature independent and temperature dependent chemical equilibrium constant. The reaction is exothermic ($\Delta_r H^\circ < 0$), which results in an increase of the chemical equilibrium constant when the temperature decreases. The two-phase system exists in temperatures lower than T_0. Therefore, when the chemical equilibrium constant is temperature independent (Figures 4.14a, 4.14c and 4.14e), its value is lower than the temperature dependent chemical equilibrium constant (Figures 4.14b, 4.14d and 4.14f). When the effect of temperature is taken into account, the reaction progresses further and there is more product in the system. The product is 2-propanol and it is heavier than propene. It is expected that the higher K^{eq} allows the liquid phase to exist at higher temperatures (or the vapor phase to start appearing at higher temperatures). However, results do not seem to be very different in Figure 4.14. In the case reactions are nearly athermic ($\Delta_r H^\circ \approx 0$), they have a very weak dependence on temperature and the assumption of a temperature independent chemical equilibrium constant is reasonable. Of course, when such dependency is more prominent, we need to account for it through the use of enthalpies of reaction for more reliable calculations.

4.1.8 Cyclohexane synthesis

George et al. (1976) examined the synthesis of cyclohexane by benzene hydrogenation at high temperature:

$$\mathrm{C_6H_6} + 3\mathrm{H_2} \rightleftharpoons \mathrm{C_6H_{12}} \tag{4.45}$$

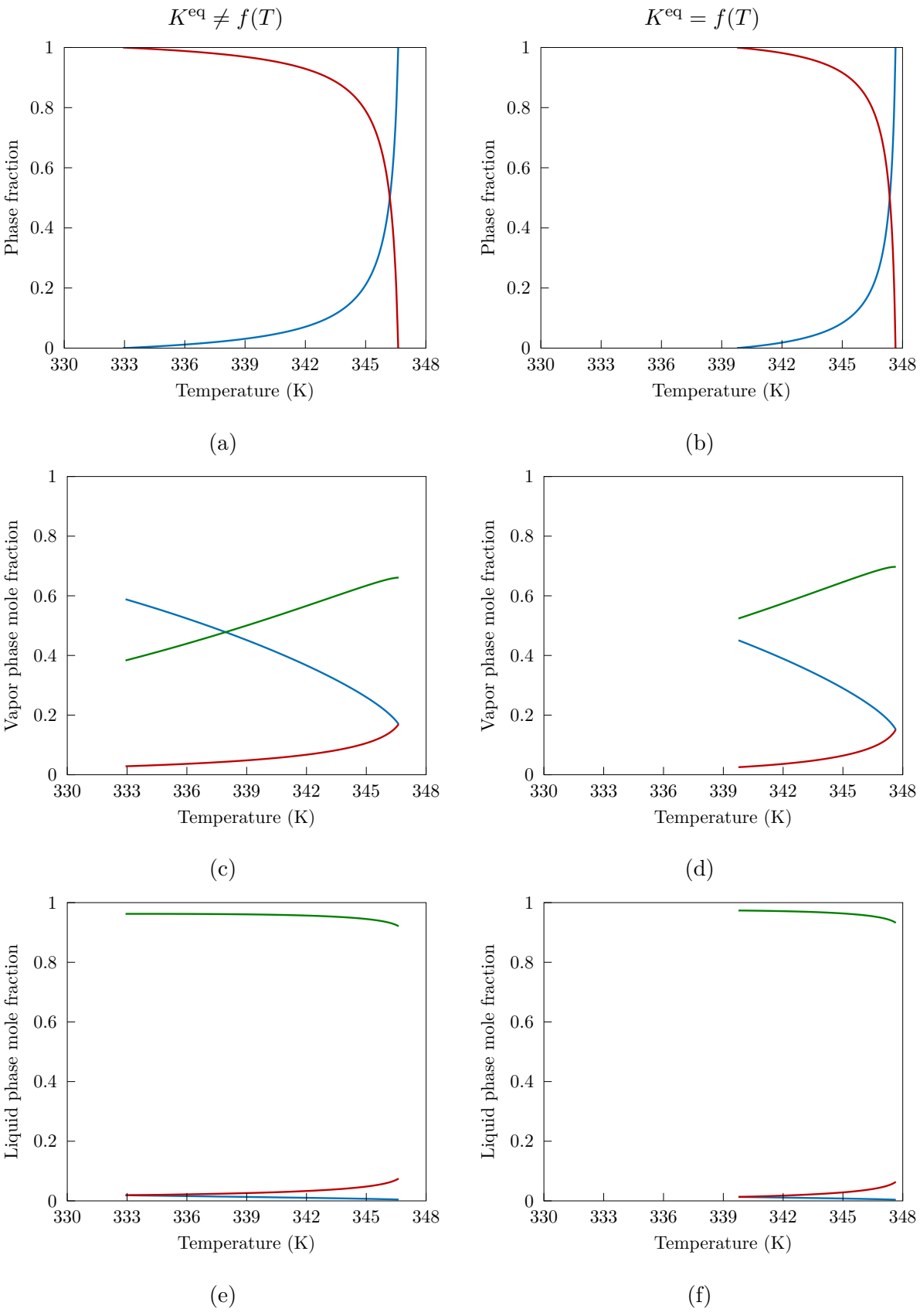

Figure 4.14: Equilibrium in propene hydration for an equimolar feed of reactants at 1 bar with temperature independent and dependent chemical equilibrium constant: (a, b) phase fractions [vapor (—), liquid (—)], (c, d, e, f) mole fractions [propene (—), water (—), 2-propanol (—)].

The number of elements is $N_E = N_C - N_R = 3 - 1 = 2$. The formula matrix and stoichiometric matrix of the system are given by:

$$\mathbf{A} = \begin{bmatrix} 1 & 0 & 1 \\ 0 & 1 & 3 \end{bmatrix} \qquad \mathbf{N} = \begin{bmatrix} -1 & -3 & 1 \end{bmatrix}^{\mathrm{T}} \tag{4.46}$$

Phase behavior is described by the Peng-Robinson equation of state (Peng and Robinson, 1976) with all binary interaction parameters k_{ij} set to zero, similar to Burgos-Solórzano et al. (2004). Gibbs energy of formation was taken from George et al. (1976). Calculations are shown in Table 4.8. Small differences with Burgos-Solórzano et al. (2004) are due to different chemical equilibrium constants. George et al. (1976) assumed that the system obeys the Lewis fugacity rule, which does not fully account for non-ideality of intermolecular forces and therefore predicted larger vapor phase fraction.

Table 4.8: Equilibrium mole fractions, phase amounts and phase fractions in cyclohexane synthesis at 500 K and 30 atm.

Component	Feed	Our work		Burgos-Solórzano et al. (2004)		George et al. (1976)	
		Vapor	Liquid	Vapor	Liquid	Vapor	Liquid
benzene	0.247	4.45×10^{-6}	5.43×10^{-6}	4.00×10^{-6}	4.92×10^{-6}	3.64×10^{-4}	3.87×10^{-4}
hydrogen	0.753	0.238	0.0204	0.249	0.0147	0.076	0.0023
cyclohexane	0	0.762	0.980	0.751	0.985	0.923	0.997
n_t (mol)	4.05	0.132	0.918	0.148	0.902	0.660	0.391
β		0.125	0.875	0.141	0.859	0.628	0.372

4.1.9 Methanol synthesis

Methanol synthesis is usually modeled in the literature (Castier et al., 1989; Stateva and Wakeham, 1997; Phoenix and Heidemann, 1998) by the following reactions:

$$\mathrm{CO} + 2\mathrm{H_2} \rightleftharpoons \mathrm{CH_4O} \tag{4.47}$$

$$\mathrm{CO_2} + \mathrm{H_2} \rightleftharpoons \mathrm{CO} + \mathrm{H_2O} \tag{4.48}$$

from a mixture of carbon monoxide, carbon dioxide, hydrogen and water with methane and *n*-octadecane as inerts. The number of elements is $N_E = N_C - N_R = 7 - 2 = 5$. The formula matrix and stoichiometric matrix of the system are given by:

$$\mathbf{A} = \begin{bmatrix} 1 & 1 & 0 & 0 & 1 & 0 & 0 \\ 0 & 1 & 0 & 1 & 0 & 0 & 0 \\ 0 & 0 & 1 & 1 & 2 & 0 & 0 \\ 0 & 0 & 0 & 0 & 0 & 1 & 0 \\ 0 & 0 & 0 & 0 & 0 & 0 & 1 \end{bmatrix} \qquad \mathbf{N} = \begin{bmatrix} -1 & 0 & -2 & 0 & 1 & 0 & 0 \\ 1 & -1 & -1 & 1 & 0 & 0 & 0 \end{bmatrix}^{\mathrm{T}} \tag{4.49}$$

Phase behavior is described by the Soave-Redlich-Kwong equation of state (Soave, 1972) with binary interaction parameters k_{ij} from Castier et al. (1989). Reference state (ideal gas) chemical potentials at 473.15 K and 1 bar were taken from Phoenix and Heidemann (1998). In Tables 4.9 and 4.10 VLE and VLLE results are presented for two different feeds. Results from Stateva and Wakeham (1997), and Castier et al. (1989) are also included for comparison. The heavy hydrocarbon *n*-octadecane leads to the separation of the liquid phases and the conditions permit the presence of a vapor phase. Larger deviations are observed with the calculations from Stateva and Wakeham (1997), while both authors use different values for the chemical equilibrium constants.

Table 4.9: Equilibrium mole fractions, phase amounts and phase fractions in methanol synthesis at 473.15 K and 300 bar.

Component	Feed	Our work		Stateva and Wakeham (1997)		Castier et al. (1989)	
		Vapor	Liquid	Vapor	Liquid	Vapor	Liquid
carbon monoxide	0.15	6.27×10^{-5}	1.09×10^{-5}	1.33×10^{-5}	traces	6.51×10^{-5}	1.08×10^{-5}
carbon dioxide	0.08	0.0006	0.0003	traces	traces	0.0005	0.0002
hydrogen	0.74	0.6597	0.0970	0.6493	0.0948	0.6589	0.0962
water	0	0.0471	0.2432	0.0464	0.2488	0.0473	0.2436
methanol	0	0.2045	0.6349	0.2120	0.6371	0.2053	0.6354
methane	0.3	0.0880	0.0246	0.0923	0.0193	0.0878	0.0246
n-octadecane	0	0	0	0	0	0	0
n_t (mol)	100	26.346	27.702	–	–	26.421	27.622
β		0.4875	0.5125	0.4968	0.5032	0.4889	0.5111

Table 4.10: Equilibrium mole fractions, phase amounts and phase fractions in methanol synthesis at 473.15 K and 101.3 bar.

Component	Feed	Our work			Stateva and Wakeham (1997)			Castier et al. (1989)		
		Vapor	Liquid (aq)	Liquid (org)	Vapor	Liquid (aq)	Liquid (org)	Vapor	Liquid (aq)	Liquid (org)
carbon monoxide	0.1071	0.0010	7.00×10^{-6}	0.0002	5.63×10^{-8}	1.27×10^{-10}	4.80×10^{-9}	0.0011	6.82×10^{-6}	0.0002
carbon dioxide	0.0571	0.0548	0.0025	0.0271	7.27×10^{-12}	2.96×10^{-6}	3.18×10^{-12}	0.0534	0.0024	0.0270
hydrogen	0.5286	0.5741	0.0059	0.1091	0.5328	0.0071	0.0600	0.5731	0.0058	0.1159
water	0.2143	0.1718	0.7715	0.1104	0.1635	0.7047	0.0070	0.1722	0.7709	0.1116
methanol	0	0.1426	0.2197	0.2767	0.2274	0.2870	0.1418	0.1441	0.2205	0.2753
methane	0.0214	0.0544	0.0004	0.0182	0.0752	0.0011	0.0210	0.0546	0.0004	0.0192
n-octadecane	0.0715	0.0014	1.18×10^{-14}	0.4582	0.0010	2.70×10^{-6}	0.7702	0.0015	1.31×10^{-15}	0.4507
n_t (mol)	140	47.702	31.285	21.673	–	–	–	46.917	31.508	22.030
β		0.4739	0.3108	0.2153	0.4843	0.3780	0.1377	0.4670	0.3136	0.2193

4.2 Transesterification of fatty acid triglycerides with methanol

Biodiesel is a liquid mixture of fatty acid esters, which are alkyl monoesters of long alkyl-chain (fatty) acids (Perdomo et al., 2013; Wu et al., 2016). It is not as toxic as traditional diesel, biodegrades faster, has a higher cetane number and flash point, and is practically free from sulfur components, that can lead to hazardous emissions from combustion. Furthermore, biodiesel is produced from renewable sources and is an alternative to conventional fossil fuels (Perdomo et al., 2013; Anikeev, 2014; Yancy-Caballero and Guirardello, 2015; Wu et al., 2016). Esters in biodiesel can be also applied in polymerizations as substrates (da Roza et al., 2012).

Biodiesel production can be achieved through a number of processes: esterification, transesterification, blending, cracking, microemulsification, and pyrolysis (Yancy-Caballero and Guirardello, 2015). Transesterification of vegetable oils and animal fats with different alcohols at low pressures is usually the preferred method for biodiesel synthesis (Voll et al., 2011) and homogeneous catalyzed transesterification is mainly employed. Acidic or basic (NaOH, KOH, CH_3ONa) catalysts are used, while non-catalytic synthesis is also reported with sub- and supercritical alcohols (Anikeev, 2014; Voll et al., 2011). Two liquid phases are expected at equilibrium, a fatty acid methyl-ester and a glycerol rich phase (Yancy-Caballero and Guirardello, 2015). Due to its low cost and availability, methanol is the alcohol selected for the reaction. Equilibrium is shifted toward favorable equilibrium yields using an excess of the alcohol (Likozar and Levec, 2014; Perdomo et al., 2013; Wu et al., 2016; Yancy-Caballero and Guirardello, 2015, 2013). Glycerol is a by-product of transesterification that is separated after equilibrium has been established (Yancy-Caballero and Guirardello, 2013) and can find different applications (Perdomo et al., 2013; Liu et al., 2016). Soybean, algal, canola, sunflower, cotton, palm, and coconut oil are used in the reactions (Likozar and Levec, 2014; Yancy-Caballero and Guirardello, 2015). Interest has shifted toward non-edible oils such as linseed, castor, Karanja, neem, rubber, jatropha and cashew oil (Mathiarasi and Partha, 2016). Second generation biofuels involve the transesterification with oils from hazardous waste (Perdomo et al., 2013). As far as the synthesis is concerned, water in the system can lead to reduced yields due to two phenomena: acceleration of ester hydrolysis to fatty acids reacting with the basic catalyst to produce even more water, and shift of the hydroxide/alkoxide equilibrium to hydroxide, reducing the concentration of the true catalyst, which is the methoxide ions (Wu et al., 2016). Finally, saponification can take place between glycerin and the basic catalyst (Wu et al., 2016).

Anikeev et al. (2012) and Anikeev (2014) examined the successive transesterifications of a triglyceride with methanol, according to the following reaction scheme:

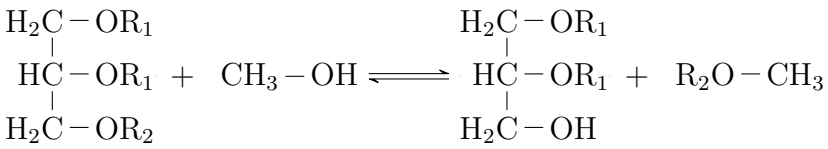

(4.50)

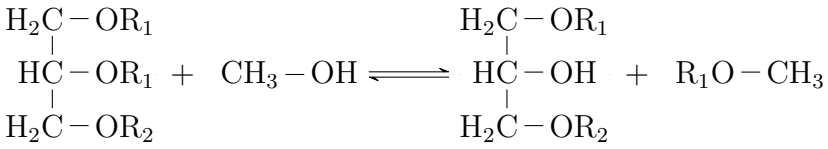

(4.51)

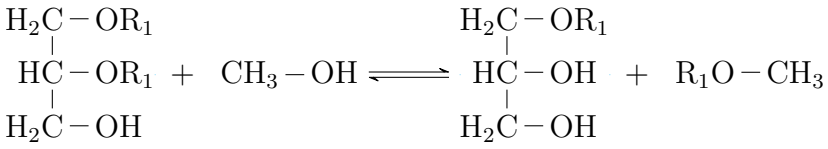

(4.52)

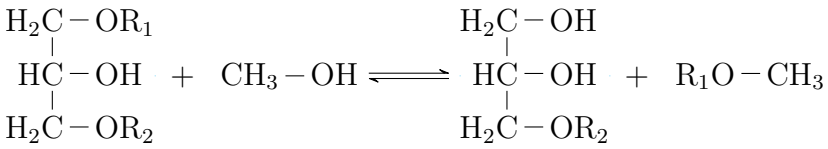

(4.53)

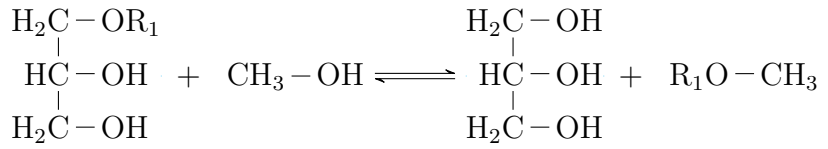

(4.54)

At each step the group $-OR_1$ or $-OR_2$ is substituted by a $-OH$, until glycerol is obtained. The authors showed calculations for a single vapor phase and two starting components: palmitic-palmitic-oleic and oleic-linoleic-linoleic triglycerides. Both compounds share the same R_2 group but differ in their R_1 group. The chemical compositions of all components and elements for the two transesterification systems is presented in Table 4.11. The number of elements is $N_E = N_C - N_R = 9 - 5 = 4$. The formula matrix and stoichiometric matrix of the system are given by:

$$\mathbf{A} = \begin{bmatrix} 1 & 3 & 3 & 3 & 3 & 3 & 3 & 1 & 1 \\ 3 & 2 & 3 & 3 & 4 & 4 & 5 & 2 & 2 \\ 0 & 2 & 2 & 1 & 1 & 0 & 0 & 1 & 0 \\ 0 & 1 & 0 & 1 & 0 & 1 & 0 & 0 & 1 \end{bmatrix}$$

$$\mathbf{N} = \begin{bmatrix} -1 & -1 & 1 & 0 & 0 & 0 & 0 & 0 & 1 \\ -1 & -1 & 0 & 1 & 0 & 0 & 0 & 1 & 0 \\ -1 & 0 & -1 & 0 & 1 & 0 & 0 & 1 & 0 \\ -1 & 0 & 0 & -1 & 0 & 1 & 0 & 1 & 0 \\ -1 & 0 & 0 & 0 & -1 & 0 & 1 & 1 & 0 \end{bmatrix}^{\mathrm{T}} \tag{4.55}$$

Table 4.11: Component and element numbering for the PPOFAG ($R_1 \equiv C_{16}H_{31}O$) and OLLFAG transesterification ($R_1 \equiv C_{18}H_{33}O$) systems (for both mixtures $R_2 \equiv C_{18}H_{31}O$).

	Component	Element
1	CH_4O	CHO
2	$C_3H_5O_3(R_1)_2R_2$	H
3	$C_3H_6O_3(R_1)_2$	R_1
4	$C_3H_6O_3R_1R_2$	R_2
5	$C_3H_7O_3R_1$	
6	$C_3H_7O_3R_2$	
7	$C_3H_8O_3$	
8	CH_3OR_1	
9	CH_3OR_2	

The compounds that exist in both mixtures are shown in Table 4.12. Phase behavior is described by the Peng-Robinson equation of state (Peng and Robinson, 1976) with all binary interaction parameters k_{ij} set to zero. Critical constants and acentric factors were predicted by Anikeev (2014) and chemical equilibrium constants were taken from the same authors. Figures 4.15 and 4.16 show phase and mole fractions at equilibrium for both systems at 1 atm and triglyceride/methanol ratio equal to 1:3.

For the temperature window selected, both systems can mostly exist as a two- or three-phase mixture. At lower temperatures, we begin with LLE of an ester-rich phase (CH_3OR_1, CH_3OR_2) and a glycerol-rich phase. At higher temperatures, a vapor phase can appear. After the vapor phase appears, increasing the temperature decreases more rapidly the amount of the glycerol-rich liquid phase, which eventually leads to VLE. For the PPOFAG transesterification, at higher temperatures both liquid phases disappear and it can exist as a single-vapor phase.

4.3 Speed and convergence[†]

Computational efficiency of algorithms in the literature is usually reported as CPU time and/or number of iterations. Total CPU time for each system at specified conditions is presented for both algorithms in Table 4.13. This reflects the time needed by each algorithm to determine the equilibrium solution including initialization, solving for simultaneous chemical and phase equilibrium, and finally, stability analysis. The successive substitution algorithm is entirely a first-order method, whereas the combined algorithm uses a second-order method for final convergence. Nevertheless, the latter requires calculation of derivatives and inversion of matrices, which could make the method not as fast as expected. In other words, absolute CPU time is not proportional to the number of the iterations. Although the speed is an indication of the efficiency of the algorithm, results in

[†]Appears in Tsanas et al. (2017a,b)

Table 4.12: Compounds in triglyceride esterification.

Compound	Abbreviation (Anikeev et al., 2012)	Chemical formula
Palmitic-palmitic-oleic fatty acid glyceride	PPOFAG	$H_2C-OOC_{16}H_{31}$ $HC-OOC_{16}H_{31}$ $H_2C-OOC_{18}H_{33}$
Oleic-linoleic-linoleic fatty acid glyceride	OLLFAG	$H_2C-OOC_{18}H_{31}$ $HC-OOC_{18}H_{31}$ $H_2C-OOC_{18}H_{33}$
Palmitic-palmitic fatty acid di-glyceride	PPDFADIG	$H_2C-OOC_{16}H_{31}$ $HC-OOC_{16}H_{31}$ H_2C-OH
Linoleic-linoleic fatty acid di-glyceride	LLDFADIG	$H_2C-OOC_{18}H_{31}$ $HC-OOC_{18}H_{31}$ H_2C-OH
Palmitic-oleic fatty acid di-glyceride	PODFADIG	$H_2C-OOC_{16}H_{31}$ $HC-OH$ $H_2C-OOC_{18}H_{33}$
Linoleic-oleic fatty acid di-glyceride	LOFADIG	$H_2C-OOC_{18}H_{31}$ $HC-OH$ $H_2C-OOC_{18}H_{33}$
Palmitic fatty acid mono-glyceride	PFAMONOG	$H_2C-OOC_{16}H_{31}$ $HC-OH$ H_2C-OH
Linoleic fatty acid mono-glyceride	LFAMONOG	$H_2C-OOC_{18}H_{31}$ $HC-OH$ H_2C-OH
Oleic fatty acid mono-glyceride	OFAMONOG	H_2C-OH $HC-OH$ $H_2C-OOC_{18}H_{33}$
Glycerol	–	H_2C-OH $HC-OH$ H_2C-OH
Palmitic fatty acid methyl ester	PFAME	$C_{16}H_{31}OOCH_3$
Linoleic fatty acid methyl ester	LFAME	$C_{18}H_{31}OOCH_3$
Oleic fatty acid methyl ester	OFAME	$C_{18}H_{33}OOCH_3$

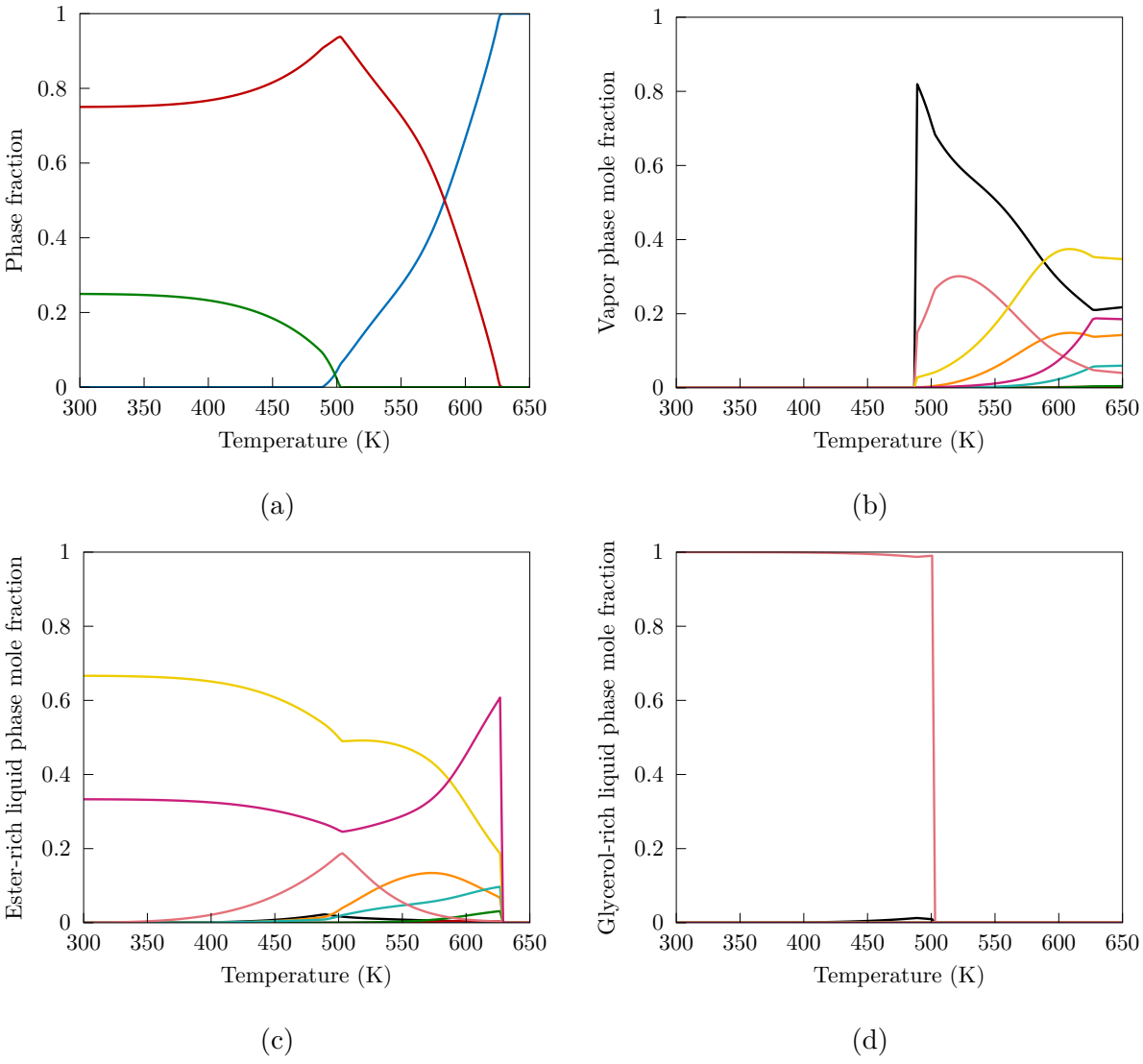

Figure 4.15: Equilibrium in PPOFAG transesterification with methanol and PPOFAG/methanol ratio equal to 1:3 at 1 atm: (a) phase fractions [vapor (—), ester-rich liquid (—), glycerol-rich liquid (—)], (b, c, d) mole fractions [methanol (—), PPOFAG (—), PPFADIG (—), POFADIG (—), PFAMONOG (—), OFAMONOG (—), glycerol (—), PFAME (—), OFAME (—)].

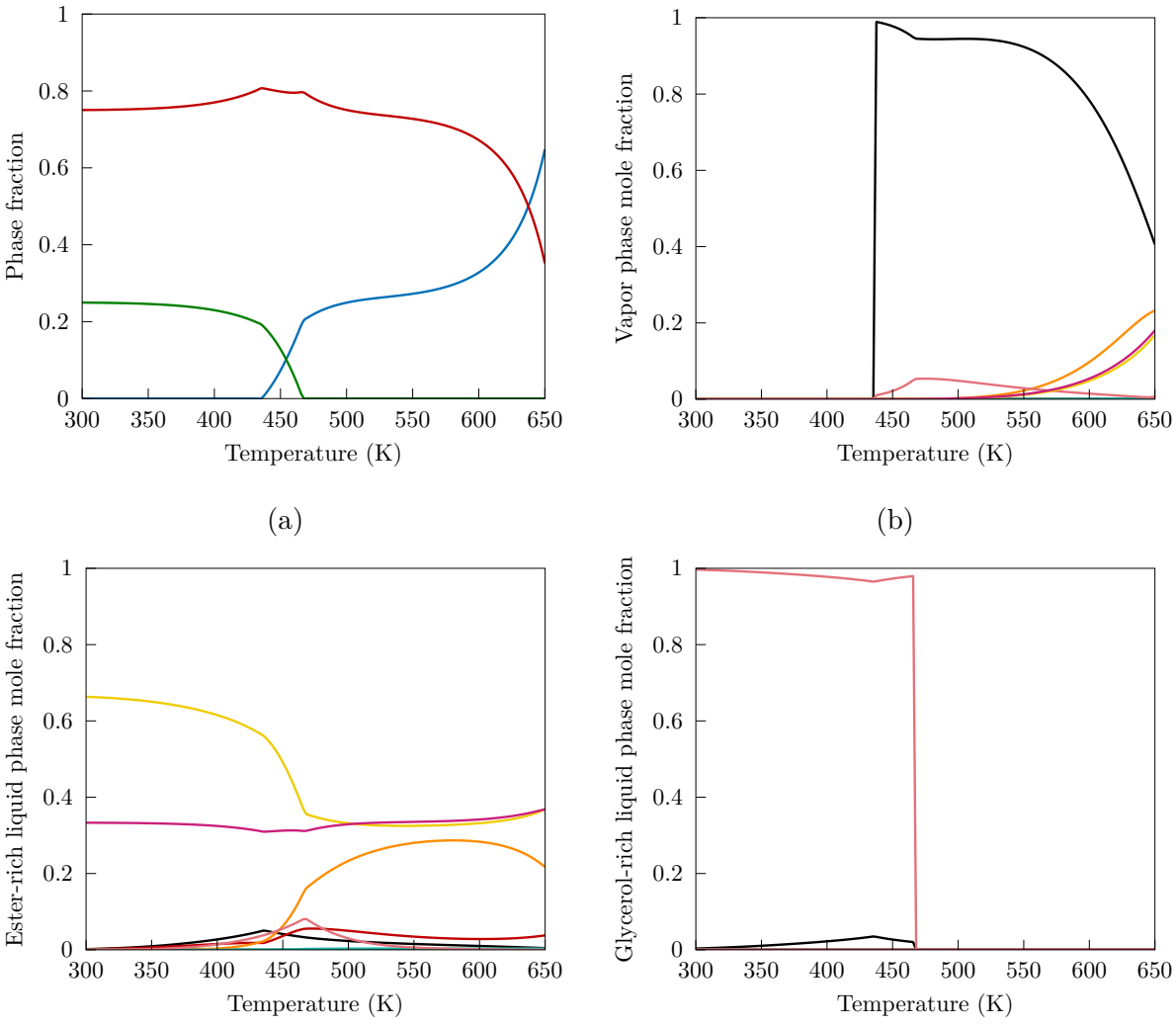

Figure 4.16: Equilibrium in OLLFAG transesterification with methanol and OLLFAG/methanol ratio equal to 1:3 at 1 atm: (a) phase fractions [vapor (—), ester-rich liquid (—), glycerol-rich liquid (—)], (b, c, d) mole fractions [methanol (—), OLLFAG (—), LLFADIG (—), LOFADIG (—), LFAMONOG (—), OFAMONOG (—), glycerol (—), LFAME (—), OFAME (—)].

Table 4.13 are not universally conclusive. CPU time depends on the thermodynamic model selected. Simple models are expected to provide faster equilibrium results. Especially for ideal systems, the outer loop (non-ideality update) in the successive substitution algorithm is not required because components have composition independent fugacity or activity coefficients. It should not be overlooked that CPU time depends also on the implementation of the method that has to do with the efficiency of matrix manipulation (e.g. inversion, solution of linear systems, etc.). Finally, CPU time can differ due to the hardware, computer language and compilers.

Table 4.13: CPU time to obtain the equilibrium solution of the systems examined (SSA: successive substitution algorithm, CA: combined algorithm, processor: Intel®Core™ i7-5500U CPU@ 2.40 GHz).

System	T (K)	p	N_P	SSA (ms)	CA (ms)
Formaldehyde/water	310	1 atm	2	1.28	–
Xylene separation	350	0.05 atm	2	1.31	–
Acetic acid/ethanol	355	1 atm	2	1.72	1.46
Acetic acid/1-butanol	370	1 atm	2	1.62	1.48
MTBE synthesis	320.92	1 atm	2	1.87	1.30
TAME synthesis ($N_R = 2$)	330	1.52 bar	2	1.60	1.37
Propene hydration [$K^{\text{eq}} \neq f(T)$]	345	1 bar	2	1.45	1.47
Cyclohexane synthesis	500	30 atm	2	1.48	1.30
Methanol synthesis	473.15	101.3 bar	3	3.08	2.23
PPOFAG	500	1 atm	3	3.07	3.25
OLLFAG	450	1 atm	3	2.82	3.06

Apart from the CPU time, we also present the number of iterations of each solution procedure in both algorithms (Figures 4.17 to 4.25): Q-function minimization, main calculation for each phase set, and the number of inner-loop (Newton) iterations per outer loop non-ideality update when the Lagrange multipliers method is employed. Stability analysis iterations are not shown. Minimization of Q-function follows the same trend in both algorithms, since this is a common initialization routine. Change of the error at each iteration reveals the convergence rate type of each algorithm. Successive substitution figures show linear convergence rate and require more iterations to reach the Gibbs energy minimum. In the figures of the combined algorithm, after three iterations of successive substitution, it is evident that the error reduces quadratically, as a result of accelerated calculations by the modified RAND method. Direct comparison of the algorithms shows in general a decrease in the iteration number when the combined algorithm is used. The difference can be small for some examples, such as propene hydration, and for others it ranges from two to even five times fewer iterations. The number of inner loop iterations in the successive substitution algorithm is decreasing the closer we approach to the final solution. However, the iteration number is sensible for the Lagrange multipliers method, taking into account that a linearly convergent method is expected to be slower. The

number of iterations is also not conclusive about the efficiency of the calculations or the speed. Single iteration cost is not the same for the different algorithms. The number of iterations depends on initial estimates and the convergence criterion tolerance. Whenever a comparison with the literature can be made, the factors that affect CPU time or number of iterations must be considered.

- Formaldehyde/water mixture and xylene separation

  Both systems are ideal and there is no need of an outer loop to update fugacity or activity coefficients. Successive substitution algorithm attains quadratic convergence rate and the combined algorithm does not require to switch calculations to the modified RAND. No convergence behavior is presented.

- Esterification of acetic acid with ethanol

  The initial assumption is a single vapor phase, which does not require the nested-loop procedure to converge. Vapor phase is ideal and the total mole numbers do not change due to the reaction. These are the conditions under which the Q-function minimization can yield the equilibrium solution of the single-phase assumption (section 3.2.3). For this reason, only the convergence behavior of the two-phase system appears in Figure 4.17.

  Xiao et al. (1989) studied the application of two stoichiometric algorithms, the S-C (Sanderson and Chien, 1973) and the KZ algorithm. The S-C algorithm follows the conventional stoichiometric approach using nested loops. In the inner loop the phase equilibrium problem is solved based on the Rachford-Rice equation and successive substitution. In the outer loop, the reaction extents are updated. The KZ algorithm is proposed by the authors as an improvement of the S-C algorithm. In this new formulation, the loops of the S-C algorithm are switched. The algorithms mentioned in Xiao et al. (1989) should be comparable with the successive substitution algorithm in this work, since all three are based on a nested-loop procedure. To fully converge to the solution, the successive substitutuion algorithm needed 44 outer loop iterations (106 Newton iterations), the combined algorithm 3 (12 Newton iterations and 4 modified RAND iterations), the S-C algorithm 10 (42 Newton iterations) and the KZ algorithm 9 (23 Newton iterations). The reason why our successive substitution algorithm needs almost three times as many iterations as the slower S-C algorithm is probably because Xiao et al. (1989) used a very lose convergence criterion. They calculated the K-factors of VLE as $K_i = y_i/x_i$ and the procedure stopped when $\sum_{i=1}^{N_C}(K_i^{\text{new}}/K_i - 1)^2 < 10^{-6}$. In our method, convergence was assumed after tighter criteria, when the error given by Eq. 3.77 is less than 10^{-10}. The combined algorithm is superior with a total of 12 inner loop iterations and only 4 additional RAND iterations to fully converge. Finally, in Xiao et al. (1989) the initial assumption is a two-phase mixture, in contrast with our approach, where we assume a single phase and later test if an additional phase must be considered.

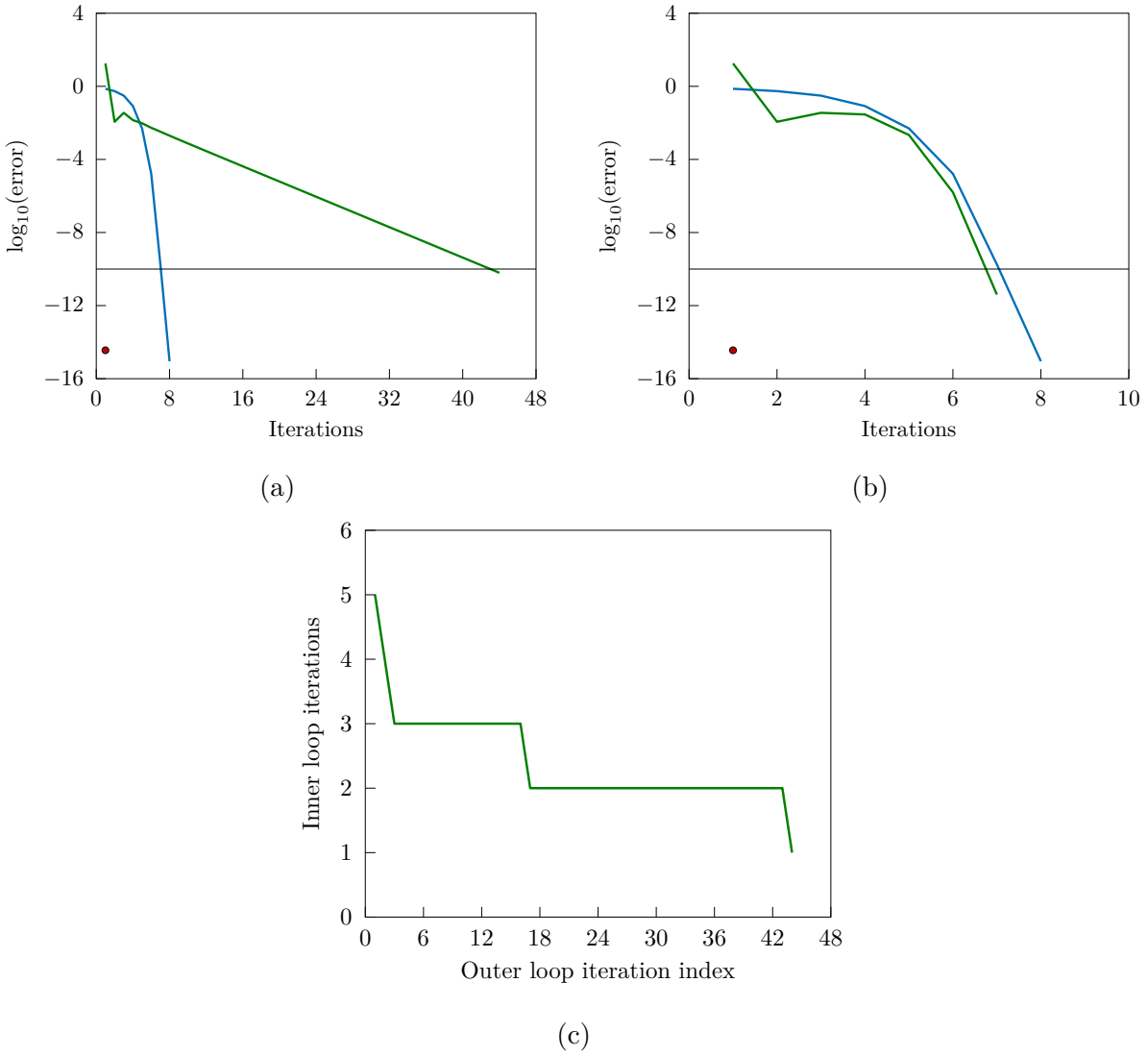

Figure 4.17: Convergence in acetic acid/ethanol esterification for an equimolar feed of reactants at 355 K and 1 atm: (a) successive substitution algorithm, (b) combined algorithm, (c) inner loop (Newton) iterations per outer loop non-ideality updates [Q-function minimization (—), V (●), VL (—)].

Castier et al. (1989) presented a second-order stoichiometric method. The authors initialize calculations with direct substitution aided by the General Dominant Eigenvalue Method (GDEM) (Crowe and Nishio, 1975) for accelerated calculations. Final convergence is achieved with Murray's minimization. It is suggested in their method to use 5 direct substitution iterations followed by 1 GDEM step for the single-phase chemical equilibrium, 2 GDEM steps for two-phase systems and 3 GDEM steps for three-phase systems. They also mention which criteria must be met to skip GDEM and enter Murray's minimization. The Murray steps are very efficient and are used only for final convergence. The authors performed their calculations at slightly higher temperature than the one in this work (358.15 K). When the vapor phase was considered ideal, a single vapor phase exists at equilibrium with 3 Murray iterations. Conversely, when an EoS that accounts for the acid dimerization is used, the inital assumption of a vapor phase needed 3 Murray iterations and the final vapor-liquid mixture needed 2 Murray iterations.

- Esterification of acetic acid with 1-butanol

  Bonilla-Petriciolet et al. (2008a) applied simulated annealing to determine the equilibrium of two-phase reaction systems. Their algorithm belongs to stochastic optimization methods formulated as a stoichiometric problem. Their procedure involves solving for CPE at specific conditions, using different feeds and initial estimates. At the end they report total number of function evaluations and success rate, showing the percentage of the initial estimates that will actually lead to the equilibrium solution. For this system, they mention total time of 40 s compared to our 1.62 ms with successive substitution and 1.48 with the combined algorithm. Moreover, the authors report 0% and 3% success rate for two feed compositions they chose to demostrate the algorithm performance, while our algorithms did not face problems with the same feeds.

- MTBE synthesis

  Castier et al. (1989) tested the system under different conditions from this work. Calculations were made for the temperature window of the two-phase system at 5.07 bar with 1-butene as inert instead of *n*-butane. Initialization in our work needed 9 iterations. The successive substitution algorithm required for the single-phase reaction 9 outer loop iterations (25 Newton iterations) and for the two-phase system 30 (73 Newton iterations). With the combined algorithm L and VL phase sets needed 3 outer loop iterations (13 and 14 Newton iterations) and additionally 3 and 4 modified RAND iterations respectively. Castier et al. (1989) reported 2 Murray iterations for the single-phase convergence and 1 Murray iteration for the two-phase system. No further information was given for the initialization iterations.

- TAME synthesis

  Bonilla-Petriciolet et al. (2008a) reported total time of 85 s compared with our 1.60 ms with successive substitution and 1.37 with the combined algorithm. For all the

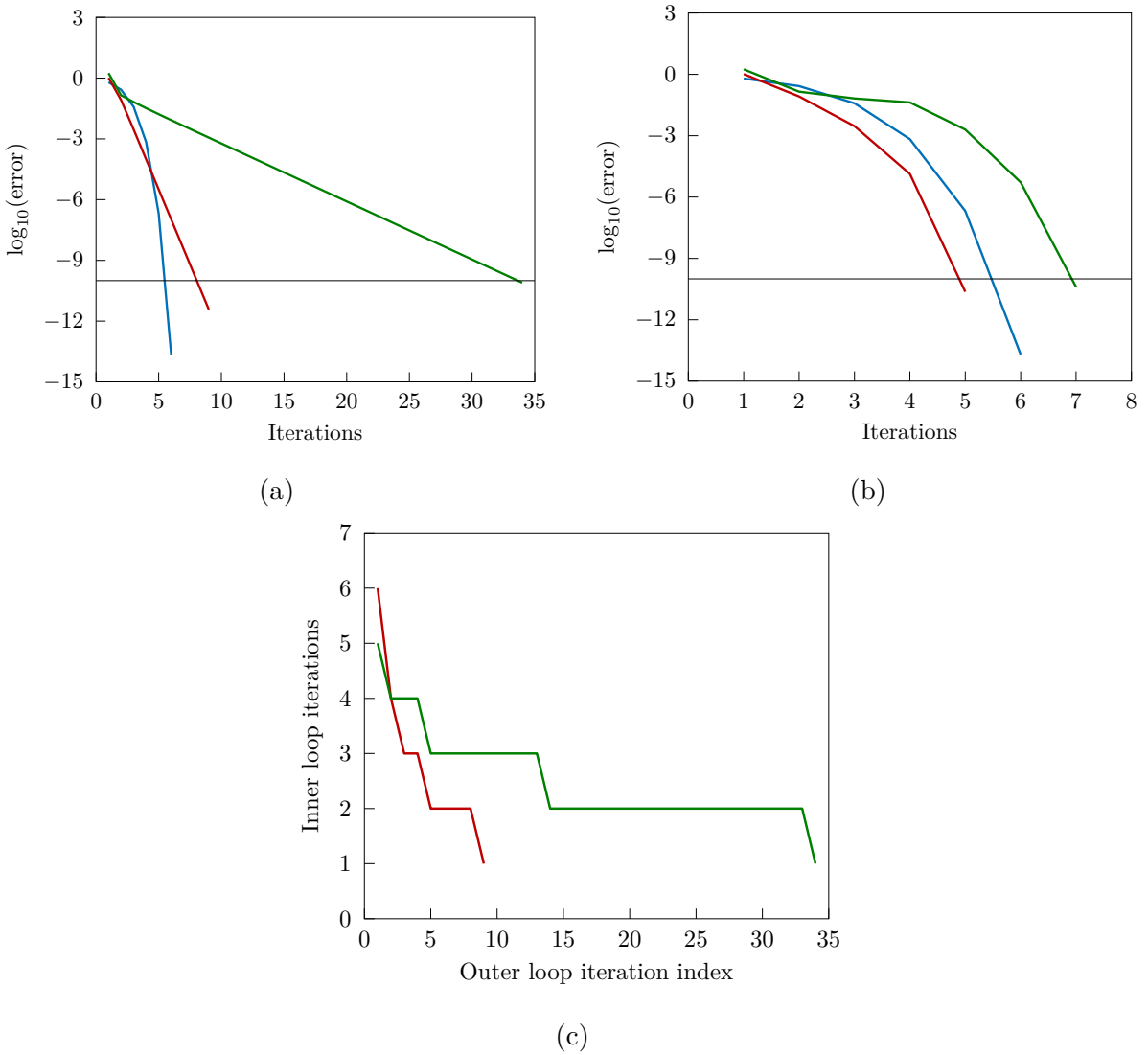

Figure 4.18: Convergence in acetic acid/1-butanol esterification for an equimolar feed of reactants at 370 K and 1 atm: (a) successive substitution algorithm, (b) combined algorithm, (c) inner loop (Newton) iterations per outer loop non-ideality updates [Q-function minimization (—), L (—), VL (—)].

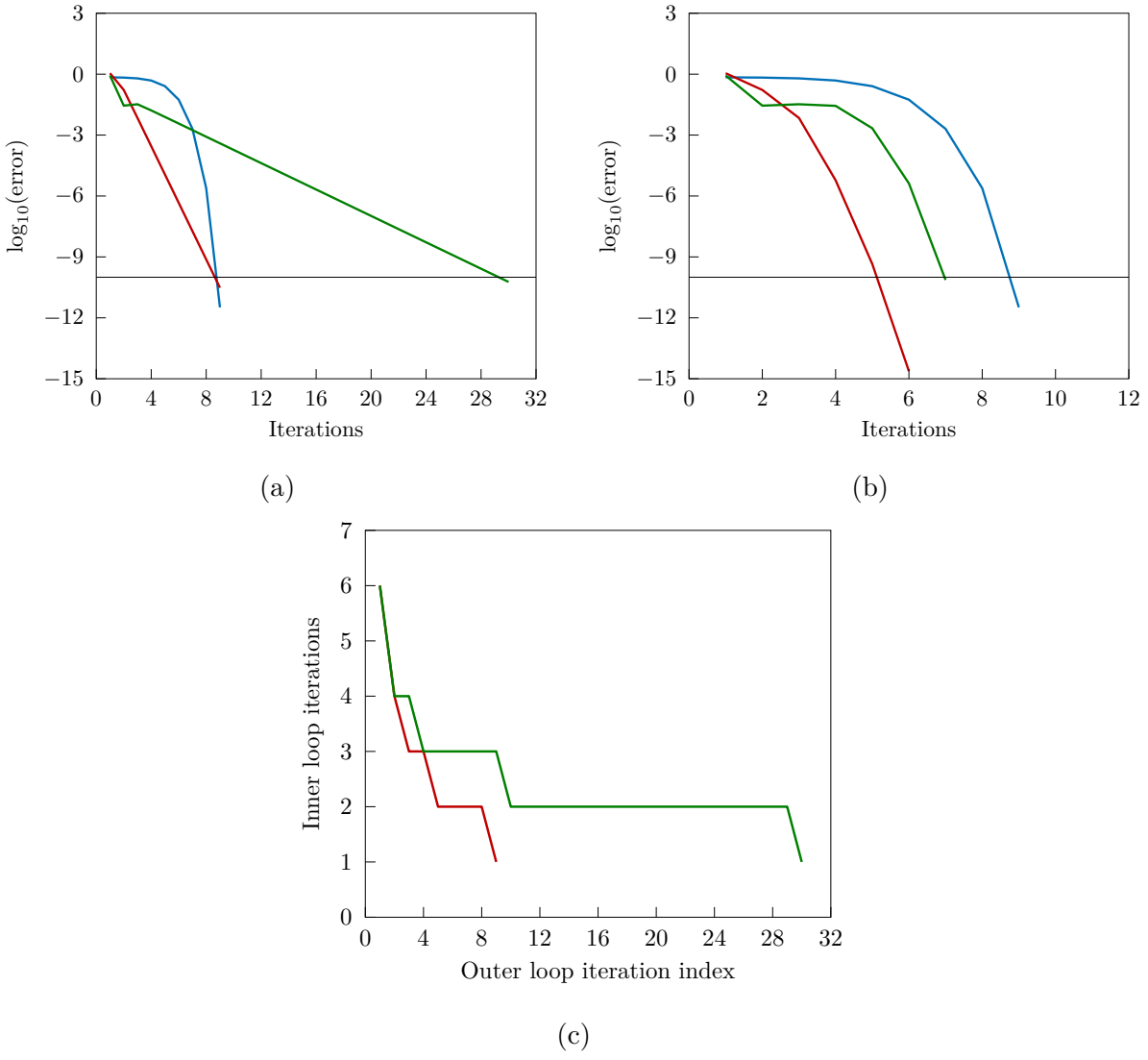

Figure 4.19: Convergence in MTBE synthesis for isobutene/methanol ratio equal to 1:1.1 without inert at 320.92 K and 1 atm: (a) successive substitution algorithm, (b) combined algorithm, (c) inner loop (Newton) iterations per outer loop non-ideality updates [Q-function minimization (—), L (—), VL (—)].

feeds selected, the authors had 100% success rate at finding the equilibrium solution. It must be mentioned that our calculations refer to the two-reaction system as presented in Chen et al. (2002) instead of the single-reaction system in Bonilla-Petriciolet et al. (2008a).

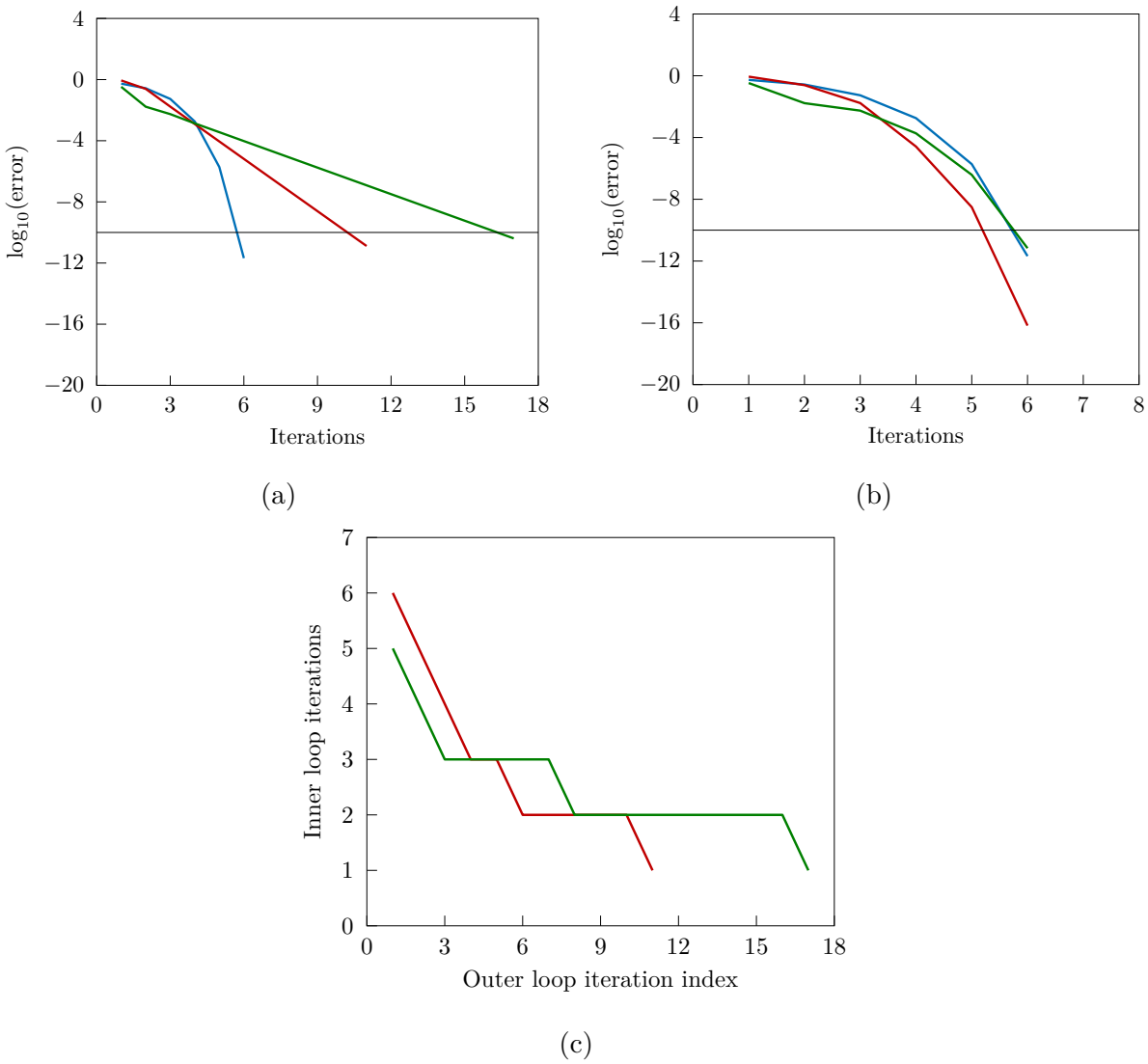

Figure 4.20: Convergence in the two-reaction TAME synthesis for a stoichiometric ratio of reactants and methanol/n-pentane ratio equal to 2:1 at 330 K and 1.52 bar: (a) successive substitution algorithm, (b) combined algorithm, (c) inner loop (Newton) iterations per outer loop non-ideality updates [Q-function minimization (—), L (—), VL (—)].

- Propene hydration

  Bonilla-Petriciolet et al. (2008a) reported total time of 30 s compared with our 1.45 ms with successive substitution and 1.47 with the combined algorithm. The lowest success rate they reported was 41%. This is an example of a system where the combined algorithm is not decisively faster than the successive substitution algorithm.

- Cyclohexane synthesis

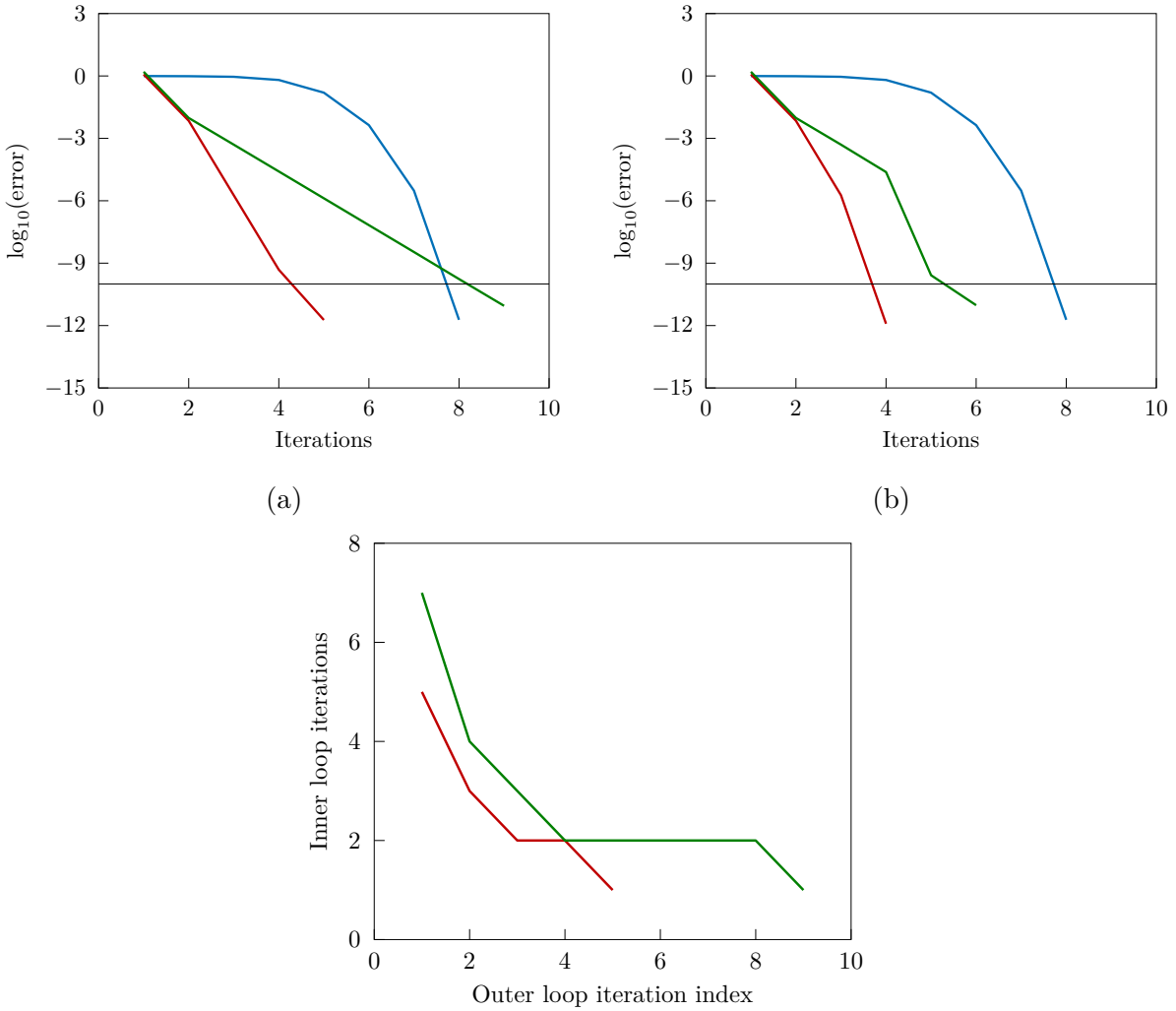

Figure 4.21: Convergence in propene hydration for an equimolar feed of reactants at 345 K and 1 bar: (a) successive substitution algorithm, (b) combined algorithm, (c) inner loop (Newton) iterations per outer loop non-ideality updates [Q-function minimization (—), L (—), VL (—)].

Burgos-Solórzano et al. (2004) study the minimization of the Gibbs energy using a validation tool, which guarantees determining the global minimum. The only time they reported is 120 ms for the validation tool calculations [Sun Blade 1000 Model 1600 (600 MHz) workstation]. In our work we spent 1.48 ms with the successive substitution and 1.30 ms with the combined algorithm for the complete calculations (initialization, convergence of single phase, stability analysis, convergence of two-phase system and final stability analysis).

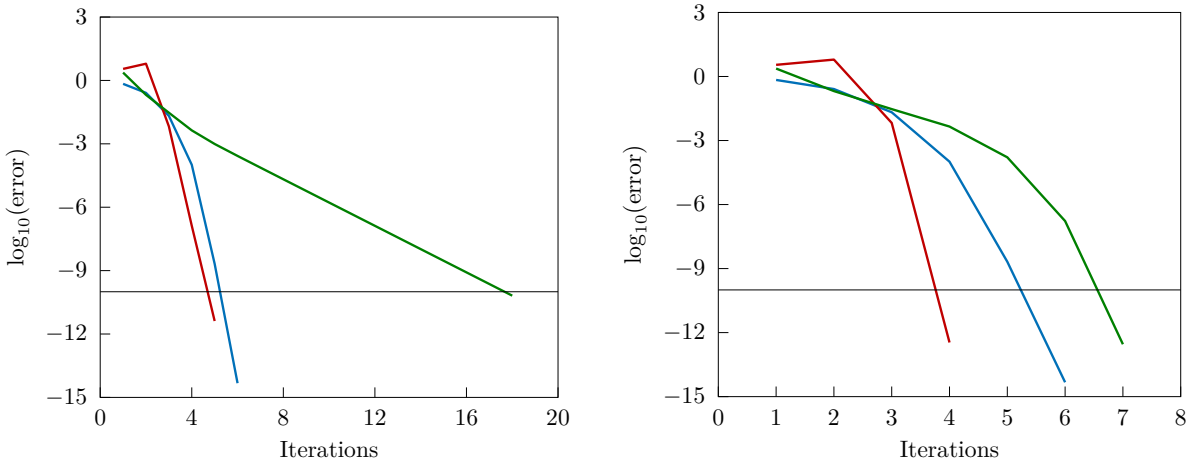

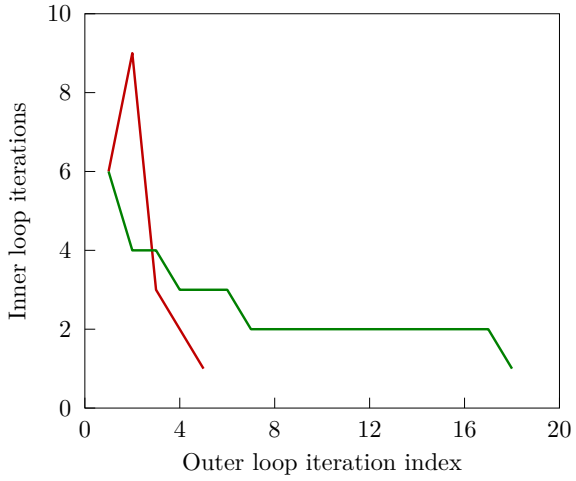

Figure 4.22: Convergence in cyclohexane synthesis for benzene/hydrogen ratio equal to 1:3.05 at 500 K and 30 atm: (a) successive substitution algorithm, (b) combined algorithm, (c) inner loop (Newton) iterations per outer loop non-ideality updates [Q-function minimization (—), V (—), VL (—)].

- Methanol synthesis

  Castier et al. (1989) reported iteration numbers for the three-phase synthesis. Initialization of L, VL and VLL required 5 iterations with 1 GDEM step, 10 iterations with 2 GDEM steps, and 12 iterations with 2 GDEM steps respectively (the third GDEM step was not needed for the three-phase convergence). For the full convergence of L, VL and VLL, the Murray iterations were 3, 4 and 1 respectively. In this work, 10 iterations were required for initialization. For the CPE calculations with the successive substitution algorithm, we had 54 outer loop iterations (149 Newton iterations) for V, 27 outer loop iterations (78 Newton iterations) for VL and 22 outer loop iterations (60 Newton iterations) for VLL. With the combined algorithm, all phases required 3 outer loop iterations (with 19 Newton iterations for V, 18 for VL and 16 for VLL) and 4, 5 and 4 modified RAND additional iterations for V, VL and VLL respectively.

- PPOFAG and OLLFAG transesterification with methanol

  For the two transesterification systems mentioned in Anikeev (2014) there were no pertinent data to compare. The only equilibrium results shown in Anikeev (2014) are for a single-vapor phase. What is worth mentioning here is that a relatively large number of iterations correspond to the first outer loop iteration (Figures 4.24c and 4.25c, 11 and 18 respectively). This happens because Q-function was minimized with the assumption of a single vapor phase. When this vapor phase was brought in the nested-loop procedure, at some point, the compositions of the phase matched better to a liquid phase. The phase was changed to liquid and the calculations continued. Subsequent calculations (LL and VLL) appear to be fast for both algorithms.

4.4 Conclusions

The non-stoichiometric algorithms introduced in Chapter 3 were first applied to systems studied in the literature. Calculations were made for the VLE, LLE or VLLE of three- to seven-component systems with one or two reactions. The same general algorithms were used for all the cases without exceptions and there was no issue excluding components from different phases (e.g. non-volatile oxydimethanol in the formaldehyde/water mixture). Comparison with the published results show that the algorithms can be successfully used for CPE calculations. Moreover, the algorithms could perform well for more complex mixtures, such as in the transesterification of two different triglyceride with methanol, involving nine components, five reactions and up to three phases.

Apart from CPE calculations at specified temperature, pressure and feed composition, it was also possible to examine the effect of various factors that could affect equilibrium: the presence of inert in MTBE synthesis, temperature dependence in the chemical equilibrium constant in propene hydration, and combination of a two-reaction synthesis into a single reaction in TAME synthesis. Although no published calculations were available for

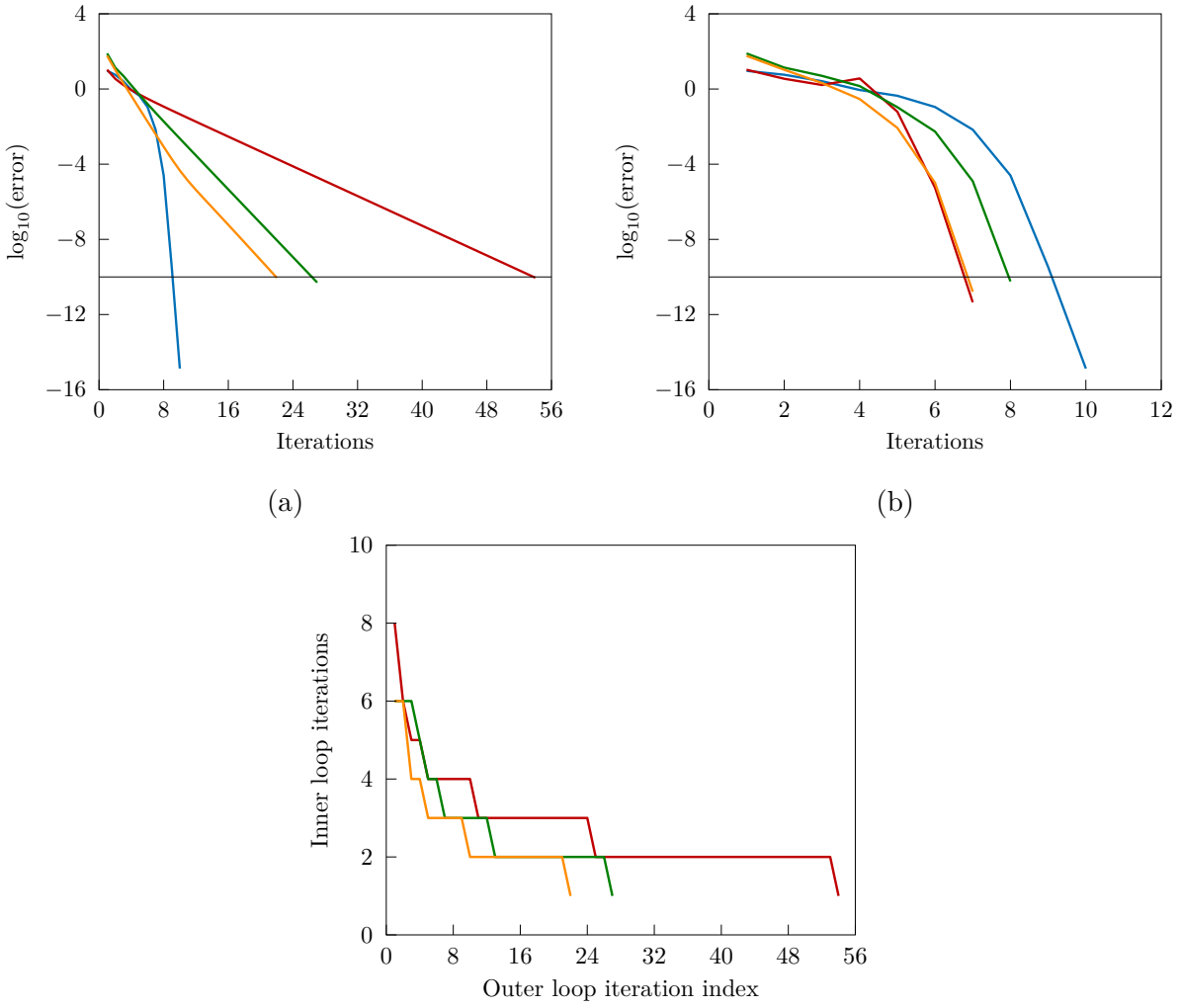

Figure 4.23: Convergence in methanol synthesis in the presence of n-octadecane at 473.15 K and 101.3 bar: (a) successive substitution algorithm, (b) combined algorithm, (c) inner loop (Newton) iterations per outer loop non-ideality updates [Q-function minimization (—), V (—), VL (—), VLL (—)].

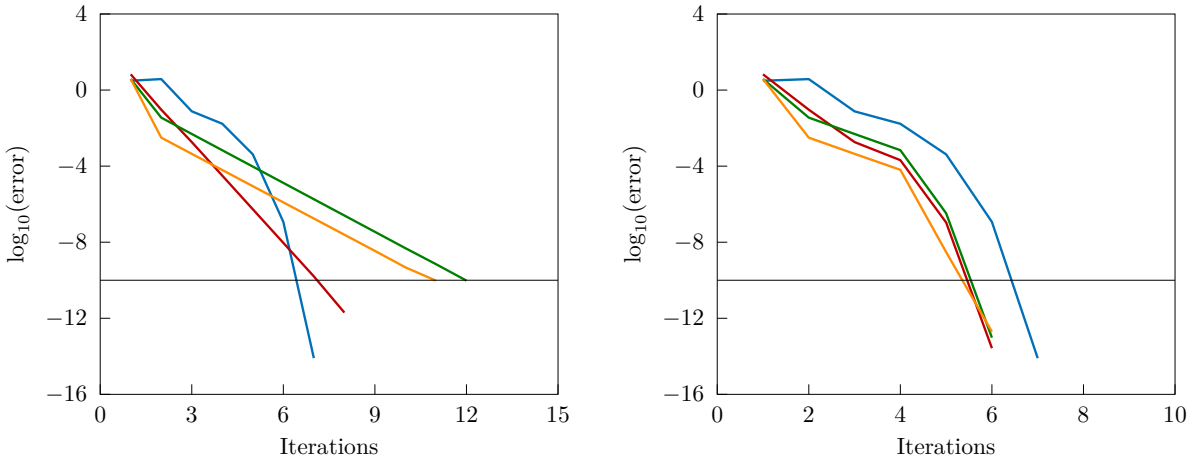

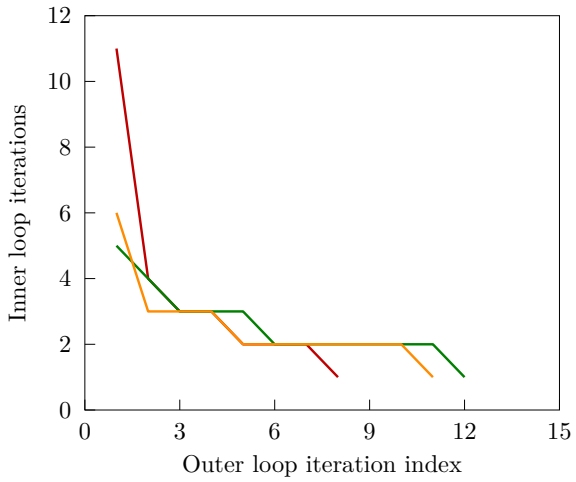

(c)

Figure 4.24: Convergence in PPOFAG transesterification with methanol for PPOFAG/methanol ratio equal to 1:3 at 450 K and 1 atm: (a) successive substitution algorithm, (b) combined algorithm, (c) inner loop (Newton) iterations per outer loop non-ideality updates [Q-function minimization (—), L (—), LL (—), VLL (—)].

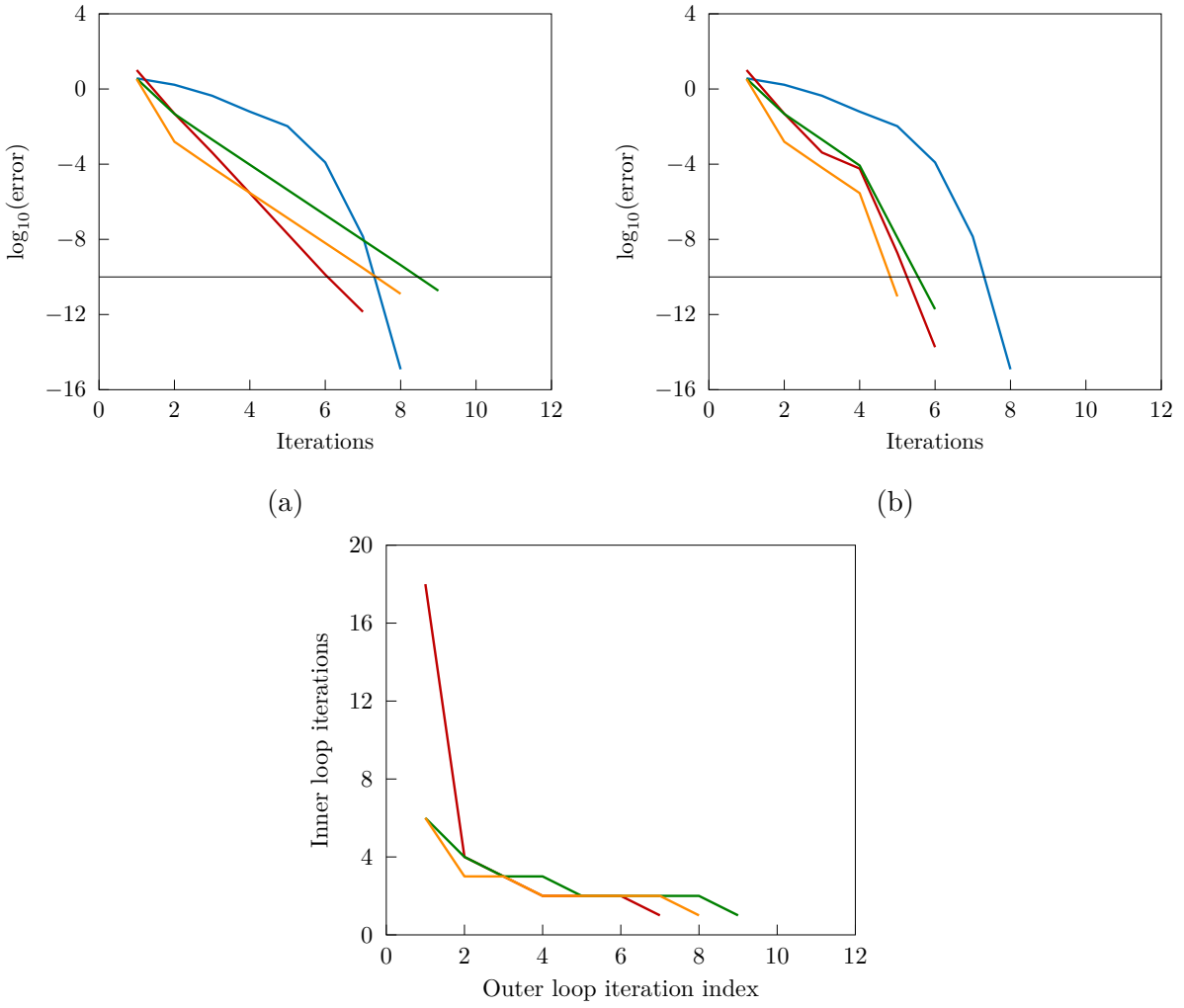

Figure 4.25: Convergence in OLLFAG transesterification with methanol for OLLFAG/methanol ratio equal to 1:3 at at 500 K and 1 atm: (a) successive substitution algorithm, (b) combined algorithm, (c) inner loop (Newton) iterations per outer loop non-ideality updates [Q-function minimization (—), L (—), LL (—), VLL (—)].

comparisons, these factors affected the equilibrium of the mixtures as expected.

Minimization of function Q provided initial estimates of good quality for the Lagrange multipliers method and we never encountered cases of divergence or oscillations. Furthermore, stability analysis could always identify a good estimate of the new phase without the need of re-initialization with function Q. Actually, it was observed that re-initialization with the new phase might lead to worse estimates because during the Q-function minimization, unlike in stability analysis, fugacity or activity coefficients are not utilized.

Speed and convergence behavior were investigated for the two non-stoichiometric algorithms. The combined algorithm converged to the solution with fewer iterations than the first-order successive substitution algorithm. Each outer loop iteration of the Lagrange multipliers method involved on average 2-4 inner loop (Newton) iterations, which reduced to 1-2 close to the solution. In the combined algorithm, successive substitution refines the initial estimates from the Q-function minimization and full convergence needs only 2-5 additional modified RAND steps. Taking into account that the Lagrange multipliers method has linear and the modified RAND method quadratic convergence, both require a reasonable number of iterations and they are much faster than reported CPU times in different publications. There have been cases where the algorithms in this work exhibited comparable CPU times but in general the combined algorithm appears to be more efficient, while the Gibbs energy monitoring during modified RAND steps is improving the robustness of calculations. Due to the modified RAND method, we propose the combined algorithm as an efficient and reliable approach for equilibrium calculations in multiphase reaction systems.

Finally, calculations were not compared with experimental data for the systems of this chapter. The focus of the study was the structure and performance of the algorithms, without concluding which model is more suitable to describe a reaction system. The use of better models will result in more accurate calculations/predictions. However, it should be mentioned that more complex models are computationally expensive and this could be reflected in increased CPU times.

CHAPTER

5

Calculation of CPE in electrolyte systems

Various models have been used to describe electrolyte behavior in solutions. One of the first successful attempts to theoretically formulate non-ideality in an electrolyte solution is attributed to Debye and Hückel (1923). Usually, when we refer to "Debye-Hückel" activity coefficients, we need to clarify how many parameters are included in the equation. There can be up to three ion independent parameters that depend on temperature and solvent properties. The limiting Debye-Hückel law has one parameter and extended Debye-Hückel equations utilize the two additional parameters. However, its use is limited to low values of ionic strength. Ionic strength in phase k is defined as:

$$I_k = \frac{1}{2} \sum_{i=1}^{N_C} z_i^2 m_{ik} \tag{5.1}$$

where:

I_k	ionic strength in phase k
z_i	charge of component i
m_{ik}	molality of component i in phase k

At higher electrolyte concentrations more complicated models are applicable, such as the Pitzer's model. It was originally proposed by Pitzer (1973) and it is worth mentioning one of its extended variants presented in Felmy and Weare (1986). Felmy and Weare (1986) show a number of different contributing terms to the activity coefficient: a Debye-Hückel based term and binary as well as ternary interactions between cations, anions and neutral solutes. Binary and ternary interaction parameters are regressed based on experimental data. Less complex Pitzer based equations might omit the ternary interaction parameters and include their own analysis predicting interaction parameters when experimental data are scarce (Edwards et al., 1978).

A number of equilibrium calculation methods based on the law of mass action have

been published, such as PHREEQC (Parkhurst and Appelo, 2013), used also in reactive transport processes. A more detailed list of similar methods is mentioned in Leal et al. (2016b). The authors followed the approach of Gibbs energy minimization to calculate geological system equilibrium and integrated their method in Reaktoro (C++ and Python framework combining chemical equilibrium and/or kinetics for chemically reactive process modeling, `reaktoro.org`). Moreover, Thomsen (1997) employed reaction extents in a second-order single phase procedure using the chemical equilibrium constants of the reactions. Finally, Xiao et al. (1989) developed the first-order KZ algorithm and applied it to the VLE of water/ammonia/carbon dioxide and Gautam and Seider (1979c) used the original single phase ideal RAND in an aqueous solution of sulfur dioxide with the ideal system approximation.

The non-stoichiometric algorithms developed in this work are applied to multiphase chemical equilibrium involving electrolyte reactions. Electroneutrality must be incorporated in the working equations due to electrolytes in the system. In general, cases of interest include weak electrolytes, ion speciation and reactions with minerals. CPE calculation in electrolyte systems is useful for geochemistry modeling such as underground carbon dioxide sequestration.

5.1 Electroneutrality in CPE calculations

Dissociation of an electrolyte can be viewed as a chemical reaction. In the general case we have a mixture of N_R electrolytes that dissociate according to the reactions:

$$\begin{gathered} \mathrm{X}_{r(y_r)}\mathrm{Y}_{r(x_r)} \rightleftharpoons y_r \mathrm{X}_r{}^{(x_r)+} + x_r \mathrm{Y}_r{}^{(y_r)-} \\ r = 1, ..., N_R \end{gathered} \tag{5.2}$$

where:

$\mathrm{X}_r^{(x_r)+}$ cation with charge $+x_r$ in dissociation reaction r

$\mathrm{Y}_r^{(y_r)-}$ anion with charge $-y_r$ in dissociation reaction r

For convenience, we assume that ions $\mathrm{X}_r^{(x_r)+}$ and $\mathrm{Y}_r^{(y_r)-}$ are unique for each dissociation r. The number of elements is $N_E = N_C - N_R = 3N_R - N_R = 2N_R$. If the elements are chosen as the ions, the formula matrix and stoichiometric matrix of the hypothetical system are given by:

$$\mathbf{A} = \begin{array}{c} \begin{matrix} \cdots & \mathrm{X}_{r(y_r)}\mathrm{Y}_{r(x_r)} & \cdots & \mathrm{X}_r{}^{(x_r)+} & \mathrm{Y}_r{}^{(y_r)-} & \cdots \end{matrix} \\ \begin{bmatrix} \vdots & \vdots & \vdots & \vdots & \vdots & \vdots \\ \vdots & y_r & \cdots & 1 & 0 & \vdots \\ \vdots & x_r & \cdots & 0 & 1 & \vdots \\ \vdots & \vdots & \vdots & \vdots & \vdots & \vdots \end{bmatrix} \end{array} \begin{matrix} \vdots \\ \mathrm{X}_r{}^{(x_r)+} \\ \mathrm{Y}_r{}^{(y_r)-} \\ \vdots \end{matrix} \tag{5.3}$$

$$\mathbf{N}^{\mathrm{T}} = \begin{array}{c} \begin{matrix} \cdots & \mathrm{X}_{r(y_r)}\mathrm{Y}_{r(x_r)} & \cdots & \mathrm{X}_r{}^{(x_r)+} & \mathrm{Y}_r{}^{(y_r)-} & \cdots \end{matrix} \\ \begin{bmatrix} \vdots & \vdots & \vdots & \vdots & \vdots & \vdots \\ \vdots & -1 & \cdots & y_r & x_r & \vdots \\ \vdots & \vdots & \vdots & \vdots & \vdots & \vdots \end{bmatrix} \end{array} \begin{matrix} \vdots \\ \text{reaction } r \\ \vdots \end{matrix}$$

An additional equation that is supposed to be satisfied in such systems is the electroneutrality equation. We start with N_R uncharged electrolytes with net charge equal to zero, which should not change after all dissociation equilibria have been established. In other words, at equilibrium:

$$\sum_{r=1}^{N_R}(n_{\mathrm{X}_r{}^{(x_r)+}})(+x_r) + \sum_{r=1}^{N_R}(n_{\mathrm{Y}_r{}^{(y_r)-}})(-y_r) = 0 \tag{5.4}$$

The material balance in non-stoichiometric methods is given by Eq. 3.7:

$$\mathbf{A}\sum_{k=1}^{N_P}\mathbf{n}_k = \mathbf{b} \tag{5.5}$$

Eq. 5.4 could be included as an additional row in the matrix and vector of the material balance constraints as (Appendix B):

$$\begin{bmatrix} \mathbf{A} \\ \mathbf{A}_{\mathrm{el}} \end{bmatrix} \sum_{k=1}^{N_P}\mathbf{n}_k = \begin{bmatrix} \mathbf{b} \\ 0 \end{bmatrix} \tag{5.6}$$

where:

$$\mathbf{A}_{\mathrm{el}} = \begin{array}{c} \begin{matrix} \cdots & \mathrm{X}_{r(y_r)}\mathrm{Y}_{r(x_r)} & \cdots & \mathrm{X}_r{}^{(x_r)+} & \mathrm{Y}_r{}^{(y_r)-} & \cdots \end{matrix} \\ \begin{bmatrix} \cdots & 0 & \cdots & x_r & -y_r & \cdots \end{bmatrix} \end{array} \tag{5.7}$$

However, this row can be obtained as a linear combination of the rows that already exist

in the formula matrix of Eq. 5.3. If we multiply the rows of $X_r^{(x_r)+}$ with x_r, the rows of $Y_r^{(y_r)+}$ with $-y_r$ and then add all the rows, we will get Eq. 5.4. Therefore, this framework already takes into account the electroneutrality equation. Reaching equilibrium does not only mean that the material balance is satisfied. It also implies that the change of the component mole numbers follows the way the reactions are written. The formula matrix "hides" reaction information because it is not independent of the stoichiometric matrix (Eq. 3.20). In fact, since the reactions are balanced out and there is no production or consumption of charge (e.g. as in redox half reactions), if the net charge in the feed is zero, the net charge at equilibrium will be also zero. A similar analysis can be made when the different dissociating electrolytes $X_{r(y_r)}Y_{r(x_r)}$ share common ions.

The way electroneutrality is satisfied by the the formula matrix in Eq. 5.6 does not prevent individual phases from being charged. It only ensures that the net charge of all the phases at equilibrium will be zero. Eq. 5.4 should be satisfied for every phase where charged particles appear. The main assumption is that charged components are excluded from all phases except for the solvent phase (in this work the aqueous phase). In this case, the entries of the vector $\sum_{k=1}^{N_P} \mathbf{n}_k$ for charged components are actually their total mole numbers in the only phase they appear. The models in this work do not account for this inherently. Instead, charged particles are artificially excluded from non-solvent phases to guarantee that phase electroneutrality coincides with overall electroneutrality in Eq. 5.6. The reason why Eq. 5.6 was presented with the sum of mole numbers of all the phases, was to keep the material balance in the form used for the non-electrolyte systems of the previous chapter.

5.2 Infinite dilution reference state

In the expression of liquid phase chemical potential, pure component reference state is usually selected if a component can be condensed at the system temperature. This is particularly favorable if the behavior of the component does not deviate much from Raoult's law. On the other hand, when the component is non-condensable at the system temperature or it is not described adequately by the pure component limiting law, the infinite dilution (Henry's law based) reference state is often preferred:

$$f_{ik}^{\circ} = H_{ik}(T, p, n_{\text{sol},k}) \tag{5.8}$$

and

$$\mu_{ik}^{\circ} = \tilde{\mu}_{ik}(T, p, n_{\text{sol},k}) \tag{5.9}$$

where:

H_{ik} Henry's constant of component i in phase k

$n_{\text{sol},k}$ solvent mole numbers in phase k
$\tilde{\mu}_{ik}$ infinite dilution chemical potential of component i in phase k

The dependence of Henry's constant on pressure is usually expressed as:

$$H_{ik} = H_{ik}^{s} \exp\left(\int_{p_{\text{sol}}^{s}}^{p} \frac{\bar{V}_{ik}^{\infty}}{RT} dp\right) \approx H_{ik}^{s} \exp\left[\frac{\bar{V}_{ik}^{\infty}(p - p_{\text{sol}}^{s})}{RT}\right] \tag{5.10}$$

where:
H_{ik}^{s} saturation Henry's constant of component i in phase k
$\bar{V}_{ik}^{\infty}$ infinite dilution partial molar volume of component i in phase k
p_{sol}^{s} solvent vapor pressure

In such mixtures the treatment is different for solvents and solutes. Solvents follow the pure component reference state and solutes the infinite dilution reference state. Henry's constants for specific solvents can be found in the literature. Nevertheless, it is difficult to predict the overall Henry's constant in the case of mixed solvents only from pure solvent Henry's constants (Michelsen and Mollerup, 2007). For this reason it is preferable to consider one component as the solvent and the rest as the solutes. Similar to the symmetric activity coefficient defined by Eq. 2.47 in the pure component reference state, using the infinite dilution reference state we define the asymmetric activity coefficient:

$$\tilde{\gamma}_{ik} \equiv \frac{\hat{f}_{ik}}{x_{ik} H_{ik}} \tag{5.11}$$

where:
$\tilde{\gamma}_{ik}$ asymmetric activity coefficient of component i in phase k

Therefore, fugacity and chemical potential expressions become:

$$\hat{f}_{ik} = x_{ik} \tilde{\gamma}_{ik} H_{ik} \tag{5.12}$$

and

$$\mu_{ik} = \tilde{\mu}_{ik} + RT \ln(x_{ik} \tilde{\gamma}_{ik}) \tag{5.13}$$

Comparing Eq. 2.48 with 5.12, we can conclude that:

$$\gamma_{ik} = \tilde{\gamma}_{ik} \frac{H_{ik}}{f_{ik}} \tag{5.14}$$

As the mole fraction of component i approaches 0, the asymmetric activity coefficient

$\tilde{\gamma}_{ik}$ approaches 1 according to the definition of Eq. 5.11. However, the infinite dilution activity coefficient of component i under the symmetric convention is usually not 1 but given by:

$$\gamma_{ik}^{\infty} = \lim_{x_{ik}\to 0} \gamma_{ik} = \lim_{x_{ik}\to 0} \left(\tilde{\gamma}_{ik} \frac{H_{ik}}{f_{ik}} \right) = \frac{H_{ik}}{f_{ik}} \tag{5.15}$$

where:

γ_{ik}^{∞} symmetric infinite dilution activity coefficient of component i in phase k

As a result, from Eq. 5.14:

$$\tilde{\gamma}_{ik} = \frac{\gamma_{ik}}{\gamma_{ik}^{\infty}} \tag{5.16}$$

Comparing Eq. 2.49 with 5.13, using Eq. 5.15:

$$\tilde{\mu}_{ik} = \mu_{ik}^{\text{pure}} + RT \ln \gamma_{ik}^{\infty} \tag{5.17}$$

When we have more than one solvent, the infinity dilution activity coefficient depends on the composition of these solvents. In the electrolyte systems presented in the following section, we assume that only water is the solvent. Therefore:

$$\begin{gathered} \left(\frac{\partial \ln \gamma_{ik}^{\infty}}{\partial n_{qk}} \right)_{T,p} = 0 \\ q = 1, ..., N_C \end{gathered} \tag{5.18}$$

Two further variations of the infinite dilution reference state can be found in the literature:

- Unit molality reference state

  Molality is a different measure of concentration defined as:

  $$m_{ik} = \frac{n_{ik}}{n_{\text{sol},k} M_{\text{sol},k}} \tag{5.19}$$

  and it shows the mole numbers of a solute dissolved per kg of solvent. We can express mole fractions as functions of molality:

  $$x_{ik} = \frac{n_{ik}}{n_{t,k}} = \frac{n_{ik}}{n_{\text{sol},k} M_{\text{sol},k}} \frac{n_{\text{sol},k} M_{\text{sol},k}}{n_{t,k}} = m_{ik} x_{\text{sol},k} M_{\text{sol},k} \tag{5.20}$$

where:

$M_{\mathrm{sol},k}$	solvent molar mass in phase k
$x_{\mathrm{sol},k}$	solvent mole fraction in phase k

Using Eq. 5.13:

$$\mu_{ik} = [\tilde{\mu}_{ik} + RT \ln(M_{\mathrm{sol},k} m^{\circ})] + RT \ln \frac{m_{ik}(\tilde{\gamma}_{ik} x_{\mathrm{sol},k})}{m^{\circ}} \tag{5.21}$$

We define:

$$\tilde{\mu}^{m}_{ik} = \tilde{\mu}_{ik} + RT \ln(M_{\mathrm{sol},k} m^{\circ}) \tag{5.22}$$

and

$$\tilde{\gamma}^{m}_{ik} = x_{\mathrm{sol},k} \tilde{\gamma}_{ik} \tag{5.23}$$

where:

$\tilde{\mu}^{m}_{ik}$	chemical potential of component i in phase k at unit molality
$\tilde{\gamma}^{m}_{ik}$	asymmetric molality activity coefficient of component i in phase k
m°	unit molality

Finally the chemical potential becomes:

$$\mu_{ik} = \tilde{\mu}^{m}_{ik} + RT \ln \frac{m_{ik} \tilde{\gamma}^{m}_{ik}}{m^{\circ}} \tag{5.24}$$

This expression is useful when the activities of solutes are expressed as:

$$\alpha_{ik} = \frac{m_{ik} \tilde{\gamma}^{m}_{ik}}{m^{\circ}} \tag{5.25}$$

- Unit molarity reference state

  Molarity is formally defined as:

$$c_{ik} = \frac{n_{ik}}{V_k} \tag{5.26}$$

  and shows how many moles are dissolved per unit volume of solution. Instead of the S.I. unit, the unit “M” is more common, defined as mol/L. Mole fractions are found as:

$$x_{ik} = \frac{n_{ik}}{n_{t,k}} = \frac{n_{ik}}{V_k}\frac{V_k}{n_{t,k}} = \frac{c_{ik}}{c_{t,k}} \tag{5.27}$$

where:

c_{ik}	molarity of component i in phase k
$c_{t,k}$	total molarity in phase k

Molality and molarity are related through:

$$m_{ik} = \frac{c_{ik}}{\rho_k - \sum_{\substack{i=1 \\ i\neq \mathrm{sol}}}^{N_C} c_{ik} M_i} \tag{5.28}$$

where:

M_i	molar mass of component i
$c_{\mathrm{sol},k}$	solvent molarity in phase k
ρ_k	density of phase k

Using Eq. 5.13:

$$\mu_{ik} = \left[\tilde{\mu}_{ik} + RT \ln \frac{c^\circ M_{\mathrm{sol},k}}{\rho_{\mathrm{sol},k}}\right] + RT \ln \left(\frac{c_{ik}}{c^\circ} \frac{\tilde{\gamma}_{ik} x_{\mathrm{sol},k} \rho_{\mathrm{sol},k}}{\rho_k - \sum_{\substack{i=1 \\ i\neq \mathrm{sol}}}^{N_C} c_{ik} M_i} \right) \tag{5.29}$$

We define:

$$\tilde{\mu}^c_{ik} = \tilde{\mu}_{ik} + RT \ln \frac{c^\circ M_{\mathrm{sol},k}}{\rho_{\mathrm{sol},k}} \tag{5.30}$$

and

$$\tilde{\gamma}^c_{ik} = \frac{x_{\mathrm{sol},k} \rho_{\mathrm{sol},k}}{\rho_k - \sum_{\substack{i=1 \\ i\neq \mathrm{sol}}}^{N_C} c_{ik} M_i} \tilde{\gamma}_{ik} \tag{5.31}$$

Chemical potentials become:

$$\mu_{ik} = \tilde{\mu}^c_{ik} + RT \ln \frac{c_{ik} \tilde{\gamma}^c_{ik}}{c^\circ} \tag{5.32}$$

where:

$\tilde{\mu}^c_{ik}$	chemical potential of component i in phase k at unit molarity
$\tilde{\gamma}^c_{ik}$	asymmetric molarity activity coefficient of component i in phase k
$\rho_{\mathrm{sol},k}$	pure solvent density in phase k

c° unit molarity

This expression is useful when the activities of solutes are expressed as:

$$\alpha_{ik} = \frac{c_{ik}\tilde{\gamma}^c_{ik}}{c^\circ} \tag{5.33}$$

In general the unit molality m° and molarity c° do not always appear in relationships in the literature. The only reason they are introduced here is to maintain dimensionless all the arguments of the logarithms while preserving the general expressions for the molality and molarity chemical potentials (Eq. 5.24 and 5.32).

5.3 Non-stoichiometric algorithms in electrolyte mixtures

5.3.1 Water/ammonia/carbon dioxide mixture

Xiao et al. (1989) included calculations in their work for the VLE of the mixture $H_2O/NH_3/CO_2$ in the presence of methane and ethane as inerts. Ammonia and carbon dioxide dissolve in water and react according to the schemes:

$$NH_3 + H_2O \rightleftharpoons NH_4^+ + OH^- \tag{5.34}$$
$$CO_2 + H_2O \rightleftharpoons HCO_3^- + H^+ \tag{5.35}$$
$$HCO_3^- \rightleftharpoons CO_3^{2-} + H^+ \tag{5.36}$$
$$H^+ + OH^- \rightleftharpoons H_2O \tag{5.37}$$
$$NH_3 + HCO_3^- \rightleftharpoons NH_2COO^- + H_2O \tag{5.38}$$

The chemical compositions of all components and elements for the electrolyte system is presented in Table 5.1. The number of elements is $N_E = N_C - N_R = 11 - 5 = 6$. The formula matrix and stoichiometric matrix of the system are given by:

$$\mathbf{A} = \begin{bmatrix} 2 & 1 & 0 & 0 & 0 & 1 & 2 & 1 & 1 & 0 & 0 \\ 1 & 0 & 0 & 0 & 0 & 0 & 0 & 1 & 1 & 1 & 0 \\ 0 & 1 & 0 & 0 & 0 & 0 & 1 & 0 & 0 & 0 & 1 \\ 0 & 0 & 1 & 0 & 0 & 0 & 0 & 0 & 1 & 1 & 1 \\ 0 & 0 & 0 & 1 & 0 & 0 & 0 & 0 & 0 & 0 & 0 \\ 0 & 0 & 0 & 0 & 1 & 0 & 0 & 0 & 0 & 0 & 0 \end{bmatrix} \tag{5.39}$$

$$\mathbf{N} = \begin{bmatrix} -1 & -1 & 0 & 0 & 0 & 0 & 1 & 1 & 0 & 0 & 0 \\ -1 & 0 & -1 & 0 & 0 & 1 & 0 & 0 & 1 & 0 & 0 \\ 0 & 0 & 0 & 0 & 0 & 1 & 0 & 0 & -1 & 1 & 0 \\ 1 & 0 & 0 & 0 & 0 & -1 & 0 & -1 & 0 & 0 & 0 \\ 1 & -1 & 0 & 0 & 0 & 0 & 0 & 0 & -1 & 0 & 1 \end{bmatrix}^{\mathrm{T}}$$

Vapor phase is described by the Soave-Redlich-Kwong equation of state (Soave, 1972) with all binary interaction parameters k_{ij} set to zero and liquid phase by the activity coefficient model presented in Edwards et al. (1978) using numerical composition derivatives. Chemical equilibrium constants and Henry's constants were taken from Edwards et al. (1978), water density and vapor pressure from Dortmund Data Bank (2017), and water dielectric constant from Pátek et al. (2009). Charged components are considered non-volatile and the inert hydrocarbons non-soluble in the aqueous phase (Xiao et al., 1989). Results are compared with Xiao et al. (1989) in Table 5.2 and convergence behavior is shown in Figure 5.1. Calculations required 2.32 ms with the successive substitution algorithm and 2.31 ms with the combined algorithm. Similar CPU times show that the fewer iterations required by the combined algorithm cost more, possibly because of the matrix inversion and calculations of numerical derivatives (central difference).

Table 5.1: Component and element numbering for the $H_2O/NH_3/CO_2$ system.

	Component	Element
1	H_2O	H^+
2	NH_3	O^{2-}
3	CO_2	NH_2^-
4	CH_4	CO_2
5	C_2H_6	CH_4
6	H^+	C_2H_6
7	NH_4^+	
8	OH^-	
9	HCO_3^-	
10	CO_3^{2-}	
11	NH_2COO^-	

Xiao et al. (1989) used a different equation of state for the vapor phase suitable for

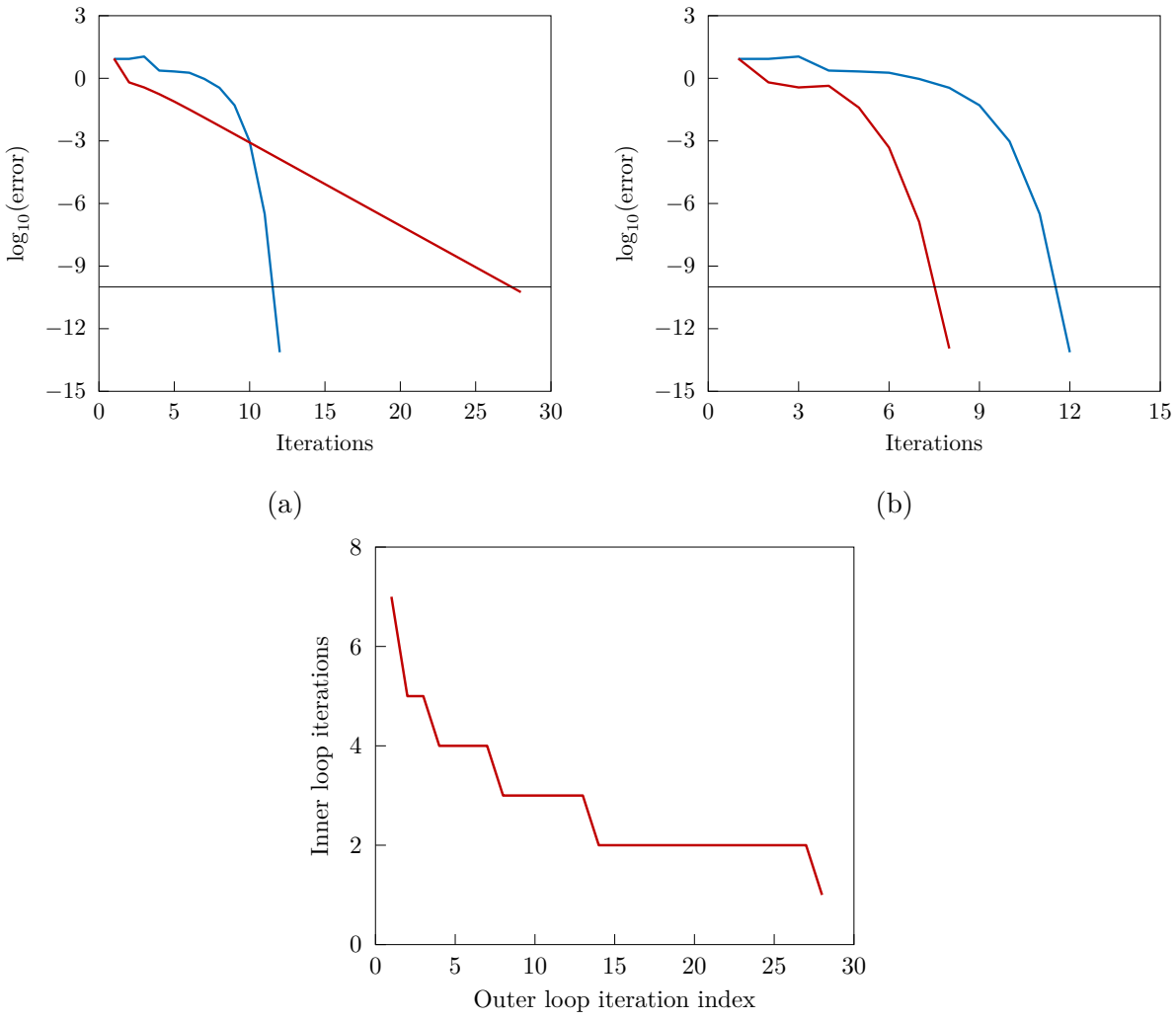

Figure 5.1: Convergence in the $H_2O/NH_3/CO_2$ system at 373 K and 10 atm: (a) successive substitution algorithm, (b) combined algorithm, (c) inner loop (Newton) iterations per outer loop non-ideality updates [Q-function minimization (—), VL (—)].

Table 5.2: Equilibrium partial pressures in the vapor phase, molalities in the liquid phase, phase amounts and phase fractions of the $H_2O/NH_3/CO_2$ system at 373 K and 10 atm.

Component	Feed	Our work		Our work (++, −− interact)		Xiao et al. (1989)	
		p_i (atm)	m_i (mol/kg)	p_i (atm)	m_i (mol/kg)	p_i (atm)	m_i (mol/kg)
H_2O	0.8473	0.9173	55.5084	0.9304	55.5084	0.9462	55.5550
NH_3	0.0458	0.2556	0.8322	0.1881	0.5926	0.1543	0.6151
CO_2	0.0458	2.1333	0.0243	1.5385	0.0178	1.8080	0.0183
CH_4	0.0305	3.3469	0	3.6714	0	3.5457	0
C_2H_6	0.0305	3.3469	0	3.6714	0	3.5457	0
H^+	0	0	3.25×10^{-8}	0	1.65×10^{-8}	0	5.34×10^{-8}
NH_4^+	0	0	1.8242	0	2.3301	0	2.2256
OH^-	0	0	3.78×10^{-5}	0	2.63×10^{-5}	0	4.61×10^{-5}
HCO_3^-	0	0	1.4090	0	2.0517	0	1.6712
CO_3^{2-}	0	0	0.0599	0	0.0822	0	0.1780
NH_2COO^-	0	0	0.2954	0	0.1139	0	0.1984
n_t (mol)	65.5084	5.9756	57.8310	5.4474	57.9161	–	–
β		0.0937	0.9063	0.0860	0.9140	–	–

polar compounds, but this does not fully explain the deviations compared with our calculations. Details about parameters and model implementation (Edwards et al., 1978) are not provided by Xiao et al. (1989). For instance, same types of charges do not interact according to Edwards et al. (1978) and their binary interaction parameters must be set to zero. If we allow such interactions, the equilibrium solution seems to be closer to the one presented by Xiao et al. (1989) (Table 5.2). We did not try to investigate further if the interpretation of binary interaction parameter rules in Edwards et al. (1978) was correct or not in the work of Xiao et al. (1989). The main purpose of this section is to show that the algorithms can be applied to electrolyte systems without modifications of the working equations. Furthermore, Figure 5.1 illustrates that the non-stoichiometric algorithms of this work exhibit the same convergence rate as for non-electrolyte mixtures: linear convergence with the successive substitution algorithm and quadratic during the final iterations of the combined algorithm where the modified RAND method is used.

Possible modifications are concerned with the change of the infinite dilution reference state of solutes (mole fraction or molality based) to the pure component reference state. The first step is to transition from the unit molality to the infinite dilution reference state with Eq. 5.22 and 5.23, since we use mole fractions in the equations instead of molalities. Additionally, derivatives of the chemical potential are required in the modified RAND method. For component i in phase k, where we use the infinite dilution reference state, we have (Eq. 5.15 and 5.17):

$$\left(\frac{\partial \ln \tilde{\gamma}_{ik}}{\partial n_{qk}}\right)_{T,p} = \left(\frac{\partial \ln \gamma_{ik}}{\partial n_{qk}}\right)_{T,p} - \left(\frac{\partial \ln \gamma_{ik}^{\infty}}{\partial n_{qk}}\right)_{T,p} \qquad q = 1, ..., N_C \tag{5.40}$$

and

$$\frac{1}{RT}\left(\frac{\partial \tilde{\mu}_{ik}}{\partial n_{qk}}\right)_{T,p} = \left(\frac{\partial \ln \gamma_{ik}^{\infty}}{\partial n_{qk}}\right)_{T,p} \qquad q = 1, ..., N_C \tag{5.41}$$

Using Eq. 5.18, we get:

$$\left(\frac{\partial \ln \tilde{\gamma}_{ik}}{\partial n_{qk}}\right)_{T,p} = \left(\frac{\partial \ln \gamma_{ik}}{\partial n_{qk}}\right)_{T,p} \qquad q = 1, ..., N_C \tag{5.42}$$

and

$$\left(\frac{\partial \tilde{\mu}_{ik}}{\partial n_{qk}}\right)_{T,p} = 0 \qquad q = 1, ..., N_C \tag{5.43}$$

5.3.2 Carbon dioxide in aqueous solutions

Carbon dioxide dissolves in water but is not an inert in an aqueous solution. It is usually assumed that the following reactions take place when carbon dioxide interacts with water:

$$CO_2 + H_2O \rightleftharpoons H^+ + HCO_3^- \tag{5.44}$$

$$HCO_3^- \rightleftharpoons H^+ + CO_3^{2-} \tag{5.45}$$

Eq. 5.44 could be split into two reactions:

$$CO_2 + H_2O \rightleftharpoons H_2CO_3 \tag{5.46}$$

$$H_2CO_3 \rightleftharpoons H^+ + HCO_3^- \tag{5.47}$$

Most studies [e.g. Leal et al. (2016a,b)] disregard the carbonic acid in the solution and use Eq. 5.44 and 5.45 to model the dissolution of carbon dioxide in water. We examined these two cases separately: a set of reactions that exclude the carbonic acid using Eq. 5.44 and 5.45, and a different set that accounts for the carbonic acid with Eq. 5.46, 5.47 and 5.45. Apart from water, calculations are also made for an aqueous solution of calcium chloride with or without solid calcium carbonate.

In the calculations, vapor phase is described by the Peng-Robinson equation of state (Peng and Robinson, 1976) with all binary interaction parameters k_{ij} set to zero, except between water and carbon dioxide that is equal to 0.189 (Mohebbinia et al., 2013). Liquid phase is described by Pitzer's activity coefficient model (Pitzer, 1973) with the extended version presented in Felmy and Weare (1986) and parameters from the Pitzer database of PHREEQC (Parkhurst and Appelo, 2013) using numerical composition derivatives. Reference state chemical potentials were taken from Venkatraman et al. (2015), except for carbon dioxide that was taken from Duan and Sun (2003). Water density was obtained from Dortmund Data Bank (2017) and water dielectric constant from Pátek et al. (2009). All solutes except carbon dioxide are considered non-volatile. Only calcium carbonate is allowed to exist in the solid phase. Results are compared with experimental solubilites of carbon dioxide in water (Wiebe and Gaddy, 1940; Prutton and Savage, 1945) and calcium chloride solutions (Prutton and Savage, 1945).

In Duan and Sun (2003), the reduced unit molality reference state chemical potential of carbon dioxide is modeled. The analysis of the authors reveals that this value is actually the Henry's constant of carbon dioxide. Henry's constant can be found at lower pressures from the equation:

$$H_{\mathrm{CO_2}} = \frac{y_{\mathrm{CO_2}} p}{x_{\mathrm{CO_2}}} \tag{5.48}$$

Experimental determination of $x_{\mathrm{CO_2}}$ does not refer only to molecular carbon dioxide dissolved in water. Solubility is the sum of all carbon dioxide related species: carbon dioxide, carbonic acid, bicarbonate and carbonate ions. Bicarbonate and carbonate ions are not produced in large amounts due to the small chemical equilibrium constants. In this case, $x_{\mathrm{CO_2}}$ is expected to be close to the aqueous molecular carbon dioxide. In contrast, carbon dioxide to carbonic acid reaction has a chemical equilibrium constant close to 1. Dissolved molecular carbon dioxide is expected to be almost as much as carbonic acid at equilibrium. With a rough approximation, ignoring the bicarbonate and carbonate ions, the Henry's constant that is calculated for the actual carbon dioxide in water should be multiplied with a factor of 2, to account for carbonic acid. Before calculating the equilibrium of the electrolyte system in the presence of carbonic acid, we attempted to find a scaling factor of the Henry's constant. This factor was determined by the following procedure:

1. Assume initially $H_{CO_2}^{scaled} = 2H_{CO_2}^{DS}$, where $H_{CO_2}^{DS}$ is calculated from the correlation in Duan and Sun (2003).

2. Solve CPE with $H_{CO_2} = H_{CO_2}^{scaled}$

3. From the solution update scaled Henry's constant as:

$$H_{CO_2}^{scaled} = \frac{x_{CO_2} + x_{H_2CO_3} + x_{HCO_3^-} + x_{CO_3^{2-}}}{x_{CO_2}} H_{CO_2}^{DS} \tag{5.49}$$

- If $H_{CO_2}^{scaled}$ has converged, accept the scaling factor
- If $H_{CO_2}^{scaled}$ has not converged, go to step 2

We found that an average value of this factor is 2.01 in the range 280-400 K and 5-15 atm. Whenever the carbonic acid was included in the calculations, the scaled Henry's constant was used for carbon dioxide. Results for both approaches (with and without carbonic acid) are presented. It is also assumed that:

$$\bar{V}_{H_2CO_3}^{\infty} = v_{H_2O} + \bar{V}_{CO_2}^{\infty} \tag{5.50}$$

Otherwise, based on the data from Venkatraman et al. (2015), only the reference state chemical potential of water and carbon dioxide will be pressure dependent and the chemical equilibrium constant at higher pressures will favor unreasonably the production of H_2CO_3. The reactions in the complete system of carbon dioxide, water, calcium chloride and calcium carbonate acid are:

- Without carbonic acid

$$H_2O \rightleftharpoons H^+ + OH^- \tag{5.51}$$
$$CO_2 + H_2O \rightleftharpoons H^+ + HCO_3^- \tag{5.52}$$
$$HCO_3^- \rightleftharpoons H^+ + CO_3^{2-} \tag{5.53}$$
$$CaCl_2 \rightleftharpoons Ca^{2+} + 2Cl^- \tag{5.54}$$
$$CaCO_3 \rightleftharpoons Ca^{2+} + CO_3^{2-} \tag{5.55}$$

The number of elements is $N_E = N_C - N_R = 10 - 5 = 5$. The formula matrix and stoichiometric matrix of the system are given by:

$$\mathbf{A} = \begin{bmatrix} 2 & 0 & 0 & 0 & 1 & 0 & 1 & 0 & 1 & 0 \\ 0 & 0 & 1 & 1 & 0 & 1 & 0 & 0 & 0 & 0 \\ 1 & 0 & 0 & 1 & 0 & 0 & 1 & 0 & 1 & 1 \\ 0 & 0 & 2 & 0 & 0 & 0 & 0 & 1 & 0 & 0 \\ 0 & 1 & 0 & 1 & 0 & 0 & 0 & 0 & 1 & 1 \end{bmatrix}$$

$$\mathbf{N} = \begin{bmatrix} -1 & 0 & 0 & 0 & 1 & 0 & 1 & 0 & 0 & 0 \\ -1 & -1 & 0 & 0 & 1 & 0 & 0 & 0 & 1 & 0 \\ 0 & 0 & 0 & 0 & 1 & 0 & 0 & 0 & -1 & 1 \\ 0 & 0 & -1 & 0 & 0 & 1 & 0 & 2 & 0 & 0 \\ 0 & 0 & 0 & -1 & 0 & 1 & 0 & 0 & 0 & 1 \end{bmatrix}^{\mathrm{T}} \tag{5.56}$$

- With carbonic acid

$$\mathrm{H_2O} \rightleftharpoons \mathrm{H^+ + OH^-} \tag{5.57}$$
$$\mathrm{CO_2 + H_2O} \rightleftharpoons \mathrm{H_2CO_3} \tag{5.58}$$
$$\mathrm{H_2CO_3} \rightleftharpoons \mathrm{H^+ + HCO_3^-} \tag{5.59}$$
$$\mathrm{HCO_3^-} \rightleftharpoons \mathrm{H^+ + CO_3^{2-}} \tag{5.60}$$
$$\mathrm{CaCl_2} \rightleftharpoons \mathrm{Ca^{2+} + 2Cl^-} \tag{5.61}$$
$$\mathrm{CaCO_3} \rightleftharpoons \mathrm{Ca^{2+} + CO_3^{2-}} \tag{5.62}$$

The number of elements is $N_E = N_C - N_R = 11 - 6 = 5$. The formula matrix and stoichiometric matrix of the systems are given by:

$$\mathbf{A} = \begin{bmatrix} 2 & 0 & 2 & 0 & 0 & 1 & 0 & 1 & 0 & 1 & 0 \\ 0 & 0 & 0 & 1 & 1 & 0 & 1 & 0 & 0 & 0 & 0 \\ 1 & 0 & 1 & 0 & 1 & 0 & 0 & 1 & 0 & 1 & 1 \\ 0 & 0 & 0 & 2 & 0 & 0 & 0 & 0 & 1 & 0 & 0 \\ 0 & 1 & 1 & 0 & 1 & 0 & 0 & 0 & 0 & 1 & 1 \end{bmatrix}$$

$$\mathbf{N} = \begin{bmatrix} -1 & 0 & 0 & 0 & 0 & 1 & 0 & 1 & 0 & 0 & 0 \\ -1 & -1 & 1 & 0 & 0 & 0 & 0 & 0 & 0 & 0 & 0 \\ 0 & 0 & -1 & 0 & 0 & 1 & 0 & 0 & 0 & 1 & 0 \\ 0 & 0 & 0 & 0 & 0 & 1 & 0 & 0 & 0 & -1 & 1 \\ 0 & 0 & 0 & -1 & 0 & 0 & 1 & 0 & 2 & 0 & 0 \\ 0 & 0 & 0 & 0 & -1 & 0 & 1 & 0 & 0 & 0 & 1 \end{bmatrix}^{\mathrm{T}} \tag{5.63}$$

The components and elements of the complete system are presented in Table 5.3.

Table 5.3: Component and element numbering for $H_2O/CO_2/CaCl_2/CaCO_3$ system.

Component	Without H_2CO_3	With H_2CO_3	Element
1	H_2O	H_2O	H^+
2	CO_2	CO_2	Ca^{2+}
3	$CaCl_2$	H_2CO_3	O^{2-}
4	$CaCO_3$	$CaCl_2$	Cl^-
5	H^+	$CaCO_3$	CO_2
6	Ca^{2+}	H^+	
7	OH^-	Ca^{2+}	
8	Cl^-	OH^-	
9	HCO_3^-	Cl^-	
10	CO_3^{2-}	HCO_3^-	
11		CO_3^{2-}	

Carbon dioxide in water

Carbon dioxide solubility in pure water is calculated without calcium chloride or calcium carbonate in the solution. Their corresponding rows and columns are decoupled from the formula and stoichiometric matrices. Figure 5.2 shows the solubility as a function of pressure at different temperatures.

Both approaches can capture adequately the experimental data at different temperatures over a large pressure range. In Figures 5.2a and 5.2c, concentrations of the bicarbonate and carbonate ions are so low, that the molecular aqueous carbon dioxide is almost as high as the total solubility. We see a different picture in Figures 5.2b and 5.2d where the carbonic acid is included in the calculations. Dissolved molecular carbon dioxide is approximately as abundant as the carbonic acid and the scaled Henry's constant must account for this to ultimately yield correct solubilities.

Carbon dioxide in aqueous solution of calcium chloride

The electrolyte system is more complex and non-ideal when calcium chloride is dissolved in water. There is no calcium carbonate in the solution and its corresponding rows and columns are decoupled from the formula and stoichiometric matrices. Experimental solubility of carbon dioxide in the solution is lower at higher salinity. Calculations are shown with experimental data in Figure 5.3.

The calculated curves at different temperatures are more distinguishable in comparison with the experimental data but they change as expected, i.e. higher temperatures result in lower solubilities. The reason for the larger deviations compared to pure water solubility, is the lack of a ternary interaction parameter involving calcium and chloride ions with carbon dioxide [Pitzer database of PHREEQC (Parkhurst and Appelo, 2013) for Pitzer's model in

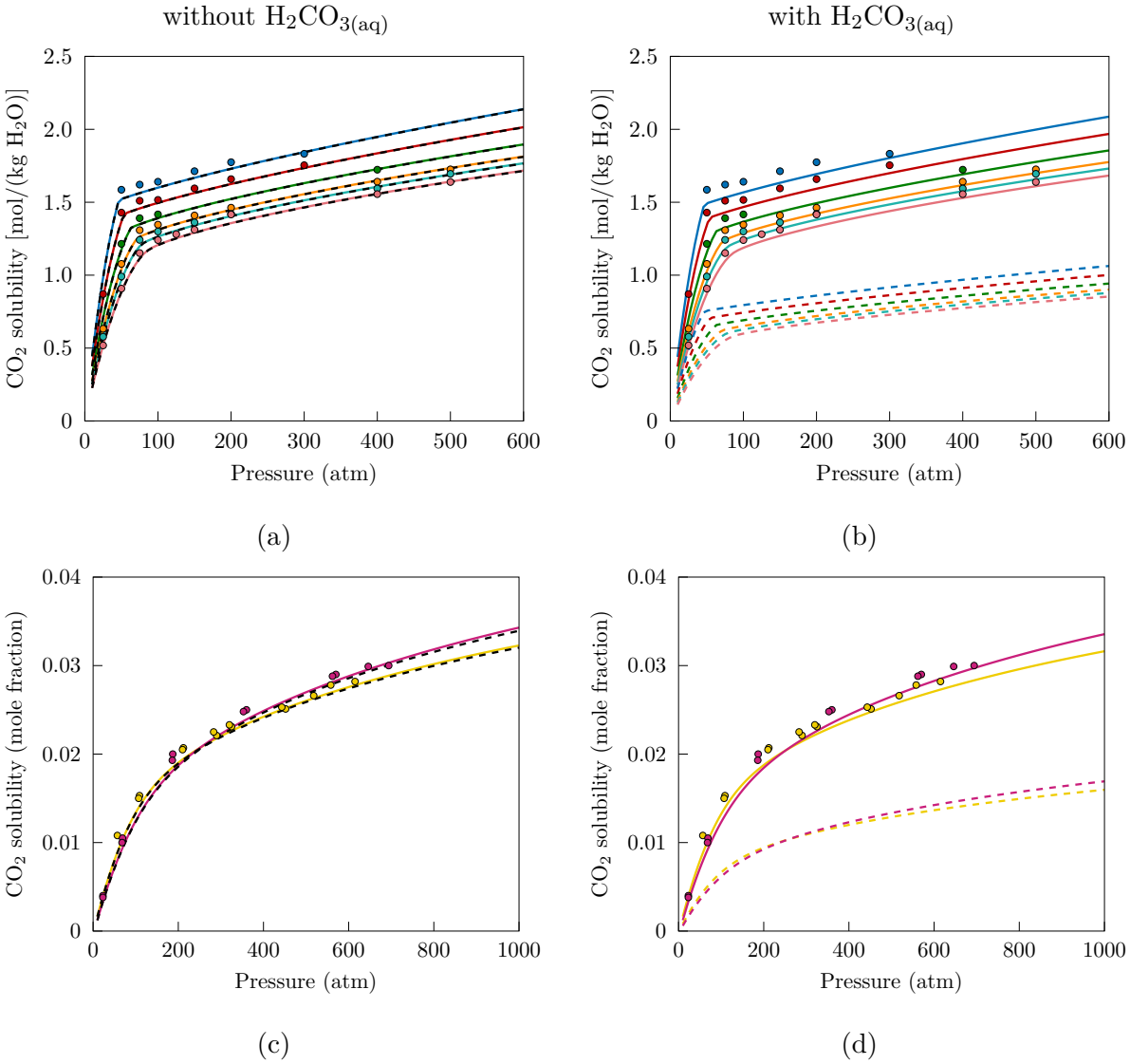

Figure 5.2: CO_2 solubility in water [experimental data at 285.15 K (●), 291.15 K (●), 298.15 K (●), 304.19 K (●), 308.15 K (●), 313.15 K (●), 374.15 K (●), 393.15 K (●), sum of all CO_2 related species (——), $CO_{2(aq)}$ (- - -)].

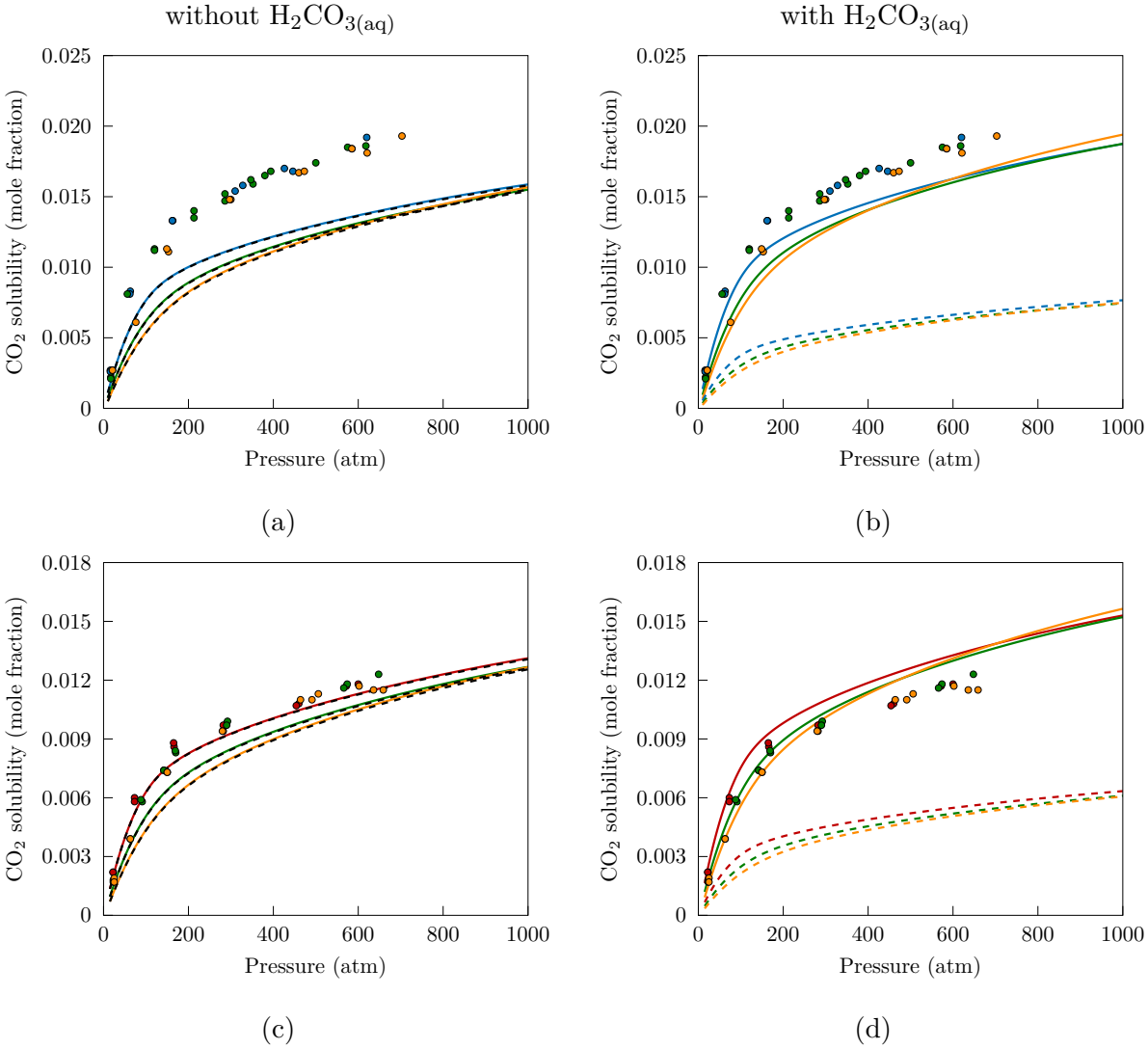

Figure 5.3: CO_2 solubility in: (a, b) 10.1% $CaCl_{2(aq)}$, (c, d) 20.2% $CaCl_{2(aq)}$ [experimental data at 348.65 K (●), 349.15 K (●), 374.15 K (●), 394.15 K (●), sum of all CO_2 related species (——), $CO_{2(aq)}$ (- - -)].

Felmy and Weare (1986)]. However, we conclude that the algorithms can produce results even when the system is highly non-ideal. Of course, better models or more available relevant parameters will shift the calculated curves closer to the experimental data.

Carbon dioxide in aqueous solution of calcium chloride with calcium carbonate

Finally, calculations are made in the presence of both calcium chloride and calcium carbonate in the solution. The latter is a solute but can also form a pure solid phase. Comparison with experimental data is shown in Figures 5.4.

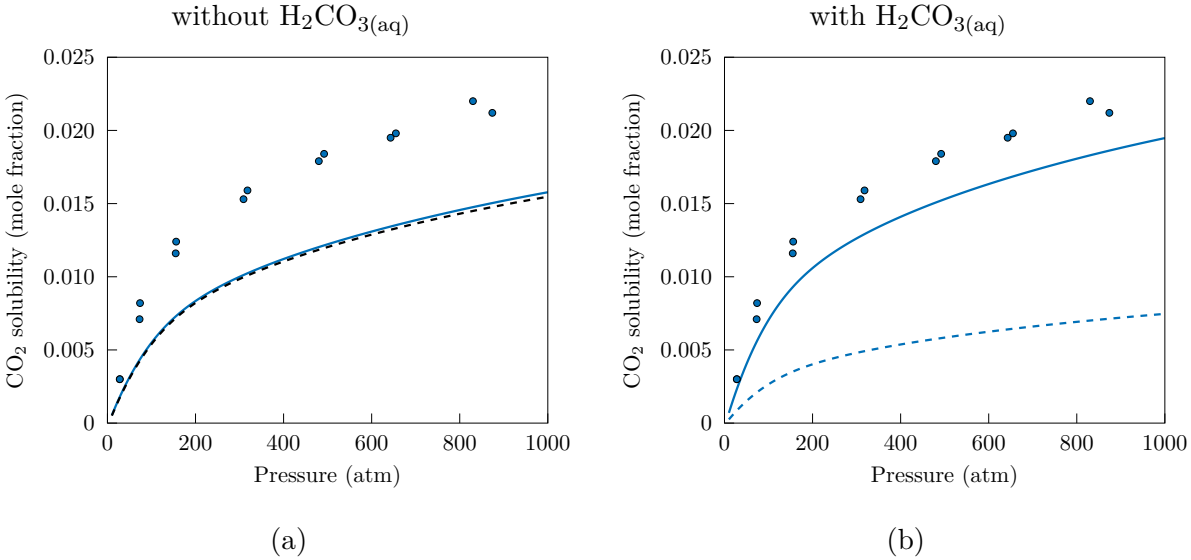

Figure 5.4: CO_2 solubility in 10.1% $CaCl_{2(aq)}$ in the presence of $CaCO_{3(s)}$ [experimental data at 393.15 K (●), sum of all CO_2 related species (——), $CO_{2(aq)}$ (- - -)].

Experimental data with or without calcium carbonate at equilibrium do not seem to be easily distinguishable (Figures 5.3a and 5.3b). The solid does not appear in the system from precipitation, but it is included in the feed. Calculations predict only a small amount of the solid dissolving in the the aqueous phase (0.01%-0.02%) and as a result it does not affect much the overall equilibrium. The main capability of the algorithms highlighted here is that with both the Lagrange multipliers method and the modified RAND we can handle pure solids in contact with highly non-ideal electrolyte aqueous phases at equilibrium.

5.4 Conclusions

The successive substitution and the combined algorithm were successfully applied to single-solvent (aqueous) electrolyte systems. Electroneutrality is already satisfied by the formula matrix in the material balance. It should be mentioned that the working equations have been derived for mole fractions and a mole fraction based reference state needs to be selected. Therefore, the main difficulty associated with these systems is to transform

the molality or molarity reference state to the infinite dilution reference state. This task is not performed by the non-stoichiometric methods presented in this work but by the fugacity or activity coefficient routine. As a result the working equations of both the Lagrange multipliers and the modified RAND method remain unchanged in electrolyte systems.

Calculations in the VLE of an ammonia/carbon dioxide aqueous solution in the presence of inerts revealed that CPU time and convergence behavior are similar to calculations for non-electrolyte systems. Furthermore, we investigated the solubility of carbon dioxide in pure water and highly non-ideal aqueous solutions of calcium chloride in the presence of solid calcium carbonate. Comparisons were made with experimental data to validate as a first step the correct qualitative description of the systems. The most accurate calculations were observed for aqueous solution of carbon dioxide at various temperatures. The models used for the electrolytes in the aqueous phase are not necessarily the most suitable because not all interaction parameters between the solutes were available. Improved calculations can be made when more relevant parameters are known or a more consistent electrolyte EoS model is used.

Finally, the most important finding of this chapter is that both algorithms were able to solve the CPE of electrolyte systems and consideration of a solid phase did not cause any problems in convergence (initialization or the actual CPE calculations). Even more complex areas of application could include geochemical systems with an aqueous phase of various charged and uncharged solutes at equilibrium with multiple solid phases, such as the systems appearing in Leal et al. (2016a,b).

CHAPTER

6

Phase equilibrium modeling for DME enhanced waterflood

Waterflooding is a secondary oil recovery method. Water/brine injected into a reservoir displaces the oil by maintaining the reservoir pressure at a sufficient level for oil production. However, primary and secondary oil recovery accounts for about 35% of the total oil amount, while further recovery with conventional methods proves to be too expensive (Lake, 1989). To extract more oil from a reservoir, enhanced oil recovery methods are employed. One EOR method is solvent enhanced waterflood, which involves phase equilibrium and component exchange with the reservoir oil, such as extraction, dissolution, etc. In the case of complete miscibility of the solvent with the oil, the process has high ultimate displacement efficiency due to the absence of residual phases (Lake, 1989). Dimethyl ether (DME) has been recently proposed as a novel solvent in the DME enhanced waterflood (DEW) process developed by Shell (Chernetsky et al., 2015), intended for mature and new wells (Groot et al., 2016).

DME or methoxymethane, a colorless gas at room temperature, is the simplest ether. The molecular structure of DME is shown in Figure 6.1. It is synthesized from synthesis gas (syngas), natural gas, coal or biomass: methanol is first produced and is subsequently dehydrated to DME (Arteconi et al., 2009; Park et al., 2007). It can be used as a propellant gas, fuel additive, pesticide, hydrogen source for fuel cells, for household cooking and heating, etc. (Wu et al., 2003, 2004; Park et al., 2007; Meng et al., 2012; Ratnakar et al., 2016a, 2017). DME is not a cryogenic liquid, which makes it easy to store (Park et al., 2007). It is a high performance refrigerant that operates at moderate pressures, being potentially a green refrigerant (ozone depletion potential equal to 0) (Meng et al., 2012).

It has similar physical properties to liquefied petroleum gases (propane, butane) and as a result is has been proposed as an alternative to LPG. DME exhibits excellent properties as a diesel fuel and has been viewed as a fossil fuel alternative because of the lower emissions of SO_x and NO_x (Arteconi et al., 2009; Meng et al., 2012; Tallon and Fenton, 2010). Use

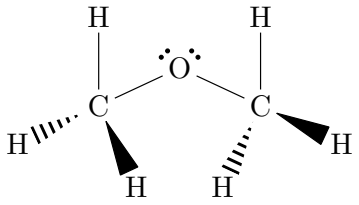

Figure 6.1: Dimethyl ether molecular structure.

in extraction is advantageous due to its higher vapor pressure compared to other liquid organic solvents, because of the easier removal from the final product. DME in air is flammable, making it ideal as a fuel, but requires provision when applied as a solvent in extraction (Tallon and Fenton, 2010). Finally, DME is non-toxic, non-corrosive and non-carcinogenic (Chahardowli et al., 2016; Ratnakar et al., 2016a, 2017).

DME is a slightly polar compound (dipole moment 1.3 D), soluble in both polar and non-polar solvents (Wu et al., 2003, 2004; Dahlhoff and Pfennig, 2000; Arteconi et al., 2009). This the reason why it was considered as a solvent in enhanced waterflood. Details of the DEW process are included in te Riele et al. (2016). Alkindi et al. (2016) mention that DME enhanced waterflood is advantageous compared with steam injection due to the miscible flow without density differences that could cause negative gravity effects. DME can be dissolved in water/brine and it is first-contact miscible with the oil. When it partitions into the oil phase, it swells the oil reducing its viscosity and therefore increasing its mobility. The solvent is then recovered and reused by chase water flooding (Groot et al., 2016). Water/brine plays the role of the DME carrier during the injection (Chernetsky et al., 2015; Ratnakar et al., 2016a). DME is imported or synthesized on site (te Riele et al., 2016).

A complex EOR process, the DEW process, involves partitioning of DME between the hydrocarbon and water/brine phases. Compared with classical waterflooding, because of DME, hydrocarbons can be dissolved to a larger extent in the aqueous phase and more water can be dissolved in the hydrocarbon phase. In order to combine the DEW process with reservoir simulation, adequate phase equilibrium modeling is needed to capture the major characteristics of the DME/water(brine)/hydrocarbon phase behavior. In particular, the most important property to describe is the partitioning of DME between the hydrocarbon and aqueous phases (K-value). In addition to phase equilibrium, other physical properties of DME-containing oils and aqueous phases, such as densities and viscosities, are important, but they are not covered in this study. In this chapter, we present the modeling of DME binary systems with different compounds relevant to the DEW process, influenced by the work of Ratnakar et al. (2016b,a, 2017). Predictions are made initially for ternary mixtures of DME/water/hydrocarbons and then for DME/water/model oil, examining the effect of oil composition, temperature, pressure and salinity on the K-values of DME.

6.1 EoS models

The models selected for the phase equilibrium modeling are the Cubic-Plus-Association equation of state and cubic equations of state with Huron-Vidal mixing rules.

- Cubic-Plus-Association equation of state (CPA EoS)

  CPA is an EoS developed to account for the association of compounds such as water, alcohols, organic acids etc. (Kontogeorgis et al., 1996). Association can take place between the same types of molecules (self-association) or different types (cross association or solvation). The equation combines the Soave-Redlich-Kwong EoS (Soave, 1972) with the association term of Huang and Radosz (1990). The original form of CPA is:

$$p = \frac{RT}{v-b} - \frac{a(T)}{v(v+b)} - \frac{RT}{v^2}\sum_{\mathrm{A}_i}\left(\frac{1}{X_{\mathrm{A}_i}} - \frac{1}{2}\right)\frac{\partial X_{\mathrm{A}_i}}{\partial(1/v)} \tag{6.1}$$

  which can also take the form (Michelsen and Hendriks, 2001):

$$p = \frac{RT}{v-b} - \frac{a(T)}{v(v+b)} - \frac{1}{2}\frac{RT}{v}\left(1 + \frac{1}{v}\frac{\partial \ln g}{\partial(1/v)}\right)\sum_i x_i \sum_{\mathrm{A}_i}(1 - X_{\mathrm{A}_i}) \tag{6.2}$$

  with

$$X_{\mathrm{A}_i} = \frac{1}{1 + (1/v)\sum_j x_j \sum_{\mathrm{B}_j} X_{\mathrm{B}_j}\Delta^{\mathrm{A}_i\mathrm{B}_j}} \tag{6.3}$$

$$\Delta^{\mathrm{A}_i\mathrm{B}_j} = g(v)\left[\exp\left(\frac{\epsilon^{\mathrm{A}_i\mathrm{B}_j}}{RT}\right) - 1\right] b_{ij}\beta^{\mathrm{A}_i\mathrm{B}_j} \tag{6.4}$$

$$g(v) = \frac{2-\eta}{2(1-\eta)^3} \tag{6.5}$$

  and

$$\eta = \frac{b}{4v} \tag{6.6}$$

  where:

v	molar volume
a	energy parameter
b	covolume parameter
$\Delta^{\mathrm{A}_i\mathrm{B}_j}$	association strength between sites A_i and B_j

X_{A_i}	mole fraction of component i not bonded at site A
$g(v)$	radial distribution function
$\epsilon^{\mathrm{A}_i\mathrm{B}_j}$	association energy of interaction between sites A_i and B_j
$\beta^{\mathrm{A}_i\mathrm{B}_j}$	parameter in the association term of CPA between sites A_i and B_j
b_{ij}	covolume parameter of components i and j

The radial distribution function is approximated as:

$$g(v) \approx \frac{1}{1 - 1.9\eta} \tag{6.7}$$

For pure components, the energy parameter is calculated by:

$$a(T) = a_0 \left[1 + c_1 \left(1 - \sqrt{T_r}\right)^2\right] \tag{6.8}$$

Combining rules of a involve the use of a binary interaction parameter:

$$a_{ij} = \sqrt{a_i a_j}(1 - k_{ij}) \tag{6.9}$$

No interaction parameters are involved in the combining rules of b:

$$b_{ij} = \frac{b_i + b_j}{2} \tag{6.10}$$

where:

a_{ij}	energy parameter of components i and j
a_i	energy parameter of component i
k_{ij}	binary interaction parameter between component i and j
b_i	covolume parameter of component i
b_{ij}	covolume parameter of components i and j

In this work, water is the only self-associating compound, hydrocarbons or inert gases in the oil are non-associating and DME is solvating in water. For DME/water the modified CR-1 rules are followed for cross association (Folas et al., 2006):

$$\beta_{\mathrm{cross}} = \beta_{\mathrm{regressed}} \tag{6.11}$$

and

$$\epsilon_{\mathrm{cross}} = \frac{\epsilon_{\mathrm{water}}}{2} \tag{6.12}$$

Classical mixing rules are used for a and b:

$$a = \sum_i \sum_j x_i x_j a_{ij} \tag{6.13}$$

and

$$b = \sum_i x_i b_i \tag{6.14}$$

- Cubic equation of state with Huron-Vidal mixing rules (CEoS-HV)

  Cubic equations of state are widely used due to their simplicity. Peng-Robinson (Peng and Robinson, 1976) and Soave-Redlich-Kwong (Soave, 1972) are expressed with the same equation:

$$p = \frac{RT}{v-b} - \frac{a(T)}{(v+\delta_1 b)(v+\delta_2 b)} \tag{6.15}$$

with

$$\delta_1 = \begin{cases} 1+\sqrt{2} & \text{PR} \\ 1 & \text{SRK} \end{cases} \qquad \delta_2 = \begin{cases} 1-\sqrt{2} & \text{PR} \\ 0 & \text{SRK} \end{cases} \tag{6.16}$$

and

$$\Delta = \frac{1}{\delta_2 - \delta_1} \ln \frac{1+\delta_2}{1+\delta_1} \tag{6.17}$$

To apply a CEoS on a mixture with polar components the Huron-Vidal mixing rules (Huron and Vidal, 1979) are used, based on a modified NRTL excess energy function:

$$\frac{a}{bRT} = \sum_i \frac{a_i}{b_i RT} - \frac{1}{\Delta} \frac{g^{E,\infty}}{RT} \tag{6.18}$$

with

$$g^{E,\infty} = \sum_i x_i \frac{\sum_j x_j b_j \exp\left(-\alpha_{ji} \frac{C_{ji}}{RT}\right) C_{ji}}{\sum_j x_j b_j \exp\left(-\alpha_{ji} \frac{C_{ji}}{RT}\right)} \tag{6.19}$$

where:

C_{ij} HV-NRTL energy interaction parameter between components i and j

α_{ij} HV-NRTL non-randomness parameter between components i and j

The advantage of the modified NRTL equation is that we can reduce the mixing rules to the classical van der Waals mixing rules by the following relations (Huron and Vidal, 1979):

$$\begin{gathered} \alpha_{ij} = 0 \qquad C_{ji} = g_{ji} - g_{ii} \qquad g_{ii} = -\frac{a_i}{b_i}\Delta \\ g_{ji} = -2\frac{\sqrt{b_i b_j}}{b_i + b_j}\sqrt{g_{ii} g_{jj}}(1 - k_{ij}) \end{gathered} \tag{6.20}$$

6.2 Regression for DME binary systems

Parameters were regressed for CPA and CEoS-HV using experimental data of binary systems of DME with different compounds. The binary systems are presented in Table 6.1 and are divided into 2 groups, DME/water and DME/hydrocarbon or inert gas. The same critical constants were used for both CPA and CEoS-HV. CPA pure component parameters are reported in Table 6.2, where Γ is given by:

$$\Gamma = \frac{a_0}{bR} \tag{6.21}$$

Table 6.1: Experimental data of DME binaries used in the regressions.

Binary	T range (K)	p range (bar)	Points	Type
water (Pozo and Streett, 1984)	323.15 – 394.21	0.12 – 346.81	74	p-y-x, p-x-x'
methane (Garcia-Sanchez et al., 1987)	282.9 – 343.8	19.7 – 123.6	23	p-y-x
propane (Horstmann et al., 2003; Giles and Wilson, 2000)	273.15 – 313.39	2.663 – 13.868	93	p-x, p-y-x
n-butane (Pozo de Fernández et al., 1992)	282.96 – 414.5	1.474 – 48.2	154	p-y-x
n-pentane (Outcalt and Lemmon, 2013)	269.99 – 380	1.8326 – 27.502	34	T-p
n-decane (Park et al., 2007)	323.15	0.0118 – 11.4231	39	p-x
n-dodecane (Park et al., 2007)	323.15	0.002 – 11.4339	36	p-x
CO_2 (Laursen et al., 2003)	298.15 – 320.15	6 – 73.2	27	p-y-x
N_2 (Laursen et al., 2003)	298.15 – 318.15	6 – 103.5	34	p-y-x

The objective function to be minimized in the regression is the sum of all deviations from experimental data: pressure and compositions in VLE, LLE. Deviations ΔX_i are calculated as:

Table 6.2: Pure component parameters for CPA.

Component	T_c (K)	Γ (K)	b (L/mol)	c_1	ϵ/R (K)	$\beta \times 10^3$	Scheme
DME (Tsivintzelis and Kontogeorgis, 2014)	400.1	2045.568	0.0496	0.72125	0	0	-
water (Kontogeorgis et al., 1999)	647.29	1017.338	0.014515	0.67359	2003.248	69.2	4C
methane (Tsivintzelis et al., 2011)	190.56	959.028	0.0291	0.44718	0	0	-
propane (Yakoumis et al., 1997)	369.83	1896.453	0.057834	0.6307	0	0	-
n-butane (Yakoumis et al., 1997)	425.18	2193.083	0.072081	0.70771	0	0	-
n-pentane (Yakoumis et al., 1997)	469.7	2405.105	0.091008	0.79858	0	0	-
n-decane (Yakoumis et al., 1997)	617.7	3190.542	0.17865	1.13243	0	0	-
n-dodecane (Tsivintzelis et al., 2011)	658	3471.038	0.21624	1.19531	0	0	-
CO_2 (Tsivintzelis et al., 2010)	304.21	1551.222	0.0272	0.7602	0	0	-
N_2 (Folas et al., 2006)	126.2	634.07	0.02605	0.49855	0	0	-

$$\Delta X_i = \begin{cases} \left| \dfrac{X_i^{\text{exp}} - X_i^{\text{calc}}}{X_i^{\text{exp}}} \right| & X \text{ is pressure} \\ \\ \left| \dfrac{X_i^{\text{exp}} - X_i^{\text{calc}}}{\min(X_i^{\text{exp}}, 1 - X_i^{\text{exp}})} \right| & X \text{ is composition} \end{cases} \tag{6.22}$$

DME/water

DME/water phase equilibrium data exhibit two vapor-liquid and one liquid-liquid region. Tsivintzelis and Kontogeorgis (2014) presented CPA modeling of this binary at two temperatures. The reason their parameters are not used in this work is because we regressed experimental data at four temperatures. A number of different regression strategies was attempted for CPA:

- regress two parameters for all temperatures: k_{ij} and β_{cross} using Eq. 6.12 to calculate ϵ_{cross}
- regress three parameters for all temperatures: k_{ij}, β_{cross} and ϵ_{cross}
- regress k_{ij} for each temperature using constant β_{cross} and Eq. 6.12 to calculate ϵ_{cross}

and for CEoS-HV:

- regress three parameters for all temperatures: C_{ij}, C_{ji} and α_{ij}
- regress C_{ij} and C_{ji} for each temperature using constant α_{ij}

Tables 6.3 and 6.4 show the parameters for each model and regression strategy. In Figure 6.2 calculations with CPA and SRK-HV are compared with experimental data. In general, the two VLE branches of the curves are represented well by all models, but temperature dependent parameters give better results for the LLE curves (Figures 6.2e and 6.2f). The worst results are obtained when only two temperature independent parameters are regressed for CPA, especially when predicting solubility of water in the DME-rich phase and DME in the water-rich phase.

Table 6.3: Regressed parameters for DME/water using CPA (non-regressed parameters in parentheses).

T (K)	k_{ij}	β_{cross}	$\epsilon_{\text{cross}}/R$ (K)
all	-0.0967	0.3799	(1001.624)
all	-0.1250	0.1438	1287.500
323.15	-0.1274	(0.3799)	(1001.624)
348.15	-0.1066	(0.3799)	(1001.624)
373.26	-0.0937	(0.3799)	(1001.624)
394.21	-0.0807	(0.3799)	(1001.624)

Table 6.4: Regressed parameters for DME/water using PR and SRK with HV mixing rules (non-regressed parameters in parentheses).

T (K)	PR			SRK		
	C_{ij}/R (K)	C_{ji}/R (K)	α_{ij}	C_{ij}/R (K)	C_{ji}/R (K)	α_{ij}
all	2104.07	-1916.56	0.0950	2147.48	-1986.72	0.0923
323.15	2293.17	-2047.16	(0.0950)	2376.86	-2147.05	(0.0923)
348.15	2036.05	-1851.43	(0.0950)	2136.14	-1974.91	(0.0923)
373.26	1940.59	-1773.66	(0.0950)	2049.42	-1907.38	(0.0923)
394.21	1511.54	-1295.47	(0.0950)	1643.92	-1479.10	(0.0923)

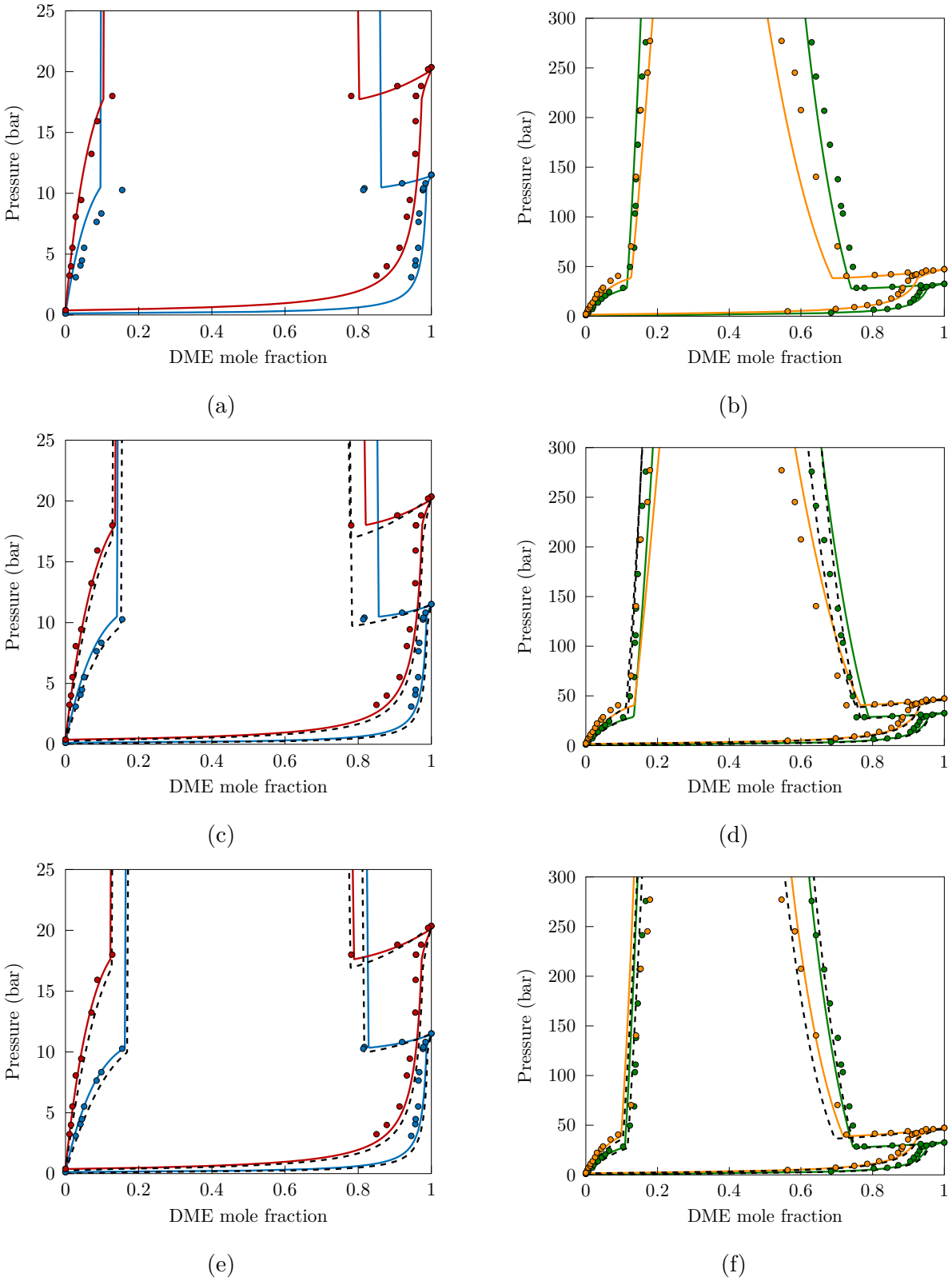

Figure 6.2: DME/water modeling with CPA and SRK-HV: (a, b) regressed k_{ij}, β_{cross} for CPA, (c, d) regressed k_{ij}, β_{cross}, ϵ_{cross} for CPA and C_{ij}, C_{ji}, α_{ij} for SRK-HV, (d, e) regressed $k_{ij} = f(T)$ for CPA and $C_{ij}, C_{ji} = f(T)$ for SRK-HV [experimental data at 323.15 K (●), 348.15 K (●), 373.26 K (●), 394.21 K (●), calculations with CPA (——), calculations with SRK-HV (- - -)].

DME/hydrocarbon and inert gas

For the DME binaries with hydrocarbons (HC) or inert gases, a binary interaction parameter was was enough to describe adequately the experimental data at different temperatures. For the CEoS-HV approach, we did not regress the HV parameters C_{ij}, C_{ji} and α_{ij}. Instead, we regressed a temperature independent k_{ij} using the corresponding EoS. Eq. 6.20 can be then used to determine the HV parameters. Performance of the models is similar (Figures 6.3a to 6.9) except for the higher temperatures in the DME/*n*-butane mixture. In Figures 6.5c, 6.5d, 6.6c and 6.6d there are isotherms that correspond to higher temperatures than pure DME critical temperature (400.1 K). CPA could not describe properly equilibrium around the critical point. Nevertheless, this is not a problem of the binary modeling but requires different parametrization for the pure components.

Table 6.5: Regressed parameters for DME/HC, DME/CO_2 and DME/N_2 using CPA, PR and SRK.

DME binary	CPA k_{ij}	PR k_{ij}	SRK k_{ij}
C1	0.0194	0.0401	0.0299
C3	0.0477	0.0486	0.0490
n-C4	0.0437	0.0425	0.0455
n-C5	0.0382	0.0402	0.0404
n-C10	0.0179	0.0174	0.0194
n-C12	0.0107	0.0091	0.0117
CO_2	0.0019	-0.0066	-0.0070
N_2	0.0495	0.1063	0.0968

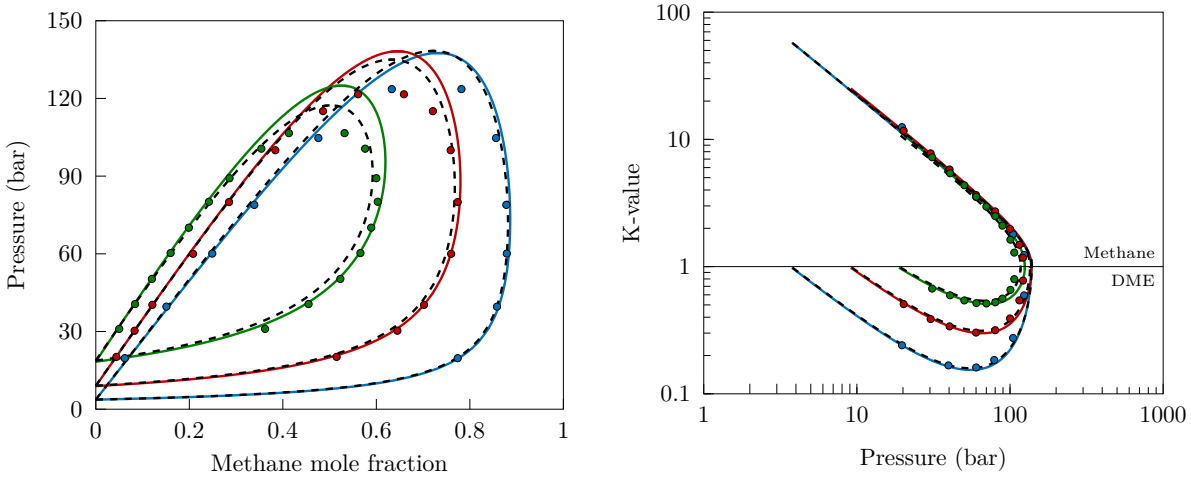

(a) (b)

Figure 6.3: DME/methane modeling with CPA and SRK: (a) *p*-*y*-*x* diagram, (b) K-values [experimental data at 282.9 K (●), 313.3 K (●), 343.8 K (●), calculations with CPA (——), calculations with SRK (- - -)].

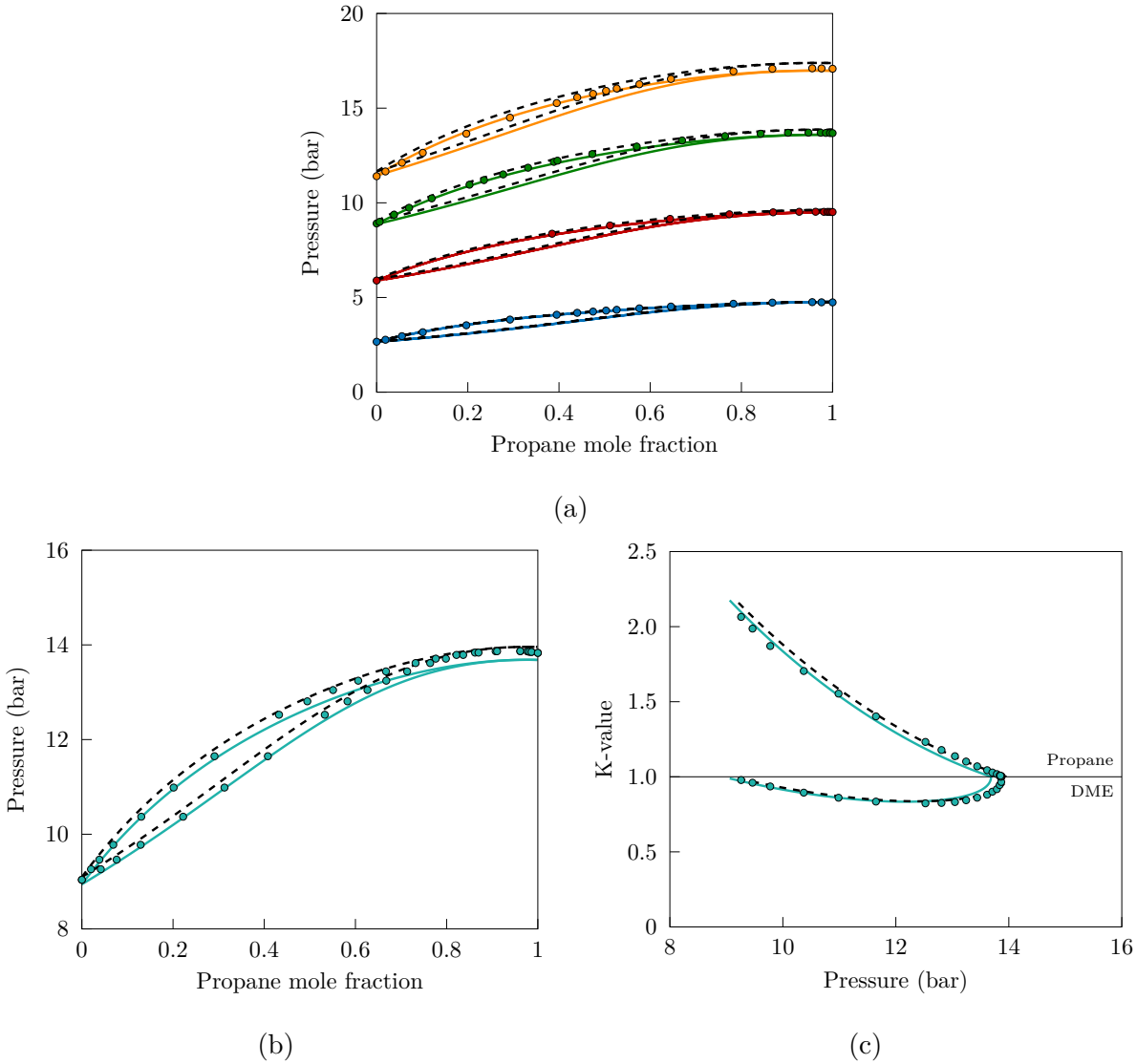

Figure 6.4: DME/propane modeling with CPA and SRK: (a, b) p-y-x diagram, (c) K-values [experimental data at 273.15 K (●), 298.15 K (●), 313.10 (●), 323.15 K (●), 313.39 K (●), calculations with CPA (——), calculations with SRK (- - -)].

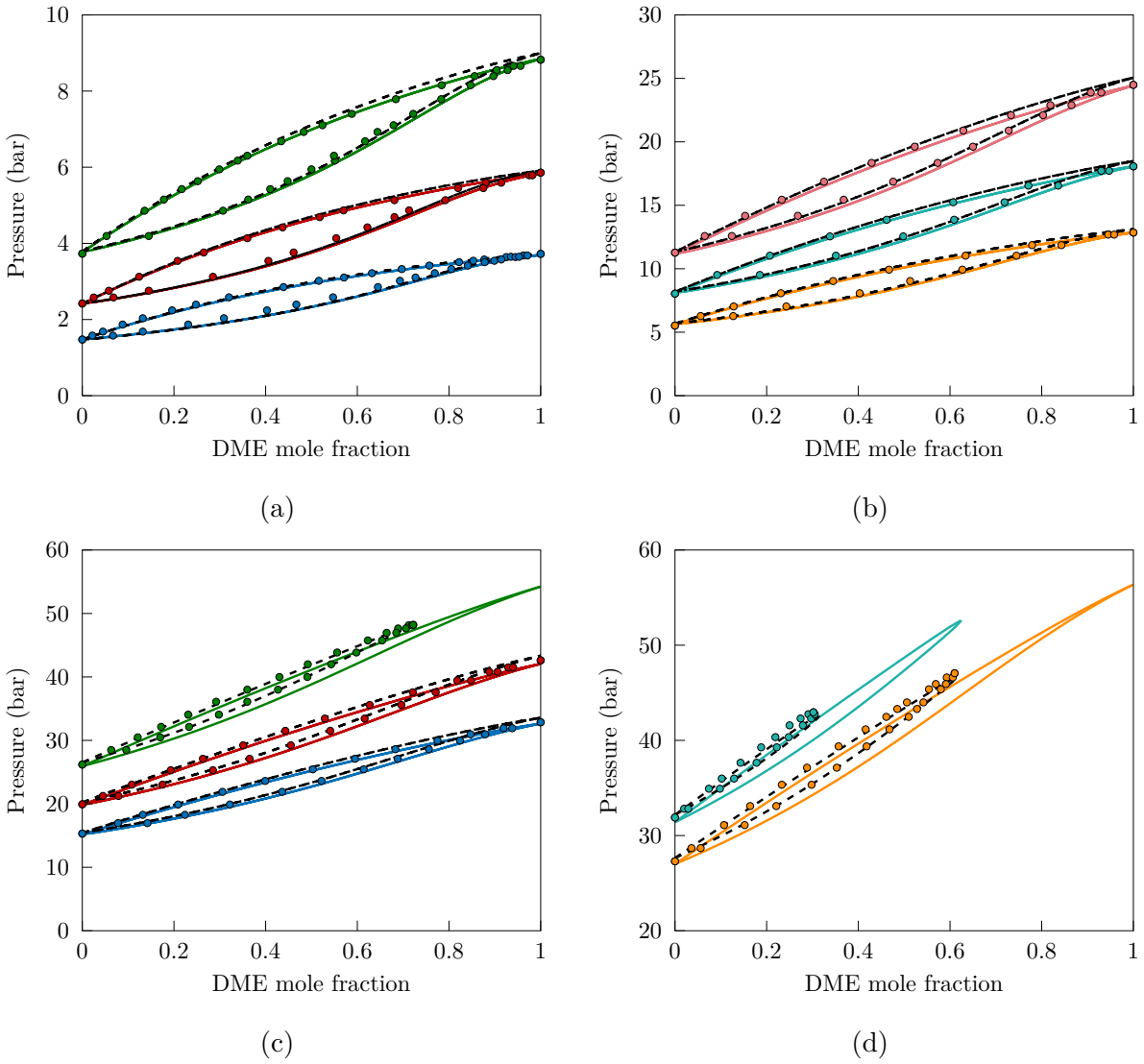

Figure 6.5: DME/*n*-butane modeling with CPA and SRK: (a, b) *p*-*y*-*x* diagram [experimental data at 282.96 K (●), 297.86 K (●), 312.98 K (●), 328.01 K (●), 343.07 K (●), 353.65 K (●)], (c, d) *p*-*y*-*x* diagram [experimental data at 372.87 K (●), 387.22 K (●), 402.71 K (●), 405.16 K (●), 414.50 K (●)] [calculations with CPA (——), calculations with SRK (- - -)].

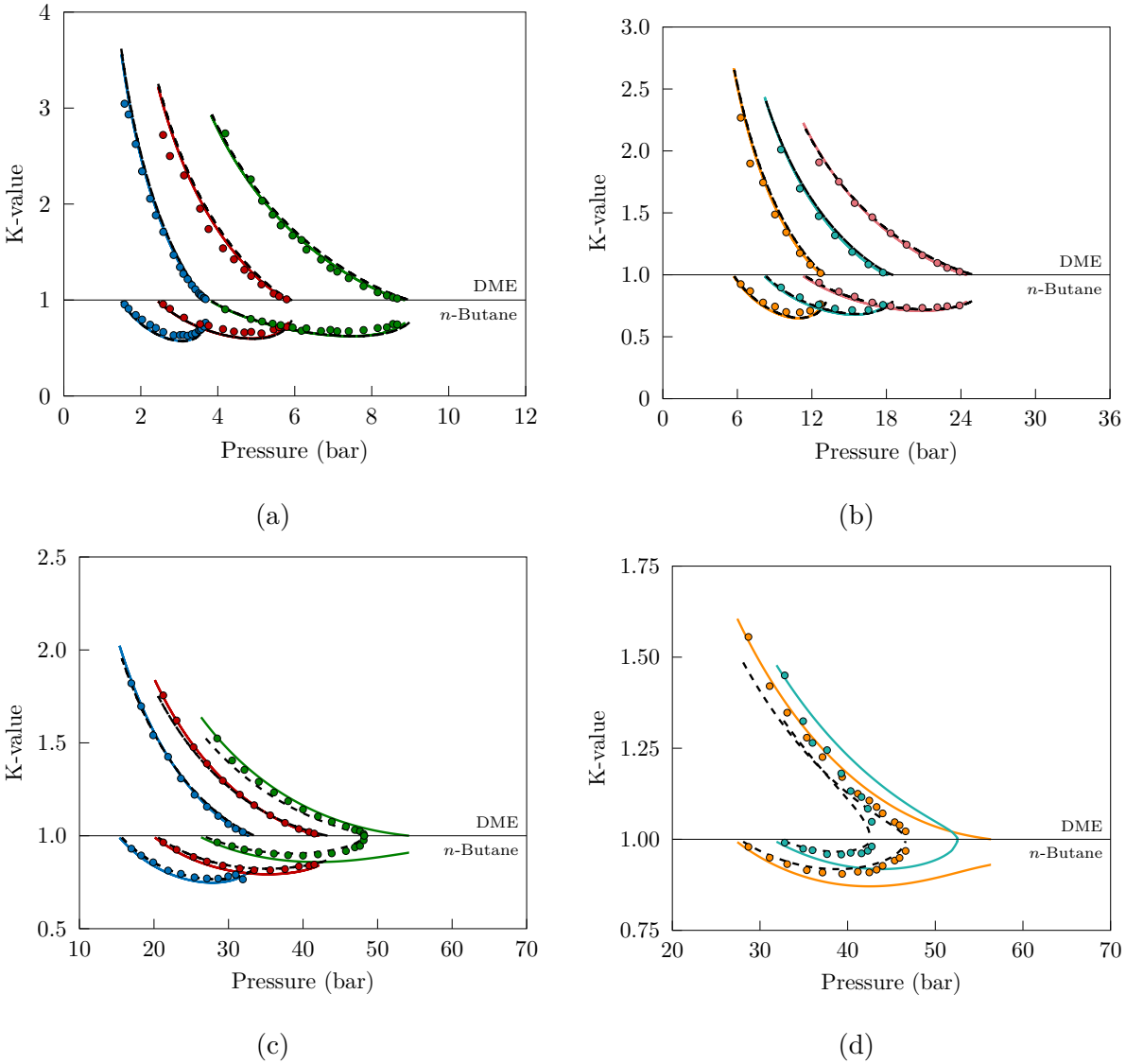

Figure 6.6: DME/*n*-butane modeling with CPA and SRK: (a, b) K-values [experimental data at 282.96 K (●), 297.86 K (●), 312.98 K (●), 328.01 K (●), 343.07 K (●), 353.65 K (●)], (c, d) K-values [experimental data at 372.87 K (●), 387.22 K (●), 402.71 K (●), 405.16 K (●), 414.50 K (●)] [calculations with CPA (——), calculations with SRK (- - -)].

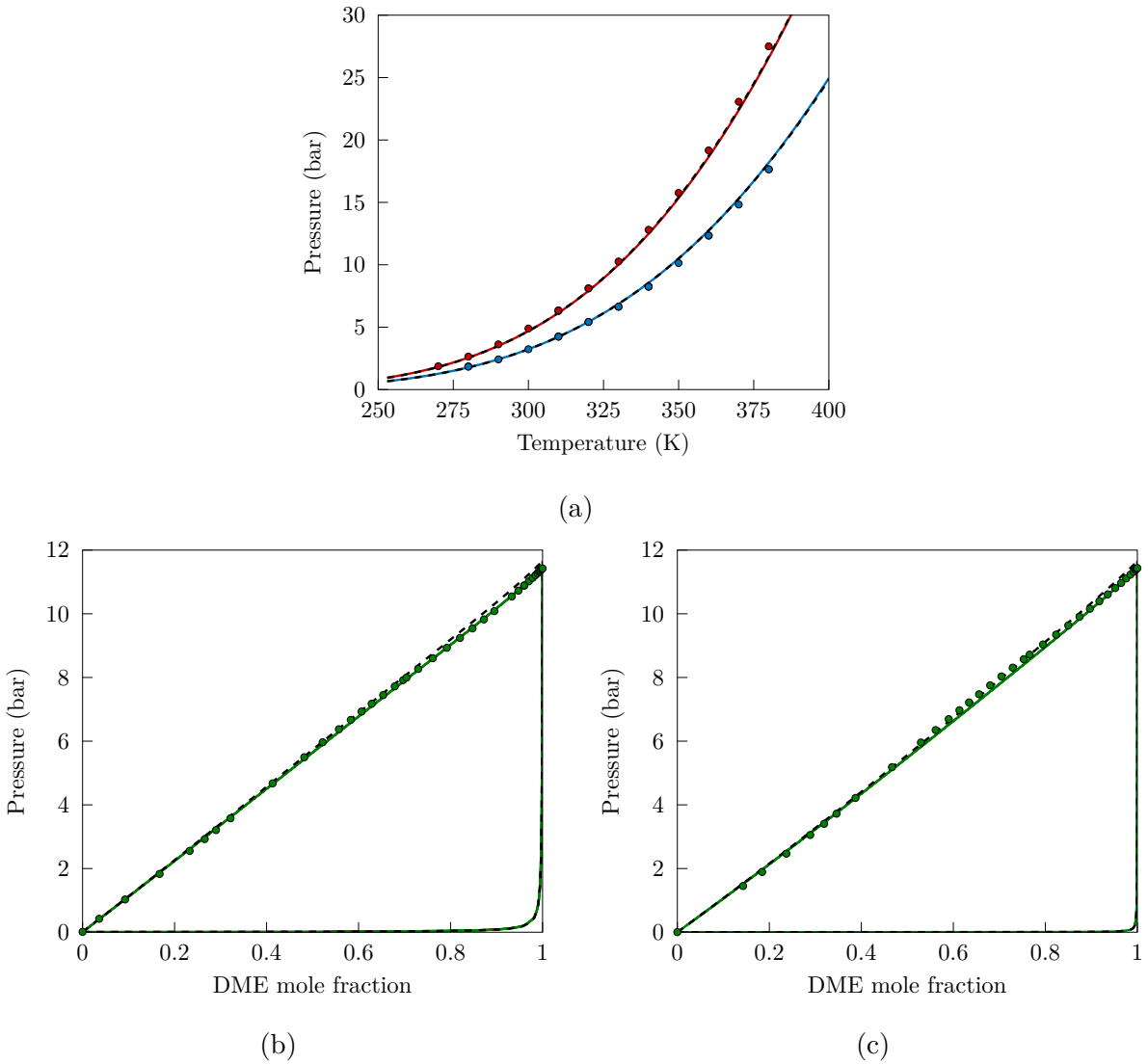

Figure 6.7: DME/hydrocarbon modeling with CPA and SRK for: (a) *n*-pentane, (b) *n*-decane, (c) *n*-dodecane [experimental data at $x_{\mathrm{DME}} = 0.392$ (●), $x_{\mathrm{DME}} = 0.679$ (●), 323.15 K (●), calculations with CPA (——), calculations with SRK (- - -)].

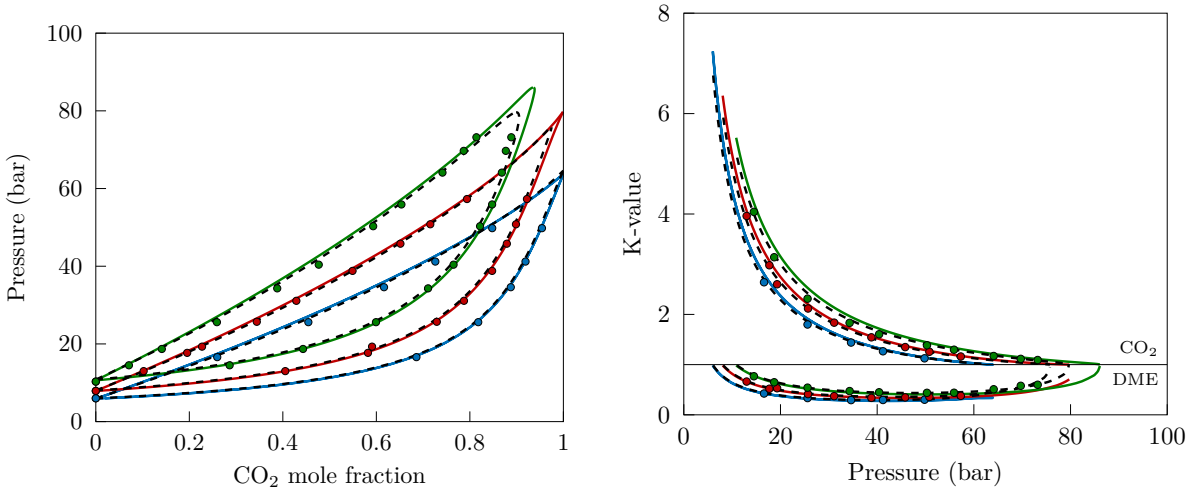

(a) (b)

Figure 6.8: DME/carbon dioxide modeling with CPA and SRK: (a) *p-y-x* diagram, (b) K-values [experimental data at 298.15 K (●), 308.65 K (●), 320.15 K (●), calculations with CPA (——), calculations with SRK (- - -)].

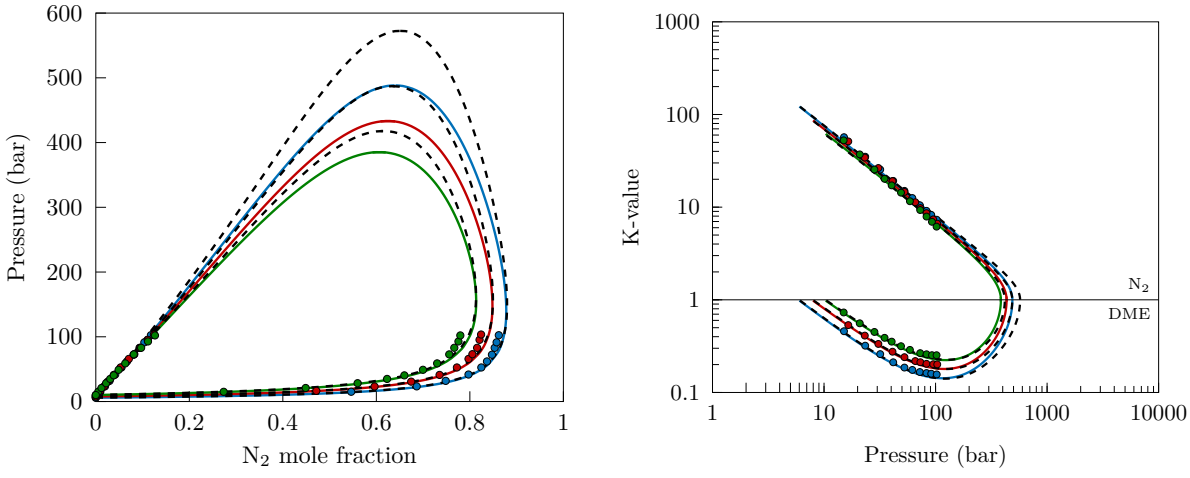

(a) (b)

Figure 6.9: DME/nitrogen modeling with CPA and SRK: (a) *p-y-x* diagram, (b) K-values [experimental data at 298.15 K (●), 308.15 K (●), 318.15 K (●), calculations with CPA (——), calculations with SRK (- - -)].

Table 6.6 shows the deviations for all the binaries and regression approaches. The error of the calculation is expressed in terms of average absolute relative deviations. Absolute relative deviation is given by:

$$\mathrm{ARD}_i = \left| \frac{X_i^{\mathrm{exp}} - X_i^{\mathrm{calc}}}{X_i^{\mathrm{exp}}} \right| \tag{6.23}$$

The formula implies that no experimental point is zero. The average absolute relative deviation is calculated by:

$$\mathrm{AARD} = \frac{1}{N} \sum_{i=1}^{N} \mathrm{ARD}_i \tag{6.24}$$

where:

N number of experimental points

The comparisons were made with experimental pressure and the mole fraction of DME in the vapor phase, the liquid phase of VLE, and the two liquid phases of LLE (whenever possible). Regression errors are acceptable and the modeling of the systems satisfactory. Larger deviations appear for DME liquid phase mole fractions in DME/water VLE, because the values of the mole fractions are small (Eq. 6.23 will result in larger values for the same absolute deviations). Finally, CPA in DME/n-butane has larger deviations than the two CEoS. This is a problem of pure component parametrization, that does not allow CPA to capture the correct behavior around the critical point (Figures 6.5c, 6.5d, 6.6c and 6.6d).

In general, it seems that CPA and CEoS-HV lead to equilibrium curves with similar deviations from the experimental data (PR-HV and SRK-HV are judged as a group since they give very similar results). For the purpose intended, we do not expect predictions with any of the models to yield much different conclusions. If conditions are not close to the critical region, CPA can model the binaries more than adequately. At the time of calculations, a CPA fugacity coefficient routine was more accessible therefore CPA was chosen to make predictions for the partitioning of DME, namely the K-value. For DME/water, the temperature dependent k_{ij} were selected. HV multicomponent mixing rules would require modifications in the routines to differentiate between water and hydrocarbons/inert gases. The parameters of the later are not supplied to the routine but must be calculated from Eq. 6.20.

Table 6.6: Average absolute relative deviations for DME binaries considering different models and regression strategies (LLE-1: water-rich liquid, LLE-2: DME-rich liquid).

System	Model	Regression parameters	$\%\Delta p$	$\%\Delta y$	$\%\Delta x_{\text{VLE}}$	$\%\Delta x_{\text{LLE-1}}$	$\%\Delta x_{\text{LLE-2}}$
DME/Water	CPA	$k_{ij}, \beta^{\text{A}_i\text{B}_j}$	1.50	26.71	2.81	6.26	4.36
	CPA	$k_{ij}, \beta^{\text{A}_i\text{B}_j}, \epsilon^{\text{A}_i\text{B}_j}$	0.62	26.46	1.80	11.99	4.94
	CPA	$k_{ij} = f(T)$	1.45	11.86	2.75	16.13	2.45
	PR-HV	$C_{ij}, C_{ji}, \alpha_{ij}$	3.51	3.65	37.61	5.63	5.97
	SRK-HV	$C_{ij}, C_{ji}, \alpha_{ij}$	2.86	3.95	32.35	7.20	5.31
	PR-HV	$C_{ij}, C_{ji} = f(T)$	3.87	3.78	31.18	12.64	2.63
	SRK-HV	$C_{ij}, C_{ji} = f(T)$	3.12	4.05	30.59	10.20	2.32
DME/C1	CPA	k_{ij}	2.99	2.49			
	PR	k_{ij}	2.66	2.91			
	SRK	k_{ij}	2.62	2.90			
DME/C3	CPA	k_{ij}	0.67	0.82			
	PR	k_{ij}	1.11	1.03			
	SRK	k_{ij}	0.58	0.80			
DME/n-C4	CPA	k_{ij}	1.18	8.18			
	PR	k_{ij}	1.20	2.59			
	SRK	k_{ij}	0.88	2.69			
DME/n-C5	CPA	k_{ij}	2.63				
	PR	k_{ij}	2.61				
	SRK	k_{ij}	2.56				
DME/n-C10	CPA	k_{ij}	1.35				
	PR	k_{ij}	1.27				
	SRK	k_{ij}	1.29				
DME/n-C12	CPA	k_{ij}	2.39				
	PR	k_{ij}	2.09				
	SRK	k_{ij}	1.78				
DME/CO_2	CPA	k_{ij}	2.73	1.68			
	PR	k_{ij}	1.33	0.95			
	SRK	k_{ij}	1.36	0.94			
DME/N_2	CPA	k_{ij}	3.80	2.11			
	PR	k_{ij}	4.18	1.93			
	SRK	k_{ij}	4.10	2.35			

6.3 Predictions of DME partitioning between water and oil

The experimental data of the DME binaries were captured successfully and therefore the next step is to predict the equilibrium behavior of DME/water/hydrocarbon mixtures. CEoS-HV could serve the same purpose, but in this work all predictions were made with CPA. As a first step, ternary mixture behavior will be predicted. In Figures 6.10 to 6.12 ternary mixtures of DME/water/hydrocarbon are shown at the same conditions. Binary interaction parameters for water/hydrocarbons were taken from Paterson (2017). Methane is the only hydrocarbon that allows the existence of two VLE and one VLLE region, as it is the lightest hydrocarbon. The number of degrees of freedom is zero in the VLLE regions at specified temperature and pressure with unique compositions of the vapor and the two liquid phases. The LLE curves of all hydrocarbons are presented in the same ternary figure (Figure 6.13). It appears that the nature of the hydrocarbon does not have a prominent effect on the overall equilibrium. Even for the DME/water/methane ternary where more complicated equilibria are observed, LLE boundaries are close to those of the remaining hydrocarbons. This implies that the K-values of DME between oil and water are not likely to have a strong dependence on the hydrocarbon concentration in the oil.

To test this hypothesis, we perform the following test. A light, intermediate and heavy hydrocarbon are chosen to represent the oil. For different hydrocarbon (methane, *n*-butane and *n*-decane) composition and DME concentration in the feed, we calculate the K-values at equilibrium. The constraint in these calculations is to use as little water as possible in the feed, which will result in a water-rich incipient phase (phase fraction $< 10^{-5}$). This leads to an oil phase with practically the same composition as the feed. The only case where this is not possible, is when the oil is too light to exist only as a liquid and we have separation into a vapor phase as well. Binary interaction parameters for methane/*n*-butane and methane/*n*-decane are -0.0005 and 0.0067 respectively, both regressed using databases developed in the work of Varzandeh (2017).

Figures 6.14 and 6.15 show the DME K-value between the oil and the aqueous phase, as a function of the oil composition in the feed. Each figure corresponds to constant DME in the feed. Because of the calculation procedure, the DME concentration is essentially the DME in the oil phase if there is only LLE (oil-rich liquid and water-rich liquid equilibrium). Figure 6.14a, 10% of DME in the feed with an incipient water-rich phase results in LLE when the heavier hydrocarbons dominate. At higher compositions of lighter hydrocarbons, the oil phase is too light and we have VLLE reducing to VLE at even higher methane concentrations in the absence of *n*-decane. Figures 6.14b and 6.15a show that by increasing DME in the feed, VLE disappears and the VLLE region shrinks. Finally at 70% DME (Figure 6.15b) in the feed, the only equilibrium that can be established is LLE at the current conditions regardless of the oil composition.

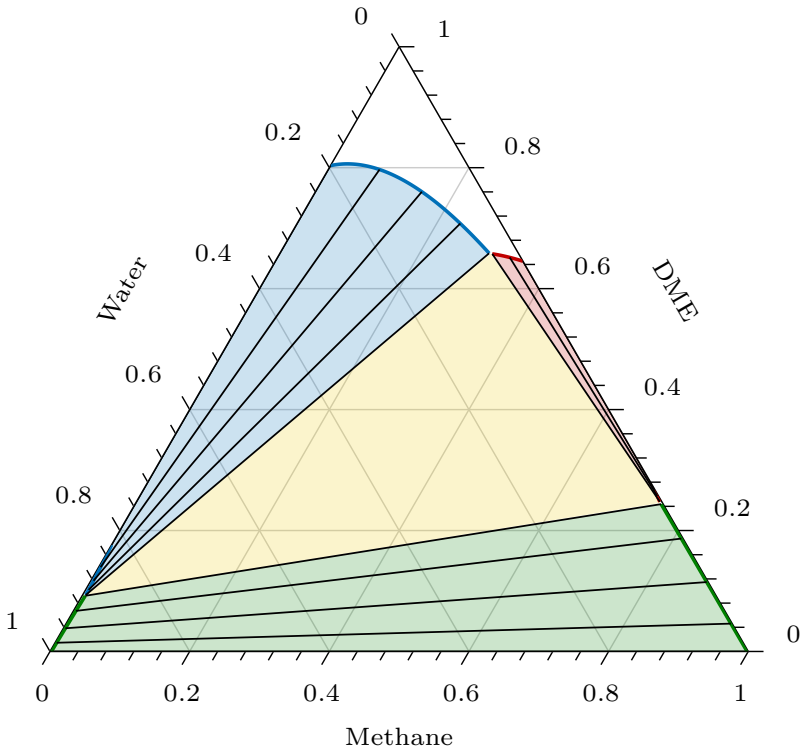

(a)

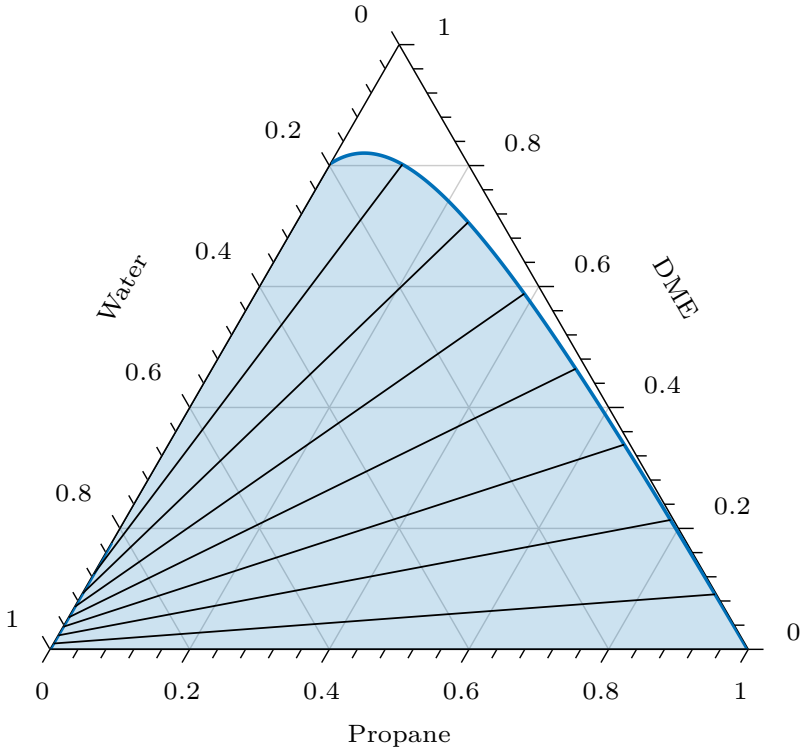

(b)

Figure 6.10: Ternary diagram of DME/water at 323.15 and 100 bar with: (a) methane, (b) propane [binodal curves for LLE (—), VLE (DME-rich liquid) (—), VLE (water-rich liquid) (—), tie lines (—), LLE region (▭), VLE (DME-rich liquid) region (▭), VLE (water-rich liquid) region (▭), VLLE region (▭)].

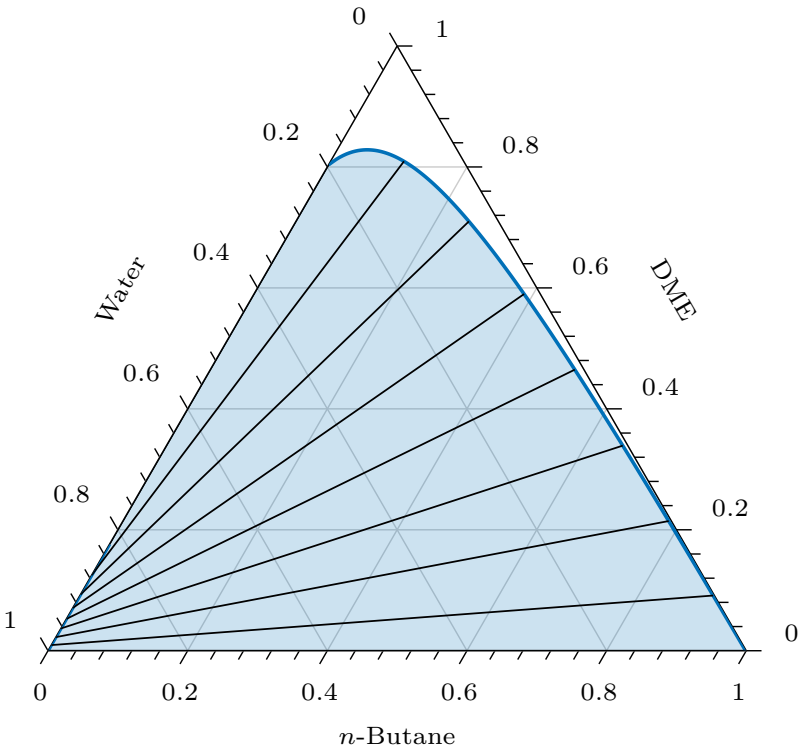

(a)

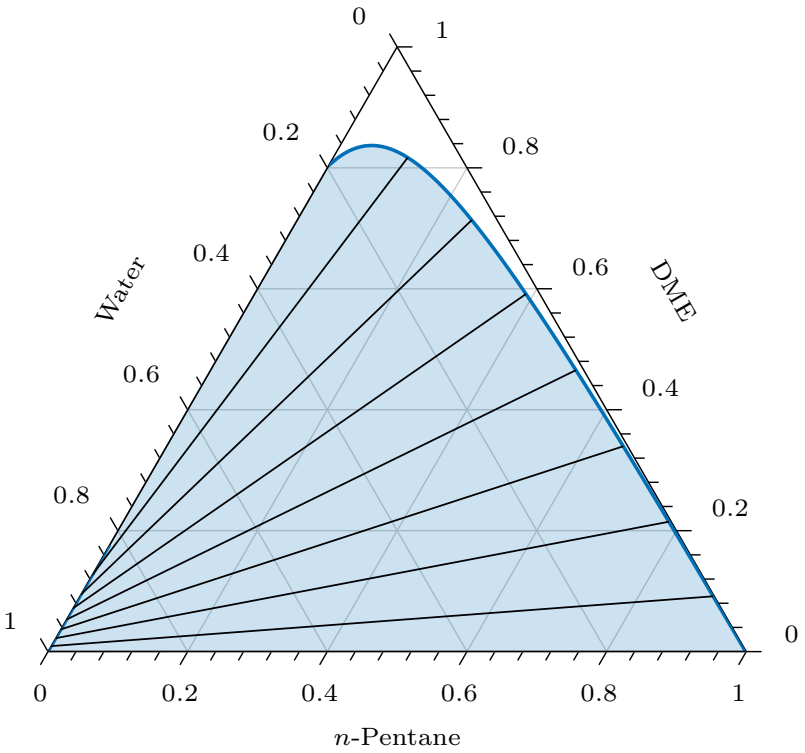

(b)

Figure 6.11: Ternary diagram of DME/water at 323.15 and 100 bar with: (a) n-butane, (b) n-pentane [binodal curve (—), tie lines (—), LLE region ( )].

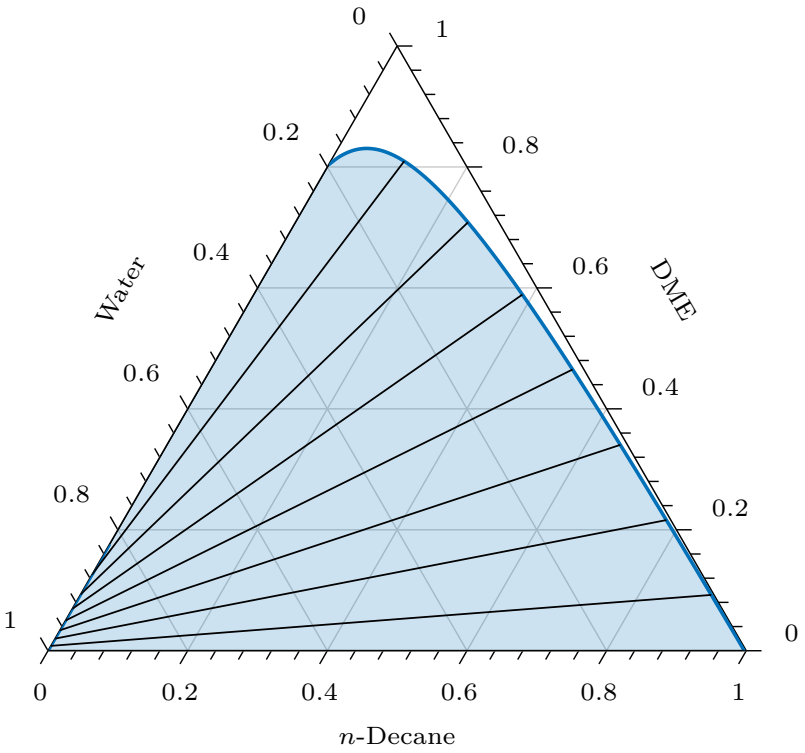

(a)

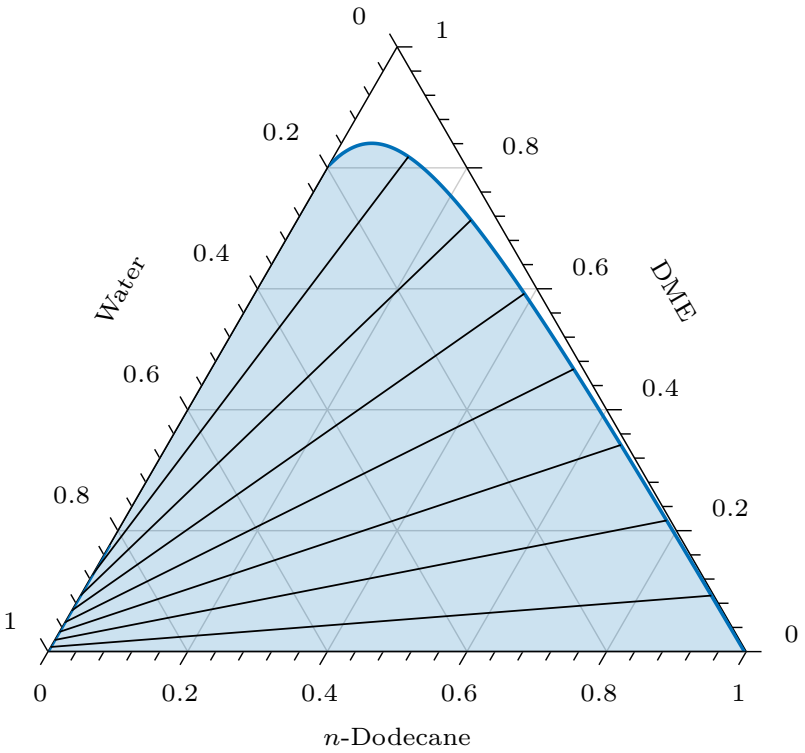

(b)

Figure 6.12: Ternary diagram of DME/water at 323.15 and 100 bar with: (a) n-decane, (b) n-dodecane [binodal curve (—), tie lines (—), LLE region ( )].

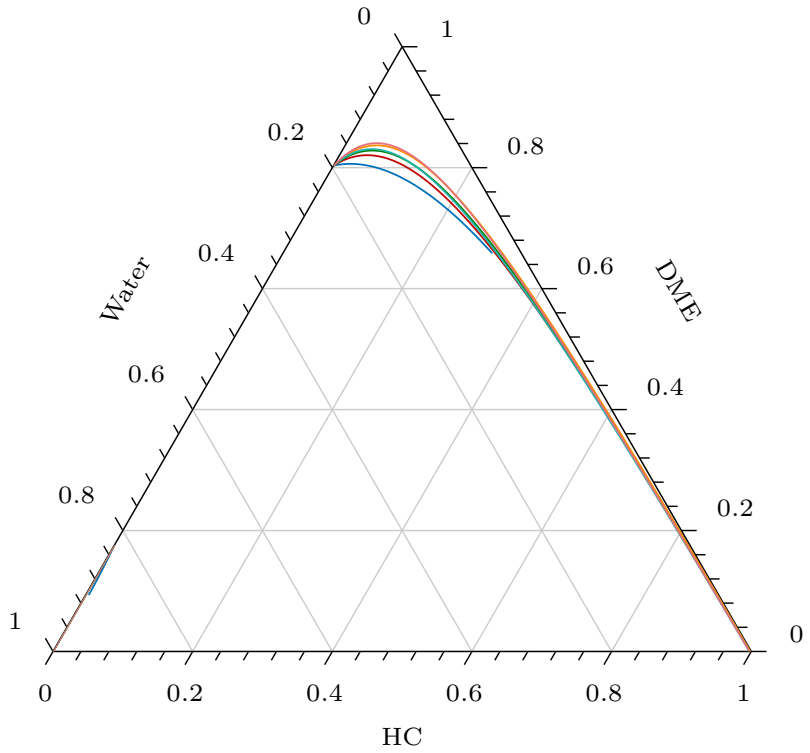

Figure 6.13: Comparison of LLE binodal curves in DME/water/HC ternaries at 323.15 K and 100 bar [methane (—), propane (—), *n*-butane (—), *n*-pentane (—), *n*-decane (—), *n*-dodecane (—)].

The common observation of the ternary diagrams is that the K-value does not change much, and the higher the DME concentration, the less impactful the nature of the hydrocarbon is. This conclusion may potentially simplify the design and modeling of core flooding experiments, because the oil composition, based on the predictions, gives very modest influence on the DME partitioning.

Temperature and pressure effects are presented in Figure 6.16 for a constant oil composition (30% methane, 30% *n*-butane, 40% *n*-decane). Keeping the aqueous phase incipient, we increase the DME until we reach 100% DME in the oil phase. This is the ending point of Figures 6.16a and 6.16b, practically DME and traces of oil in the oil phase. In other words, it is the limiting K-value of the binary DME/water at the conditions specified. Increasing the pressure causes a slight decrease in the K-value, but change of temperature leads to larger differences in the distribution ratio of DME. Higher temperatures favor the partitioning from water into oil, especially at lower to medium DME mole fractions.

Figure 6.16 reveals a maximum DME mole fraction in the oil phase that does not appear in the work of Ratnakar et al. (2016b,a, 2017). By increasing the DME mole fraction, the hydrocarbon mole fractions and the oil/water ratio decrease. After the oil is diluted enough with DME and water, the oil phase cannot dissolve as much DME as before. It decreases to ultimately reach the DME mole fraction of the DME/water LLE in the DME-rich

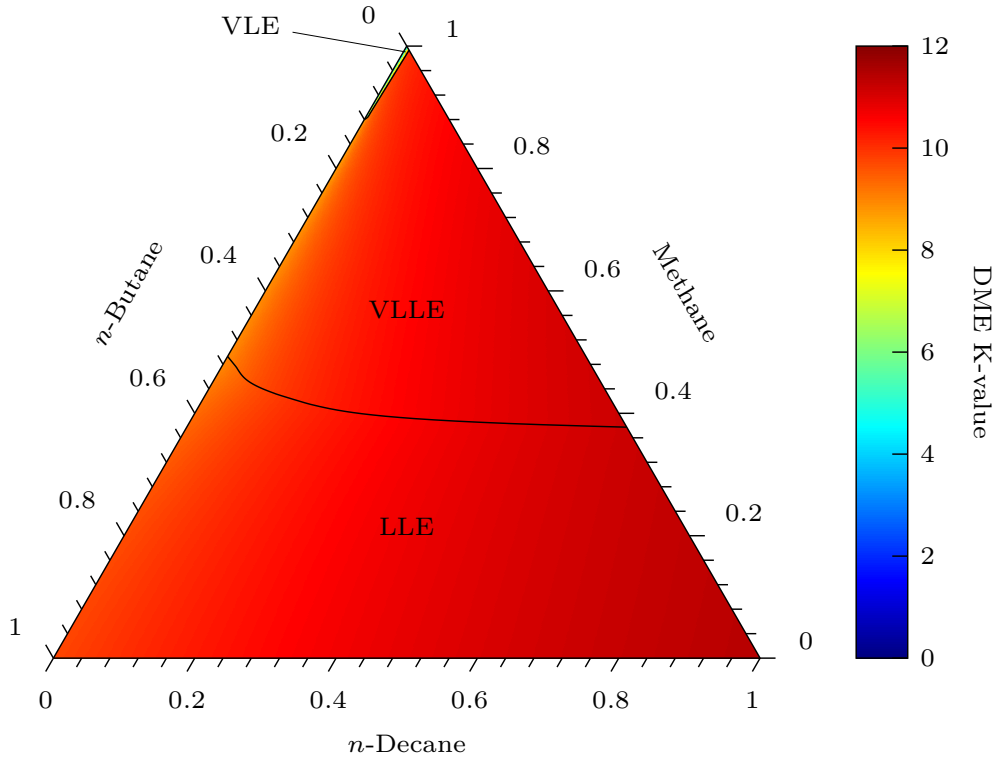

(a)

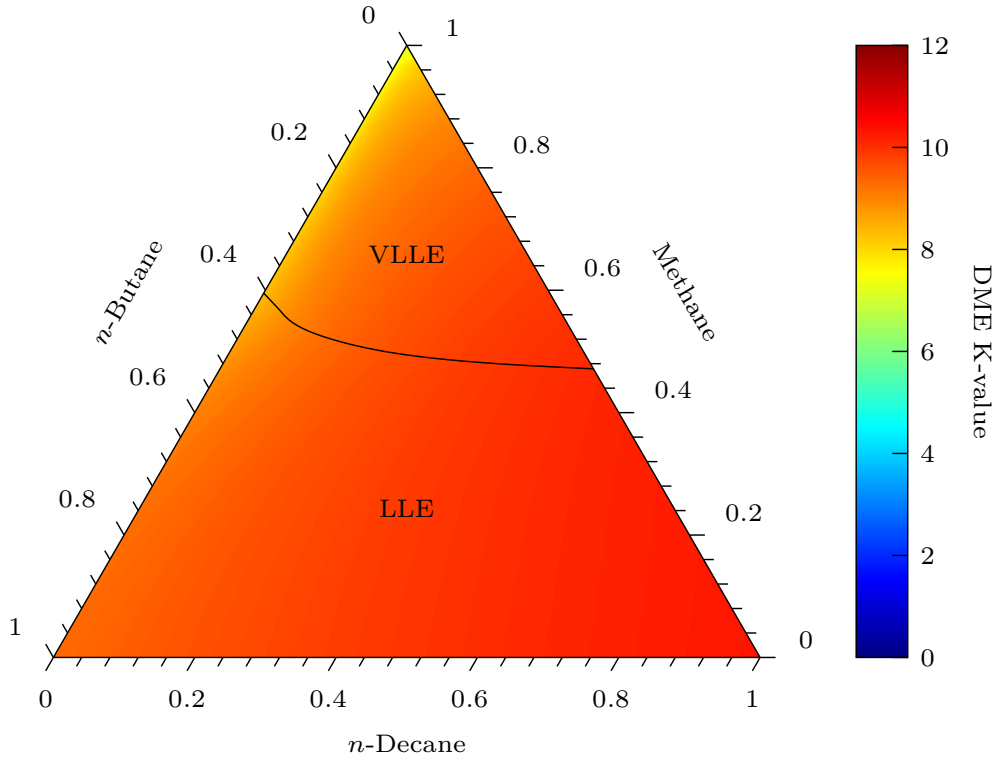

(b)

Figure 6.14: K-values of DME partitioning between oil and aqueous phase at 323.15 and 100 bar for different oil composition with DME mole fraction in the feed: (a) $z_{\mathrm{DME}} = 0.1$, (b) $z_{\mathrm{DME}} = 0.3$.

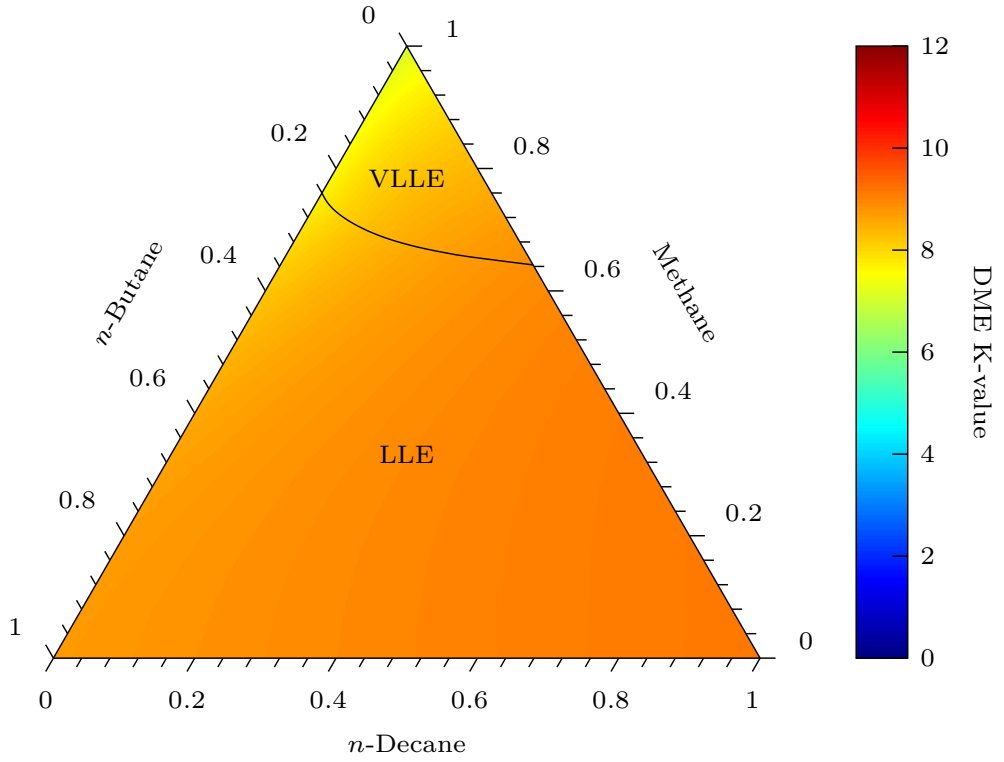

(a)

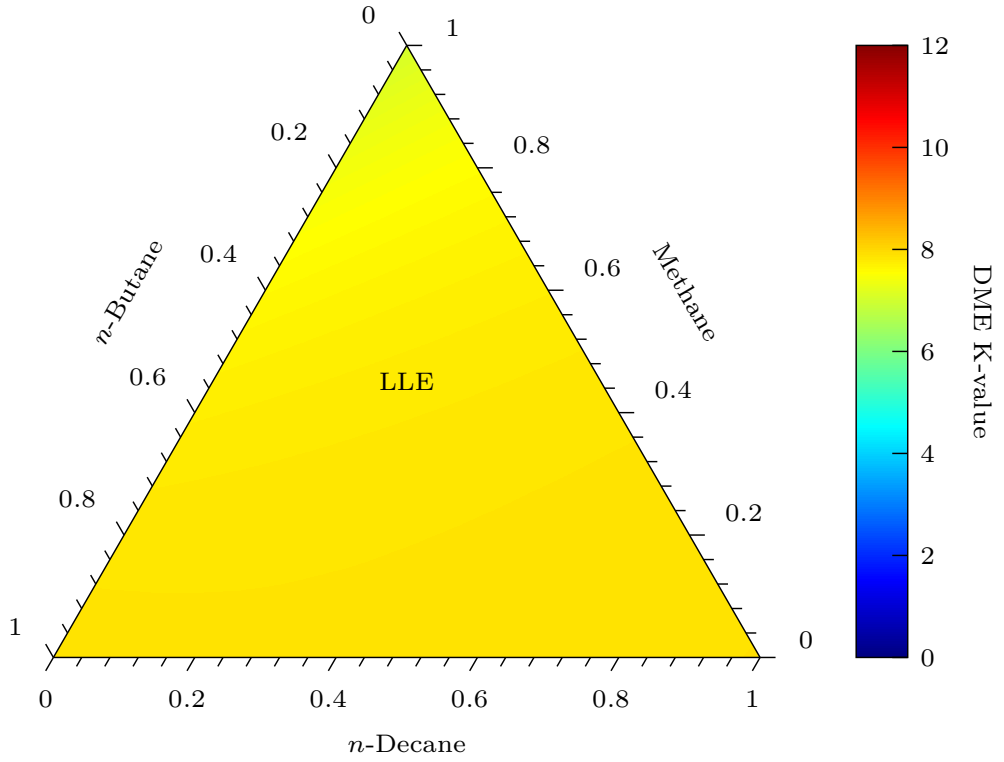

(b)

Figure 6.15: K-values of DME partitioning between oil and aqueous phase at 323.15 and 100 bar for different oil composition with DME mole fraction in the feed: (a) $z_{\mathrm{DME}} = 0.5$, (b) $z_{\mathrm{DME}} = 0.7$.

phase, which is practically a limiting oil phase. This change does not mean that DME stops preferring partitioning in the oil phase, since K-values are larger than 1. Instead, the "capacity" of the oil phase for DME is lower. This maximum DME concentration in the oil phase reduces with increasing temperate and pressure, while temperature still has a more obvious effect.

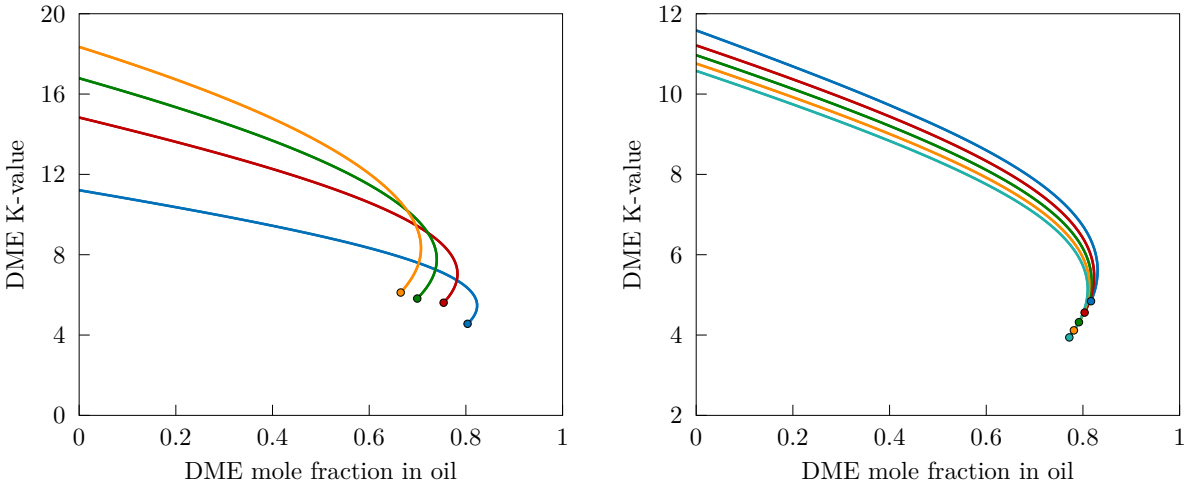

(a) (b)

Figure 6.16: K-values of DME partitioning between oil (30% methane, 30% n-butane, 40% n-decane) and aqueous phase at: (a) 100 bar [323.15 K (—), 348.15 K (—), 373.26 K (—), 394.21 K (—)], (b) 323.15 K [50 bar (—), 100 bar (—), 150 bar (—), 200 bar (—), 250 bar (—)].

6.4 Effect of salinity on DME partitioning

Instead of fresh water usually brine is involved in waterflooding. It is also possible for brine to be the DME carrier during the injection process. Consequently, it is more relevant to study the DME partitioning between hydrocarbon and brine phases. Models such as the Electrolyte CPA EoS (eCPA) proposed by Maribo-Mogensen et al. (2015), can be applied to mixtures of electrolytes under the unified framework of an equation of state. However, it requires significant effort to implement a complex model like eCPA into practical simulations. It is advantageous to choose a simpler model to generate quick results for analysis, which is more easily used for the purpose of simulation. The treatment of brine is inspired by the study of Søreide and Whitson (1992). Despite its theoretical non-rigorousness, the approach can account for the major effects of salt with a simple procedure, particularly suitable for quick implementation in simulators by slight modification of the existing models. According to their method, brine is treated as "pseudo-water", a special form of water. The method predicts the reduced water vapor pressure in the presence of salt by modifying the $a(T)$ function. This works well far from the critical point of water but since the critical constants of the "pseudo-water" are not changed, larger deviations at higher reduced temperatures are expected.

Brine is modeled as a pseudo-component with the same critical constants and CPA parameters as water except for c_1. This parameter is allowed to be a function of salinity and its value is determined through regression of experimental vapor pressures of brine solution at different mass fractions of NaCl (Haas Jr., 1976). Results are presented in Table 6.7 with average absolute relative vapor pressure deviations and Figure 6.17.

Table 6.7: Regressed values of CPA c_1 parameter at different NaCl concentrations.

$\%w_{\mathrm{NaCl}}$	c_1	%AARD
2.84	0.68624	0.90
5.00	0.70752	1.30
5.52	0.71108	1.44
8.06	0.74120	1.93
10.00	0.76080	2.35
10.46	0.77208	2.48
12.75	0.79516	3.02
14.92	0.82260	3.59
15.00	0.82468	3.60
16.98	0.85448	4.15
18.95	0.87204	4.75
20.00	0.88464	5.12

Vapor pressures are described adequately by the model and as expected higher temperatures exhibit larger deviations. Change of c_1 cannot capture vapor pressure at the critical temperature. More accurate modeling would require correlations of the critical constants with salinity. For most reservoir applications, the influence is not supposed to be large, because it will mainly influence the water content in vapor phase.

For salinities other than the ones regressed, a relationship between c_1 and w_{NaCl} is presented in Figure 6.18. For 0% NaCl, we force the equation to give the c_1 of pure water. With such a correlation, experimental data of DME/brine can be regressed (Ratnakar et al., 2017). Binary interaction parameters are presented in Table 6.8 and model prediction with experimental data in Figure 6.19.

Figure 6.20 shows how binary interaction parameters change with NaCl mass fraction at 323 K. A liner equation can be fitted to the data to allow predictions at salinities where experimental data was not available. The equation $k_{ij} = f(w_{\mathrm{NaCl}})$ was used to predict the sensitivity of the K-value with different NaCl concentrations in the brine (Figure 6.21). For brine/hydrocarbon, k_{ij} of water/hydrocarbon were used for simplicity. It is evident that the salting-out effect at larger salinity forces more DME to migrate to the oil phase, as the aqueous phase becomes more and more undesirable. Not as obvious as in Figure 6.16, a maximum DME mole fraction in the oil phase is identified. In the case of constant temperature and pressure, this maximum DME mole fraction is eliminated at high salinity.

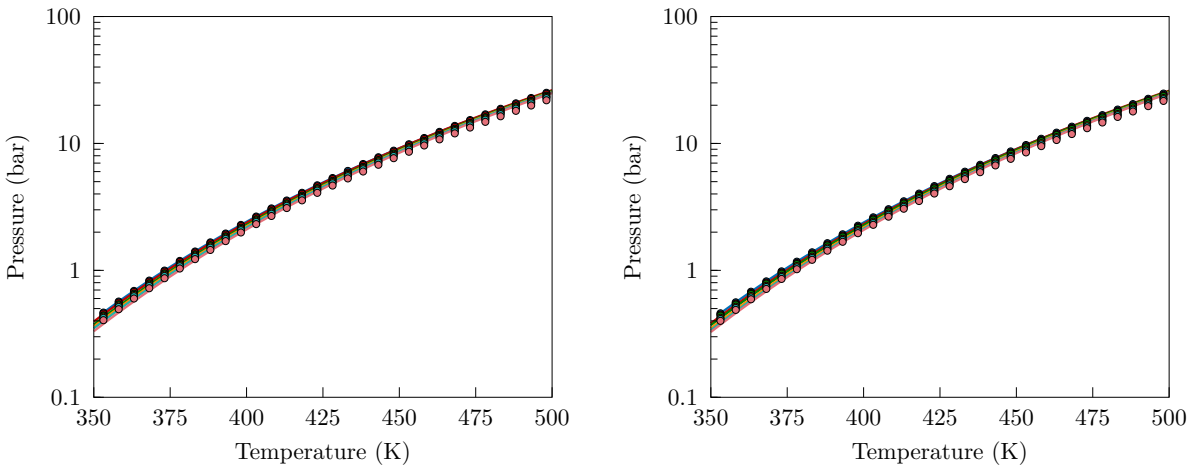

Figure 6.17: Brine vapor pressure modeling with CPA for different w_{NaCl}: (a) p-T diagram [experimental data for 2.84% (●), 5.52% (●), 10.00% (●), 12.75% (●), 15.00% (●), 18.95% (●)], (b) p-T diagram [experimental data for 5.00% (●), 8.06% (●), 10.46% (●), 14.92% (●), 16.98% (●), 20.00% (●)] [calculations with CPA (——)].

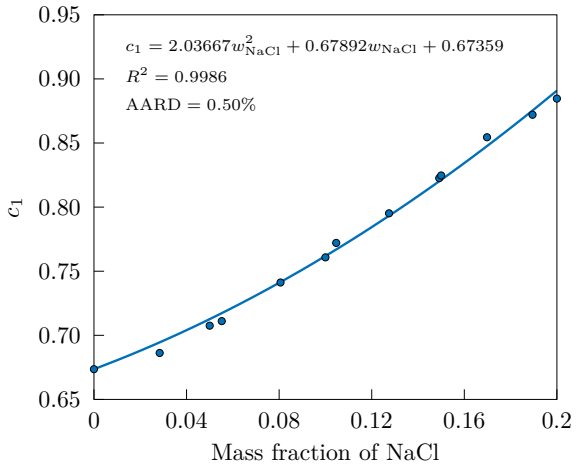

Figure 6.18: Correlation of CPA c_1 parameter for different NaCl mass fractions [regressed c_1 (●), polynomial $n = 2$ trend line (——), AARD: average absolute relative deviation of the fitting].

Table 6.8: Regressed k_{ij} for the pseudo-binary system DME/brine (VLE AARD 3.71%, LLE AARD 2.19%).

T (K)	$\%w_{\mathrm{NaCl}}$	k_{ij}
303	10	-0.0997
353	10	-0.0538
323	3	-0.1037
323	10	-0.0815
323	17	-0.0576

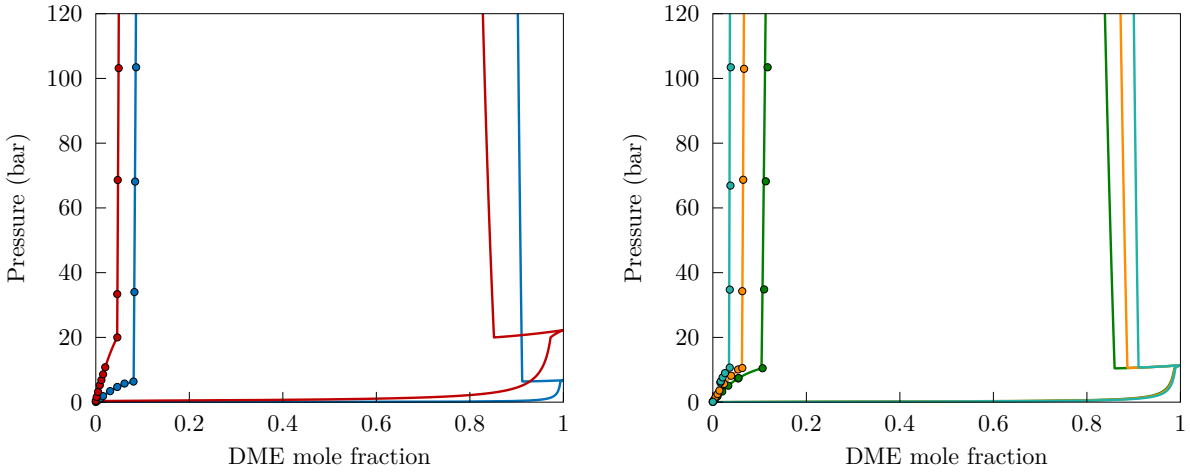

(a) (b)

Figure 6.19: DME/brine modeling with CPA: (a) 10% w/w NaCl, (b) 323 K [experimental data 303 K (●), 353 (●), 3% w/w NaCl (●), 10% w/w NaCl (●), 17% w/w NaCl (●)] [calculations with CPA (——)].

Following the decreasing K-value curve, mole fractions after some aqueous mass fraction of NaCl show a monotonically increasing trend. Brine is a pseudo-component and therefore the DME mole fraction can be considered as salt-free.

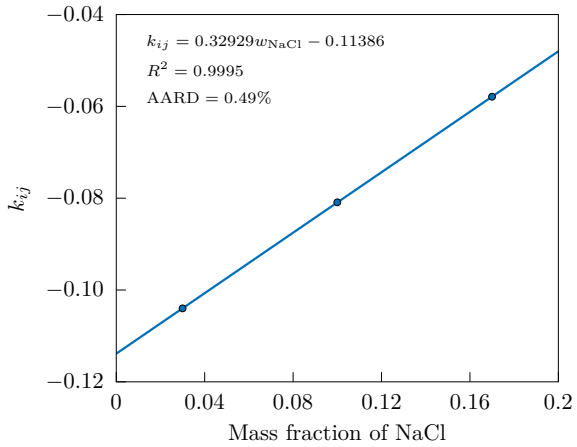

Figure 6.20: Correlation of CPA k_{ij} for the pseudo-binary DME/brine at 323 K for different NaCl mass fractions [regressed k_{ij} (●), linear trend line (——), AARD: average absolute relative deviation of the fitting].

6.5 Conclusions

The DEW process requires adequate phase equilibrium modeling for mixtures of DME in water and oil. For this reason parameters for CPA and CEoS-HV (PR and SRK) were regressed using DME binary systems with water, hydrocarbons and inert gases. Both models resulted in satisfactory phase equilibrium calculations with relatively small

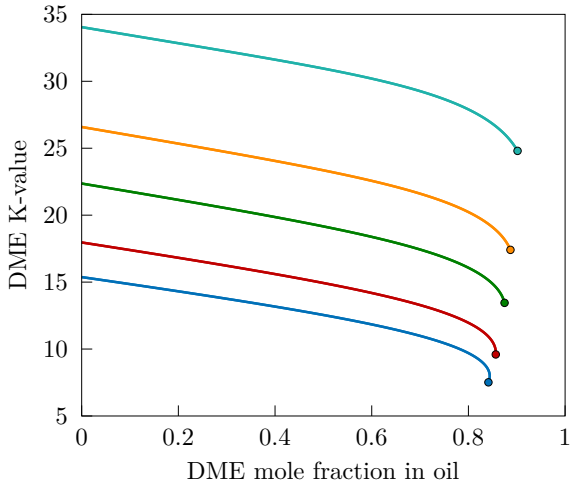

Figure 6.21: K-values of DME partitioning between oil (30% methane, 30% *n*-butane, 40% *n*-decane) and aqueous phase at 323 K and 100 bar for different w_{NaCl} [3% (—), 6% (—), 10% (—), 13% (—), 17% (—)].

deviations from experimental data. For DME/water, temperature dependent interaction parameters provided the best fit, while only one temperature independent parameter was enough in DME/hydrocarbon and DME/inert gas binaries.

Predictions were made for ternary mixtures of DME/water with various hydrocarbons at the same temperature and pressure. It was observed that the size of the hydrocarbon had a minor effect on the overall equilibrium. This was validated by K-value calculations in DME/water/oil mixtures, where the oil was modeled as a ternary system of methane, *n*-butane and *n*-decane. For different oil compositions, the K-values of DME between the oil and the aqueous phase changed only slightly. This weak dependence of the DME partitioning on the oil compositions might simplify core flood experiments and DEW simulations, allowing simpler "model" oils to be used for quick but acceptable estimation of the DME partitioning. Temperature, pressure and salinity sensitivity of the K-value was also investigated. Larger K-values are found at higher temperatures, lower pressures and higher salinities. K-values are more sensitive to temperature than pressure, whereas salinity has a profound effect on the DME partitioning, resulting much larger compositions of DME in the oil phase at high concentrations of NaCl in water.

CHAPTER

7

Conclusions and future work

7.1 Chemical and phase equilibrium calculations

Conlcusions

Various methods and algorithms have been proposed in the literature for chemical and phase equilibrium calculations in multicomponent mixtures. The Gibbs energy minimization approach includes stoichiometric methods, which involve reaction extents, and non-stoichiometric methods, which minimize the Gibbs energy under material balance constraints. Most implementations of stoichiometric methods are inefficient nested loops using the ideal system approximation, while multiphase quadratic methods result in a cumbersome framework. On the other hand, non-stoichiometric methods are advantageous for multiple reactions but are usually applied to single-phase or slightly non-ideal two-phase systems. There is still need of a systematic, reliable and straightforward approach to CPE calculations. In this work two non-stoichiometric methods are presented for non-ideal multiphase chemical equilibrium calculations: the Lagrange multipliers method and the modified RAND method. The Lagrangian of the reduced Gibbs energy is defined incorporating the material balance constraints and equations based on the Lagrangian conditions at the minimum are solved in both methods.

The Lagrange multipliers method is a nested-loop procedure: in the inner loop the working equations are solved for constant fugacity/activity coefficients and their values are updated in the outer loop. As a result, the method can attain quadratic convergence for ideal systems, where the outer loop is redundant. The modified RAND is a second-order method that takes advantage of fugacity/activity coefficient composition derivatives to accelerate calculations. The advantages of the modified RAND method are quadratic convergence for multiphase non-ideal mixtures, same treatment for all components in all the phases, and monitoring the value of the Gibbs energy to control convergence. The latter is possible because the material balance is satisfied at every modified RAND iteration.

Two algorithms are applied to the VLE, LLE and VLLE of reaction systems in this study: the successive substitution algorithm, which includes calculations only with the Lagrange multipliers method and the combined algorithm, which uses the modified RAND method after a few steps of successive substitution. Our initialization could provide good initial estimates and stability analysis could successfully identify if a phase split should occur. All calculations converged to the equilibrium solution without issues, even when components were be excluded from a phase (e.g. non-volatile components). CPU times of both algorithms showed that they are faster than different methods in the literature and the number of iterations was acceptable considering their convergence rate and calculation tolerances set. The recommended approach for CPE calculations is the combined algorithm as it exhibits clear advantages: efficient second-order convergence with increased robustness provided by the Gibbs energy monitoring.

Finally, the algorithms were used for calculations in electrolyte mixtures. Equilibrium involves speciation reactions in a highly non-ideal aqueous phase, a vapor phase of the volatile solutes and a pure solid phase. The material balance accounts for electoneutrality indirectly when the electrolytes are confined to the aqueous phase and there are no additional working equations for electrolyte solutions. If the molality or molarity reference state, usually selected for such systems, is transformed to the infinite dilution reference state (mole fraction based), the equations of the algorithms do not require any modifications. It should be stressed that the tested electrolyte systems show similar CPU time and convergence behavior to non-electrolyte reaction systems.

Future work

The algorithms in this study provide a general approach to multiphase reaction equilibrium and their application is not limited to specific systems. The efficient combined algorithm could be useful in simulations of industrial processes such as reactive distillation, reactive extraction and weak electrolyte equilibrium (e.g. sour water stripping). Simulations involve a large number of PT flash problems, therefore adjustments are required to further improve the speed of calculations. If the maximum number of equilibrium phases is known beforehand, the time used in stability analysis can be reduced. Furthermore, during successive substitution the highest number of inner-loop iterations are found during the first few outer-loop non-ideality updates. Excessive computation could be avoided if successive substitution was used only once before the modified RAND steps. Finally, comparison of stoichiometric algorithm with the non-stoichiometric algorithms of this work, could illustrate more clearly the weaknesses and the advantages of both formulations, either for CPE calculations at constant temperature and pressure or in process simulation.

The Lagrange multipliers method is based on Gibbs energy minimization equations, but it is not a minimization itself. The material balance belongs to the working equations and the Gibbs energy decrease cannot be controlled. In this work the successive substitution algorithm never failed to converge for any of the systems tested. Nevertheless, there is no

mathematical guarantee of convergence, which can cause oscillations in strongly non-ideal systems. Heidemann and Michelsen (1995) published examples of unstable successive substitution calculations when solving phase equilibrium with the Rachford-Rice equations for two-phase systems. A similar analysis could be performed for the current formulation to conclude when the method cannot be successfully used for CPE calculations and determine the non-ideality limits that can be tolerated.

Despite the advantages of the modified RAND method, a non-descent direction could be produced during calculations. In this case, regardless of the step control parameter in Eq. 3.70, the Gibbs energy cannot decrease. Corrections to the $\mathbf{M}^{-1}$ matrix in phase equilibrium problems have been proposed by Paterson et al. (2018), suggesting that the ascent direction issues are likely to be encountered close to critical points. This correction was not needed in the examples tested in our work, but including it in the algorithm clearly provides an extra level of robustness. Extension to CPE calculations is easily achieved by substituting the phase equilibrium formula matrix (identity matrix) with the corresponding formula matrix of the reaction system. Moreover, the RAND method (original and modified) can lead to negative mole numbers of trace components. White et al. (1958) and Smith and Missen (1982) addressed the issue of small concentrations, using essentially Eq. 3.34 to determine compositions of trace components more accurately. This was not attempted in this work, but it could be applied in future analysis with a systematic investigation of the improvement they offer.

Finally, successful calculation of electrolyte equilibrium with the two non-stoichiometric algorithms allows the study of more complex geochemical systems, pertinent to the research of geologists and oil reservoir engineers. Geochemical reactions appearing in Leal et al. (2016a,b) with multiple solutes and calcite/dolomite/quartz solid phases could be an interesting application of the CPE algorithms proposed in this work. In the current framework, speciation of electrolytes is a different type of reaction, and the consideration of a solid is the addition of a pure component phase (remaining components are excluded). However, the number of electrolyte systems we tested might not be enough to identify further provisions we should take into account when dealing with a strongly non-ideal electrolyte aqueous phase or pure solid phases. The suitability of electrolyte models and analysis of solute behavior should be also carefully investigated. Equilibrium results appeared to be rather sensitive to different sets of parameters for the same models or different correlations for the Henry's constant corresponding to the same component.

7.2 DME phase equilibrium modeling

Conlcusions

Accurate DME phase modeling is necessary for simulations of the DEW process. Parameters for CPA and CEoS-HV (PR and SRK) were regressed for binary systems of DME with water, methane, propane, *n*-butane, *n*-pentane, *n*-decane, *n*-dodecane, carbon dioxide

and nitrogen. Deviations from experimental data revealed that temperature dependent parameters are needed for adequate description of DME/water (DME modeled as cross associating with CPA), while only one binary interaction parameter was required for the remaining binaries. CPA was selected for predictions in multicomponent DME mixtures with water and hydrocarbons. Calculations for the LLE of ternary systems of DME/water/hydrocarbon produced similar curves for different hydrocarbons, suggesting that the hydrocarbon size may not have a strong effect on the DME partitioning.

To examine the extent of this effect, predictions of the DME K-values between oil and water were made, modeling the oil as a methane/n-butane/n-decane mixture. K-values seemed to exhibit a stronger dependence on the DME mole fraction in the oil phase rather than the oil composition. Temperature, pressure and salinity sensitivities of K-value were also investigated. Temperature has a larger effect on the K-value than pressure, with higher temperatures and lower pressures resulting in higher concentrations of DME in the oil phase. For the salinity effect, brine was considered as "pseudo-water". Salinity was introduced with CPA in the c_1 parameter. Vapor pressures of brine solutions were regressed to determine a correlation of the form $c_1 = f(w_{\mathrm{NaCl}})$ and then binary interaction parameters for CPA were regressed using DME/brine experimental data. K-values were predicted at different NaCl concentrations in water, showing that high salinity improves appreciably the partitioning of DME into the oil phase.

Future work

The DME phase equilibrium modeling was aimed to provide a quick and preliminary analysis with the focus on the K-values of DME between oil and aqueous phases. There is obviously room for further refinement and improvement. More accurate electrolyte models, such as eCPA Maribo-Mogensen et al. (2015), can apparently be used. If we want to select a simpler model for reservoir simulation, the current approach based on Søreide and Whitson (1992) can also be improved, e.g. by introducing salinity dependent critical constants of "pseudo-water" and brine/hydrocarbon k_{ij}. Finally, although we believe the current analysis has captured the main characteristics of the temperature, pressure and salinity influences, future work should include calculations for live oils or multicomponent oils with more realistic composition of hydrocarbons and inerts.

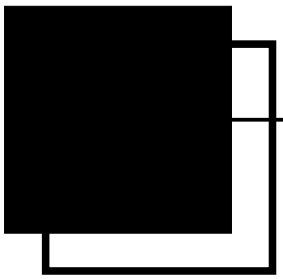

Appendices

A Matrix-vector operations

Equations in different chapters involve the use of operations between matrices and vectors. This section presents simple mathematical operations between the quantities in a more compact way. Vectors are considered to be equivalent to single column matrices. For vector $\mathbf{v} \in \mathbb{R}^{q\times 1}$ and matrix $\mathbf{M} \in \mathbb{R}^{p\times q}$, we have:

- sum of vector components:

$$\sum_{i=1}^{q} v_i = \mathbf{v}^{\mathrm{T}}\mathbf{e}_q \tag{A.1}$$

- vector of matrix columns sum:

$$\begin{bmatrix} \sum_{j=1}^{q} M_{1j} \\ . \\ . \\ . \\ \sum_{j=1}^{q} M_{pj} \end{bmatrix} = \sum_{j=1}^{q} \mathbf{M}_j = \mathbf{M}\mathbf{e}_q \tag{A.2}$$

- vector of matrix rows sum:

$$\begin{bmatrix} \sum_{i=1}^{p} M_{i1} \\ . \\ . \\ . \\ \sum_{i=1}^{p} M_{iq} \end{bmatrix} = \sum_{i=1}^{p} \mathbf{M}_i^{\mathrm{T}} = \mathbf{M}^{\mathrm{T}}\mathbf{e}_p \tag{A.3}$$

- sum of matrix components:

$$\sum_{i=1}^{p}\sum_{j=1}^{q} M_{ij} = \mathbf{e}_p^{\mathrm{T}}\mathbf{M}\mathbf{e}_q \tag{A.4}$$

where:

$\mathbf{M}_j$	column j of matrix $\mathbf{M}$
$\mathbf{M}_i^{\mathrm{T}}$	column i of matrix $\mathbf{M}^{\mathrm{T}}$ (row i of matrix $\mathbf{M}$ in column form)
$\mathbf{e}_X$	vector of ones with dimensions $X \times 1$

B Degrees of freedom analysis

In a general chemical and phase equilibrium problem (Smith and Missen, 1982), the ranks of the stoichiometric and formula matrix are linked by:

$$\text{rank}(\mathbf{N}) \leq N_C - \text{rank}(\mathbf{A}) \tag{B.1}$$

To use these matrices in calculations, the equality must be valid. In the case of inequality, the number of additional stoichiometric constraints to be defined is found by:

$$N_S = N_C - \text{rank}(\mathbf{A}) - \text{rank}(\mathbf{N}) \tag{B.2}$$

and they have the form:

$$\mathbf{A}_{ac} \sum_{k=1}^{N_P} \mathbf{n}_k = \mathbf{b}_{ac} \tag{B.3}$$

where:
$\mathbf{A}_{ac}, \mathbf{b}_{ac}$ additional stoichiometric constraints

It is easy to incorporate these constraints in a modified formula matrix and element abundance vector:

$$\mathbf{A}' = \begin{bmatrix} \mathbf{A} \\ \mathbf{A}_{ac} \end{bmatrix} \qquad \mathbf{b}' = \begin{bmatrix} \mathbf{b} \\ \mathbf{b}_{ac} \end{bmatrix} \tag{B.4}$$

It follows that:

$$\text{rank}(\mathbf{A}_{ac}) = N_S \tag{B.5}$$

The Gibbs phase rule for reaction systems and additional specifications is (Rao, 1985):

$$F = (N_C - N_R - N_S) + (N_V - N_T) - N_P + 2 \tag{B.6}$$

where:
N_V number of additional variables
N_T number of additional constraints not included in $\mathbf{A}_{ac}, \mathbf{b}_{ac}$

The quantity $N_E = N_C - N_R - N_S$ represents the number of the elements in the system (independent entities). Eq. B.6 can be rewritten as:

$$F = N_E + (N_V - N_T) - N_P + 2 \tag{B.7}$$

When no additional constraints or variables are assumed, the Gibbs phase rule becomes:

$$F = N_E - N_P + 2 \tag{B.8}$$

where:

$$N_E = N_C - N_R \tag{B.9}$$

In this work, calculations take place at specified temperature and pressure. Since $F \geq 0$, the number of phases cannot be larger than the number of elements (Eq. B.8):

$$N_P \leq N_E \tag{B.10}$$

C Reference state chemical potentials

In a phase equilibrium problem, when the reference states are the same for all components, reference state chemical potentials can be assumed equal to zero. Conversely, determination of simultaneous chemical and phase equilibrium implies that reference state chemical potentials satisfy the following equation:

$$\frac{\Delta_r G^\circ_{rk}}{RT} = \sum_{i=1}^{N_C} \frac{\nu_{ir}\mu^\circ_{ik}}{RT} = -\ln K^{\text{eq}}_{rk} \qquad r = 1, ..., N_R \tag{C.1}$$

where the reference state Gibbs energy of the reaction and chemical potentials are at the same conditions. However, databases for standard state chemical potentials are not always available. Individual values of μ° do not affect the equilibrium solution, as long as they are consistent with Eq. C.1. Reference state Gibbs energy of formation or combustion can be found in the literature for individual components and we can set:

$$\mu^\circ_{ik} = \Delta_f G^\circ_{ik} \qquad \text{or} \qquad \mu^\circ_{ik} = -\Delta_c G^\circ_{ik} \qquad i = 1, ..., N_C \tag{C.2}$$

What is usually reported in the literature is chemical equilibrium constants for specific reactions. We have N_R chemical reactions and therefore N_R equations as Eq. C.1. The number of the reference chemical potentials required for the calculations is N_C. For this reason, when chemical equilibrium constants are given, we must "decompose" them into fictitious values of μ°. The first step is to select N_R reference components and set at the desired temperature and pressure:

$$\mu^\circ_{ik} = \begin{cases} \hat{\mu}_{ik}, & i \in \text{reference components} \\ 0, & i \notin \text{reference components} \end{cases} \tag{C.3}$$

The following system is solved for the non-zero $\hat{\boldsymbol{\mu}}_k$:

$$\frac{1}{RT}\hat{\mathbf{N}}^{\mathrm{T}}\hat{\boldsymbol{\mu}}_k = \begin{bmatrix} -\ln K^{\text{eq}}_{1k} \\ . \\ . \\ . \\ -\ln K^{\text{eq}}_{N_R k} \end{bmatrix} \tag{C.4}$$

Matrix $\hat{\mathbf{N}}$ is the stoichiometric matrix corresponding only to the reference components. This matrix must be invertible, therefore the general rule is to choose reference components

that result in rank($\hat{\mathbf{N}}$) = N_R. There can be cases where this is not true: if we select an inert as a reference component, the corresponding row of the matrix will be all zeros. Another case when the rank can be less than N_R is when the reference components participate in all reactions with the same stoichiometric coefficients. If the same reference state is selected for all phases, then $\hat{\boldsymbol{\mu}}_k$ is common between the different phases. Otherwise, Eq. 2.54 must be used appropriately to change reference states for the remaining phases. To determine the reaction extents at equilibrium we can use the mole numbers of the reference components in the feed and in phase k, $\hat{\mathbf{n}}_F$ and $\hat{\mathbf{n}}_k$:

$$\boldsymbol{\xi} = \hat{\mathbf{N}}^{-1} \left(\sum_{k=1}^{N_P} \hat{\mathbf{n}}_k - \hat{\mathbf{n}}_F \right) \tag{C.5}$$

In this way, we can calculate reaction extents even for a non-stoichiometric method in simultaneous chemical and phase equilibrium computation.

D Determination of the formula matrix

The formula matrix is vital for the material balance in non-stoichiometric methods, because it is a summary of the elemental composition of each component. Moreover, it includes reaction information, since the mole numbers must not only lead to constant total mass, but their change should be also consistent with the chemical reactions. The link between the formula matrix and the reactions is proven by Eq. 3.20: the choice of elements depends on the way the reactions are selected and vice versa. In an equation of the form:

$$\mathbf{WZ} = \mathbf{0} \tag{D.1}$$

matrix $\mathbf{Z}$ is a basis of the null space of $\mathbf{W}$. The solution is not a unique matrix $\mathbf{Z}$. It is obvious that $\mathbf{Z} = \mathbf{0}$ satisfies the equation. Eq. 3.20 has the same form in a CPE problem, where it is implied that $\mathbf{A} \neq \mathbf{0}$ and $\mathbf{N} \neq \mathbf{0}$. Smith and Missen (1982) presented a method, where they determine $\mathbf{N}$ from $\mathbf{A}$ in Eq. 3.20. This method produces a number of linearly independent reactions that will be satisfied at equilibrium.

According to Eq. 3.5, when the number of components is fixed, increasing the number of elements decreases the number of independent chemical reactions. In the literature, we usually find chemical equilibrium constants for well-defined reactions that were observed experimentally. Thus, $\mathbf{N}$ is already specified by the authors. Determination of $\mathbf{A}$ is therefore more desirable: chemical equilibrium will be established only for the equations that were observed experimentally. When the number of reactions is small, it might be easy to select the elements by observation. However, in systems with many reactions and complex components we need a systematic way of determining the formula matrix. For this reason, we take the transpose of Eq. 3.20:

$$\mathbf{N}^{\mathrm{T}}\mathbf{A}^{\mathrm{T}} = \mathbf{0} \tag{D.2}$$

The command `null`$(\cdot,$ 'r') in MATLAB® calculates the "rational" basis for the null space of a matrix obtained from the reduced row echelon form of the matrix. The reduced row echelon form of matrix $\mathbf{A}$ is a relatively simple form of $\mathbf{A}$ which also satisfies Eq. 3.20 and D.2. The command `rref`$(\cdot)$ calculates the reduced row echelon form of a matrix, which is unique. In MATLAB®:

$$\mathbf{A} = \texttt{rref}\left\{[\texttt{null}(\mathbf{N}^{\mathrm{T}}, \text{'r'})]^{\mathrm{T}}\right\} \tag{D.3}$$

In this matrix, each leading 1 in every row is the only non-zero entry in its column. This form implies that all the elements are selected as components. When an element is

defined as a component, its Lagrange multiplier is equal to the chemical potential of the corresponding component. In the following reaction:

$$\mathrm{A} + \mathrm{B} \rightleftharpoons \mathrm{D} \qquad \mathrm{C\ inert} \tag{D.4}$$

the number of elements is $N_E = N_C - N_R = 4 - 1 = 3$ and the stoichiometric matrix is $\mathbf{N} = [-1, -1, 0, 1]^{\mathrm{T}}$. The formula matrix $\mathbf{A}$ is found by Eq. D.3:

$$\mathbf{A} = \begin{matrix} \\ \mathrm{A} \\ \mathrm{B} \\ \mathrm{C} \end{matrix} \begin{matrix} \begin{matrix} \mathrm{A} & \mathrm{B} & \mathrm{C} & \mathrm{D} \end{matrix} \\ \begin{bmatrix} 1 & 0 & 0 & 1 \\ 0 & 1 & 0 & 1 \\ 0 & 0 & 1 & 0 \end{bmatrix} \end{matrix} \tag{D.5}$$

Matrix $\mathbf{A}$ illustrates what we intuitively understand: elements A and B must be combined to produce component D. It is crucial to stress that when elements have been defined as components, the latter share only the chemical composition of the corresponding components. Unlike elements, system components are chemical substances with certain physical and chemical properties (boiling point, density, etc.). Elements are artificial entities we define to facilitate the mathematical formulation of a CPE material balance. In other words, elements are a mathematical convenience. Furthermore, elements are reaction invariant entities, which makes the element abundance vector a constant. Only component mole numbers change throughout the course of reactions.

Nevertheless, reactions can have multiple products. If reactants and products are chosen as elements and multiple-product reactions exist, some A_{ji} might be negative for products not selected as elements. For instance, in reaction:

$$\mathrm{A} + \mathrm{B} \rightleftharpoons \mathrm{C} + \mathrm{D} \tag{D.6}$$

the number of elements must be $N_E = N_C - N_R = 4 - 1 = 3$. The stoichiometric matrix is $\mathbf{N} = [-1, -1, 1, 1]^{\mathrm{T}}$ and the formula matrix $\mathbf{A}$ is calculated by Eq. D.3:

$$\mathbf{A} = \begin{matrix} \\ \mathrm{A} \\ \mathrm{B} \\ \mathrm{C} \end{matrix} \begin{matrix} \begin{matrix} \mathrm{A} & \mathrm{B} & \mathrm{C} & \mathrm{D} \end{matrix} \\ \begin{bmatrix} 1 & 0 & 0 & 1 \\ 0 & 1 & 0 & 1 \\ 0 & 0 & 1 & -1 \end{bmatrix} \end{matrix} \tag{D.7}$$

Although elements A and B are combined to produce D, we need to remove the chemical

composition of element C from the complex AB to match the exact chemical composition of component D. This could also lead to $b_j \leq 0$. Therefore, we need to broaden the interpretation of vector **b**: total mole numbers of element j, as the net result of contributing to form components and being removed as excess from components. We can calculate different values of **b** using Eq. 3.7 for each feed, focusing on element C and components C, D:

1. $\mathbf{n}_F = [1\ 1\ 1\ 0]^{\mathrm{T}}$

   $\mathbf{b} = [1\ 1\ 1]^{\mathrm{T}}$: Initially there is no component D and all of element C is used to form component C. At an arbitrary reaction extent, x mol of component C and x mol of component D are produced. Element C contributes $x+1$ mol to form component C and x mol are removed from component D as excess. The net result is $1 + x - x = 1 = b_C$.

2. $\mathbf{n}_F = [1\ 1\ 0\ 0]^{\mathrm{T}}$

   $\mathbf{b} = [1\ 1\ 0]^{\mathrm{T}}$. Initially, there is no component C or component D. At an arbitrary reaction extent, x mol of component C and x mol of component D are produced. Element C contributes x mol to form component C and x mol are removed from component D as excess. The net result is $x - x = 0 = b_C$.

3. $\mathbf{n}_F = [1\ 1\ 0\ 1]^{\mathrm{T}}$

   $\mathbf{b} = [2\ 2\ -1]^{\mathrm{T}}$. Initially, there is only component D. At an arbitrary reaction extent, x mol of component C and x mol of component D are produced. Element C contributes x mol to form component C and $x + 1$ mol are removed from component D as excess. The net result is $x - (x + 1) = -1 = b_C$.

Positive and negative values of the formula matrix can be separated in the matrices $\mathbf{A}^+$ and $\mathbf{A}^-$. For the matrix of Eq. D.7 we have:

$$\mathbf{A} = \mathbf{A}^+ + \mathbf{A}^- = \begin{bmatrix} 1 & 0 & 0 & 1 \\ 0 & 1 & 0 & 1 \\ 0 & 0 & 1 & 0 \end{bmatrix} + \begin{bmatrix} 0 & 0 & 0 & 0 \\ 0 & 0 & 0 & 0 \\ 0 & 0 & 0 & -1 \end{bmatrix} \tag{D.8}$$

The mole numbers of element j that actually exist in the system correspond to the positive values of the formula matrix $\sum_{i=1}^{N_C} A_{ji}^+ \sum_{k=1}^{N_P} n_{ik}$. The "artificial" excessive mole numbers of element j in other element combinations to form components is $-\sum_{i=1}^{N_C} A_{ji}^- \sum_{k=1}^{N_P} n_{ik}$. Although each of these numbers is not constant, their difference (material balance) is:

$$\sum_{i=1}^{N_C} A_{ji}^+ \sum_{k=1}^{N_P} n_{ik} + \sum_{i=1}^{N_C} A_{ji}^- \sum_{k=1}^{N_P} n_{ik} = \sum_{i=1}^{N_C} A_{ji} \sum_{k=1}^{N_P} n_{ik} = b_j \tag{D.9}$$

Unless we desire all elements to be a tangible entity as actual building blocks (strictly parts of molecules, $A_{ji} \geq 0$), there should not be any problem using them with a broader interpretation in the calculations, allowing negative entries in the formula matrix.

E Initialization of calculations

Minimization of function Q (section 3.2.3) is a robust procedure to initialize the main calculations. This is a numerical method, where initialization is required as well. Lagrange multipliers are the chemical potentials of the elements at equilibrium. A reasonable initial estimate is:

$$\lambda_j^{(0)} = \begin{cases} \ln \dfrac{|b_j|}{\sum_{q=1}^{N_E} |b_q|}, & b_j \neq 0 \\ 0, & b_j = 0 \end{cases} \qquad j = 1, ..., N_E \tag{E.1}$$

Absolute values are used for negative entries in vector $\mathbf{b}$. In this case, it is not implied that an element does not exist when $b_j = 0$ (Appendix D). There is also the need of initial estimates for the phase amounts. We follow a simple analysis: mole numbers will be between a minimum and a maximum number, because reactions tend to decrease or increase the total mole numbers. If there is no change in the mole numbers, the phase amount estimate is equal to the feed total mole numbers. There are two directions for reactions, forward and backward. To calculate the theoretical maximum extents for the forward and backward reactions, we have:

$$\xi_r^F = \min_i \left(-\frac{n_{F,i}}{\nu_{ir}} \right), \quad \frac{n_{F,i}}{\nu_{ir}} < 0 \tag{E.2}$$

$$\xi_r^B = \min_i \left(\frac{n_{F,i}}{\nu_{ir}} \right), \quad \frac{n_{F,i}}{\nu_{ir}} > 0 \tag{E.3}$$

where:

ξ_r^F maximum extent of the forward reaction r

ξ_r^B maximum extent of the backward reaction r

The total mole numbers for each reaction happening independently are:

$$n_{t,r}^F = n_{t,F} + \nu_{t,r} \xi_r^F \tag{E.4}$$

$$n_{t,r}^B = n_{t,F} - \nu_{t,r} \xi_r^B \tag{E.5}$$

where:

$n_{t,r}^F$ phase amount estimate for the full forward reaction r

$n_{t,r}^B$ phase amount estimate for the full backward reaction r

To calculate an average value of mole numbers based on forward and backward reactions, a weighted average can be used, with chemical equilibrium constants as weights:

$$\bar{n}_t^F = \frac{\sum_{r=1}^{N_R} K_{rk}^{\mathrm{eq}}\, n_{t,r}^F}{\sum_{r=1}^{N_R} K_{rk}^{\mathrm{eq}}} \tag{E.6}$$

$$\bar{n}_t^B = \frac{\sum_{r=1}^{N_R} (1/K_{rk}^{\mathrm{eq}}) n_{t,r}^B}{\sum_{r=1}^{N_R} (1/K_{rk}^{\mathrm{eq}})} \tag{E.7}$$

to finally obtain the initial estimate of the total mole numbers of the single phase k:

$$n_{t,k}^{(0)} = \frac{\bar{n}_t^F + \bar{n}_t^B}{2} \tag{E.8}$$

Rigorous generalization to multiple phases has not been attempted. In case we need to start with more than one phases, we can calculate an average number of $\bar{n}_t^F$ and $\bar{n}_t^B$, distributing it equally to all phases:

$$\begin{gathered} n_{t,k}^{(0)} = \frac{\bar{n}_t^F + \bar{n}_t^B}{2N_P} \\ k = 1, ..., N_P \end{gathered} \tag{E.9}$$

It has been found that phase amounts initial estimates are not crucial for convergence.

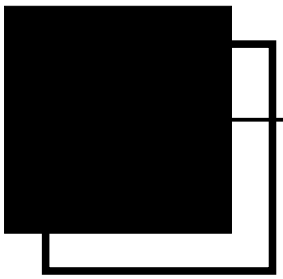

Bibliography

Abrams, D. S. and Prausnitz, J. M. (1975). Statistical thermodynamics of liquid mixtures: A new expression for the excess gibbs energy of partly or completely miscible systems. *AIChE Journal*, 21(1):116–128.

Alkindi, A., Al-Azri, N., Said, D., AlShuaili, K., and Te Riele, P. (2016). Persistence in EOR - design of a field trial in a carbonate reservoir using solvent-based water-flood process. Muscat, Oman. SPE EOR Conference at Oil and Gas West Asia, Society of Petroleum Engineers.

Anikeev, V. (2014). Chapter 1 – synthesis of biodiesel fuel in supercritical lower alcohols with and without heterogeneous catalysts (thermodynamics, phase and chemical equilibriums, experimental studies). *Supercritical Fluid Technology for Energy and Environmental Applications*, pages 1–29.

Anikeev, V., Stepanov, D., and Yermakova, A. (2012). Thermodynamics of phase and chemical equilibrium in the processes of biodiesel fuel synthesis in subcritical and supercritical methanol. *Industrial & Egineering Chemistry Research*, 51(13):4783–4796.

Arteconi, A., Di Nicola, G., Santori, G., and Stryjek, R. (2009). Second virial coefficients for dimethyl ether. *Journal of Chemical & Engineering Data*, 54(6):1840–1843.

Avami, A. and Saboohi, Y. (2011). A simultaneous method for phase identification and equilibrium calculations in reactive mixtures. *Chemical Engineering Research and Design*, 89(10):1901–1908.

Barbosa, D. and Doherty, M. F. (1988). The influence of equilibrium chemical reactions on vapor-liquid phase diagrams. *Chemical Engineering Science*, 43(3):529–540.

Bonilla-Petriciolet, A., Bravo-Sánchez, U. I., Castillo-Borja, F., Frausto-Hernández, S., and Segovia-Hernández, J. G. (2008a). Gibbs energy minimization using simulated

annealing for two-phase equilibrium calculations in reactive systems. *Chemical and Biochemical Engineering Quarterly*, 22(3):285–298.

Bonilla-Petriciolet, A., Iglesias-Silva, G. A., and Hall, K. R. (2008b). An effective calculation procedure for two-phase equilibria in multireaction systems. *Fluid Phase Equilibria*, 269(1–2):48–55.

Bonilla-Petriciolet, A., Moreno-Virgen, M. d. R., and Soto-Bernal, J. J. (2012). Global Gibbs free energy minimization in reactive systems via harmony search. *International Journal of Chemical Reactor Engineering*, 10(1).

Bonilla-Petriciolet, A., Rangaiah, G. P., and Segovia-Hernández, J. G. (2011). Constrained and unconstrained Gibbs free energy minimization in reactive systems using genetic algorithm and differential evolution with tabu list. *Fluid Phase Equilibria*, 300(1–2):120–134.

Bonilla-Petriciolet, A. and Segovia-Hernández, J. G. (2010). A comparative study of particle swarm optimization and its variants for phase stability and equilibrium calculations in multicomponent reactive and non-reactive systems. *Fluid Phase Equilibria*, 289(2):110–121.

Bonilla-Petriciolet, A., Vázquez-Román, R., Iglesias-Silva, G. A., and Hall, K. R. (2006). Performance of stochastic global optimization methods in the calculation of phase stability analyses for nonreactive and reactive mixtures. *Industrial & Egineering Chemistry Research*, 45(13):4764–4772.

Boynton, P. F. (1960). Chemical equilibrium in multicomponent polyphase systems. *The Journal of Chemical Physics*, 32(6):1880–1881.

Brinkley, Jr, S. R. (1946). Note on the conditions of equilibrium for systems of many constituents. *The Journal of Chemical Physics*, 14(9):563–564.

Brinkley, Jr, S. R. (1947). Calculation of the equilibrium composition of systems of many constituents. *The Journal of Chemical Physics*, 15(2):107–110.

Burgos-Solórzano, G. I., Brennecke, J. F., and Stadtherr, M. A. (2004). Validated computing approach for high-pressure chemical and multiphase equilibrium. *Fluid Phase Equilibria*, 219(2):245–255.

Castier, M., Rasmussen, P., and Fredenslund, A. (1989). Calculation of simultaneous chemical and phase equilibria in nonideal systems. *Chemical Engineering Science*, 44(2):237–248.

Castillo, J. and Grossmann, I. E. (1981). Computation of phase and chemical equilibria. *Computers & Chemical Engineering*, 5(2):99–108.

Cavallotti, P., Celeri, G., Leonardis, B., and Gardini, L. (1980). Calculation of multicomponent multiphase equilibria. *Chemical Engineering Science*, 35(11):2297–2304.

Chahardowli, M., Farajzadeh, R., and Bruining, H. (2016). Experimental investigation of dimethyl ether/polymer hybrid as an enhanced oil recovery method. Muscat, Oman. SPE EOR Conference at Oil and Gas West Asia, Society of Petroleum Engineers.

Chang, T., Rousseau, R. W., and Kilpatrick, P. K. (1986). Methanol synthesis reactions: calculations of equilibrium conversions using equations of state. *Industrial & Engineering Chemistry Process Design and Development*, 25(2):477–481.

Chen, F., Huss, R. S., Doherty, M. F., and Malone, M. F. (2002). Multiple steady states in reactive distillation: kinetic effects. *Computers & Chemical Engineering*, 26(1):81–93.

Chernetsky, A., Masalmeh, S., Eikmans, D., Boerrigter, P. M., Fadili, A., Parsons, C. A., Parker, A., Boersma, D. M., Cui, J., Dindoruk, B., te Riele, P. M., Alkindi, A., and Azri, N. (2015). A novel enhanced oil recovery technique: Experimental results and modelling workflow of the DME enhanced waterflood technology. Abu Dhabi, UAE. Abu Dhabi International Petroleum Exhibition and Conference, Society of Petroleum Engineers.

Chong, M. F., Chen, J., Oh, P. P., and Chen, Z.-S. (2014). Modeling study of chemical phase equilibrium of canola oil transesterification in a CSTR. *Chemical Engineering Science*, 87:371–380.

Crowe, C. M. and Nishio, M. (1975). Convergence promotion in the simulation of chemical processes - the general dominant eigenvalue method. *AIChE Journal*, 21(3):528–533.

Cruise, D. R. (1964). Notes on the rapid computation of chemical equilibria. *The Journal of Physical Chemistry*, 68(12):3797–3802.

da Roza, M. B., Nicolau, A., Angeloni, L. M., Sidou, P. N., and Samios, D. (2012). Thermodynamic and kinetic evaluation of the polymerization process of epoxidized biodiesel with dicarboxylic anhydride. *Molecular Physics*, 110(11–12):1375–1381.

Dahlhoff, G. and Pfennig, A. (2000). Vapor-liquid equilibria in quaternary mixtures of dimethyl ether + *n*-butane + ethanol + water. *Journal of Chemical & Engineering Data*, 45(4):887–892.

Darnoko, D. and Cheryan, M. (2000). Kinetics of palm oil transesterification in a batch reactor. *Journal of the American Oil Chemists' Society*, 77(12):1263–1267.

Debye, P. and Hückel, E. (1923). Zur theorie der elektrolyte. *Physikalische Zeitschrift*, 24:179–207.

Dortmund Data Bank (Accessed: 25.08.2017).

Duan, Z. and Sun, R. (2003). An improved model calculating CO_2 solubility in pure water and aqueous NaCl solutions from 273 to 533 K and from 0 to 2000 bar. *Chemical Geology*, 193(3):257–271.

Edwards, T. J., Maurer, G., Newman, J., and Prausnitz, J. M. (1978). Vapor-liquid

equilibria in multicomponent aqueous solutions of volatile weak electrolytes. *AIChE Journal*, 24(6):966–976.

Elnabawy, A. O., Fateen, S.-E. K., and Bonilla-Petriciolet, A. (2014). Phase stability analysis and phase equilibrium calculations in reactive and nonreactive systems using charged system search algorithms. *Industrial & Egineering Chemistry Research*, 53(6):2382–2395.

Fateen, S.-E. K., Bonilla-Petriciolet, A., and Rangaiah, G. P. (2012). Evaluation of covariance matrix adaptation evolution strategy, shuffled complex evolution and firefly algorithms for phase stability, phase equilibrium and chemical equilibrium problems. *Chemical Engineering Research and Design*, 90(12):2051–2071.

Felmy, A. R. and Weare, J. H. (1986). The prediction of borate mineral equilibria in natural waters: Application to Searles Lake, California. *Geochimica et Cosmochimica Acta*, 50(12):2771–2783.

Floudas, C. A. and Visweswaran, V. (1990). A global optimization algorithm (GOP) for certain classes of nonconvex NLPs–I. Theory. *Computers & Chemical Engineering*, 14(12):1397–1417.

Folas, G. K., Kontogeorgis, G. M., Michelsen, M. L., and Stenby, E. H. (2006). Application of the Cubic-Plus-Association equation of state to mixtures with polar chemicals and high pressures. *Industrial & Engineering Chemistry Research*, 45(4):1516–1526.

Garcia-Sanchez, F., Laugier, S., and Richon, D. (1987). Vapor-liquid equilibrium data for the methane-dimethylether and methane-diethylether systems between 282 and 344 K. *Journal of Chemical & Engineering Data*, 32(2):211–215.

Gautam, R. and Seider, W. D. (1979a). Computation of phase and chemical equilibrium: Part I. Local and constrained minima in Gibbs free energy. *AIChE Journal*, 25(6):991–999.

Gautam, R. and Seider, W. D. (1979b). Computation of phase and chemical equilibrium: Part II. Phase-splitting. *AIChE Journal*, 25(6):999–1006.

Gautam, R. and Seider, W. D. (1979c). Computation of phase and chemical equilibrium: Part III. Electrolytic solutions. *AIChE Journal*, 25(6):1006–1015.

Gautam, R. and Wareck, J. S. (1986). Computation of physical and chemical equilibria–alternate specifications. *Computers & Chemical Engineering*, 10(2):143–151.

George, B., Brown, L. P., Farmer, C. H., Buthod, P., and Manning, F. S. (1976). Computation of multicomponent, multiphase equilibrium. *Industrial & Engineering Chemistry Process Design and Development*, 15(3):372–377.

Giles, N. F. and Wilson, G. M. (2000). Phase equilibria on seven binary mixtures. *Journal of Chemical & Engineering Data*, 45(2):146–153.

Greiner, H. (1988a). The chemical equilibrium problem for a multiphase system formulated as a convex program. *Calphad*, 12(2):155–170.

Greiner, H. (1988b). Computing complex chemical equilibria by generalized linear programming. *Mathematical and Computer Modelling*, 10(7):529–550.

Greiner, H. (1988c). The Gibbs energy of a chemical reaction system considered as a function of its elemental abundancies. *Calphad*, 12(2):143–154.

Greiner, H. (1991). An efficient implementation of Newton's method for complex nonideal chemical equilibria. *Computers & Chemical Engineering*, 15(2):115–123.

Grob, S. and Hasse, H. (2005). Thermodynamics of phase and chemical equilibrium in a strongly nonideal esterification system. *Journal of Chemical & Engineering Data*, 50(1):92–101.

Groot, J. A. W. M., Eikmans, D., Fadili, A., and Romate, J. E. (2016). Field-scale modelling and sensitivity analysis of DME enhanced waterflooding. Muscat, Oman. SPE EOR Conference at Oil and Gas West Asia, Society of Petroleum Engineers.

Gupta, A. K., Bishnoi, P. R., and Kalogerakis, N. (1991). A method for the simultaneous phase equilibria and stability calculations for multiphase reacting and non-reacting systems. *Fluid Phase Equilibria*, 63(1–2):65–89.

Haas Jr., J. L. (1976). Physical properties of the coexisting phases and thermochemical properties of the H_2O component in boiling NaCl solutions. *Geological Survey Bulletin*, 1421-A.

Harvie, C. E., Greenberg, J. P., and Weare, J. H. (1987). A chemical equilibrium algorithm for highly non-ideal multiphase systems: Free energy minimization. *Geochimica et Cosmochimica Acta*, 51(5):1045–1057.

Hayden, J. G. and O'Connell, J. P. (1975). A generalized method for predicting second virial coefficients. *Industrial & Engineering Chemistry Process Design and Development*, 14(3):209–216.

Heidemann, R. A. and Michelsen, M. L. (1995). Instability of successive substitution. *Industrial & Engineering Chemistry Research*, 34(3):958–966.

Hildebrandt, D. and Glasser, D. (1994). Predicting phase and chemical equilibrium using the convex hull of the gibbs free energy. *The Chemical Engineering Journal and the Biochemical Engineering Journal*, 54(3):187–197.

Horstmann, S., Birke, G., and Fischer, K. (2003). Vapor-liquid equilibrium and excess enthalpy data for the binary systems propane + dimethyl ether and propene + dimethyl ether at temperatures from (298 to 323) K. *Journal of Chemical & Engineering Data*, 49(1):38–42.

Huang, S. H. and Radosz, M. (1990). Equation of state for small, large, polydisperse, and associating molecules. *Industrial & Engineering Chemistry Research*, 29(11):2284–2294.

Huff, V. N., Gordon, S., and Morrell, V. E. (1951). General method and thermodynamic tables for computation of equilibrium composition and temperature of chemical reactions. *National Advisory Committee for Aeronautics*, NACA Technical Report 1037:829–885.

Huron, M.-J. and Vidal, J. (1979). New mixing rules in simple equations of state for representing vapour-liquid equilibria of strongly non-ideal mixtures. *Fluid Phase Equilibria*, 3(4):255–271.

Jaime-Leal, J. E., Bonilla-Petriciolet, A., Segovia-Hernández, J. G., Hernández, S., and Hernández-Escoto, H. (2012). Analysis and prediction of input multiplicity for the reactive flash separation using reaction-invariant composition variables. *Chemical Engineering Research and Design*, 90(11):1856–1870.

Jalali, F., Seader, J. D., and Khaleghi, S. (2008). Global solution approaches in equilibrium and stability analysis using homotopy continuation in the complex domain. *Computers & Chemical Engineering*, 32(10):2333–2345.

Jalali-Farahani, F. and Seader, J. D. (2000). Use of homotopy-continuation method in stability analysis of multiphase, reacting systems. *Computers & Chemical Engineering*, 24(8):1997–2008.

Jiménez, L. and Costa-López, J. (2002). The production of butyl acetate and methanol via reactive and extractive distillation. II. Process modeling, dynamic simulation, and control strategy. *Industrial & Egineering Chemistry Research*, 41(26):6735–6744.

Kanth, M. V. S. R. R., Pushpavanam, S., Narasimhan, S., and Narasimha, M. B. (2014). A robust and efficient algorithm for computing reactive equilibria in single and multiphase systems. *Industrial & Egineering Chemistry Research*, 53(39):15278–15286.

Kiss, A. A., Dimian, A. C., and Rothenberg, G. (2006). Solid acid catalysts for biodiesel production —towards sustainable energy. *Advanced Synthesis & Catalysis*, 348(1–2):75–81.

Kontogeorgis, G. M., Voutsas, E. C., Yakoumis, I. V., and Tassios, D. P. (1996). An equation of state for associating fluids. *Industrial & Engineering Chemistry Research*, 35(11):4310–4318.

Kontogeorgis, G. M., Yakoumis, I. V., Meijer, H., Hendriks, E., and Moorwood, T. (1999). Multicomponent phase equilibrium calculations for water–methanol–alkane mixtures. *Fluid Phase Equilibria*, 158-160(Supplement C):201–209.

Koukkari, P. and Pajarre, R. (2007). Combining reaction kinetics to the multi-phase Gibbs energy calculation. *Computer Aided Chemical Engineering*, 24:153–158.

Lake, L. W. (1989). *Enhanced oil recovery*. Prentice-Hall, Inc, Upper Saddle River, NJ.

Lantagne, G., Marcos, B., and Cayrol, B. (1988). Computation of complex equilibria by nonlinear optimization. *Computers & Chemical Engineering*, 12(6):589–599.

Laursen, T., Rasmussen, P., and Andersen, S. I. (2003). VLE and VLLE measurements of dimethyl ether containing systems. *Journal of Chemical & Engineering Data*, 47(2):198–202.

Leal, A. M. M., Kulik, D. A., and Kosakowski, G. (2016a). Computational methods for reactive transport modeling: A Gibbs energy minimization approach for multiphase equilibrium calculations. *Advances in Water Resources*, 88:231–240.

Leal, A. M. M., Kulik, D. A., and Saar, M. O. (2016b). Enabling Gibbs energy minimization algorithms to use equilibrium constants of reactions in multiphase equilibrium calculations. *Chemical Geology*, 437:170–181.

Lee, Y. P., Rangaiaha, G. P., and Luus, R. (1999). Phase and chemical equilibrium calculations by direct search optimization. *Computers & Chemical Engineering*, 23(9):1183–1191.

Likozar, B. and Levec, J. (2014). Transesterification of canola, palm, peanut, soybean and sunflower oil with methanol, ethanol, isopropanol, butanol and tert-butanol to biodiesel: Modelling of chemical equilibrium, reaction kinetics and mass transfer based on fatty acid composition. *Applied Energy*, 123(Supplement C):108–120.

Liu, J., Daoutidis, P., and Yang, B. (2016). Process design and optimization for etherification of glycerol with isobutene. *Chemical Engineering Science*, 144(Supplement C):326–335.

Lucia, A. and Xu, J. (1990). Chemical process optimization using Newton-like methods. *Computers & Chemical Engineering*, 14(2):119–138.

Ma, Y. H. and Shipman, C. W. (1972). On the computation of complex equilibria. *AIChE Journal*, 18(2):299–304.

Madeley, W. D. and Toguri, J. M. (1973). Computing chemical equilibrium compositions in multiphase systems. *Industrial & Engineering Chemistry Fundamentals*, 12(2):261–262.

Mandagaran, B. A. and Campanella, E. A. (2009). Modeling of phase and chemical equilibrium on the quaternary system acetic acid, *n*-butanol, water and *n*-butylacetate. *Chemical Product and Process Modeling*, 4(1).

Maribo-Mogensen, B., Thomsen, K., and Kontogeorgis, G. M. (2015). An electrolyte CPA equation of state for mixed solvent electrolytes. *AIChE Journal*, 61(9):2933–2950.

Mathiarasi, R. and Partha, N. (2016). Optimization, kinetics and thermodynamic studies on oil extraction from Daturametel Linn oil seed for biodiesel production. *Renewable Energy*, 96(Part A):583–590.

Maurer, G. (1986). Vapor-liquid equilibrium of formaldehyde-and water-containing multicomponent mixtures. *AIChE Journal*, 32(6):932–948.

McDonald, C. M. and Floudas, C. A. (1995). Global optimization for the phase and chemical equilibrium problem: Application to the NRTL equation. *Computers & Chemical Engineering*, 19(11):1111–1139.

McDonald, C. M. and Floudas, C. A. (1997). GLOPEQ: A new computational tool for the phase and chemical equilibrium problem. *Computers & Chemical Engineering*, 121(1):1–23.

McNaught, A. D. and Wilkinson, A. (1997). *IUPAC Compendium of Chemical Terminology*. Blackwell Scientific Publications, Oxford, second edition.

Meng, X., Zhang, J., Wu, J., and Liu, Z. (2012). Experimental measurement and modeling of the viscosity of dimethyl ether. *Journal of Chemical & Engineering Data*, 57(3):988–993.

Michelsen, M. L. (1982). The isothermal flash problem. Part I. Stability. *Fluid Phase Equilibria*, 9(1):1–19.

Michelsen, M. L. (1989). Calculation of multiphase ideal solution chemical equilibrium. *Fluid Phase Equilibria*, 53:73–80.

Michelsen, M. L. and Hendriks, E. M. (2001). Physical properties from association models. *Fluid Phase Equilibria*, 180(1–2):165–174.

Michelsen, M. L. and Mollerup, J. M. (2007). *Thermodynamic Models: Fundamentals & Computational Aspects*. Tie-Line Publications, Holte, Denmark, second edition.

Mohebbinia, S., Sepehrnoori, K., and Johns, R. T. (2013). Four-phase equilibrium calculations of carbon dioxide/hydrocarbon/water systems with a reduced method. *SPE Journal*, 18(5):943–951.

Moodley, K., Rarey, J., and Ramjugernath, D. (2015). Application of the bio-inspired Krill Herd optimization technique to phase equilibrium calculations. *Computers & Chemical Engineering*, 74:75–88.

NIST Chemistry WebBook (Accessed: 19.02.2016). *NIST Standard Reference Database Number 69*.

NIST Chemistry WebBook (Accessed: 28.08.2017). *NIST Standard Reference Database Number 69*.

Nothnagel, K.-H., Abrams, D. S., and Prausnitz, J. M. (1973). Generalized correlation for fugacity coefficients in mixtures at moderate pressures. Application of chemical theory of vapor imperfections. *Industrial & Engineering Chemistry Process Design and Development*, 12(1):25–35.

Okasinski, M. J. and Doherty, M. F. (2000). Prediction of heterogeneous reactive azeotropes in esterification systems. *Chemical Engineering Science*, 55(22):5263–5271.

Omota, F., Dimian, A. C., and Bliek, A. (2001). Design of reactive distillation process for fatty acid esterification. *Computer Aided Chemical Engineering*, 9:463–468.

Omota, F., Dimian, A. C., and Bliek, A. (2003). Fatty acid esterification by reactive distillation. Part 1: equilibrium-based design. *Chemical Engineering Science*, 58(14):3159–3174.

Osorio-Viana, W., Duque-Bernal, M., Quintero-Arias, J. D., Dobrosz-Gómez, I., Fontalvo, J., and Gómez-García, M. Á. (2013). Activity model and consistent thermodynamic features for acetic acid-isoamyl alcohol-isoamyl acetate-water reactive system. *Fluid Phase Equilibria*, 345:68–80.

Outcalt, S. L. and Lemmon, E. W. (2013). Bubble-point measurements of eight binary mixtures for organic Rankine cycle applications. *Journal of Chemical & Engineering Data*, 58(6):1853–1860.

Pal, D., Tripathi, A., Shukla, A., Gupta, K. R., and Keshav, A. (2015). Reactive extraction of pyruvic acid using tri-*n*-octylamine diluted in decanol/kerosene: Equilibrium and effect of temperature. *Industrial & Egineering Chemistry Research*, 60(3):860–869.

Park, S.-J., Han, K.-J., and Gmehling, J. (2007). Isothermal phase equilibria and excess molar enthalpies for binary systems with dimethyl ether at 323.15 K. *Journal of Chemical & Engineering Data*, 52(5):1814–1818.

Parkhurst, D. L. and Appelo, C. A. J. (2013). *Description of input and examples for PHREEQC version 3 – A computer program for speciation, batch-reaction, one-dimensional transport, and inverse geochemical calculations*, volume Book 6, Chapter 43. U.S. Geological Survey Techniques and Methods.

Pátek, J., Hrubý, J., Klomfar, J., Souăková, M., and Harvey, A. H. (2009). Reference correlations for thermophysical properties of liquid water at 0.1 MPa. *Journal of Physical and Chemical Reference Data*, 38(1):21–29.

Paterson, D. (2017). *Flash Computation and EoS Modelling for Compositional Thermal Simulation of Flow in Porous Media*. PhD thesis, Technical University of Denmark.

Paterson, D., Michelsen, M. L., Stenby, E. H., and Yan, W. (2017). New formulations for isothermal multiphase flash. Montgomery, Texas, USA. SPE Reservoir Simulation Conference, Society of Petroleum Engineers. Submitted under the title "RAND-Based Formulations for Isothermal Multiphase Flash" to Society of Petroleum Engineers Journal (accepted).

Paterson, D., Michelsen, M. L., Yan, W., and Stenby, E. H. (2018). Extension of modified RAND to multiphase flash specifications based on state functions other than (T,P). *Fluid Phase Equilibria*, 458(41):288–299.

Peng, D.-Y. and Robinson, D. B. (1976). A new two-constant equation of state. *Industrial & Engineering Chemistry Fundamentals*, 15(1):59–64.

Perdomo, F. A., Millán-Malo, B. M., Mendoza-Díaz, G., and Gil-Villegas, A. (2013). Predicting reactive equilibria of biodiesel's fatty-acid-methyl-esters compounds. *Journal of Molecular Liquids*, 185(Supplement C):8–12.

Pérez Cisneros, E. S., Gani, R., and Michelsen, M. L. (1997). Reactive separation systems–I. Computation of physical and chemical equilibrium. *Chemical Engineering Science*, 52(4):527–543.

Phoenix, A. V. and Heidemann, R. A. (1998). A non-ideal multiphase chemical equilibrium algorithm. *Fluid Phase Equilibria*, 150–151:255–265.

Pitzer, K. S. (1973). Thermodynamics of electrolytes. I. Theoretical basis and general equations. *The Journal of Physical Chemistry*, 77(2):268–277.

Powell, M. J. D. (1971). Recent advances in unconstrained optimization. *Mathematical Programming*, 1(1):26–57.

Pozo, M. E. and Streett, W. B. (1984). Fluid phase equilibria for the system dimethyl ether/water from 50 to 220 °C and pressures to 50.9 MPa. *Journal of Chemical & Engineering Data*, 29(3):324–329.

Pozo de Fernández, M. E., Calado, J. C. G., Zollweg, J. A., and Streett, W. B. (1992). Vapor-liquid equilibria in the binary system dimethyl ether + *n*-butane from 282.9 to 414.5 K at pressures to 4.82 MPa. *Fluid Phase Equilibria*, 74:289–302.

Prigogine, I. and Defay, R. (1947). On the number of independent constituents and the phase rule. *The Journal of Chemical Physics*, 15(8):614–615.

Prutton, C. F. and Savage, R. L. (1945). The solubility of carbon dioxide in calcium chloride-water solutions at 75, 100, 120° and high pressures. *Journal of the American Chemical Society*, 67(9):1550–1554.

Rao, Y. K. (1983). The analysis and calculation of equilibria in complex metallurgical systems. *Metallurgical Transactions B*, 14(4):701–710.

Rao, Y. K. (1985). Extended form of the Gibbs phase rule. *Chemical Engineering Education*, 19(1):46–49.

Ratnakar, R. R., Dindoruk, B., and Wilson, L. (2016a). Experimental investigation of DME-water-crude oil phase behavior and PVT modeling for the application of DME-enhanced waterflooding. *Fuel*, 182:188–197.

Ratnakar, R. R., Dindoruk, B., and Wilson, L. (2016b). Use of DME as an EOR agent: Experimental and modeling study to capture interactions of DME, brine and crudes at reservoir conditions. Dubai, UAE. SPE Annual Technical Conference and Exhibition, Society of Petroleum Engineers.

Ratnakar, R. R., Dindoruk, B., and Wilson, L. C. (2017). Phase behavior experiments and PVT modeling of DME-brine-crude oil mixtures based on Huron-Vidal mixing rules for EOR applications. *Fluid Phase Equilibria*, 434:49–62.

Rossi, C. C. R. S., Berezuk, M. E., Cardozo-Filho, L., and Guirardello, R. (2011). Simultaneous calculation of chemical and phase equilibria using convexity analysis. *Computers & Chemical Engineering*, 35(7):1226–1237.

Saim, S. and Subramaniam, B. (1988). Chemical reaction equilibrium at supercritical conditions. *Chemical Engineering Science*, 43(8):1837–1847.

Saito, S., Michishita, T., and Maeda, S. (1971). Separation of meta- and para-xylene mixture by distillation accompanied by chemical reactions. *Journal of Chemical Engineering of Japan*, 4(1):37–43.

Sander, B., Rasmussen, P., and Fredenslund, A. (1986). Calculation of solid-liquid equilibria in aqueous solutions of nitrate salts using an extended UNIQUAC equation. *Chemical Engineering Science*, 41(5):1197–1202.

Sanderson, R. V. and Chien, H. H. Y. (1973). Simultaneous chemical and phase equilibrium calculation. *Industrial & Engineering Chemistry Process Design and Development*, 12(1):81–85.

Schott, G. L. (1964). Computation of restricted equilibria by general methods. *The Journal of Chemical Physics*, 40(7):2065–2066.

Schuchardt, U., Sercheli, R., and Vargas, R. M. (1998). Transesterification of vegetable oils: a review. *Journal of the Brazilian Chemical Society*, 9(3):199–210.

Seider, W. D. and Widagdo, S. (1996). Multiphase equilibria of reactive systems. *Fluid Phase Equilibria*, 123(1–2):283–303.

Shah, V. H., Pham, V., Larsen, P., Biswas, S., and Frank, T. (2016). Liquid-liquid extraction for recovering low margin chemicals: Thinking beyond the partition ratio. *Industrial & Egineering Chemistry Research*, 55(6):1731–1739.

Smith, W. R. and Missen, R. W. (1982). *Chemical Reaction Equilibrium Analysis: Theory and Algorithms*. Wiley, New York, United States of America.

Soave, G. (1972). Equilibrium constants from a modified Redlich-Kwong equation of state. *Chemical Engineering Science*, 27(6):1197–1203.

Solsvik, J., Haug-Warberg, T., and Jakobsen, H. A. (2016). Implementation of chemical reaction equilibrium by Gibbs and Helmholtz energies in tubular reactor models: Application to the steam-methane reforming process. *Chemical Engineering Science*, 140:261–278.

Søreide, I. and Whitson, C. H. (1992). Peng-Robinson predictions for hydrocarbons, CO_2, N_2, and H_2S with pure water and NaCl brine. *Fluid Phase Equilibria*, 77:217–240.

Stateva, R. P. and Wakeham, W. A. (1997). Phase equilibrium calculations for chemically reacting systems. *Industrial & Engineering Chemistry Research*, 36(12):5474–5482.

Suzuki, I., Komatsu, H., and Hirata, M. (1970). Formulation and prediction of quaternary vapor-liquid equilibria accompanied by esterification. *Journal of Chemical Engineering of Japan*, 3(2):152–157.

Tallon, S. and Fenton, K. (2010). The solubility of water in mixtures of dimethyl ether and carbon dioxide. *Fluid Phase Equilibria*, 298(1):60–66.

te Riele, P., Parsons, C., Boerrigter, P., Plantenberg, J. Suijkerbuijk, B., Burggraaf, J., Chernetsky, A., Boersma, D., and Broos, R. (2016). Implementing a water soluble solvent based enhanced oil recovery technology - aspects of field development planning. Muscat, Oman. SPE EOR Conference at Oil and Gas West Asia, Society of Petroleum Engineers.

Thomsen, K. (1997). *Aqueous Electrolytes Model Parameters and Process Simulation*. PhD thesis, Technical University of Denmark.

Toikka, A. M., Toikka, M. A., and Trofimova, M. A. (2012). Chemical equilibrium in a heterogeneous fluid phase system: thermodynamic regularities and topology of phase diagrams. *Russian Chemical Bulletin*, 61(4):741–751.

Tsanas, C., Stenby, E. H., and Yan, W. (2017a). Calculation of multiphase chemical equilibrium by the modified RAND method. *Industrial & Engineering Chemistry Research*, 56(41):11983–11995.

Tsanas, C., Stenby, E. H., and Yan, W. (2017b). Calculation of simultaneous chemical and phase equilibrium by the method of Lagrange multipliers. *Chemical Engineering Science*, 174:112–126.

Tsivintzelis, I. and Kontogeorgis, G. M. (2014). On the predictive capabilities of CPA for applications in the chemical industry: Multicomponent mixtures containing methyl-methacrylate, dimethyl-ether or acetic acid. *Chemical Engineering Research and Design*, 92(12):2947–2969.

Tsivintzelis, I., Kontogeorgis, G. M., Michelsen, M. L., and Stenby, E. H. (2010). Modeling phase equilibria for acid gas mixtures using the CPA equation of state. I. Mixtures with H_2S. *AIChE Journal*, 56(11):2965–2982.

Tsivintzelis, I., Kontogeorgis, G. M., Michelsen, M. L., and Stenby, E. H. (2011). Modeling phase equilibria for acid gas mixtures using the CPA equation of state. Part II: Binary mixtures with CO_2. *Fluid Phase Equilibria*, 306(1):38–56.

Uchida, M. (1987). MPEC2: A code for multi-phase chemical equilibria. *Computers & Chemistry*, 11(1):19–24.

Ung, S. and Doherty, M. F. (1995a). Calculation of residue curve maps for mixtures with

multiple equilibrium chemical reactions. *Industrial & Engineering Chemistry Research*, 34(10):3195–3202.

Ung, S. and Doherty, M. F. (1995b). Necessary and sufficient conditions for reactive azeotropes in multireaction mixtures. *AIChE Journal*, 41(11):2383–2392.

Ung, S. and Doherty, M. F. (1995c). Synthesis of reactive distillation systems with multiple equilibrium chemical reactions. *Industrial & Engineering Chemistry Research*, 34(8):2555–2565.

Ung, S. and Doherty, M. F. (1995d). Theory of phase equilibria in multireaction systems. *Chemical Engineering Science*, 50(20):3201–3216.

Ung, S. and Doherty, M. F. (1995e). Vapor-liquid phase equilibrium in systems with multiple chemical reactions. *Chemical Engineering Science*, 50(1):23–48.

Varzandeh, F. (2017). *Modeling Study of High Pressure and High Temperature Reservoir Fluids*. PhD thesis, Technical University of Denmark.

Venkatraman, A., Lake, L. W., and Johns, R. T. (2015). Modelling the impact of geochemical reactions on hydrocarbon phase behavior during CO_2 gas injection for enhanced oil recovery. *Fluid Phase Equilibria*, 402:56–68.

Voll, F. A. P., da Silva, C., Rossi, C. C. R. S., Guirardello, R., de Castilhos, F., Oliveira, J. V., and Cardozo-Filho, L. (2011). Thermodynamic analysis of fatty acid esterification for fatty acid alkyl esters production. *Biomass and Bioenergy*, 35(2):781–788.

Voňka, P. and Leitner, J. (1995). Calculation of chemical equilibria in heterogeneous multicomponent systems. *Calphad*, 19(1):25–36.

Wasylkiewicz, S. K. and Ung, S. (2000). Global phase stability analysis for heterogeneous reactive mixtures and calculation of reactive liquid-liquid and vapor-liquid-liquid equilibria. *Fluid Phase Equilibria*, 175(1–2):253–272.

White, III, C. W. and Seider, W. D. (1981). Computation of phase and chemical equilibrium: Part IV. Approach to chemical equilibrium. *AIChE Journal*, 27(3):466–471.

White, W. B., Johnson, S. M., and Dantzig, G. B. (1958). Chemical equilibrium in complex mixtures. *The Journal of Chemical Physics*, 28(5):751–755.

Wiebe, R. and Gaddy, V. L. (1940). The solubility of carbon dioxide in water at various temperatures from 12 to 40° and at pressures to 500 atmospheres. Critical phenomena. *Journal of the American Chemical Society*, 62(4):815–817.

Wilson, G. M. (1964). Vapor-liquid equilibrium. xi. a new expression for the excess free energy of mixing. *Journal of the American Chemical Society*, 86(2):127–130.

Wu, J., Liu, Z., Pan, J., and Zhao, X. (2004). Vapor pressure measurements of dimethyl ether from (233 to 399) K. *Journal of Chemical & Engineering Data*, 49(1):32–34.

Wu, J., Liu, Z., Wang, F., and Ren, C. (2003). Surface tension of dimethyl ether from (213 to 368) K. *Journal of Chemical & Engineering Data*, 48(6):1571–1573.

Wu, L., Wei, T., Lin, Z., Zou, Y., Tong, Z., and Sun, J. (2016). Bentonite-enhanced biodiesel production by NaOH-catalyzed transesterification: Process optimization and kinetics and thermodynamic analysis. *Fuel*, 182(Supplement C):920–927.

Xiao, W.-d., Zhu, K.-h., Yuan, W.-k., and Chien, H. H.-y. (1989). An algorithm for simultaneous chemical and phase equilibrium calculation. *AIChE Journal*, 35(11):1813–1820.

Yakoumis, I. V., Kontogeorgis, G. M., Voutsas, E. C., and Tassios, D. P. (1997). Vapor-liquid equilibria for alcohol/hydrocarbon systems using the CPA equation of state. *Fluid Phase Equilibria*, 130(1):31–47.

Yancy-Caballero, D. M. and Guirardello, R. (2013). Thermodynamic simulation of transesterification reaction by gibbs energy minimization. *Fluid Phase Equilibria*, 341(Supplement C):12–22.

Yancy-Caballero, D. M. and Guirardello, R. (2015). Modeling and parameters fitting of chemical and phase equilibria in reactive systems for biodiesel production. *Biomass and Bioenergy*, 81(Supplement C):544–555.

Zeleznik, F. J. and Gordon, S. (1968). Calculation of complex chemical equilibria. *Industrial & Engineering Chemistry*, 60(6):27–57.

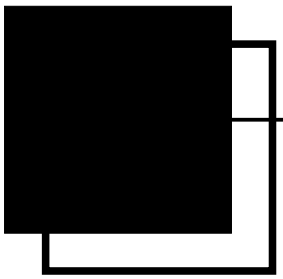

Glossaries

Abbreviations

ARD	absolute relative deviation
AARD	average absolute relative deviation
CEoS	cubic equation of state
CPA	Cubic-Plus-Association
CPE	chemical and phase equilibrium
DME	dimethyl ether
EoS	equation of state
HC	hydrocarbon
LLE	liquid-liquid equilibrium
VLE	vapor-liquid equilibrium
VLLE	vapor-liquid-liquid equilibrium

Symbols

$\mathbf{A}$	formula matrix
$\mathbf{A}_{ac}, \mathbf{b}_{ac}$	additional stoichiometric constraints
A_{ji}	number of elements j in the chemical formula of component i

$\mathcal{A}_i$	component i in a chemical reaction
a	energy parameter
a_i	energy parameter of component i
a_0	parameter in the energy term of CPA
a_{ij}	energy parameter of components i and j
$\mathbf{B}$	element abundance matrix
$\mathbf{B}_k$	element abundance vector in phase k
$\mathbf{b}$	element abundance vector
B_{jk}	total mole numbers of element j in phase k
b_j	total mole numbers of element j
b	covolume parameter
b_i	covolume parameter of component i
b_{ij}	covolume parameter of components i and j
$C^\circ_{p,i}$	reference state heat capacity at constant pressure of component i
C_{ij}	HV-NRTL energy interaction parameter between components i and j
c_{ik}	molarity of component i in phase k
$c_{\mathrm{sol},k}$	solvent molarity in phase k
$c_{t,k}$	total molarity in phase k
c°	unit molarity
c_1	parameter in the energy term of CPA
$\mathbf{e}_X$	vector of ones with dimensions $X \times 1$
$\mathbf{F}$	vector of working equations in the successive substitution method
$\hat{f}_{ik}$	fugacity of component i in phase k
f_{ik}	fugacity of pure component i in phase k
f_{il}	fugacity of pure liquid i

f_{ik}°	reference state fugacity of component i in phase k
G	Gibbs energy
G_k	Gibbs energy of phase k
$g(v)$	radial distribution function
H	enthalpy
H_{ik}	Henry's constant of component i in phase k
H_{ik}^{s}	saturation Henry's constant of component i in phase k
I_k	ionic strength in phase k
$\mathbf{J}$	Jacobian of $\mathbf{F}$ in the Lagrange multiplier method
K_{rk}^{eq}	thermodynamic equilibrium constant of reaction r in phase k
k_{ij}	binary interaction parameter between component i and j
K_{ik}	K-factor of component i in phase k with respect to a reference phase
$\mathcal{L}$	Lagrangian function
M_i	molar mass of component i
$M_{\mathrm{sol},k}$	solvent molar mass in phase k
m_{ik}	molality of component i in phase k
m°	unit molality
$\mathbf{N}$	stoichiometric matrix
$\hat{\mathbf{N}}$	stoichiometric matrix for the assignment of $\hat{\mu}$
$\mathbf{n}$	component abundance matrix
$\mathbf{n}_k$	component abundance vector in phase k
$\mathbf{n}_t$	phase amount vector
$\mathbf{n}_F$	component abundance vector in the feed
N	number of experimental points
N_C	number of components

N_E	number of elements
N_P	number of phases
N_R	number of independent chemical reactions
N_S	number of special stoichiometric conditions
N_T	number of additional constraints not included in $\mathbf{A}_{ac}, \mathbf{b}_{ac}$
N_V	number of additional variables
n_{ik}	mole numbers of component i in phase k
$n_{t,k}$	amount of phase k
$n_{F,i}$	mole numbers of component i in the feed
$n_{t,F}$	total mole numbers in the feed
$n_{\mathrm{sol},k}$	solvent mole numbers in phase k
$n_{t,r}^{B}$	phase amount estimate for the full backward reaction r
$n_{t,r}^{F}$	phase amount estimate for the full forward reaction r
OF	objective function in the regressions of DME binaries
Pe_i	Poynting effect (Poynting correction) for component i
p	pressure
p_k	pressure of phase k
p_i	partial pressure of component i
p_i^s	vapor pressure of component i
$p_{c,i}$	critical pressure of component i
p_{sol}^s	solvent vapor pressure
p^*	ideal gas reference pressure
Q	function minimized during intialization
R	gas constant
R_j	transformed tie line slopes defined in Bonilla-Petriciolet et al. (2008a)

$\mathbf{s}$	phase amount correction vector
S	entropy
S_k	entropy of phase k
s_k	correction for the amount of phase k
T	temperature
T_k	temperature of phase k
$T_{c,i}$	critical temperature of component i
T_r	reduced temperature
TPD	tangent plane distance
tpd	reduced tangent plane distance
tm	modified tangent plane distance
U	internal energy
U_k	internal energy of phase k
$\boldsymbol{\mathcal{V}}$	stoichiometric matrix of reference components in Ung and Doherty (1995b,d)
V	volume
V_k	volume of phase k
$\bar{V}_{ik}$	partial molar volume of component i in phase k
$\bar{V}_{ik}^{\infty}$	infinite dilution partial molar volume of component i in phase k
v	molar volume
v_{ik}	molar volume of component i in phase k
v_{il}	molar volume of component i in the liquid phase
$\mathbf{W}$	vector of trial phase mole numbers
$\mathbf{w}$	vector of trial phase mole fractions
W_i	trial phase mole numbers of component i
w_i	trial phase mole fraction of component i

$\mathbf{x}$	matrix of mole fractions
$\mathbf{x}_{\text{ref}}$	reference component mole fractions in Ung and Doherty (1995b,d)
$\mathbf{x}_k$	vector of mole fractions in phase k
$\mathrm{X}_r^{(x_r)+}$	cation with charge $+x_r$ in dissociation reaction r
X_{A_i}	mole fraction of component i not bonded at site A
x_{ik}	mole fraction of component i in phase k
$\bar{x}_i$	overall mole fraction of component i
x_{jk}^{el}	mole fraction of element j in phase k
$x_{\text{sol},k}$	solvent mole fraction in phase k
$\mathrm{Y}_r^{(y_r)-}$	anion with charge $-y_r$ in dissociation reaction r
$\mathbf{z}$	vector of mole fractions in the feed
z_i	mole fraction of component i in the feed
z_i	charge of component i

Greek letters

α	step-size control parameter
α_{ik}	activity of component i in phase k
α_{ij}	HV-NRTL non-randomness parameter between components i and j
β_k	mole fraction of phase k
$\beta^{\mathrm{A}_i\mathrm{B}_j}$	parameter in the association term of CPA between sites A_i and B_j
β_{cross}	cross association β parameter of CPA in DME/water
γ_{ik}	symmetric activity coefficient of component i in phase k
γ_{ik}^{∞}	symmetric infinite dilution activity coefficient of component i in phase k
$\tilde{\gamma}_{ik}$	asymmetric activity coefficient of component i in phase k
$\tilde{\gamma}_{ik}^{m}$	asymmetric molality activity coefficient of component i in phase k
$\tilde{\gamma}_{ik}^{c}$	asymmetric molarity activity coefficient of component i in phase k

$\Delta_c G^\circ_{ik}$	reference state Gibbs energy of combustion of component i in phase k
$\Delta_f G^\circ_{ik}$	reference state Gibbs energy of formation of component i in phase k
$\Delta_r G^\circ_{rk}$	reference state Gibbs energy of reaction r in phase k
$\Delta_r H^\circ_{rk}$	reference state enthalpy of reaction r in phase k
$\Delta_r V^\circ_{rk}$	reference state volume change of reaction r in phase k
$\Delta^{\mathrm{A}_i\mathrm{B}_j}$	association strength between sites A_i and B_j
$\delta\mathbf{b}$	mass balance satisfaction vector
δ_{ij}	Kronecker delta
$\epsilon^{\mathrm{A}_i\mathrm{B}_j}$	association energy of interaction between sites A_i and B_j
$\epsilon_{\mathrm{cross}}$	cross association ϵ parameter of CPA in DME/water
θ_{ik}	yield factor of component i in phase k
$\boldsymbol{\lambda}$	vector of Lagrange multipliers
λ_j	Lagrange multiplier of element j
$\boldsymbol{\mu}_k$	vector of chemical potentials in phase k
μ_{ik}	chemical potential of component i in phase k
μ°_{ik}	reference state chemical potential of component i in phase k
μ^*_i	ideal gas chemical potential of component i
μ^{pure}_{ik}	chemical potential of pure component i in phase k
$\tilde{\mu}_{ik}$	infinite dilution chemical potential of component i in phase k
$\tilde{\mu}^m_{ik}$	chemical potential of component i in phase k at unit molality
$\tilde{\mu}^c_{ik}$	chemical potential of component i in phase k at unit molarity
$\hat{\mu}_{ik}$	chemical potential of component i in phase k assigned from a chemical equilibrium constant
$\boldsymbol{\nu}_r$	vector of stoichiometric coefficients in reaction r
$\boldsymbol{\nu}_i$	vector of all stoichiometric coefficients for component i

$\boldsymbol{\nu}_t$	vector of total stoichiometric coefficients
ν_{ir}	stoichiometric coefficient of component i in reaction r
$\nu_{t,r}$	total stoiometric coefficient in reaction r
$\boldsymbol{\xi}$	vector of reaction extents
ξ_r	extent of reaction r
ξ_r^B	maximum extent of the backward reaction r
ξ_r^F	maximum extent of the forward reaction r
ρ_k	density of phase k
$\rho_{\text{sol},k}$	pure solvent density in phase k
$\boldsymbol{\Phi}_k$	matrix of fugacity coefficient composition derivatives in phase k
$\hat{\phi}_{ik}$	fugacity coefficient of component i in phase k
ϕ_i^s	saturation fugacity coefficient of component i
ω_i	acentric factor of component i

Superscripts

0	initial value
$\circ$	reference state
calc	calculated value
exp	experimental value
s	saturation
T	transpose of matrix or vector

Subscripts

$(\cdot)$	state of matter indicator (solid, liquid, etc.)
i	component
j	element

k	phase
l	liquid phase
q	dummy variable
r	reaction
s	solid phase
sol	solvent
v	vapor phase

Operators

∇	gradient
∇^2	Laplacian
Δ	finite difference, correction quantity in iterative calculations
Δ_c	change of a property during combustion reaction
Δ_f	change of a property during formation reaction
Δ_r	change of a property during reaction
$\mathcal{F}_i^f$	Legendre transformation of function $f(\mathbf{x})$ with respect to variable x_i

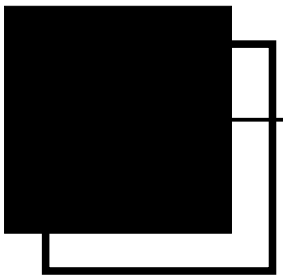

Index

Center for Energy Resources Engineering (CERE)

Department of Chemistry
Kemitorvet, Building 207
Technical University of Denmark
DK-2800 Kgs. Lyngby

+45 45 25 24 19
www.kemi.dtu.dk